

Electronic Thesis and Dissertation Repository

---

4-30-2020 9:30 AM

## Structure and Function of Asthma Evaluated Using Pulmonary Imaging

Rachel L. Eddy, *The University of Western Ontario*

Supervisor: Parraga, Grace, *The University of Western Ontario*

A thesis submitted in partial fulfillment of the requirements for the Doctor of Philosophy degree in Medical Biophysics

© Rachel L. Eddy 2020

Follow this and additional works at: <https://ir.lib.uwo.ca/etd>



Part of the [Medical Biophysics Commons](#)

---

### Recommended Citation

Eddy, Rachel L., "Structure and Function of Asthma Evaluated Using Pulmonary Imaging" (2020).  
*Electronic Thesis and Dissertation Repository*. 6871.  
<https://ir.lib.uwo.ca/etd/6871>

This Dissertation/Thesis is brought to you for free and open access by Scholarship@Western. It has been accepted for inclusion in Electronic Thesis and Dissertation Repository by an authorized administrator of Scholarship@Western. For more information, please contact [wlsadmin@uwo.ca](mailto:wlsadmin@uwo.ca).

## Abstract

Asthma has been understood to affect the airways in a spatially heterogeneous manner for over six decades. Computational models of the asthmatic lung have suggested that airway abnormalities are diffusely and randomly distributed throughout the lung, however these mechanisms have been challenging to measure *in vivo* using current clinical tools. Pulmonary structure and function are still clinically characterized by the forced expiratory volume in one-second (FEV<sub>1</sub>) – a global measurement of airflow obstruction that is unable to capture the underlying regional heterogeneity that may be responsible for symptoms and disease worsening. In contrast, pulmonary magnetic resonance imaging (MRI) provides a way to visualize and quantify regional heterogeneity *in vivo*, and preliminary MRI studies in patients suggest that airway abnormalities in asthma are spatially persistent and not random. Despite these disruptive results, imaging has played a limited clinical role because the etiology of ventilation heterogeneity in asthma and its long-term pattern remain poorly understood. Accordingly, the objective of this thesis was to develop a deeper understanding of the pulmonary structure and function of asthma using functional MRI in conjunction with structural computed tomography (CT) and oscillometry, to provide a foundation for imaging to guide disease phenotyping, personalized treatment and prediction of disease worsening. We first evaluated the biomechanics of ventilation heterogeneity and showed that MRI and oscillometry explained biomechanical differences between asthma and other forms of airways disease. We then evaluated the long-term spatial and temporal nature of airway and ventilation abnormalities in patients with asthma. In nonidentical twins, we observed a spatially-matched CT airway and MRI ventilation abnormality that persisted for seven-years; we estimated the probability of an identical defect occurring in time and space to be 1 in 130,000. In unrelated asthmatics, ventilation defects were spatially-persistent over 6.5-years and uniquely predicted longitudinal bronchodilator reversibility. Finally, we investigated the entire CT airway tree and showed that airways were truncated in severe asthma related to thickened airway walls and worse MRI ventilation heterogeneity. Together, these results advance our understanding of asthma as a non-random disease and support the use of MRI ventilation to guide clinical phenotyping and treatment decisions.

## **Keywords**

Asthma, Airways, Chronic Obstructive Pulmonary Disease, Computed Tomography, Hyperpolarized Noble Gas MRI, Pulmonary Imaging, Pulmonary Structure-function, Ventilation Heterogeneity

## **Summary for Lay Audience**

Asthma is a chronic lung disease that causes the air a person breathes in to unevenly spread throughout their lungs. The causes of this are still not well-known because the current tools to measure lung function cannot locate where inside the lungs the air does not go. To better understand this, computer models have been created and showed that asthma lung abnormalities are randomly spread throughout the whole lungs, but magnetic resonance imaging (MRI) of the lung showed that abnormalities stay in the same lung locations over time and are not random. Despite these new results, MRI of the lungs is not used often for asthma patients because the causes of MRI measurements and how they change over long periods of time are not known. This thesis measured lung structure and function in asthma using functional MRI and structural computed tomography (CT) imaging to better understand how and why air unevenly spreads throughout the lungs in patients with asthma and create a new way to guide asthma treatments to help air spread more evenly. First, we evaluated lung biomechanics and saw different biomechanical measurements in patients with asthma compared to different lung diseases and healthy people. We then evaluated MRI and CT lung abnormalities twice over 6-7 years in two different groups of patients. Twins with asthma had a lung abnormality in the exact same location that stayed the same after 7 years. We calculated the chances of an identical abnormality like this occurring in two people to be 1-in-130,000, or less likely than the chances of someone being struck by lightning. In a larger group of non-related asthma patients, MRI and CT abnormalities remained in the same lung locations over 6.5 years and MRI abnormalities predicted future asthma worsening. Finally, we evaluated all airways we could see on CT images and saw that patients with severe asthma had less airways and this was related to thicker airway walls and worse lung function. Together, these results provide a better understanding of lung structure-function in asthma that are not random and support the use of MRI to guide patient-specific treatment.

## Co-Authorship Statement

This thesis contains four manuscripts that have been published in scientific journals. As first author of these four manuscripts, I significantly contributed to all aspects of the studies as well as manuscript preparation and submission. Specifically, I made intellectual contributions to all study designs and was responsible for participant recruitment, organization and management of study visits, and acquisition of pulmonary function test and participant data. Following data acquisition, I was responsible for image analysis, database organization, statistical analysis and interpretation, clinical/physiological interpretation, drafting and final approval of the manuscripts. As Principal Investigator and Supervisor, Dr. Grace Parraga provided ongoing guidance and was responsible for study conception and experimental design, data analysis and interpretation, drafting and final revisions and approval of the manuscripts. She is also the guarantor of the integrity of the data and responsible for Good Clinical Practice. Management of study visits and acquisition of pulmonary function test and imaging data were performed under the supervision of Sandra Blamires, Lyndsey Reid-Jones and Danielle Knipping. MRI of research participants was performed by Trevor Szekeres and David Reese. Polarization of  $^3\text{He}$  gas was performed by Andrew Wheatley, Dante Capaldi, Heather Young and Andrew Westcott. For each manuscript within this thesis, all co-authors approved the final draft and their specific contributions are listed below.

**Chapter 2** is an original research article entitled “*Oscillometry and Pulmonary Magnetic Resonance Imaging in Asthma and COPD*” and was published in the journal *Physiological Reports* in 2019. This manuscript was co-authored by Rachel L Eddy, Andrew Westcott, Geoffrey N Maksym, Grace Parraga and Ronald J Dandurand. Andrew Westcott and Geoffrey N Maksym assisted with data interpretation. Ronald J Dandurand conceived and designed the study, and was responsible for clinical/physiological interpretation of the data.

**Chapter 3** is an original research article entitled “*Nonidentical Twins with Asthma: Spatially-matched CT Airway and MRI Ventilation Abnormalities*” and was published in the journal *Chest* in 2019 as a selected report. This manuscript was co-authored by Rachel L Eddy, Alexander M Matheson, Sarah Svenningsen, Danielle Knipping, Christopher Licskai, David G McCormack and Grace Parraga. Alexander M Matheson assisted with data analysis and interpretation. Sarah Svenningsen was responsible for data acquisition and interpretation.

Danielle Knipping assisted with clinical interpretation of the data. David G McCormack and Christopher Licskai were responsible for recruitment of study participants, clinical input in the study design and clinical/physiological interpretation of the data.

**Chapter 4** is an original research article entitled “*Hyperpolarized Helium 3 MRI in Mild-to-Moderate Asthma: Prediction of Postbronchodilator Reversibility*” and was published in the journal *Radiology* in 2019. This manuscript was co-authored by Rachel L Eddy, Sarah Svenningsen, Christopher Licskai, David G McCormack and Grace Parraga. Sarah Svenningsen assisted with participant recruitment and data acquisition and interpretation. Christopher Licskai and David G McCormack were responsible for recruitment of study participants, clinical input in the study design and clinical/physiological interpretation of the data.

**Chapter 5** is an original research article entitled “*Is Computed Tomography Total Airway Count Related to Asthma Severity and Airway Structure-function?*” and was published in the *American Journal of Respiratory and Critical Care Medicine* in 2020. This manuscript was co-authored by Rachel L Eddy, Sarah Svenningsen, Miranda Kirby, Danielle Knipping, David G McCormack, Christopher Licskai, Parameswaran Nair and Grace Parraga. Sarah Svenningsen was responsible for data acquisition and interpretation. Miranda Kirby assisted with data interpretation. Danielle Knipping assisted with clinical interpretation of the data. David G McCormack, Christopher Licskai and Parameswaran Nair were responsible for recruitment of study participants, clinical input in the study design and clinical/physiological interpretation of the data.

**Appendix A** contains an additional published manuscript that is complimentary to the objective and hypothesis of this thesis. The article entitled “*What is the Minimal Clinically Important Difference for Helium-3 Magnetic Resonance Imaging Ventilation Defects?*” was published in the *European Respiratory Journal* in 2018 as a research letter. This manuscript was co-authored by Rachel L Eddy, Sarah Svenningsen, David G McCormack and Grace Parraga. Sarah Svenningsen assisted with data acquisition and interpretation and David G McCormack was responsible for clinical interpretation of the data.

*To the study participants,  
for showing me first-hand the importance of our research*

## Acknowledgments

First and foremost, I thank my supervisor and mentor Dr. Grace Parraga for taking a chance on me, drawing out my potential, and providing endless opportunities for personal, professional and scholarly development. Your inherent drive for research and innovation has encouraged my own; thank you for continuously pushing me beyond my boundaries to reach new goals and achievements I never thought possible. I will always value your past, present and future mentorship and support in all of my endeavors.

To my advisory committee, Dr. Hanif Ladak, Dr. David McCormack and Dr. Aaron Fenster: thank you for your guidance and support for my research as well as my career trajectory. To Dr. Ladak, thank you for pushing me on technical and image processing details I tended to neglect early in my graduate career. To Dr. McCormack, thank you for pushing me on the clinical details of my work and to see the big picture. To Dr. Fenster, thank you for your continued support of my career development and trajectory. I am also grateful to other mentors, advisors and collaborators both at Western and other institutions: Drs. Aaron Ward, Christopher Liciskai, Nicole Campbell, Ron Dandurand and Geoff Maksym.

To the members of the Parraga lab, thank you for making this research possible and fostering a collaborative, collegial and enjoyable graduate school experience. To Dave, thank you for always supporting my push for better image quality. I have been fortunate to work with you for countless research studies, and am even more fortunate to have you as a friend. To Alexei, thank you for teaching me the fundamentals of hyperpolarized gas MRI and how to troubleshoot like an expert. To Danielle, thank you for your patient-centred approach to our research and for appreciating my Friends jokes. To Miranda, though our time in the lab never overlapped, I am fortunate to call you a mentor. I will always take it as the greatest compliment when I am mistaken for you at conferences. To Sarah, Khadija, Fumin and Dante: I could not have asked for a better group of senior students and mentors to help me navigate the beginning of grad school and my research career. Sarah, thank you for setting the best example, for your collaboration and for continuously raising the bar and challenging me to reach higher. To Khadija, thank you for your detailed help with all the grad school firsts, from committee meetings to conference abstracts. To Fumin, thank you for being the image processing guru. To Dante, thank you for help with anything and everything, no matter what else you had to do;

for example, jumping my car battery at 5:30 in the morning. You are the embodiment of what it means to be an innovative scientist, collaborative colleague and genuine friend. To Eric, thank you for navigating the beginning of grad school with me. To Andrew, thank you for taking on senior studentship with me, and for being my travel buddy in Paris. To Heather, Alex, Andrea B, Jonathan, Fabio, Marrison and Maksym, thank you for teaching me more than I could ever teach you. Thank you to all other lab members and colleagues who I've had the pleasure of working with: Tamas, Damien, Anurag, Hana, Robert, Andrea K, Hannah and Jenna. Outside the Parraga lab, thank you to those around Robarts who supported me in and outside of my grad school journey: Lisa, Dickson, Patrick, Amy, Olivia, Megan, Derek, Patricia, David T, Amanda, Janette, Johanne, Trevor and Paco.

Most importantly, I thank my friends and family. To Laura, thank you for always being there. After three years as house-mates and five more in the same city, I'm not sure how I will survive so far away from you. To Lyndsey, the impact you have had on me is unmeasurable. Thank you for all the little things, for Tim, for O&O and mostly, for being my person. To Tim, thank you for your genuine kindness and sharing your home with me. And to my parents, thank you for your unwavering love, patience and support in my pursuit of my goals and dreams. Mom, thank you for being my biggest fan and always reminding me to be humble. Dad, thank you for teaching me to be independent and consistently pushing me to think two steps ahead.

Finally, I express my sincere gratitude towards the various sources of funding I have received over my tenure as a graduate student. I acknowledge funding support from the Natural Sciences and Engineering Research Council of Canada (NSERC) and Schulich School of Medicine and Dentistry Western Graduate Research Scholarship, as well as travel funding from the Canadian Institutes of Health Research (CIHR).

# Table of Contents

<b>Abstract</b> .....	ii
<b>Summary for Lay Audience</b> .....	iv
<b>Co-Authorship Statement</b> .....	v
<b>Acknowledgments</b> .....	viii
<b>Table of Contents</b> .....	x
<b>List of Tables</b> .....	xv
<b>List of Figures</b> .....	xvii
<b>List of Appendices</b> .....	xix
<b>List of Abbreviations</b> .....	xx
<b>CHAPTER 1</b> .....	1
<b>1 INTRODUCTION</b> .....	1
<b>1.1 Motivation and Overview</b> .....	1
<b>1.2 Respiratory Structure and Function</b> .....	5
1.2.1 Airways: Conducting and Respiratory Zones .....	5
1.2.2 Alveoli: Site of Gas Exchange .....	8
1.2.3 Ventilation.....	8
<b>1.3 Pathophysiology of Asthma and COPD</b> .....	9
1.3.1 Asthma .....	9
1.3.2 COPD .....	10
1.3.3 Asthma-COPD Overlap .....	12
<b>1.4 Clinical Tools to Measure Pulmonary Function</b> .....	13
1.4.1 Spirometry.....	13
1.4.2 Plethysmography.....	14
1.4.3 Diffusing Capacity of the Lung .....	17

1.4.4	Oscillometry.....	18
<b>1.5</b>	<b>Clinical Assessments to Characterize Asthma and COPD .....</b>	<b>21</b>
1.5.1	Bronchodilator Reversibility.....	22
1.5.2	Airway Hyperresponsiveness.....	22
1.5.3	Questionnaires.....	24
1.5.4	Disease Severity .....	25
<b>1.6</b>	<b>Imaging of Pulmonary Structure and Function.....</b>	<b>26</b>
1.6.1	Planar X-ray .....	26
1.6.2	X-ray Computed Tomography .....	27
1.6.3	Nuclear Medicine.....	34
1.6.4	Magnetic Resonance Imaging.....	37
<b>1.7</b>	<b>Thesis Hypotheses and Objectives.....</b>	<b>48</b>
<b>1.8</b>	<b>References.....</b>	<b>50</b>
<b>CHAPTER 2</b>	<b>.....</b>	<b>75</b>
<b>2</b>	<b>OSCILLOMETRY AND PULMONARY MAGNETIC RESONANCE IMAGING IN ASTHMA AND COPD.....</b>	<b>75</b>
<b>2.1</b>	<b>Introduction.....</b>	<b>75</b>
<b>2.2</b>	<b>Materials and Methods.....</b>	<b>77</b>
2.2.1	Study Participants and Design .....	77
2.2.2	Pulmonary Function Tests .....	77
2.2.3	Oscillometry.....	78
2.2.4	Image Acquisition and Analysis .....	78
2.2.5	Statistical Analysis.....	79
<b>2.3</b>	<b>Results .....</b>	<b>80</b>
<b>2.4</b>	<b>Discussion.....</b>	<b>87</b>
<b>2.5</b>	<b>References.....</b>	<b>91</b>

<b>CHAPTER 3</b> .....	96
<b>3 NONIDENTICAL TWINS WITH ASTHMA: SPATIALLY-MATCHED CT AIRWAY AND MRI VENTILATION ABNORMALITIES</b> .....	96
<b>3.1 Introduction</b> .....	96
<b>3.2 Case</b> .....	97
<b>3.3 Discussion</b> .....	101
<b>3.4 References</b> .....	103
<b>CHAPTER 4</b> .....	105
<b>4 HYPERPOLARIZED HELIUM 3 MRI IN MILD-TO-MODERATE ASTHMA: PREDICTION OF POSTBRONCHODILATOR REVERSIBILITY</b> .....	105
<b>4.1 Introduction</b> .....	105
<b>4.2 Materials and Methods</b> .....	106
4.2.1 Study Participants and Design .....	106
4.2.2 Pulmonary Function Tests and Methacholine Challenge .....	107
4.2.3 MRI Parameters and Analysis .....	108
4.2.4 CT Parameters and Analysis .....	109
4.2.5 Statistical Analysis .....	110
<b>4.3 Results</b> .....	110
4.3.1 Study Participants .....	110
4.3.2 <sup>3</sup> He MRI Ventilation at Baseline and Follow-up .....	114
4.3.3 FEV <sub>1</sub> and Ventilation Defect Postbronchodilator Reversibility Measurements .....	118
4.3.4 Multivariable Analysis .....	121
<b>4.4 Discussion</b> .....	122
<b>4.5 References</b> .....	124
<b>4.6 Supplement</b> .....	128
<b>CHAPTER 5</b> .....	133

<b>5 IS COMPUTED TOMOGRAPHY TOTAL AIRWAY COUNT RELATED TO ASTHMA SEVERITY AND AIRWAY STRUCTURE-FUNCTION?.....</b>	<b>133</b>
<b>5.1 Introduction.....</b>	<b>133</b>
<b>5.2 Materials and Methods.....</b>	<b>134</b>
5.2.1 Study Participants and Design .....	134
5.2.2 Pulmonary Function Tests .....	134
5.2.3 CT .....	135
5.2.4 MRI.....	136
5.2.5 Statistical Analysis.....	136
<b>5.3 Results .....</b>	<b>137</b>
5.3.1 Participant Demographics, Pulmonary Function and Imaging Measurements .....	137
5.3.2 Is TAC Reduced with Increasing Asthma Severity? .....	138
5.3.3 Is TAC Associated with Abnormal Airway Structure and Function? ....	140
5.3.4 Is TAC Related to FEV <sub>1</sub> and Airway Wall Area? .....	145
<b>5.4 Discussion.....</b>	<b>149</b>
5.4.1 TAC is Reduced with Increasing Asthma Severity .....	149
5.4.2 TAC is Associated with Abnormal Airway Structure and Function .....	150
5.4.3 TAC is Related to FEV <sub>1</sub> and Airway Wall Area .....	151
5.4.4 Limitations and Unanswered Questions .....	152
5.4.5 Conclusions.....	154
<b>5.5 References.....</b>	<b>154</b>
<b>5.6 Supplement .....</b>	<b>158</b>
<b>CHAPTER 6.....</b>	<b>159</b>
<b>6 CONCLUSIONS AND FUTURE DIRECTIONS.....</b>	<b>159</b>
<b>6.1 Overview and Research Questions .....</b>	<b>159</b>
<b>6.2 Summary and Conclusions.....</b>	<b>160</b>

<b>6.3</b>	<b>Limitations</b> .....	163
6.3.1	Study Specific Limitations.....	163
6.3.2	General Limitations .....	166
<b>6.4</b>	<b>Future Directions</b> .....	168
6.4.1	Between-participant Probability Maps of MRI Ventilation Defects in Asthma .....	168
6.4.2	Contributions of Large versus Small Airways to Ventilation Heterogeneity in Asthma.....	171
6.4.3	Imaging Phenotypes of Asthma.....	174
<b>6.5</b>	<b>Significance and Impact</b> .....	176
<b>6.6</b>	<b>References</b> .....	177
<b>APPENDICES</b>	.....	182

## List of Tables

Table 1-1 GINA criteria for asthma severity classification .....	25
Table 1-2 GOLD criteria for COPD severity classification.....	26
Table 2-1 Participant demographics .....	81
Table 2-2 Multivariable models to predict VDP from oscillometry.....	86
Table 2-3 Advantages and limitations of oscillometry measurements .....	90
Table 4-1 Participant and MRI measurements at baseline and follow-up .....	113
Table 4-2 CT measurements .....	117
Table 4-3 Changes in forced expiratory volume in 1 second and ventilation defects .....	119
Table 4-4 Multivariable model to predict bronchodilator reversibility .....	121
Table 4-5 Baseline measurements for participants who completed longitudinal follow-up and lost to follow-up.....	128
Table 4-6 Participant listing of demographic characteristics and pulmonary function and MRI measurements at baseline and follow-up. ....	129
Table 4-7 Medication use at both visits .....	130
Table 4-8 Baseline measurement differences between reversible and not reversible participant groups.....	131
Table 4-9 Correlation coefficients for univariable relationships with post-bronchodilator $\Delta$ FEV <sub>1</sub> at follow-up .....	132
Table 5-1 Participant demographics, pulmonary function and imaging measurements.....	138
Table 5-2 Participants with missing subsegmental and sub-subsegmental daughter branches by whole-lung and lung lobe.....	140

Table 5-3 Segmental airway branch variants .....	144
Table 5-4 CT airway count and airway occlusion .....	145
Table 5-5 Multivariable models.....	147
Table 5-6 Total airway count by airway generation .....	158

## List of Figures

Figure 1-1 Prevalence of asthma in Canada .....	1
Figure 1-2 Hospitalizations for chronic diseases in Canada.....	2
Figure 1-3 Airway tree schematic and airway labels.....	7
Figure 1-4 Airway and parenchymal pathophysiology in asthma and COPD.....	11
Figure 1-5 Handheld spirometer and typical volume-time curve .....	14
Figure 1-6 Whole-body plethysmograph and typical volume-time curve .....	15
Figure 1-7 Handheld oscillometer and impedance-frequency curve .....	20
Figure 1-8 Inspiratory coronal CT with corresponding airway trees.....	29
Figure 1-9 $^1\text{H}$ MRI of the lungs .....	38
Figure 1-10 Hyperpolarized $^3\text{He}$ and $^{129}\text{Xe}$ MRI.....	42
Figure 1-11 Functional $^1\text{H}$ FDMRI.....	48
Figure 2-1 Pulmonary function test and MRI VDP measurements .....	82
Figure 2-2 Relationships between MRI ventilation heterogeneity and impedance measurements in representative subjects .....	84
Figure 2-3 Quantitative relationships between MRI VDP and impedance measurements.....	85
Figure 3-1 Spatially-matched MRI ventilation defects and CT airways for twins with asthma .....	99
Figure 3-2 Co-registered CT airway trees .....	100
Figure 4-1 Study flowchart of patient inclusion and exclusion .....	111

Figure 4-2 $^3\text{He}$ MRI ventilation in a representative participant with stable ventilation between baseline and follow-up.....	115
Figure 4-3 $^3\text{He}$ MRI ventilation in a representative participant with worse ventilation at 6-year follow-up.....	116
Figure 4-4 Group differences and univariable relationships for postBD FEV <sub>1</sub> reversibility	120
Figure 5-1 CT airway count by airway tree generation .....	139
Figure 5-2 Airway morphology and VDP by number of missing sub-subsegmental airways .....	141
Figure 5-3 MRI VDP by lung lobe .....	143
Figure 5-4 CT total airway count relationships .....	146
Figure 5-5 Airway count and wall area relationship with MRI ventilation defects and FEV <sub>1</sub> .....	148
Figure 6-1 Ventilation defect probability maps for mild-moderate and severe asthma .....	170
Figure 6-2 Small versus large airways image analysis pipeline .....	172
Figure 6-3 Relationships between FEV <sub>1</sub> and whole-lung, large and small airway VDP .....	173
Figure 6-4 MR and CT imaging-based clusters of asthma .....	175

## **List of Appendices**

Appendix A – What is the Minimal Clinically Important Difference for Helium-3 Magnetic Resonance Imaging Ventilation Defects?.....	182
Appendix B – Permission for Reproduction of Scientific Articles and Figures.....	188
Appendix C – Health Sciences Research Ethics Board Approval Notices.....	194
Appendix D – Curriculum Vitae.....	199

## List of Abbreviations

ACQ	Asthma Control Questionnaire
ANOVA	Analysis of Variance
AQLQ	Asthma Quality of Life Questionnaire
ATS	American Thoracic Society
A <sub>x</sub>	Reactance Area
BD	Bronchodilator
BMI	Body Mass Index
COPD	Chronic Obstructive Pulmonary Disease
CT	Computed Tomography
DL <sub>CO</sub>	Diffusing Capacity of the Lung for Carbon Monoxide
ERS	European Respiratory Society
ERV	Expiratory Reserve Volume
FDMRI	Fourier Decomposition Magnetic Resonance Imaging
FEV <sub>1</sub>	Forced Expiratory Volume in One Second
FOV	Field of View
FRC	Functional Residual Capacity
f <sub>res</sub>	Resonant Frequency
FVC	Forced Vital Capacity
GINA	Global Initiative for Asthma
GOLD	Global Initiative for Chronic Obstructive Lung Disease
HU	Hounsfield Unit
IC	Inspiratory Capacity
ICS	Inhaled Corticosteroid
IRV	Inspiratory Reserve Volume
LA	Lumen Area
LABA	Long-acting Beta-agonist
MCh	Methacholine Challenge
MCID	Minimal Clinically Important Difference
MRI	Magnetic Resonance Imaging
OCS	Oral Corticosteroids
PC <sub>20</sub>	Provocative Concentration Required to Decrease FEV <sub>1</sub> by 20%
PET	Positron Emission Tomography
R <sub>5</sub>	Resistance at 5 Hz
R <sub>5-19</sub>	Resistance at 5 Hz minus Resistance at 19 Hz
RA <sub>950</sub>	Relative Area of the Lung <-950 HU
R <sub>aw</sub>	Airways Resistance
RV	Residual Volume
SABA	Short-acting Beta-agonist
SD	Standard Deviation
SPECT	Single Photon Emission Computed Tomography
TAC	Total Airway Count
TE	Echo Time
TLC	Total Lung Capacity
TR	Repetition Time
UTE	Ultra-short Echo Time
VC	Vital Capacity

VD	Deadspace
VDP	Ventilation Defect Percent
VDV	Ventilation Defect Volume
VT	Tidal Volume
WA%	Wall Area Percent
WT	Wall thickness
X <sub>5</sub>	Reactance at 5 Hz

# CHAPTER 1

## 1 INTRODUCTION

*Asthma is a chronic airways disease; for over 2500 years, airway abnormalities in asthma have been understood to be distributed randomly throughout the lung. There is now evidence to suggest that asthma is regionally heterogeneous and not random. In this thesis, the structure and function of asthma are studied using pulmonary magnetic resonance imaging (MRI) and computed tomography (CT) to develop a deeper understanding of the asthmatic lung.*

### 1.1 Motivation and Overview

Asthma is a chronic respiratory disease that affects approximately 300 million people in the world.<sup>1</sup> Worldwide prevalence rates of asthma have been consistently increasing over the last 20 years and this estimate is expected to increase to 400 million by 2025.<sup>1</sup> In Canada, asthma prevalence has increased 67% since 2000 and currently affects 3.8 million people (10.8%).<sup>2</sup> As shown in **Figure 1-1**, asthma is the most common chronic respiratory disease in Canada, accounting for 78% of all cases.<sup>3</sup> Asthma affects people of all ages, although prevalence rates are highest for those younger than 20 years old and prevalence rates drop until age 65 and older, after which the rates begin to increase.<sup>4</sup>

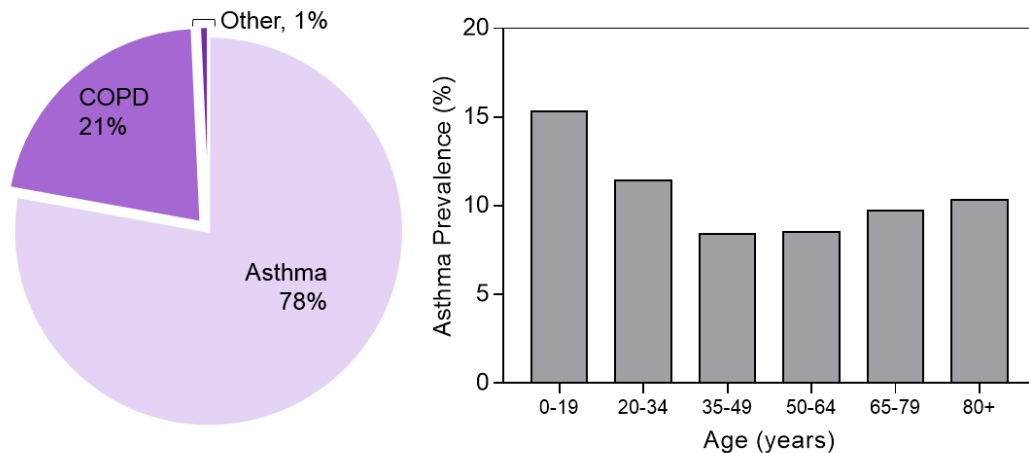


**Figure 1-1** Prevalence of asthma in Canada

Left: Proportion of all respiratory diseases. Data from the Public Health Agency of Canada, Life and Breath: Respiratory Disease in Canada (2007).<sup>3</sup>

Right: Asthma prevalence by age. Data from Public Health Agency of Canada, A Trend Analysis of the Health of Canadians from a Healthy Living and Chronic Disease Perspective (2016).<sup>4</sup>

Because of its high prevalence and chronicity, asthma poses a large burden on the economy and healthcare system. The number of patients hospitalized annually for asthma is greater than that of heart failure and diabetes and approximately 16% of these patients will experience a repeat hospitalization within one year of initial admission (**Figure 1-2**).<sup>5</sup> In contrast to other chronic diseases however, hospitalizations related to asthma are most common for patients younger than 20 years of age.<sup>5</sup> In Ontario alone, asthma care cost approximately \$1.8 billion in 2011 and is estimated to grow to \$97 billion in the next 20 years.<sup>6</sup>

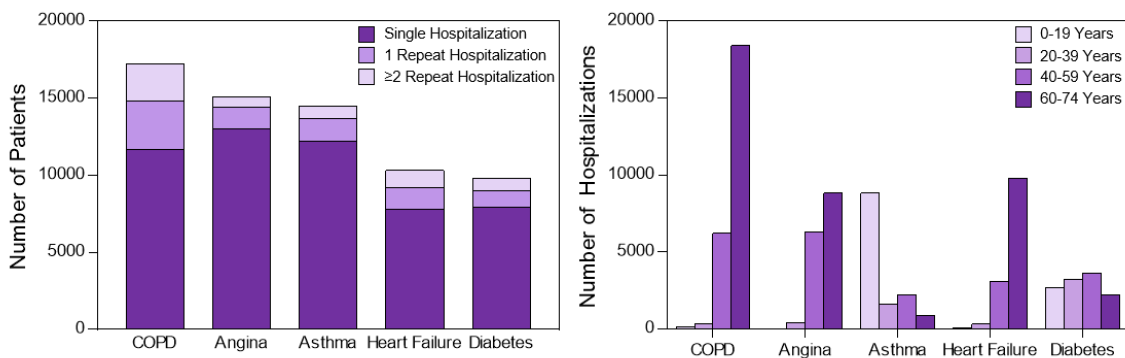


**Figure 1-2** Hospitalizations for chronic diseases in Canada

Left: Repeat hospitalizations after first admission. Right: Hospitalizations by age groups. Data from Canadian Institute for Health Information (CIHI) Health Indicators 2008.<sup>5</sup>

Notably from **Figure 1-1** and **Figure 1-2**, chronic obstructive pulmonary disease (COPD) is the second most common respiratory disease in Canada<sup>3</sup> and accounts for the greatest total number of hospitalizations, especially for people aged 60 and older.<sup>5</sup> COPD is even more costly than asthma, costing approximately \$3.9 billion in Ontario in 2011.<sup>6</sup> Moreover, in the next 20 years, the economic burden of COPD is expected to rise to \$311 billion.<sup>6</sup> Together, asthma and COPD affect over 5 million people in Canada<sup>2</sup> and 500 million people in the world,<sup>7</sup> and contribute to the third leading cause of death worldwide.<sup>8</sup> Although often recognized as distinct chronic respiratory diseases, asthma and COPD have also been regarded by some as heterogeneous and overlapping conditions. Despite the traditional idea that COPD is caused by tobacco smoke and largely preventable, asthma is also a risk factor for development of COPD independent of tobacco smoking.<sup>9,10</sup> Epidemiological studies suggest that 10% of patients with asthma will progressively

develop persistent airflow obstruction and COPD in their lifetime<sup>11,12</sup> and these patients utilize more healthcare resources<sup>13</sup> and experience more hospitalizations<sup>14</sup> than those with COPD alone. These alarming findings highlight the need for a deeper understanding of pathophysiology, treatment and management of chronic respiratory disease.

Since its first description over 2500 years ago,<sup>15</sup> asthma has been idealized as a diffuse airways disease with variable symptoms and airflow limitation. Substantive research has generated new knowledge that has driven a paradigm shift in the understanding of these concepts. The notion of ventilation heterogeneity in asthma was first introduced over 60 years ago using inert gas washout<sup>16,17</sup> and nuclear medicine imaging techniques.<sup>18,19</sup> Currently however, airflow limitation and its response to treatment or progression over time are monitored using the forced expiratory volume in one second (FEV<sub>1</sub>) – a simple and inexpensive spirometry measurement of airflow obstruction. FEV<sub>1</sub> provides only a global measurement of lung function that is unable to capture the regional heterogeneity of airway abnormalities that may be responsible for symptoms and disease worsening. Computational modeling studies have suggested that the regional heterogeneity in asthma can be described by randomly distributed airway abnormalities throughout the whole lung,<sup>20,21</sup> however these mechanisms have been challenging to measure *in vivo* using current clinical tools. As a result, asthma is still regarded as a random disease and treatments are geared towards all airways and not individualized. Moreover, inhaled therapies are not effective in all patients with asthma for various reasons such as poor regional drug distribution or drug resistance, but spirometry is not able to identify the reasons that cause lack of treatment efficacy.

Pulmonary functional magnetic resonance imaging (MRI) using inhaled noble gases provides a means to directly visualize and quantify regional gas distribution *in vivo*. Preliminary MRI findings in asthma demonstrate focal ventilation abnormalities that are spatially persistent over time.<sup>22,23</sup> These disruptive results contradict *in silico* results and suggest that asthmatic airway abnormalities may not be random, yet pulmonary imaging has played a limited role in asthma research and clinical care because the etiology of ventilation heterogeneity and its long-term pattern remains poorly understood. In contrast, imaging has played a large role in developing an understanding of the pulmonary structure-

function relationships in COPD owing to multiple large cohort studies that have incorporated imaging using x-ray computed tomography (CT)<sup>24-27</sup> and inhaled gas MRI.<sup>28</sup> Whereas COPD is characterized by persistent and progressive airflow limitation, overlap between asthma and COPD exists<sup>11,12,29</sup> and there is something to be learned from the imaging results in COPD. Pulmonary imaging has the potential to uncover the structural mechanisms and physiological relevance of regional ventilation heterogeneity in asthma and accordingly, this thesis focuses on the investigation of the pulmonary imaging structure-function relationships in asthma to develop a deeper understanding of the asthmatic lung. Armed with such an understanding, we have the potential to guide treatment decisions and regional therapies, predict disease worsening, and improve patient outcomes.

In this Chapter, the relevant background information is provided to motivate the original research presented in **Chapters 2-5**. A general overview of typical pulmonary structure and function is first provided (**1.2**), followed by the pathophysiology of asthma and COPD (**1.3**) and a brief description of current knowledge of asthma-COPD overlap. Clinical tools to measure pulmonary function are then described including the expected measurement deviations for asthma and COPD (**1.4**) as well as clinical assessments for characterizing each (**1.5**). The current state of imaging techniques is subsequently described in the context of imaging biomarkers to measure and understand pulmonary structure and function in asthma and COPD (**1.6**). Finally, the specific hypotheses and objectives of the work presented in this thesis are introduced (**1.7**).

## 1.2 Respiratory Structure and Function

The primary function of the respiratory system is gas exchange. The respiratory system comprises the nasal and oral cavities, pharynx, larynx, airways, lungs, chest wall and diaphragm; in this section, the structure and function of the airways and alveoli within the lungs are presented. The airways serve as conduits for the movement of air to the alveoli where gas exchange occurs across the alveolar-capillary interface. The overall function of the airways and alveoli is to deliver oxygen and remove carbon dioxide from the bloodstream by the process of ventilation.

### 1.2.1 Airways: Conducting and Respiratory Zones

Inhaled air first enters the respiratory system through the nasal or oral passages and then moves through the pharynx followed by the larynx, collectively known as the upper airways. Below the larynx, and as shown in **Figure 1-3**, the lower airways are grouped into the conducting and respiratory zones based on their structural and functional characteristics. The conducting zone acts as a conduit to carry air to the respiratory zone where gas exchange occurs. In general, each airway starting from the trachea continuously bifurcates into two daughter branches until the alveolar sacs at generation 23.

#### *Conducting Zone*

The conducting zone comprises the first 16 airway generations from the trachea (generation 0) to the terminal bronchioles (generation 16).<sup>30</sup> The trachea is a long tube lined with cartilage and muscle that connects the upper airways directly to the lungs and asymmetrically bifurcates into the left and right main bronchi to supply each lung. The main bronchi divide into the lobar bronchi that supply the five lung lobes – the upper, middle and lower lobes in the right lung and upper and lower lobes in the left lung. Lobar bronchi subsequently divide into segmental bronchi, which supply air to the 19 bronchopulmonary segments that are anatomically and functionally distinct. **Figure 1-3** shows the anatomical labels for the airways from the trachea to the segmental level. The airways are not individually named beyond the segmental bronchi. From here, the airways become narrower, shorter and more numerous as they branch to supply all areas of the lungs. The airways from the trachea up to the small bronchi at generation 11 are lined with

cartilage to maintain patency. Smooth muscle is interleaved with cartilage beginning in the lobar and segmental bronchi and is typically circumferentially wrapped around the airway walls. At the 12<sup>th</sup> generation, the airways become embedded in the lung parenchyma and are lined with smooth muscle only, relying on the elastic forces to tether the airways open.<sup>31</sup> The conducting zone ends at the terminal bronchioles, where the number of airways has increased more rapidly than the calibre diminished such that the total cross-sectional area exponentially increases. As the name suggests, the conducting zone conducts and humidifies air to the distal lung. These airways do not participate in gas exchange and are thus known as the anatomic deadspace – approximately 150 mL of air remains in the conducting airways during each breath.<sup>30</sup>

### *Respiratory Zone*

The respiratory zone begins at the respiratory bronchioles (generation 17) and includes the remaining distal airways up to the alveolar sacs (generation 23). Compared with the conducting zone, the airways in the respiratory zone change little in diameter as they branch. As shown in **Figure 1-3**, the respiratory bronchioles are the point where the airways begin to be lined with alveoli to facilitate gas exchange. There are increasingly more alveoli in the airway walls as the respiratory bronchioles branch and increase in airway generation. The alveolar ducts directly follow the respiratory bronchioles and have no airway walls but are completely lined with alveoli. The respiratory zone and entire airway tree terminate at the alveolar sacs, which are completely surrounded by alveoli to maximize surface area available for gas exchange. Although the distance from the first respiratory bronchiole to the most distal alveolus is only a few millimetres, the respiratory zone accounts for approximately 2.5-3.0 L of lung volume at rest<sup>30</sup> because of its millions of airways.



### 1.2.2 Alveoli: Site of Gas Exchange

The alveoli are the direct site of gas exchange at the terminal ends of the airway tree on the respiratory bronchioles, alveolar ducts and alveolar sacs. On average, there are 480 million alveoli in the human lung (range 274-790 million depending on height and lung volume of the individual),<sup>35</sup> each with a diameter of approximately 200  $\mu\text{m}$ .<sup>30</sup> Pulmonary capillaries wrap around each alveolus to create the blood-gas interface between the alveolar epithelium and capillary endothelium. Oxygen and carbon dioxide are exchanged across the blood-gas interface by passive diffusion according to Fick's law – the amount of gas that moves across the membrane is proportional to its area and inversely proportional to its thickness.<sup>30</sup> The blood-gas interface is extremely thin (0.2-0.3  $\mu\text{m}$ )<sup>36</sup> and, together with the large alveolar surface area (50-100  $\text{m}^2$ ),<sup>30</sup> this makes the lung well-suited for efficient exchange of oxygen and carbon dioxide.

### 1.2.3 Ventilation

The process by which air travels to and from the alveoli is known as ventilation. Pressure gradients between the external environment and the alveoli drive airflow from the upper airways to the alveoli by bulk flow.<sup>30</sup> Inspiration is actively initiated when the diaphragm and intercostal muscles contract, causing the alveolar pressure to decrease below that of the environment and air to flow into the lungs. Expiration occurs passively when the muscles relax and alveolar pressure increases beyond that of the environment, driving the gas out of the lungs. The lung and chest wall are elastic and will tend to return to their equilibrium positions via elastic recoil after being actively expanded during inspiration. Ventilation is expressed as the volume of air that is exchanged between the external environment and body as a function of time in **Equation 1-1**:

$$\text{Equation 1-1} \quad \text{Total ventilation [L/minute]} = \text{Breathing rate [1/min]} \cdot \text{VT [L]}$$

The total volume of air inhaled with each breath, known as tidal volume (VT), is 0.5 L on average. The ventilation rate for healthy adults is 12-20 breaths/minute – assuming a rate of 15 breaths per minute, the total ventilation would be 7.5 L/min. However, as described previously, not all inhaled gas reaches the alveoli and participates in gas exchange because of the 150 mL of deadspace (VD) in the conducting zone. Thus, **Equation 1-1** represents

total ventilation to the entire lung. It is important to determine the amount of fresh air participating in gas exchange, known as the alveolar ventilation as in **Equation 1-2**:

$$\text{Equation 1-2} \quad \text{Alveolar ventilation [L/min]} = \text{Breathing rate [1/min]} \cdot (\text{VT-VD}) [\text{L}]$$

In the same way as previously, assuming a breathing rate of 15 breaths per minute, the alveolar ventilation would be 5.25 L/min. Although 7.5 L of air enters the lungs every minute, only 5.25 L reaches the alveoli.

### 1.3 Pathophysiology of Asthma and COPD

Asthma and COPD are both obstructive lung diseases characterized by expiratory airflow limitation. Though once recognized as distinct disease entities, new understandings and definitions in the last 20 years acknowledge overlap of asthma and COPD and highlight similarities and differences between the two. Importantly, the airway and parenchymal abnormalities within an individual patient are regionally heterogeneous in both asthma and COPD. Here, the underlying pathophysiologies of the respiratory system in asthma and COPD are first presented as distinct entities, followed by a description of overlap between asthma and COPD.

#### 1.3.1 Asthma

Asthma is characterized by variable airflow limitation that results in intermittent symptoms of shortness of breath, wheeze, cough and chest tightness.<sup>37</sup> Pathophysiology of asthma is confined to the airways and derives from a complex interplay of structural and inflammatory changes that lead to airway wall thickening and edema, airway hyperresponsiveness, mucus hypersecretion and ultimately, luminal narrowing. This phenomenon is shown in **Figure 1-4** – compared with a healthy airway, the asthmatic airway wall is markedly thickened and encroaches on the airway lumen.<sup>38</sup> Structural airway changes include goblet cell hyperplasia,<sup>39</sup> subepithelial fibrosis,<sup>40</sup> angiogenesis,<sup>41</sup> submucosal gland hyperplasia and hypersecretion,<sup>42</sup> and smooth muscle hypertrophy and hyperplasia,<sup>43</sup> collectively known as airway remodeling. Airway remodeling and inflammation together lead to thickening of the airway wall and subsequent airflow obstruction via bronchoconstriction by smooth muscle and luminal obstruction by mucus

and debris. Airway inflammation in asthma involves the interactions of many immune cells, however is predominantly eosinophilic.<sup>38</sup> Eosinophil levels are increased in both the airway wall and lumen,<sup>44</sup> and contribute to wall thickening and luminal plugging, trigger bronchoconstriction and mucus secretion, and may also play a role in driving the remodeling process.<sup>45</sup> Bronchoconstriction occurs when the smooth muscle in the airway walls contracts and narrows the airway lumen; bronchoconstriction may be further exaggerated in airway hyperresponsiveness to various stimuli or irritants, such as allergens or exercise. Ultimately, narrowed and obstructed airway lumens increase the resistance to airflow in asthmatic airways and restricts airflow into and out of the lung. Although the lung parenchyma is spared in asthma, airway abnormalities affect the entire bronchial tree including large and small airways.<sup>46</sup> It is important to note that asthma is a heterogeneous condition and the relative contributions of each underlying component may be different between patients.

There is no one single cause of asthma, but rather a number of host and environmental factors are thought to contribute to its development.<sup>47</sup> The causes of asthma are beyond the scope of this thesis, however briefly, host factors may include genetic variants,<sup>48</sup> family history of asthma<sup>49</sup> or sex,<sup>50</sup> whereas environmental factors may include allergen sensitization,<sup>51</sup> respiratory viruses<sup>52</sup> and air pollution.<sup>53</sup> Onset of asthma commonly begins in childhood, but may occur at any age. Airflow obstruction in asthma is conventionally recognized as reversible with bronchodilator treatment, however may become persistent over time.<sup>29</sup>

### 1.3.2 COPD

In contrast to asthma, COPD is characterized by persistent airflow limitation and symptoms of shortness of breath, cough and sputum production.<sup>54</sup> COPD arises from chronic inflammation that, as shown in **Figure 1-4**, affects both the airways and lung parenchyma. Notably, inflammation in COPD consists primarily of neutrophils and macrophages.<sup>55</sup> The mechanisms of airflow obstruction in COPD are associated with airway remodeling which increases resistance to airflow,<sup>56,57</sup> and parenchymal damage that reduces the lung's elastic recoil force.<sup>58</sup> Structural airway remodeling in COPD occurs primarily in the small conducting airways<sup>59</sup> (generations 4-16 with diameter <2 mm) and causes bronchial wall

thickening by submucosal gland hypertrophy<sup>60</sup> and connective tissue deposition.<sup>42</sup> Inflammatory infiltrates also trigger mucus hypersecretion, which can lead to luminal plugging as is seen in the COPD-afflicted airway in **Figure 1-4**.

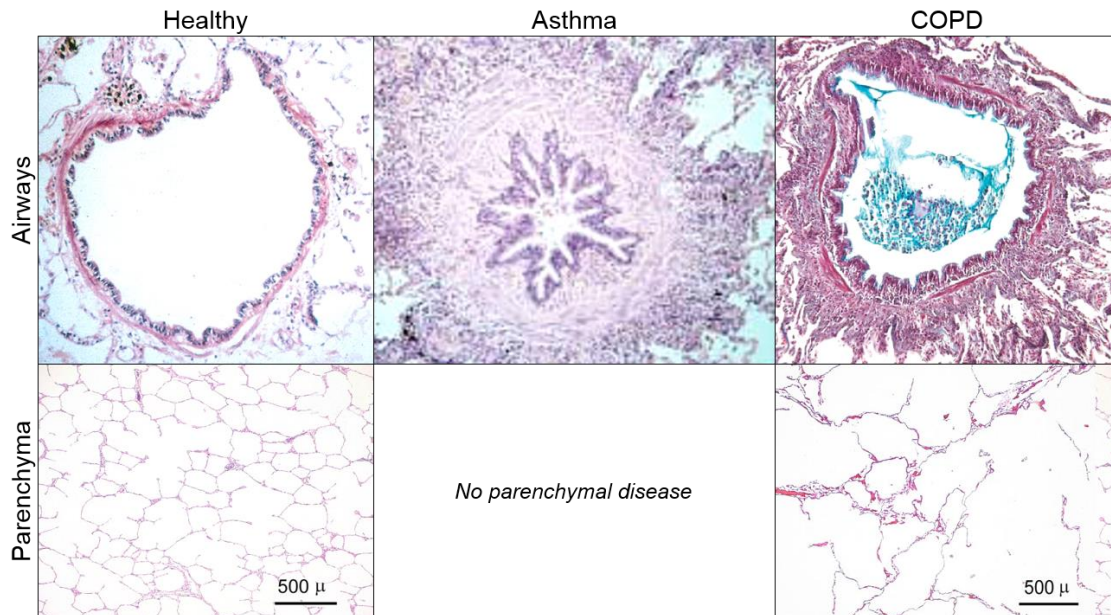


**Figure 1-4** Airway and parenchymal pathophysiology in asthma and COPD

Top: Compared with healthy airways where the wall is thin and lumen is patent, asthmatic airway shows thickened airway wall via increased smooth muscle mass, muscle constriction and inflammation. In COPD, airway walls are inflamed and thickened with inflammatory exudate of mucus and cells partially occluding the lumen. Healthy and COPD airway histology adapted from Hogg, *Lancet* (2004).<sup>59</sup> Asthma airway histology adapted from Saetta & Turato, *Eur Respir J* (2001).<sup>38</sup>

Bottom: Healthy lung parenchyma shows in-tact alveoli, whereas in COPD, alveolar walls are destroyed and airspaces are enlarged. There is no parenchymal disease in asthma. Parenchymal histology adapted from Woods et al, *Magn Reson Med* (2006).<sup>61</sup>

Permissions to reproduce all images are provided in Appendix A.

Emphysema refers to destruction of the lung parenchyma within the respiratory zone. This loss of tissue reduces the elasticity of the lung tissue such that the lungs are unable to completely empty and become hyperinflated. Emphysema also contributes to loss of tethering forces holding the small airways open and in severe cases, obliterates terminal airways causing reduced total airway cross-sectional area. Emphysema can be divided into different types based on where along the respiratory zone the damage occurs.<sup>62,63</sup> Most relevant to this thesis is centrilobular emphysema, which results from the destruction of the respiratory bronchioles while preserving the alveolar ducts and sacs and is the pattern most

commonly observed in COPD caused by cigarette smoking.<sup>59</sup> Regardless of the type of emphysematous lung damage, the airspaces become permanently enlarged, reducing the surface area of the lung available for gas exchange. Most patients with COPD will have some combination of both airways disease and emphysema, while few patients have extremes of one or the other.<sup>64</sup>

Tobacco cigarette smoking has been recognized as the main cause of and largest risk factor for COPD development, however it is well understood now that only approximately 20% of smokers will develop COPD and up to 30% of patients with COPD are life-long never-smokers.<sup>65,66</sup> A number of other host and environmental factors have now been identified,<sup>67</sup> including genetic variants,<sup>68,69</sup> suboptimal lung development in childhood,<sup>70</sup> occupational exposures,<sup>71</sup> air pollution,<sup>72</sup> childhood respiratory infections,<sup>73</sup> as well as life-long asthma.<sup>9</sup> Onset of COPD typically occurs after age 40,<sup>54</sup> however may occur earlier in life due to genetic conditions such as alpha-one antitrypsin deficiency.

### 1.3.3 Asthma-COPD Overlap

The two previous sections describe the extremes of asthma and COPD that are easily identified. Consistent with this idea, asthma and COPD are often treated as unique conditions with separate and distinct pathophysiologies.<sup>74</sup> Some argue though that the two are heterogeneous and overlapping conditions with common origins and clinical expressions. This idea was originally proposed in 1961 and is known as the Dutch hypothesis.<sup>75</sup> Although loosely defined, it is acknowledged now that 15-45% of patients with obstructive lung disease will exhibit some overlap of both asthma and COPD.<sup>76,77</sup> Despite the high prevalence, no prospective studies have been conducted to evaluate this group of patients; patients with overlapping features are often excluded from respective asthma and COPD trials<sup>78,79</sup> and very little is known to date about the pathogenesis of asthma-COPD overlap. The most recent consensus guidelines suggest key features of asthma-COPD overlap to be persistent airflow limitation in symptomatic patients over the age of 40, documented history of asthma in childhood or early adulthood and significant exposure to cigarette or biomass smoke,<sup>79</sup> however this definition is still not standardized. It is well-known now that asthma is a risk factor for COPD development<sup>9,10</sup> and that up to 10% of asthmatics will progressively develop irreversible airflow limitation or COPD.<sup>11,12</sup>

## 1.4 Clinical Tools to Measure Pulmonary Function

Objective measures of pulmonary function, collectively known as pulmonary function tests, play an important role in the diagnosis and monitoring of patients with asthma and COPD. Importantly, pulmonary function tests are simple, inexpensive and relatively quick to perform. There are a number of tools currently available, each serving a unique purpose to measure different aspects of lung disease. In this section, the clinical tools used to measure pulmonary function relevant to the original work presented in this thesis and their corresponding measurements are introduced. The measurement deviations in the context of asthma and COPD are also discussed.

### 1.4.1 Spirometry

Spirometry measures volume and airflow from the lungs as air is inhaled and exhaled as a function of time<sup>80</sup> and is the most commonly reported pulmonary function test. Spirometry has been extensively standardized by international societies and these criteria are widely implemented.<sup>80</sup> **Figure 1-5** shows an example of a handheld spirometer used to measure airflow at the mouth and a corresponding volume-time curve. The patient holds the spirometer while seated in the upright position with nose clips on and makes a tight seal around the mouthpiece with their lips. After 3-4 tidal breaths, the patient is instructed to inhale completely and then fully and forcefully exhale until their lungs are completely empty. Airflow is measured at the mouth over the entire maneuver to calculate exhaled volumes, as shown in **Figure 1-5**. The volume of air expired during the first second is the forced expiratory volume in one second ( $FEV_1$ ), whereas the volume of air expired over the entire exhalation maneuver is the forced vital capacity (FVC).  $FEV_1$  and FVC are measured in litres and are commonly expressed as a percentage of a predicted value using reference equations based on the patient's age, sex, height and ethnicity.<sup>81</sup> The ratio of  $FEV_1$  to FVC ( $FEV_1/FVC$ ) is also commonly reported.

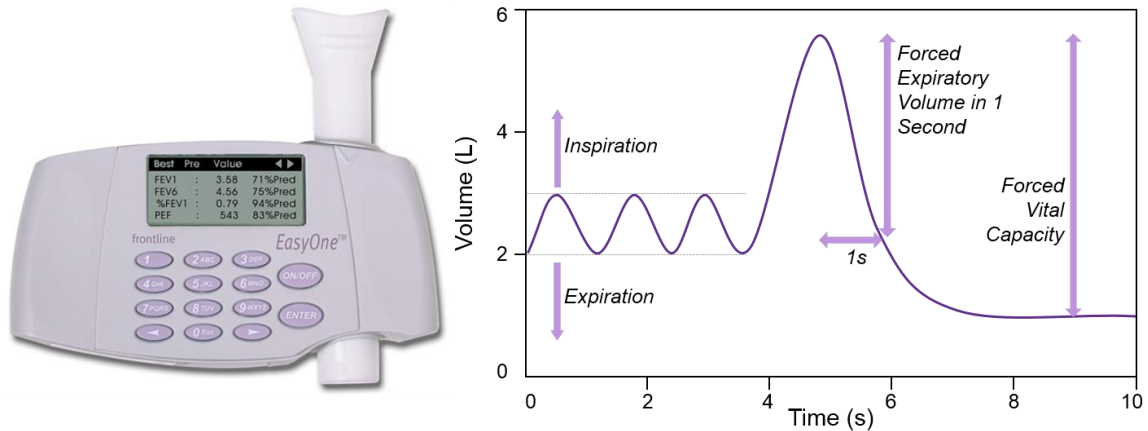


**Figure 1-5** Handheld spirometer and typical volume-time curve

Handheld spirometer records volume-time curve to measure the forced expiratory volume in one second (FEV<sub>1</sub>) and forced vital capacity (FVC).

Expiratory airflow becomes limited in both asthma and COPD due to luminal narrowing and airway obstruction. In asthma, FEV<sub>1</sub>, FVC and FEV<sub>1</sub>/FVC may be reduced because of airway smooth muscle thickening and constriction, inflammation or intraluminal plugging. In COPD, FEV<sub>1</sub>, FVC and FEV<sub>1</sub>/FVC may be reduced because of airway inflammation, intraluminal plugging or collapsed airways. In both cases, FVC may also be reduced because of premature airway closure during forced expiration. FEV<sub>1</sub> and FEV<sub>1</sub>/FVC are important diagnostic and classification markers of COPD and this is described in more detail in section 1.5.4.

## 1.4.2 Plethysmography

### *Lung Volumes and Capacities*

Plethysmography measures changes in volume in the body and accordingly, can be used to measure lung volumes and capacities. **Figure 1-6** shows a common whole-body plethysmograph and corresponding volume-time curve. The lung volumes and capacities measured are also shown on the volume-time curve. Tidal volume (VT) is the total volume of gas inhaled and exhaled during normal tidal breathing. Functional residual capacity (FRC) is the volume of gas in the lungs after exhalation during normal tidal breathing and residual volume (RV) is the volume of gas in the lungs after a complete exhalation. Inspiratory reserve volume (IRV) is the volume of gas maximally inhaled from the top of normal inhalation during normal tidal breathing, whereas expiratory reserve volume (ERV)

is the volume of gas maximally exhaled from the end of a normal exhalation during tidal breathing. Inspiratory capacity (IC) is the volume of gas inhaled from the end of a normal exhalation during tidal breathing and vital capacity (VC) is the volume of gas inhaled from end of a complete exhalation. Finally, total lung capacity (TLC) is the volume of gas in the lungs at end full inhalation. Although many of these volumes and capacities can also be measured using simple spirometry, plethysmography is required to determine FRC, RV and TLC.

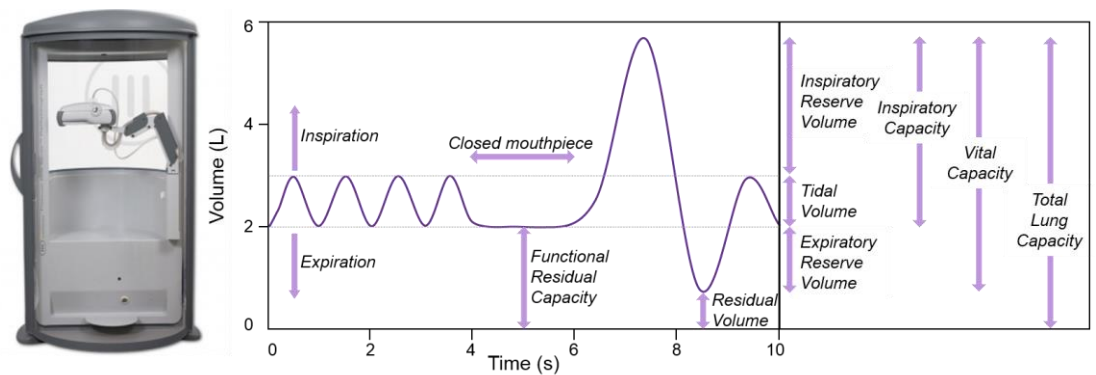


**Figure 1-6** Whole-body plethysmograph and typical volume-time curve  
Whole-body plethysmograph measures lung capacities and volumes.

During testing, patients are seated upright inside the plethysmograph with nose clips on and their hands on their cheeks; the chamber is sealed to create an airtight closed system with known interior volume. After 3-4 tidal breaths, the mouthpiece is closed by a shutter at end tidal expiration and the patient is instructed to perform a series of gentle pants for 2-3 seconds against the closed shutter. Once the shutter reopens and following a few tidal breaths, the patient is instructed to inhale fully and then passively exhale fully. During the panting maneuver, the lungs expand causing the pressure and volume inside the lungs to decrease and increase, respectively. In turn, the pressure within the sealed chamber increases and the volume within the box decreases to accommodate the new volume of the patient's lungs. The pressure within the box and at the mouth are measured and in this way, plethysmography directly measures FRC using Boyle's Law relating pressure and volume in an isothermal environment.<sup>82</sup> VT, IRV, ERV, IC and VC are determined from the spirometry-like maneuver performed after the shutter is re-opened. RV is then calculated as FRC minus ERV, and TLC as the sum of FRC and IC. It is important to note

that body plethysmography is just one option to measure FRC; nitrogen washout or helium dilution techniques may also be used and the lung volumes measured by each technique are standardized,<sup>82</sup> however the work in this thesis employs plethysmography. Similar to spirometry, lung volumes can be expressed as a percent of a predicted value based on the patient's age, sex, height and ethnicity.<sup>83</sup>

Gas trapping in both asthma and COPD causes RV, FRC and TLC to increase. The ratio of RV to TLC (RV/TLC) is often expressed as an indication for gas trapping. In asthma, gas trapping may be due to increased smooth muscle and inflammation that cause narrowing of the airway lumen, particularly in the small airways. In COPD, small airways inflammation may cause gas trapping, and loss of elastic recoil from emphysematous tissue destruction may also contribute to increased RV, FRC and TLC.

#### *Airways Resistance*

In general, resistance is defined as the ratio of driving pressure to flow; thus, in the context the lungs, airways resistance ( $R_{aw}$ ) is the ratio of the difference between alveolar and mouth pressure and the flow rate measured at the mouth as shown in **Equation 1-3**:

$$\mathbf{Equation\ 1-3} \quad R_{aw} \text{ [cmH}_2\text{O}\cdot\text{s/L]} = \frac{\text{Alveolar pressure - Mouth pressure [cmH}_2\text{O]}}{\text{Flow rate } (\dot{V}) \text{ [L/s]}}$$

Similar to the panting maneuver described previously for the measurement of lung volumes, a panting maneuver is also performed to measure airways resistance, this time with additional open-shutter panting prior to closed-shutter panting. Although flow rate may be directly measured at the mouth, alveolar pressure is not directly available during the panting maneuver. Instead, the pressure differential is inferred from the box pressure and the inverse slope of the pressure-flow plot is known as specific airways resistance ( $sR_{aw}$ ), a corrected index for airways resistance regardless of lung volume.

As shown in **Equation 1-4**,  $R_{aw}$  is then derived from  $sR_{aw}$  normalized to FRC:

$$\text{Equation 1-4} \quad R_{aw} [\text{cmH}_2\text{O}\cdot\text{s/L}] = \frac{sR_{aw} [\text{cmH}_2\text{O}\cdot\text{s}]}{\text{FRC [L]}}$$

Predictive reference equations exist for  $R_{aw}$  based on patient age, sex, height and ethnicity.<sup>84,85</sup> Resistance of the airways is directly related to the luminal diameter of the branches.  $R_{aw}$  is especially increased in asthma due to increased smooth muscle and inflammation that cause narrowing of the airway lumen. Parenchymal pathologies in COPD typically do not influence  $R_{aw}$ , however small airways inflammation in COPD can lead to narrowing of the airway lumen and increase  $R_{aw}$ .

### 1.4.3 Diffusing Capacity of the Lung

The efficiency of gas exchange within the lungs can be determined using the single-breath carbon monoxide uptake technique<sup>86</sup> to measure the diffusing capacity of the lung for carbon monoxide ( $DL_{CO}$ ), which provides an indirect measure of oxygen diffusion across the alveolar membrane. Carbon monoxide is used instead of oxygen because its uptake in the pulmonary capillaries is diffusion-limited only – oxygen, on the other hand, is limited by diffusion and perfusion. Because of its binding affinity for hemoglobin that is approximately 210-times greater than that of oxygen and the use of an extremely low concentration of carbon monoxide that does not cause complete saturation of hemoglobin, the pressure of carbon monoxide in the pulmonary capillary remains constant over time.<sup>87</sup>

Patients are again seated upright with nose clips on; after four tidal breaths, patients are instructed to exhale completely to RV, then to rapidly inhale a test gas mixture to TLC and hold their breath at TLC for 8-10 seconds before exhalation. The test gas contains a mixture of 0.3% carbon monoxide, 21% oxygen, a balance of nitrogen and a tracer gas. During the breath-hold at TLC, the carbon monoxide diffuses across the alveolar-capillary membrane into the blood. The first 150 mL of exhaled gas is discarded to account for anatomical dead space within the lungs, after which a discrete sample of alveolar gas is analyzed by comparing the concentrations of carbon monoxide in the exhaled sample to that of the inhaled gas.  $DL_{CO}$  then is the conductance (flow normalized to pressure) of carbon monoxide from the inspired test gas to the bloodstream and is measured in units of

mL·min<sup>-1</sup>·mmHg. DL<sub>CO</sub> may also be expressed as a percent of a predicted value based on the patient's age, sex, height and ethnicity.<sup>88</sup> Notably, the tracer gas also serves to measure the initial alveolar carbon monoxide concentration and the alveolar volume from which the carbon monoxide uptake is occurring. The tracer gas must be one that is insoluble, biologically inert and has a diffusivity similar to that of carbon monoxide so as not to interfere with the measurement of carbon monoxide concentration; typical tracer gases are neon (0.5%) or helium (10%).

The capacity of the lung to exchange gas across the alveolar-capillary interface, and thus the DL<sub>CO</sub> measurement, is dependent on a number of structural and functional factors that reflect a variety of physiological conditions. For the purposes of this thesis, DL<sub>CO</sub> is measured to determine the effective alveolar-capillary surface area available for gas exchange within the lung. In patients with COPD, DL<sub>CO</sub> may be reduced due to decreased surface area of the alveolar-capillary membrane caused by emphysematous tissue destruction. DL<sub>CO</sub> is not commonly measured in asthma because of the nature of its pathophysiology that does not impact the pulmonary parenchyma.

#### 1.4.4 Oscillometry

First developed over 60 years ago,<sup>89,90</sup> oscillometry is an emerging pulmonary function test that measures lung biomechanics. Oscillometry views the lungs as a linear dynamic system, which allows the lungs to be considered from a systems analysis perspective (inputs converted to outputs) and treated as an electrical circuit. Some background information on the mechanical properties of the lungs is first required to understand the basis of oscillometry.

As described previously in section **1.2.3**, the respiratory system functions through the mechanical expansion and contraction of the thoracic cavity, which alters the pressure inside the lungs and results in airflow. The key to oscillometry is respiratory system impedance ( $Z_{rs}$ ) – the quantity that directly relates pressure and airflow in the lungs and reflects how difficult it is for air to flow through the airways.<sup>91</sup> By applying airflow at a known rate (input) and measuring pressure over time (output) at the mouth, impedance can be calculated. All pulmonary function measurements previously described in this thesis

are viewed in the time domain (ie, lung volume over time). When considering the lungs as a linear dynamic system,<sup>91</sup> in the time domain, inputs are converted to outputs by convolution, which is a computationally expensive and challenging task. By taking the Fourier transform of the pressure and flow signals to convert to the frequency domain, the relationship between pressure (P) and airflow ( $\dot{V}$ ) is reduced to multiplication and the impedance calculation becomes computationally simpler as shown in **Equation 1-5**:

$$\text{Equation 1-5} \quad P(f) [\text{cmH}_2\text{O}] = Z_{rs}(f) [\text{cmH}_2\text{O}\cdot\text{s/L}] \cdot \dot{V}(f) [\text{L/s}]$$

Airflows are applied at the mouth using small-amplitude pressure oscillations that contain multiple frequencies at once to determine impedance over a frequency range. Pressure is measured at the mouth for each of the frequencies in the signal, and the impedance is subsequently calculated over the same frequency range.

Again in contrast to the other pulmonary function tests described previously, which measure only the magnitude of pressure, flow and volume, impedance describes the relationship for both magnitude and phase between pressure and flow and is therefore a complex number. As shown in **Equation 1-6**, respiratory system resistance ( $R_{rs}$ ) is the in-phase or real component of impedance, whereas reactance ( $X_{rs}$ ) is the out-of-phase or imaginary component:

$$\text{Equation 1-6} \quad Z_{rs}(f) [\text{cmH}_2\text{O}\cdot\text{s/L}] = R_{rs}(f) + iX_{rs}(f)$$

Resistance and reactance are the intrinsic properties of the respiratory system that determine how it responds to input, or airflow in this case. Taken together, oscillometry measures respiratory system resistance and reactance over a frequency range. A common handheld oscillometer and corresponding impedance-frequency curve are shown in **Figure 1-7**. While seated in the upright position with nose clips on and hands on their cheeks, the patient performs normal tidal breathing into the mouthpiece on the handheld device for 16 seconds as the pressure oscillations are superimposed over the normal breathing pattern. The patient is instructed to use their hands to support the cheeks and upper airways to avoid shunting of the applied oscillations in the upper airways and force the applied oscillations

to travel to the lungs. The applied oscillations typically begin at 4-5 Hz to avoid overlap with the patient's normal breathing pattern, which is typically 0.5 Hz or less.<sup>91</sup>

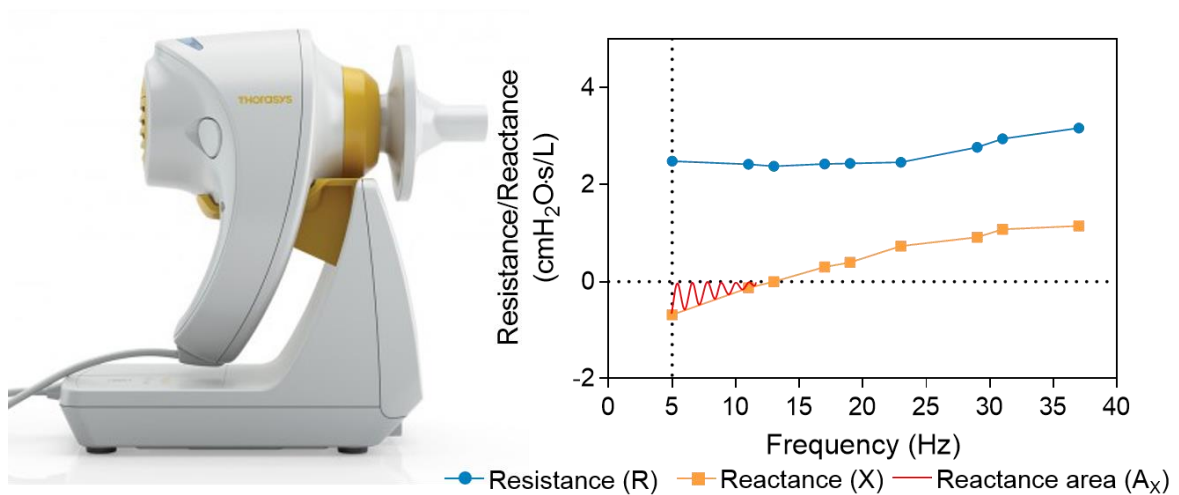


**Figure 1-7** Handheld oscillometer and impedance-frequency curve

Handheld oscillometer measures respiratory system impedance, including resistance and reactance, over 5-37 Hz frequency range.

The impedance-frequency curve in **Figure 1-7** is that of a healthy person without respiratory disease. Resistance is always positive and normally not frequency dependent. Analogous to airways resistance measured by plethysmography described previously, oscillometry-measured resistance is related to airway lumen calibre. Reactance always begins negative at low frequencies, and is frequency-dependent such that it crosses zero at some frequency and becomes positive. Reactance is related to elastic properties of the lung, but the exact property measured depends on the frequency at which the measurement is made; at low frequencies, reactance is negative and reflects tissue elastance, whereas at higher frequencies, reactance is positive and reflects tissue inertance. The point at which reactance equals zero is the resonant frequency ( $f_{res}$ ) – here, elastic and inertive forces are equal and overall impedance is completely resistive. The area under the reactance curve may also be integrated up to  $f_{res}$  and this value is known as the reactance area ( $A_X$ ).<sup>92</sup>

In asthma and COPD, oscillometry-derived resistance may increase as a result of airway obstruction for the same reasons as outlined previously for plethysmography-derived resistance. The resistance-frequency curve may be elevated at low frequencies causing it to become frequency-dependent (scooped shape), with or without additional increases

across all frequencies (upwards shift). The frequency-dependent nature of resistance reflects heterogeneous airway obstruction and is often attributed to increased resistance in the small airways; this enhanced sensitivity to small airways disease<sup>93</sup> demonstrates the major advantage of oscillometry over plethysmography-derived airways resistance and other pulmonary function tests. The frequency-dependence of resistance is quantified as the resistance at 5 Hz minus the resistance at 19 Hz ( $R_{5-19}$ ). Reactance may also be increased as a result of inflammation in the small airways that causes reduced elasticity of the lungs in both asthma and COPD. In emphysematous COPD, reactance may increase because of loss of elastic recoil of the parenchyma. In all cases, the reactance curve will typically become more negative at low frequencies (downward shift) and  $f_{res}$  may also increase, both of which subsequently cause  $A_x$  to increase.

Oscillometry has recently gained clinical traction because, compared with the pulmonary function tests described previously, it requires minimal coaching and patient effort. Reference values exist for oscillometry measurements<sup>94</sup> but the current equations were developed based only on Caucasian adults in European countries. The Global Health Initiative is currently developing global reference values for oscillometry which will be similar to that of spirometry, plethysmography and  $DL_{CO}$ . There are multiple commercially available oscillometers, however in contrast with spirometry and plethysmography, oscillometry techniques and devices are not yet well standardized. There exists many variations in the functions used to generate the oscillations as well as the frequency ranges used. Oscillometry is an overarching term to include the forced oscillation technique and impulse oscillometry, which differ by the way the oscillations are generated. The work in this thesis employs the forced oscillation technique over a frequency range of 5-37 Hz. It is important to note that here, ‘forced’ describes the forcing function used to generate the oscillations, not a forced exhalation maneuver as is performed during spirometry.

## **1.5 Clinical Assessments to Characterize Asthma and COPD**

The tools outlined above, particularly spirometry, can be used to assess features of asthma and COPD to provide characterization towards certain phenotypes and classify disease severity. Validated questionnaires have also been developed to sensitively probe patient-reported outcomes.

### 1.5.1 Bronchodilator Reversibility

Reversible airflow limitation is a key feature of asthma. The goal of reversibility testing is to determine whether a patient's lung function improves with bronchodilator treatment, which is assessed using spirometry before and after bronchodilator administration. The most common regimen to evaluate bronchodilator reversibility is using a short-acting beta-agonist (SABA) such as salbutamol. Following baseline spirometry, four separate 100 µg doses of aerosolized salbutamol are administered and spirometry is repeated after 15 minutes. Salbutamol acts directly on smooth muscle receptors in the airway wall to relieve muscle constriction and dilate the airway lumen. A total dose of 400 µg and wait time of 15 minutes are used and standardized to ensure that the response is high enough on the salbutamol dose-response curve.<sup>95</sup> Reversibility is assessed by evaluating the difference between pre- and post-bronchodilator FEV<sub>1</sub> or FVC in absolute volume and as a percent of baseline measurements. Clinically relevant bronchodilator response is defined as an improvement in FEV<sub>1</sub> or FVC of 200 mL and 12% from baseline.<sup>95</sup> These thresholds were chosen to be confidently greater than the error in spirometry measurements; changes less than 150 mL or 8% are likely to be within the normal measurement variability.<sup>96,97</sup> Patients are also instructed to withhold their prescribed bronchodilator medications prior to reversibility testing.

Spirometry is the test of choice for confirming bronchodilator reversibility, although changes in plethysmography- and oscillometry-derived metrics also typically respond to bronchodilator. Airflow limitation in COPD is generally regarded as incompletely reversible; pulmonary function tests in COPD are typically performed post-bronchodilator only.

### 1.5.2 Airway Hyperresponsiveness

Airway hyperresponsiveness is another common feature of asthma, and is defined as increased sensitivity of the airways to inhaled stimuli.<sup>98</sup> Methacholine challenge testing is the most commonly performed method for the assessment of airway hyperresponsiveness in patients and standardized guidelines are published.<sup>99</sup> Methacholine is nebulized and inhaled by the patient, after which it directly stimulates airway smooth muscle to contract

and cause bronchoconstriction and a decrease in FEV<sub>1</sub>; increasing methacholine doses are inhaled until FEV<sub>1</sub> decreases by 20%. In this way, methacholine challenge testing creates an ideal, controlled environment to simulate an asthma attack. Baseline spirometry is first performed to determine pre-challenge FEV<sub>1</sub> and the target decrease in FEV<sub>1</sub>. Saline diluent or a methacholine dose of 0.03 mg/mL is then administered, and after nebulization, spirometry is repeated. If FEV<sub>1</sub> has not decreased by 20%, the next highest concentration of methacholine is administered and this process is repeated until FEV<sub>1</sub> has decreased at least 20% or the 16 mg/mL maximum methacholine dose has been administered. Similar to reversibility testing, patients are again instructed to withhold their prescribed asthma medications prior to completing methacholine challenge testing according to guidelines.<sup>99</sup>

The provocative concentration required to decrease FEV<sub>1</sub> by 20% (PC<sub>20</sub>) is the primary outcome measurement from methacholine challenge testing and is estimated according to **Equation 1-7**:

$$\text{Equation 1-7 } PC_{20} \text{ [mg/mL]} = \text{antilog} \left[ \log C_1 + \frac{(\log C_2 - \log C_1)(20 - R_1)}{R_2 - R_1} \right]$$

C and R are the methacholine concentration and percent decrease in FEV<sub>1</sub> from baseline, respectively, and the 1 and 2 subscripts represent the second-to-last and last measurements, respectively. PC<sub>20</sub> greater than 16 mg/mL indicates normal airway hyperresponsiveness, whereas PC<sub>20</sub> less than 4 mg/mL indicates abnormal airway hyperresponsiveness. PC<sub>20</sub> between 4-16 mg/mL is recognized as borderline hyperresponsiveness and is more challenging to interpret.<sup>99</sup>

Although methacholine challenge testing for airway hyperresponsiveness is sensitive for asthma, it is not specific.<sup>99</sup> This means that the lack of airway hyperresponsiveness (PC<sub>20</sub> > 16 mg/mL) can help to exclude asthma, but the presence of airway hyperresponsiveness (PC<sub>20</sub> < 4 mg/mL) is not always perfectly indicative of asthma.<sup>37</sup>

### 1.5.3 Questionnaires

Questionnaires are important clinical tools to evaluate a patient's perception of their respiratory disease. The asthma control questionnaire (ACQ)<sup>100</sup> evaluates asthma control during the previous week using five symptom-related questions (night awakening, symptoms on awakening, activity limitation, shortness of breath and wheezing), as well as questions for daily bronchodilator use and pre-bronchodilator FEV<sub>1</sub>. Each question is scored on a scale of 0-6 and the total score is calculated as a mean the individual question scores; all seven questions may be used for the ACQ-7, or abbreviated versions<sup>101</sup> may be used to omit pre-bronchodilator FEV<sub>1</sub> (ACQ-6) or both pre-bronchodilator FEV<sub>1</sub> and daily bronchodilator use (ACQ-5). The primary goal of asthma care is to achieve and maintain asthma control, which refers to the extent to which a patient's asthma symptoms can be reduced or eliminated by treatment.<sup>102</sup> Accordingly, the ACQ is widely used as a clinical trial endpoint.<sup>103,104</sup> Total scores range from 0 to 6, where 0 reflects total control and 6 reflects severely uncontrolled. The minimal clinically important difference for ACQ is 0.5.<sup>101</sup>

The asthma quality of life questionnaire (AQLQ),<sup>105</sup> as the name suggests, probes asthma-related quality-of-life during the previous two weeks. The AQLQ consists of 32 questions related to symptoms, activity limitation, emotional function and exposure to environmental stimuli. Each question is scored on Likert scale from 1 for totally limited/limited a very great deal/limited all of the time/severely limited to 7 for limited none of the time/not at all limited, depending on the question. Total AQLQ score is calculated as the mean of all 32 question; total scores close to 1 represent poor asthma quality-of-life and scores close 7 represent very good quality-of-life. AQLQ score is also commonly used as a clinical trial endpoint<sup>104</sup> and its minimal clinically important difference is 0.5.<sup>106</sup>

It is important to acknowledge that there are a number of variations of questionnaires designed to probe asthma control and quality-of-life – ACQ and AQLQ are employed in this thesis, although they are not the only options. It is also worth acknowledging the St. George's Respiratory Questionnaire (SGRQ),<sup>107</sup> which measures the impact of respiratory disease on an individual's overall health, daily activities and perceived well-being, is mostly commonly used for patients with COPD.

## 1.5.4 Disease Severity

### *Asthma*

Asthma severity is determined by the type and amount of treatment required to control symptoms and prevent exacerbations. Asthma therapies can be grouped into three main types: controllers, relievers and add-ons.<sup>37</sup> Controller medications are used to continuously reduce airway inflammation, control symptoms and reduce exacerbations. Controller therapy is typically in the form of inhaled corticosteroids (ICS), with or without long-acting beta-agonist (LABA) combination. As shown in **Table 1-1**, it is the daily dose of controller ICS which forms the basis of asthma severity classification. The Global Initiative for Asthma (GINA) defines ‘treatment steps’ based on the required daily dose of ICS (low, medium, high), from as-needed, reliever-only use for very mild asthma at treatment step 1 to daily high dose for very severe asthma at treatment step 5.<sup>37</sup> Reliever therapies are provided to all patients for as-needed acute symptom relief, and are now also in the form of ICS-LABA combination. Add-on therapies are considered when symptoms and exacerbations persist despite optimized treatment with ICS-LABA, and take many forms from bronchodilator to anti-inflammatory actions.

**Table 1-1** GINA criteria for asthma severity classification

		ICS/ICS-LABA Use
GINA Step 1	Very Mild	As needed
GINA Step 2	Mild	Daily low dose ICS
GINA Step 3	Moderate	Daily low dose ICS-LABA
GINA Step 4	Severe	Daily medium dose ICS-LABA
GINA Step 5	Very Severe	Daily high dose ICS-LABA

Adapted from GINA Global Strategy for Asthma Management and Prevention 2019 report<sup>37</sup>

### *COPD*

COPD severity criteria are comparatively more straightforward. Spirometry thresholds are used to both diagnose and stratify COPD severity according to the Global Initiative for Chronic Obstructive Lung Disease (GOLD) guidelines.<sup>54</sup> Post-bronchodilator FEV<sub>1</sub>/FVC less than 0.70 is the diagnostic criteria for COPD, and disease severity is subsequently stratified from mild (GOLD I) to very severe (GOLD IV) based on FEV<sub>1</sub> percent predicted (%<sub>pred</sub>). **Table 1-2** shows the FEV<sub>1</sub> thresholds that define each level of COPD severity.

**Table 1-2** GOLD criteria for COPD severity classification

---

*FEV<sub>1</sub>/FVC < 0.70*

---

GOLD I	Mild	$FEV_1 \geq 80\%_{\text{pred}}$
GOLD II	Moderate	$50\% \leq FEV_1 < 80\%_{\text{pred}}$
GOLD III	Severe	$30\% \leq FEV_1 < 50\%_{\text{pred}}$
GOLD IV	Very Severe	$FEV_1 < 30\%_{\text{pred}}$

---

Adapted from GOLD Global Strategy for the Diagnosis, Management, and Prevention of Chronic Obstructive Pulmonary Disease 2019 report.<sup>54</sup>

## 1.6 Imaging of Pulmonary Structure and Function

The pulmonary function tests described previously in section 1.4 provide rapid, inexpensive measurements that are well understood. Unfortunately, these measurements cannot inform on regional disease heterogeneity,<sup>108,109</sup> are weakly predictive of early disease and disease progression,<sup>24,110</sup> and are insensitive to the small airways.<sup>111,112</sup> Pulmonary imaging, on the other hand, provides regional structural and functional measurements of lung disease that are sensitive to the entire bronchial tree. With respect to the lungs and this thesis, planar x-ray, x-ray computed tomography (CT), nuclear medicine and magnetic resonance imaging (MRI) are reviewed here.

### 1.6.1 Planar X-ray

Planar x-ray imaging, as the name suggests, uses x-ray radiation to generate two-dimensional images of the body. Since its advent in 1895 by Wilhelm Röntgen, planar x-ray has become the most common method to image the chest and lung disease because of its low cost, low radiation dose, short acquisition window and ease of access. Planar x-ray images (also known as radiographs) are produced by positioning the patient between an x-ray source and detector that are directly opposite each other. While the patient holds their breath, x-rays are passed through the thorax and are differentially attenuated by different anatomical structures. The detector measures the relative attenuation of the x-rays after they exit the body and generates a two-dimensional projection image that is a superposition of all anatomy along the x-ray path. Image contrast is thus generated by the relative attenuation of x-rays across the body; high-attenuating structures, such as bone, appear bright on an x-ray image, whereas low-attenuating structures, such as lung parenchyma, appear dark. Images of the thorax are typically acquired while the patient stands upright for anterior-posterior or lateral projections, or both. The radiation dose associated with

planar chest x-rays is on the order of 0.01 mSv,<sup>113</sup> or 0.6% that of the average annual background radiation in Toronto, Canada.<sup>114</sup>

Lung volume abnormalities on planar x-ray are commonly assessed by the shape of the lungs. Hyperinflation is detected by elongated lung volumes and flattening of the diaphragm in asthma<sup>115-117</sup> and COPD,<sup>118</sup> especially in severe emphysema.<sup>119</sup> Bronchial wall thickening or plugging may also be evident on chest x-ray in patients with asthma.<sup>115,117</sup> Lung abnormalities typically need to be quite severe in order to be detectable by chest x-ray; in fact, chest x-ray imaging in the clinical care of asthma and COPD often serves to rule out alternative causes of respiratory-related symptoms such as shortness of breath. Moreover, the two-dimensional projection nature of planar x-ray images has motivated the development of three-dimensional x-ray approaches to capture depth and tomographic information.

## 1.6.2 X-ray Computed Tomography

X-ray computed tomography (CT) imaging also leverages the body's x-ray attenuating properties, however it does so in a three-dimensional manner. CT was first developed in the 1970s and continuous improvements in acquisition speeds and image quality since have made CT the modality of choice for the evaluation of lung disease. Multi-detector technology now allows for sub-millimetre isotropic imaging of the entire lung volume in a single breath-hold, permitting multi-planar and three-dimensional reconstructions.

### 1.6.2.1 Conventional CT

CT images are produced using an x-ray source and detector array that are positioned opposite one another and rotate around the patient acquiring multiple x-ray projection images at different angles. As the x-ray source and detector rotate, the scanner bed with the patient laying supine passes through the imaging components of the system to acquire axial images of the entire thorax as the patient holds their breath. The projections are then reconstructed into a three-dimensional volumetric image, typically using filtered back projection or iterative reconstruction techniques.<sup>120</sup>

Each voxel in the reconstructed image is represented by a measurement of the tissue density relative to that of water, known as Hounsfield units (HU)<sup>121</sup> according to **Equation 1-8**:

$$\text{Equation 1-8} \quad \text{Hounsfield unit [HU]} = \left( \frac{\mu_{\text{tissue}} - \mu_{\text{water}}}{\mu_{\text{water}}} \right) \cdot 1000$$

where  $\mu$  represents the linear attenuation coefficient for the tissue of interest or water. The attenuation of water is normalized to 0 HU, and it follows that the HU of air is -1000, low-attenuating structures such as the lung parenchyma have HU near -800, and high-attenuating structures such as bone have HU near +1000. The typical radiation dose associated with clinical chest CT protocols is much greater than that of planar x-ray at 7-8 mSv.<sup>122</sup> Low-dose research CT protocols have been established with doses on the order of 1.6 mSv,<sup>24,25,27</sup> or roughly equivalent to the average annual background radiation in Toronto, Canada.<sup>114</sup> Advanced image reconstruction methods have more recently been developed to achieve ultra-low-doses on the order of 0.1-0.4 mSv,<sup>123,124</sup> however such techniques have not yet been widely implemented clinically.<sup>125</sup> CT images of the lungs may be acquired after inspiratory or expiratory maneuvers, depending on the evaluation of interest.

In patients with asthma and COPD, CT is commonly used to assess structure of the airways, lung parenchyma and pulmonary vessels; this thesis primarily focuses on airway and parenchymal measurements. **Figure 1-8** shows inspiratory CT images in the coronal plane for comparison between a healthy control and patients with asthma and COPD. Airway findings on CT include bronchial wall thickening, bronchial dilation, luminal narrowing, bronchiectasis, mucous plugging, atelectasis or mosaic lung attenuation, whereas parenchymal abnormalities are reflected in focal regions of low attenuation. In **Figure 1-8**, airway wall thickening is evident in the asthmatic patient, and a narrow window highlights regions of low attenuation in the patient with COPD. CT evaluation of lung disease has been revolutionized by the application of computational analysis to generate quantitative CT imaging biomarkers, collectively known as quantitative CT.<sup>126</sup> A number of software platforms are commercially available for quantitative CT analysis – Pulmonary

Workstation 2.0, Apollo and VIDAVision are examples from VIDA Diagnostics Inc. (Coralville, IA, USA) which have been approved for clinical use.

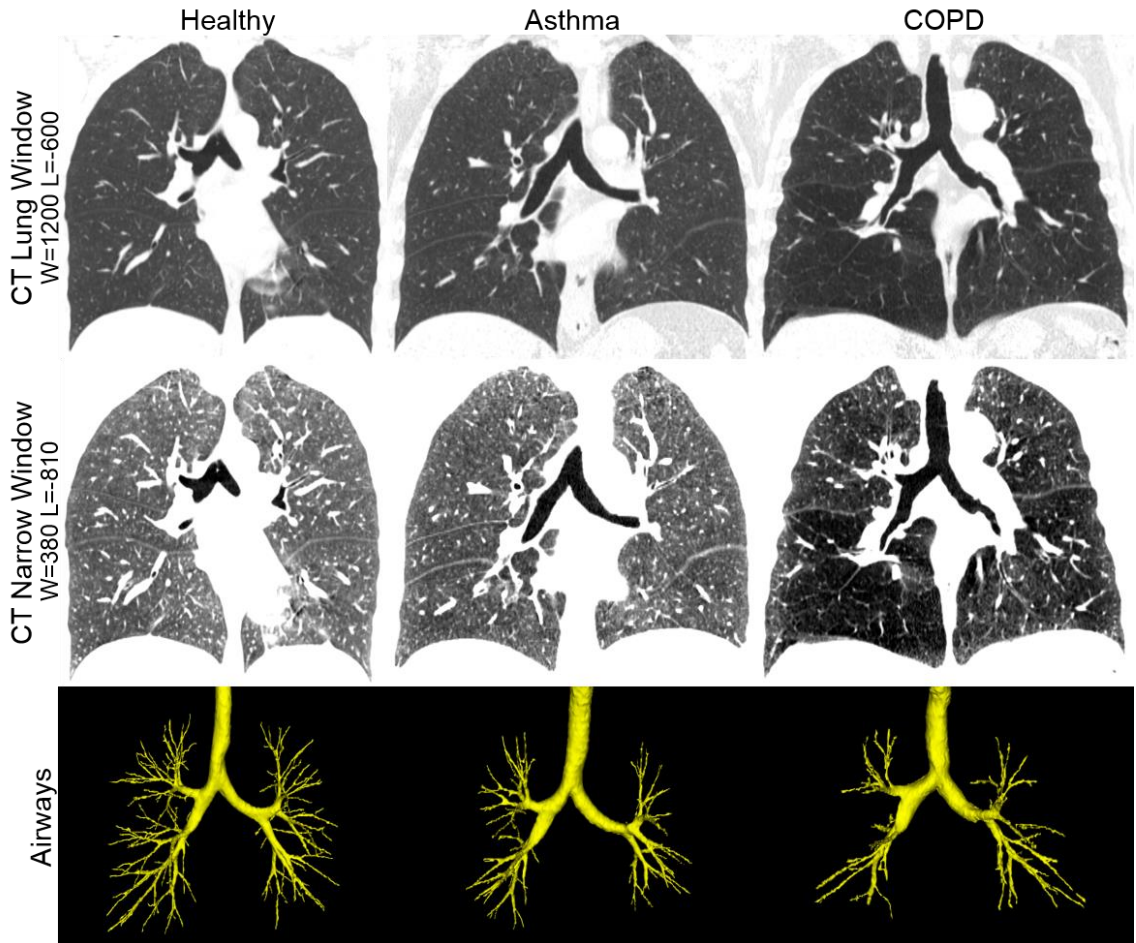


**Figure 1-8** Inspiratory coronal CT with corresponding airway trees

Top: CT images in typical lung window (W) and level (L) used to visualize structural airway and parenchymal abnormalities.

Middle: CT images with narrow window to highlight low attenuating areas. Compared with healthy participant, COPD participant shows regions with low x-ray attenuation indicative of parenchymal disease and airspace enlargement, whereas parenchyma in asthmatic participant appears normal.

Bottom: Three-dimensional airway reconstructions show fewer CT-resolved airways in asthma and COPD.

## Airways

Semi- and fully-automated approaches have been developed to segment the large airways in three dimensions. Such techniques take advantage of the cylindrical shape of the airways and the inherent contrast between the air within the airway lumen and highly vascularized airway wall. In an inspiratory CT image, airways can typically be resolved and segmented up to the tenth generation and reliably measured up to the fifth and sixth generations.<sup>127</sup>

**Figure 1-8** also shows three-dimensional airway reconstructions for each patient. Large airway morphology is measured using metrics analogous to those used in histology, such as airway wall area percent and wall thickness, as shown in in **Equation 1-9** and **Equation 1-10** respectively:

$$\text{Equation 1-9} \quad \text{Wall area percent [\%]} = \frac{\text{Airway wall area [mm}^2\text{]}}{\text{Total area [mm}^2\text{]}} \cdot 100$$

$$\text{Equation 1-10} \quad \text{Wall thickness [mm]} = \text{Outer diameter} - \text{Inner diameter [mm]}$$

The large airways in asthma have been extensively evaluated using CT. Asthmatics show greater wall thickness compared with healthy controls<sup>128-134</sup> and wall thickness increases with increasing disease severity.<sup>129,135,136</sup> Wall thickness in asthma is directly related to airway remodeling on pathology<sup>131,136,137</sup> and correlates with airway obstruction<sup>130,131,134,136,138</sup> and airway hyperresponsiveness.<sup>133,136,139</sup> Airway wall thickness on CT also decreases in response to inhaled corticosteroid treatment<sup>132,140,141</sup> and bronchial thermoplasty.<sup>142</sup> Beyond airway morphology, a quantitative scoring system has been developed to measure the burden of intraluminal airway plugging, and in patients with asthma, a high plug score was associated with worse airflow obstruction and airway eosinophilia.<sup>143</sup> Evaluation of the large airways in COPD using CT has been less straightforward. Although early CT work observed narrowed airway lumens and fewer peripheral airways in patients with COPD compared with never-smokers controls<sup>144-146</sup> and relationships between airway wall thickness and airflow obstruction,<sup>145,147-149</sup> more recent work by Smith and colleagues demonstrated thinner airway walls relative to controls when comparing spatially-matched airways.<sup>150</sup> These recent results highlight the importance of airway sampling technique when reporting and comparing quantitative CT airway measurements in patients with COPD. In contrast, the total number of airways visible and

segmented on CT may be quantified as total airway count (TAC).<sup>151</sup> Airway count was first investigated in patients with COPD and was shown to be reduced with greater emphysematous destruction in the right upper lobe,<sup>151</sup> and in following was shown to be decreased relative to never-smoking controls in the whole lung and before the onset of emphysema.<sup>152</sup> Overall, the common quantitative CT airway measurements at the disposal of clinical and research studies include lumen diameter, lumen area (LA), wall area percent (WA%), wall thickness (WT), total airway count (TAC), square root of wall area of a hypothetical airway of internal perimeter 10 mm (Pi10), and airway circularity.

As described previously in section **1.3**, the small airways (<2 mm diameter) play an important role in the pathogenesis of both asthma and COPD. Although the small airways are beyond the spatial resolution limits of CT, small airways disease can be indirectly assessed via air trapping on expiratory CT. Air trapping appears as mosaic attenuation, which is defined as variable lung attenuation that results in a heterogeneous appearance of the lung parenchyma.<sup>153</sup> Automated thresholds are applied to the lung density histogram and air trapping is quantified as the relative area of the lung with Hounsfield units less than -856 (RA<sub>856</sub>)<sup>154</sup> – -856 HU is chosen because it is the attenuation value of normally inflated lung, thus the lungs at end expiration contain less air and should have higher attenuation than -856 HU.<sup>155</sup> In asthma, air trapping is elevated compared with healthy controls<sup>156,157</sup> and related to disease severity,<sup>158</sup> airflow obstruction<sup>138,154,156</sup> and airway hyperresponsiveness.<sup>154</sup> CT air trapping has been shown to be sensitive to treatment effects with inhaled corticosteroids,<sup>159,160</sup> bronchial thermoplasty<sup>142</sup> and montelukast, a leukotriene receptor antagonist.<sup>161</sup> In COPD, CT air trapping is related to airflow obstruction,<sup>162,163</sup> however it can be difficult to distinguish from emphysema using a simple threshold.<sup>155</sup> For this reason, expiratory CT is not commonly assessed alone in COPD, but rather in conjunction with inspiratory CT using image registration techniques as described subsequently.

### *Parenchyma*

The parenchyma is assessed for emphysema also using densitometric thresholds on inspiratory CT. The key feature of emphysema on CT is decreased lung density,<sup>164</sup> and regions of low attenuation in a COPD participant compared with the healthy and asthma participants are highlighted using a narrow window in **Figure 1-8**. Similar to that of air trapping on expiratory CT, automated thresholds are applied to the lung density histogram to quantify the extent of emphysema on inspiratory CT. Thresholds ranging from -910 to -970 HU<sup>165-167</sup> or the 15<sup>th</sup> percentile of the density histogram (HU<sub>15</sub> or PD<sub>15</sub>)<sup>168</sup> have been validated against histology. The relative area of the lung less than -950 HU provides the best balance of sensitivity and specificity and is therefore most commonly used.<sup>155</sup> Emphysema is considered present when RA<sub>950</sub> is greater than 6.8%.<sup>167</sup> Unsurprisingly, RA<sub>950</sub> is typically less than 6.8% in asthma. In COPD, RA<sub>950</sub> is elevated and shows good agreement with manual emphysema scores by radiologists<sup>169</sup> and is related to airflow obstruction.<sup>170</sup>

Beyond single image sets at inspiration or expiration, novel quantitative CT methods and biomarkers have been developed by co-registering inspiratory and expiratory images. As alluded to previously, this is particularly useful for patients with COPD to distinguish emphysematous regions from regions of air trapping and this forms the basis of parametric response mapping<sup>171</sup> and disease probability measure.<sup>172</sup> Parametric response mapping uses the density thresholds previously described for emphysema and air trapping on inspiratory and expiratory CT, respectively, to classify lung tissue into normal, emphysematous or gas-trapped regions on a voxel-wise basis. Disease probability measure uses the same fundamental principles, however instead of using single thresholds, it uses a probability of each category based on normalized densities at inspiration and expiration on a continuous scale. The non-emphysematous air trapping category has been termed ‘functional small airway disease’, and together, these categories make up the primary imaging phenotypes of COPD that are well-recognized and widely implemented in COPD research.<sup>173</sup> Ostridge and colleagues directly compared parametric response mapping and disease probability measure and observed good agreement between the two methods.<sup>174</sup> This study also demonstrated relationships between disease probability measure air trapping and oscillometry measures of small airways disease,<sup>174</sup> providing physiological

validation for the air trapping measurement. Parametric response mapping has been extensively applied in COPD to sensitively identify regions of gas trapping,<sup>175-177</sup> and these regions were recently validated against pathology as measure of small airways disease in severe COPD.<sup>178</sup> Preliminary work in asthma has demonstrated an increase in regions of parametric response map gas trapping in patients with severe asthma compared with nonsevere asthma and controls,<sup>179</sup> however given its dependence on emphysema, the technique has not been widely applied in asthma studies. Alternatively, the air volume change and amount of deformation between inspiratory and expiratory CT images may be quantified<sup>180</sup> and these quantitative CT metrics show differing volume changes and tissue deformations between asthmatics and healthy controls.<sup>181</sup> Choi and colleagues used a combination of airway and parenchymal measurements to develop quantitative CT clusters of asthma patients,<sup>182</sup> providing for the first time, quantitative imaging phenotypes of asthma. The same authors subsequently used similar methods to compare quantitative CT phenotypes of asthma and COPD patients.<sup>183</sup>

#### 1.6.2.2 Dual-energy CT

The previous section summarizes the rich structural CT measurements of the lung, with the exception of some that indirectly represent pulmonary function. Direct functional assessments of the lungs are also possible using CT with inhaled contrasts and advanced CT techniques. Functional CT imaging of the lungs was first performed using a conventional-CT-like acquisition with inhaled xenon-133 (<sup>133</sup>Xe) to measure regional ventilation. After a wash-in period, regions ventilated with <sup>133</sup>Xe have increased CT density compared with non-ventilated regions.<sup>184</sup> The poor xenon enhancement associated with this technique limited its application though and has motivated xenon ventilation imaging using a dual-energy CT approach. Although first introduced in the 1970s,<sup>185</sup> dual-energy CT has only recently been applied to measure regional ventilation using <sup>133</sup>Xe.<sup>186</sup> Compared with conventional CT, dual-energy CT acquires two separate images at different x-ray tube voltages, one each at a high and low energy. Moreover, dual-source technology enables simultaneous acquisition of these two images; as the name suggests, dual-source systems are equipped with two x-ray sources and two corresponding detectors oriented 90° from each other that simultaneously rotate around the patient. The real advantage of dual-

energy CT over conventional methods is that it is sensitive to both tissue attenuation in HU and chemical composition of the lung. Regional gas distribution is generated using three-material decomposition based on attenuation differences at different energy levels to differentiate inhaled xenon from the lung parenchyma and air.<sup>187</sup> Following a wash-in period where patients breathe a mixture of xenon and oxygen for 2-3 minutes, static ventilation images may be acquired during an inspiratory breath-hold or dynamic images may be acquired during wash-in and wash-out phases.<sup>188</sup> The average radiation dose associated with dual-energy CT is approximately 3 mSv for static acquisitions and 8 mSv for dynamic acquisitions.<sup>187</sup>

As expected, xenon ventilation on dual-energy CT is homogeneous in healthy controls.<sup>188</sup> In patients with asthma, dual-energy CT shows ventilation abnormalities<sup>189,190</sup> that are associated with thicker airway walls also measured using CT,<sup>189</sup> sensitive to bronchodilator treatment<sup>190,191</sup> and related to asthma symptoms.<sup>192,193</sup> In COPD, dual-energy CT demonstrates structural and ventilation abnormalities related to airways disease and emphysema.<sup>194</sup> Another study used xenon ventilation dual-energy CT to classify areas of normal, air trapped and emphysematous tissue in patients with COPD,<sup>195</sup> similar to that described previously for parametric response mapping.

The wealth and utility of structural and functional information from all CT methods is clear, yet the application of quantitative CT is still limited beyond the research setting. Dual-energy CT in particular is limited due to the high concentrations of inhaled xenon required to provide adequate contrast that may cause respiratory depression. Even using low-dose conventional CT protocols, the risks stemming from ionizing radiation exposure limits the use of CT in serial studies of treatment response or longitudinal monitoring, especially in children and young adults with chronic lung disease.

### 1.6.3 Nuclear Medicine

Nuclear medicine imaging techniques employ radioactive tracers to measure lung function, and are used to measure ventilation, perfusion and ventilation-perfusion mismatch. As it is most relevant to this thesis, this section specifically focuses on nuclear medicine measurements of pulmonary ventilation. It is important to note that nuclear medicine

imaging methods alone only provide functional information and must be combined with other modalities to obtain structure-function relationships.

#### 1.6.3.1 Scintigraphy

Scintigraphy measures gamma radiation to form a two-dimensional projection image of radioactivity in the body. While the patient lays supine, radionuclide tracers are either injected or inhaled and once inside the body, undergo radioactive decay and emit gamma rays. The gamma rays are detected by gamma cameras around the patient which convert the absorbed energy into an electrical signal to form an image. Regions of high radionuclide content appear as hot spots on the image.

Tracers may be radioactive themselves or labeled with a radionuclide. Evaluation of regional ventilation is typically performed used radioactive gases, radioactively-labeled aerosols or Technegas.<sup>196</sup> Common radioactive tracer gases are  $^{133}\text{Xe}$  and krypton-81m ( $^{81\text{m}}\text{Kr}$ ) and the radionuclide technetium-99m ( $^{99\text{m}}\text{Tc}$ ) is used to label  $^{99\text{m}}\text{Tc}$ -diethylene-triamine pentaacetate (DTPA) aerosol and Technegas. Early research and clinical applications most commonly employed inhaled  $^{133}\text{Xe}$ , however Technegas distribution in the lungs is similar to  $^{133}\text{Xe}$  and is actually is favoured now because its deposition remains stable for more than 20 minutes.<sup>197</sup>

Although the primary pulmonary application of scintigraphy is diagnosis of pulmonary embolism,<sup>198</sup> scintigraphy was the first method to regionally identify ventilation abnormalities in patients with asthma in the 1960s<sup>18,19</sup> and studies identifying the same in COPD followed shortly thereafter.<sup>199,200</sup> In patients with asthma, the effects of methacholine-<sup>201</sup> and histamine-induced<sup>202</sup> bronchoconstriction on regional ventilation distribution were also demonstrated using scintigraphy. Similar to planar x-ray, the two-dimensional nature of scintigraphy has motivated the development of three-dimensional approaches.

#### 1.6.3.2 Single Photon Emission Computed Tomography

By the late 1990s, nuclear medicine studies of the lung transitioned to single photon emission computed tomography (SPECT) for three-dimensional imaging. Analogous to

planar x-ray and CT, SPECT offers a three-dimensional tomographic approach to image gamma radiation.<sup>196</sup> The same radionuclide tracers may be used for SPECT, and two-dimensional scintigraphy projections are acquired at multiple angles around the patient and reconstructed to form three-dimensional image. The radiation exposure associated with SPECT is dependent on the radionuclide used, though a typical ventilation-perfusion study using <sup>99m</sup>Tc is approximately 2-3 mSv.<sup>196</sup> Hybrid SPECT/CT systems are available for simultaneous structure-function imaging.<sup>203</sup>

Physiological studies have employed SPECT to measure airway closure<sup>204</sup> and predictably have shown increased ventilation abnormalities in asthma relative to controls<sup>205</sup> and demonstrated bronchoconstrictive response to methacholine.<sup>206</sup> In COPD, SPECT demonstrated increased ventilation abnormalities compared with control participants<sup>207</sup> and has been used to determine severity of airflow obstruction<sup>208</sup> and the degree of ventilation within emphysematous bullae.<sup>209</sup> Beyond ventilation imaging, SPECT lends itself to the investigation of regional deposition of inhaled aerosols when labelled with <sup>99m</sup>Tc to evaluate the delivery efficacy of inhaled treatments.<sup>210,211</sup>

#### 1.6.3.3 Positron Emission Tomography

Positron emission tomography (PET) imaging also offers three-dimensional information, however in contrast to SPECT, PET uses positron-emitting isotopes to form images of metabolic activity. A radionuclide is either injected or inhaled and once inside the body, begins to decay and emits a positron. The positron will only travel a short distance before colliding with an electron and undergoing annihilation – this process produces two gamma photons of equal energy that are emitted 180° from each other and detected coincidentally using gamma cameras oriented circumferentially around the patient. The source particle is subsequently spatially located along the straight line between the two detector elements, and all detected sources are reconstructed into a volumetric image.<sup>212</sup> Hybrid PET/CT<sup>213</sup> and PET/MRI<sup>214</sup> systems are available for simultaneous structure-function imaging, however applications of each are not common for the study of asthma and COPD.

Although PET imaging is less common than scintigraphy and SPECT for pulmonary applications, pulmonary ventilation has been assessed using nitrogen-13 (<sup>13</sup>NN), either as

a bolus injection or inhaled aerosol.  $^{13}\text{N}$  is not soluble in blood or tissue and is eliminated exclusively in the lungs;<sup>212</sup> when injected, it travels to the lungs, crosses the alveolar membrane to the airspaces and is eliminated from the body by ventilation. Accordingly, well-ventilated lung regions will quickly wash out the tracer whereas unventilated regions retain the tracer because of gas trapping. Alternatively, when inhaled,  $^{13}\text{N}$  does not reach poorly-ventilated lung regions.<sup>212</sup> The primary studies employing  $^{13}\text{N}$  PET in asthma have studied the effects of methacholine on regional ventilation and observed regions of poor ventilation following bronchoconstriction.<sup>20,215</sup> In COPD,  $^{13}\text{N}$  PET was observed to be sensitive to airways disease versus emphysematous phenotypes.<sup>216</sup> Because of the short half-life (approximately 10 minutes) and rapid elimination of  $^{13}\text{N}$  from the body, the radiation dose associated with  $^{13}\text{N}$  PET ventilation-perfusion studies is quite low at approximately 0.2 mSv.<sup>212</sup> Although beyond the scope of this thesis, it is worth noting that fluorine-18-fluorodeoxyglucose ( $^{18}\text{F}$ -FDG) PET has been suggested as a biomarker for pulmonary inflammation,<sup>217,218</sup> however future work is required to determine its utility in asthma and COPD.

Although SPECT and PET offer three-dimensional imaging (versus scintigraphy) and functional information, both methods are inherently limited by low spatial resolution and still carry risk due to the radiation exposure. SPECT is further affected by motion artifacts owing to long acquisition times, and PET relies on cyclotrons for the production of radioisotopes that make it less widely available. SPECT and PET have unique applications for physiological studies of ventilation, perfusion and ventilation-perfusion mismatch, however remain research tools for asthma and COPD.

#### 1.6.4 Magnetic Resonance Imaging

Magnetic resonance imaging (MRI) uses non-ionizing radiofrequency waves to generate images by manipulating magnetic spins of different nuclei in the body. Conventional MRI leverages the nuclear spins of protons ( $^1\text{H}$ ) and provides excellent soft tissue contrast based on proton density of the tissue of interest. Radiofrequency waves excite the nuclei and the image is acquired as the nuclei relax and resultant signal decays back to equilibrium. A range of MRI methods currently available to obtain structural and functional information of the lungs are described here.

#### 1.6.4.1 Conventional $^1\text{H}$ MRI

MRI examinations of the chest and lungs make up 2% of all examinations worldwide.<sup>219</sup> MRI of the lungs is challenging technically because of the inherent properties of the lung compared with, for example, the brain. The tissue density of the lungs is approximately  $0.1 \text{ g/cm}^3$ , which contributes to extremely low  $^1\text{H}$  signal intensity.<sup>220</sup> For context, the density of the lungs is approximately 10% that of the brain.<sup>221</sup> Moreover, the same reasons that make the lung so efficient for gas exchange pose additional challenges for lung MRI; the 480 million alveoli and  $100 \text{ m}^2$  of air tissue-interfaces in the lung further degrade the pulmonary MRI signal by creating local magnetic field inhomogeneities, or susceptibility artifacts.<sup>222,223</sup> This causes extremely rapid signal dephasing and decay (0.4-0.9 ms), making it challenging to acquire sufficient signal to generate contrast within the lungs using conventional sequences. Finally, pulmonary MRI is highly impacted by artifacts from cardiac and respiratory motion. Together, these factors contribute to low pulmonary MRI signal such that the lungs appear as dark signal voids, as shown in **Figure 1-9** and making it challenging to differentiate between health and disease.

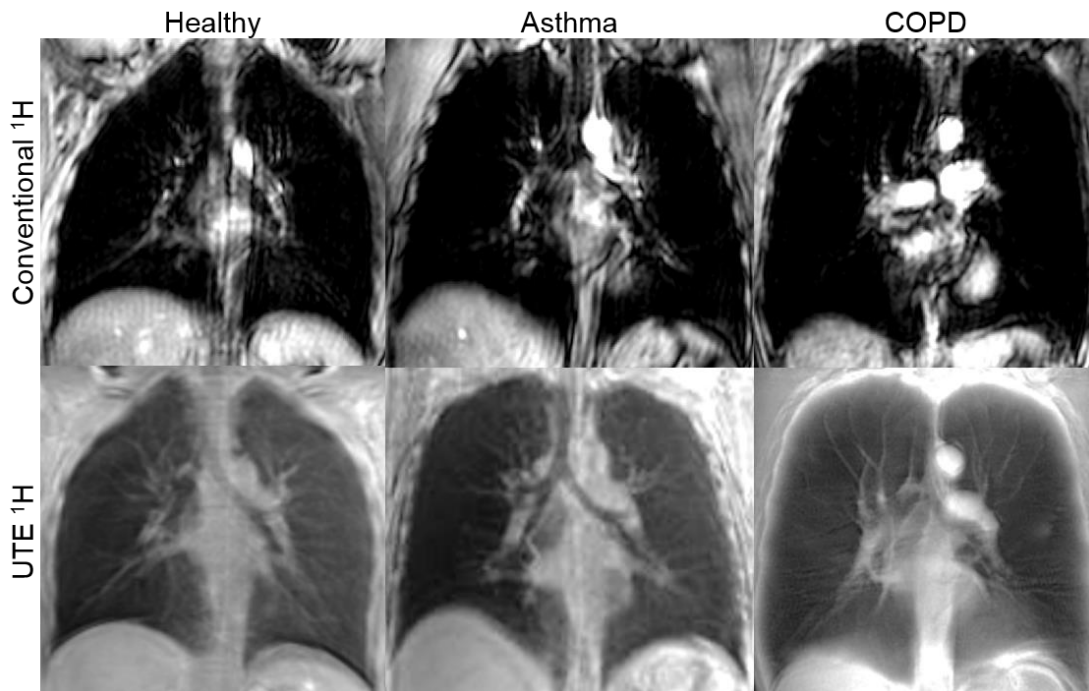


**Figure 1-9**  $^1\text{H}$  MRI of the lungs

Top row: Conventional  $^1\text{H}$  shows structural information and differences are indistinguishable between healthy participant and those with asthma and COPD.

Bottom row: UTE  $^1\text{H}$  MRI shows more structural information, where regions of low signal intensity are visible in asthma and COPD participants compared with healthy participant.

The obvious safety advantage of MRI over CT and nuclear medicine has motivated the development and of novel methods to overcome these technical challenges in order to achieve increased pulmonary MRI signal and obtain structural information. Ultra-short echo time (UTE) MRI methods do so by reducing time between radiofrequency excitation and data acquisition to acquire signal from lung tissue before it decays.<sup>220</sup> UTE  $^1\text{H}$  images are shown in **Figure 1-9**, demonstrating enhanced signal within lung parenchyma in comparison to conventional  $^1\text{H}$ . UTE MRI is particularly useful for evaluating parenchymal diseases – using a free-breathing approach in conjunction with respiratory gating, Ohno and colleagues demonstrated comparable visualization of pulmonary anatomy using UTE MRI versus CT in a variety of parenchymal diseases.<sup>224</sup> In COPD, a multi-volume breath-hold approach showed strong relationships with CT measurements of emphysema<sup>225</sup> and similar work in asthma showed decreased parenchymal signal intensity in asthma compared with healthy controls.<sup>226</sup> These preliminary results highlight the potential for UTE MRI in patients with asthma and COPD and developments are ongoing to achieve increased parenchymal signal using more rapid acquisition times. Although anatomical  $^1\text{H}$  MRI of the lung is developing rapidly, it does not provide information beyond that of a low-dose CT so the field has pushed towards pulmonary functional MRI.

#### 1.6.4.2 Inhaled Gas MRI

MRI of inhaled fluorinated and hyperpolarized gases has been used extensively over the last 25 years to evaluate regional lung structure and function in patients with lung disease. Using specialized multi-nuclear hardware and pulse sequences, the gases are imaged directly once inhaled by the patient. Although the gases are not endogenous and provide excellent contrast in that way, intrapulmonary tracer gases have low spin density at thermal equilibrium that generates three orders of magnitude less MRI signal than that of solid tissue or fluids in the body. Each gas requires different techniques to improve the spin density and MR visibility, and have their own respective advantages and disadvantages that lend themselves to different applications. In all cases, anatomical  $^1\text{H}$  is typically also acquired to provide matched anatomical information.

Of the inhaled gas MRI applications, inhaled fluorinated gas MRI was the first to be proposed in 1984,<sup>227</sup> although it was not evaluated in humans until 2008.<sup>228</sup> Fluorinated

gas MRI is enabled using inhaled sulfur hexafluoride ( $\text{SF}_6$ ), hexafluoroethane ( $\text{C}_2\text{F}_6$ ), tetrafluoromethane ( $\text{CF}_4$ ), perfluoropropane (PFP;  $\text{C}_3\text{F}_8$ ) or octafluorobutane ( $\text{C}_4\text{F}_8$ ), all of which are non-toxic and contain multiple fluorine-19 ( $^{19}\text{F}$ ) nuclei to increase the spin density. Moreover,  $^{19}\text{F}$  has a rapid signal relaxation time that allows for extensive signal averaging to improve image signal-to-noise. Importantly,  $^{19}\text{F}$  is naturally abundant and does not require hyperpolarization, so the associated costs for  $^{19}\text{F}$  MRI are lower than that of hyperpolarized gases. Dedicated  $^{19}\text{F}$  radiofrequency coils are generally desired but not required; the gyromagnetic ratio of  $^{19}\text{F}$  is close to that of  $^1\text{H}$  (40.052 MHz/T) so  $^{19}\text{F}$  can be imaged using conventional  $^1\text{H}$  hardware, however at the cost of reduced image quality due to slight off-resonance effects. Patients are instructed to breathe the fluorinated gas mixed with oxygen for 5-7 breaths to reach steady state concentration of  $^{19}\text{F}$  in the lungs, after which images may be acquired in a static breath-hold or during the wash-in and wash-out of the contrast gas.  $^{19}\text{F}$  MRI shows homogeneous ventilation in healthy volunteers<sup>229,230</sup> and a visual increase in heterogeneity of gas distribution in patients with asthma<sup>230</sup> and COPD<sup>230,231</sup> compared with healthy controls. These studies demonstrate that sufficient and clinically relevant signal may be achieved using  $^{19}\text{F}$  MRI, however it still suffers from low spatial resolution that has limited its widespread application in asthma and COPD.

On the other hand, hyperpolarized gas MRI provides images of pulmonary structure and function with high spatial and temporal resolution. Hyperpolarized gas MRI is enabled using noble gases helium-3 ( $^3\text{He}$ ) or xenon-129 ( $^{129}\text{Xe}$ ) which, as the name suggests, are hyperpolarized to increase their spin densities.<sup>232</sup> In contrast to  $^{19}\text{F}$ , signal averaging cannot be performed because  $^3\text{He}$  and  $^{129}\text{Xe}$  have long signal relaxation times. The technique was originally discovered using  $^{129}\text{Xe}$  when Albert and colleagues recognized that the polarization of the nuclei could be increased by approximately 100,000 times and provided the first  $^{129}\text{Xe}$  MR image of excised mouse lungs in 1994.<sup>233</sup> For both  $^3\text{He}$  and  $^{129}\text{Xe}$ , hyperpolarization is achieved via spin-exchange optical pumping<sup>234</sup> whereby a circularly polarized laser is used to bombard a glass cell housing rubidium and the noble gas. The circularly polarized light, with wavelength corresponding to the transition energy of rubidium, is absorbed by and polarizes the rubidium. Subsequent collisions between polarized rubidium and the noble gas transfer angular momentum to the noble gas, effectively increasing the nuclear-spin polarization of the noble gas and improving its MR

signal. The cell itself is housed inside Helmholtz coils to maintain a constant magnetic field and minimize the rate at which the polarized noble gas atoms decay back to thermal equilibrium. A single inhalation of up to 1.0 L of hyperpolarized gas is sufficient to generate high resolution static breath-hold MR images.

Following Albert and colleagues' initial results using  $^{129}\text{Xe}$ ,<sup>233</sup> the field quickly transitioned to  $^3\text{He}$ <sup>235</sup> because of its three-fold greater gyromagnetic ratio (32.434 MHz/T for  $^3\text{He}$  versus 11.777 MHz/T for  $^{129}\text{Xe}$ ) and greater achievable polarization levels with simpler turn-key systems (30-40% for  $^3\text{He}$  versus 8-25% for  $^{129}\text{Xe}$ ). This meant that greater MRI signal and thus image quality could be achieved using small volumes of polarized  $^3\text{He}$ . The field was entirely dominated by  $^3\text{He}$  until recently when the global shortage and high cost of  $^3\text{He}$ <sup>236</sup> pushed researchers back towards  $^{129}\text{Xe}$ .<sup>237,238</sup> As a result,  $^{129}\text{Xe}$  polarizer technology has significantly advanced to achieve polarization to the same order as  $^3\text{He}$ .<sup>239-241</sup> Differences have been observed between the results produced by  $^3\text{He}$  and  $^{129}\text{Xe}$  which are further discussed later on, however importantly, both have excellent safety and tolerability in healthy participants and patients with respiratory disease.<sup>242-244</sup>  $^{129}\text{Xe}$  MRI is now approved for clinical use in the United Kingdom and positive phase III clinical trial results for  $^{129}\text{Xe}$  MRI against gold-standard  $^{133}\text{Xe}$  scintigraphy just completed this year will support clinical approval in the United States later in 2020.<sup>245</sup> These methods allow for measurement of regional ventilation, lung microstructure and gas exchange. It is important to note that both  $^3\text{He}$  and  $^{129}\text{Xe}$  MRI require dedicated multi-nuclear MR systems, radiofrequency coils and hyperpolarizers. In the grand scheme of inhaled gas MRI, hyperpolarized gas applications are much more predominant than fluorinated gas; the remainder of this section is dedicated to hyperpolarized gas imaging of the lung.

### *Ventilation Imaging*

Imaging the spin density of hyperpolarized gases provides a visualization of the regional distribution of inhaled  $^3\text{He}$  or  $^{129}\text{Xe}$  in the lungs, highlighting regions that do and do not ventilate well. **Figure 1-10** demonstrates regional distribution of hyperpolarized  $^3\text{He}$  (cyan) and  $^{129}\text{Xe}$  (purple) in a healthy volunteer and participants with asthma and COPD. Compared with the healthy volunteer, where ventilation is homogeneous throughout,  $^3\text{He}$  and  $^{129}\text{Xe}$  show visually obvious ventilation heterogeneity in asthma and COPD. Noble

gas ventilation images are co-registered to anatomical  $^1\text{H}$  (grey-scale) to delineate regions of hyperpolarized gas signal void, which are termed ventilation defects. Early work by Altes and colleagues demonstrated good agreement between  $^3\text{He}$  MRI and  $^{133}\text{Xe}$  scintigraphy ventilation images.<sup>246</sup> Notably, when comparing paired  $^3\text{He}$  and  $^{129}\text{Xe}$  images, both remain homogenous in the healthy volunteer, but  $^{129}\text{Xe}$  ventilation is more heterogeneous than  $^3\text{He}$  in the asthma and COPD participants with larger and more numerous defects. These results have been observed systematically in asthma<sup>247</sup> and COPD<sup>248,249</sup> and suggest that  $^{129}\text{Xe}$  is more sensitive to lung abnormalities than  $^3\text{He}$ . It is important to note that the images shown in **Figure 1-10** were acquired after a single static inhalation of hyperpolarized gas; dynamic wash-in and wash-out investigations have been carried out,<sup>250,251</sup> however single, static inhalations remain the most commonly employed method.

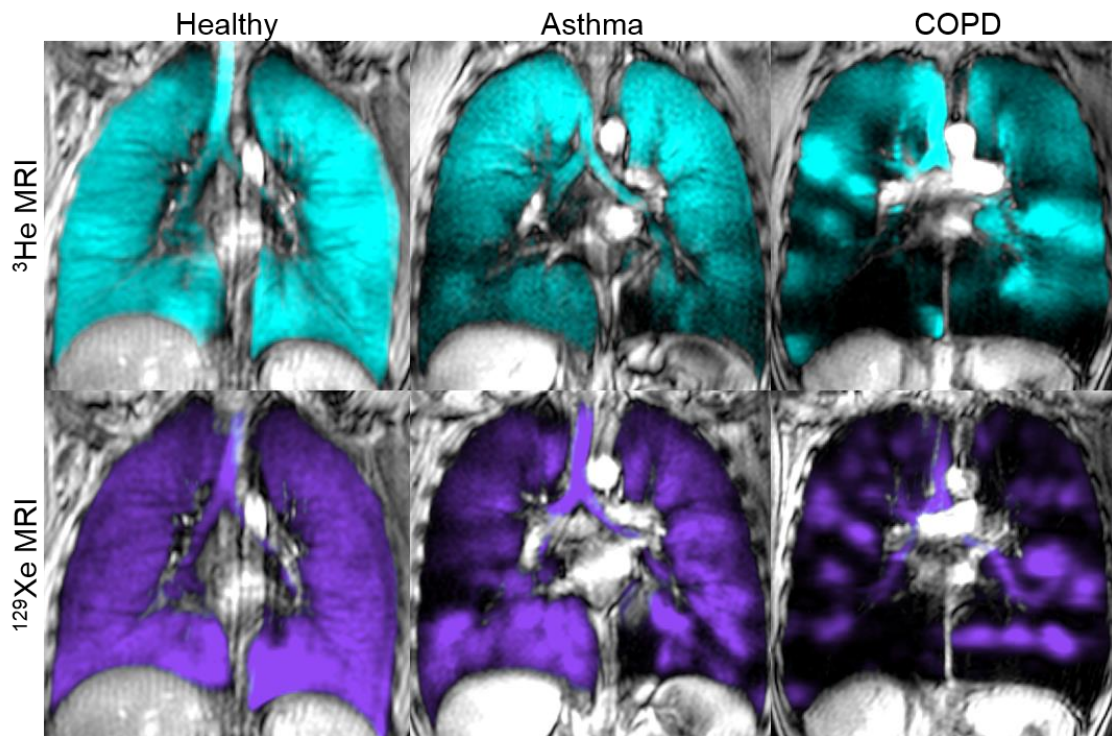


**Figure 1-10** Hyperpolarized  $^3\text{He}$  and  $^{129}\text{Xe}$  MRI  
 $^3\text{He}$  (cyan) and  $^{129}\text{Xe}$  (purple) MRI co-registered to anatomical  $^1\text{H}$  (grey-scale) show homogeneous ventilation for healthy participant and ventilation heterogeneity for asthma and COPD participants. In asthma and COPD,  $^{129}\text{Xe}$  MRI ventilation is visually more heterogeneous than  $^3\text{He}$ .

The extent of ventilation abnormalities was initially quantified using visual scoring and manual segmentation, however semi-automated<sup>252-254</sup> and automated<sup>255,256</sup> approaches are now widely used. Quantitative MRI biomarkers include the ventilated volume,<sup>257</sup> ventilation coefficient of variation,<sup>258</sup> ventilation defect volume<sup>259,260</sup> and ventilation defect percent.<sup>252,253,257,261</sup> Second-order texture features of MRI signal have also been quantified.<sup>262</sup> VDP is the most widely disseminated biomarker to date, owing to its robust reproducibility<sup>23,259</sup> and well-established relationships with clinical indices.<sup>248,263</sup> VDP is calculated as the ventilation defect volume normalized (VDV) to the thoracic cavity volume (TCV)<sup>252</sup> as shown in **Equation 1-11**:

$$\text{Equation 1-11} \quad \text{Ventilation defect percent [\%]} = \frac{\text{Ventilation defect volume [mL]}}{\text{Thoracic cavity volume [mL]}} \cdot 100$$

In asthma, and as shown in **Figure 1-10**, ventilation is typically more heterogeneous than healthy controls,<sup>258,263-265</sup> although not all asthmatics have ventilation defects.<sup>264,266</sup> Asthmatics with defects tend to be older,<sup>266</sup> and ventilation defects increase with increasing disease severity,<sup>263,267</sup> are related to airflow obstruction<sup>22,260,263,266</sup> and related to plethysmography airways resistance.<sup>265</sup> By lung lobe, one study showed a predominance of defects in the right upper and middle lobes in patients with asthma.<sup>267</sup> Ventilation defects increase in size and number following methacholine-<sup>265,268</sup> and exercise-induced<sup>268-270</sup> bronchoconstriction, and partially or completely resolve with bronchodilation.<sup>247,264,268</sup> Investigations of the short-term temporal nature of ventilation defects in asthma demonstrated persistence in the same spatial locations for same-day,<sup>23,264</sup> 7-14 day,<sup>271</sup> and up 1.5-year repeat evaluations.<sup>22,23</sup> Repeat methacholine challenges also revealed the same regions of lung affected by bronchoconstriction for up to 1.5 years.<sup>22</sup> Although long-term investigations have not yet been undertaken, these MRI findings refute the idea of diffuse and random airway abnormalities in asthma and suggest the importance of regional heterogeneity within the asthmatic lung.<sup>272</sup> Moreover, ventilation defects are unique predictors of asthma control<sup>273</sup> and exacerbations,<sup>274</sup> suggesting an important role for MRI ventilation defects as an indicator of patient outcomes.

Ventilation defects in asthma may arise from any of the underlying airway pathologies introduced in section **1.3.1** and the pathology has been investigated using a number of

different approaches. Using CT airway measurements, ventilation defects have been shown to be quantitatively and spatially related to abnormally remodeled large airways<sup>266</sup> and intraluminal plugging by mucus and cellular debris.<sup>275</sup> Fain and colleagues also demonstrated the contribution of small airways to ventilation defects via spatial correlations with regions of air trapping on expiratory CT<sup>260</sup> and relationships with oscillometry small airways resistance further suggest the role of small airways in ventilation defects in asthma.<sup>276</sup> Using a more invasive approach, a preliminary investigation of image-guided bronchoscopic biopsies in regions of ventilation defects demonstrated increased goblet cell hyperplasia and squamous metaplasia in regions of defects versus well-ventilated regions in the same participants.<sup>277</sup> With respect to airway inflammation, ventilation defects have been shown to be related to fractional exhaled nitric oxide,<sup>265</sup> neutrophils in bronchoalveolar lavage<sup>260</sup> and sputum eosinophils.<sup>278</sup> In conjunction with sputum measurements and pre- and post-bronchodilator evaluations, MRI can distinguish regions with inflammatory versus non-inflammatory contributions to ventilation heterogeneity.<sup>278</sup> With an understanding of the pathophysiology, it follows that ventilation defect response to treatment has been demonstrated with montelukast,<sup>270</sup> bronchial thermoplasty<sup>279</sup> and dupilumab.<sup>280</sup> Preliminary results of a randomized control trial for MRI-guided bronchial thermoplasty demonstrated non-inferior results compared with the conventional whole-lung approach,<sup>281</sup> and larger-scale image-guided studies are ongoing.<sup>282</sup>

Many similar results have been observed in patients with COPD. Ventilation is also more heterogeneous in COPD compared with healthy controls,<sup>248,259,283</sup> and ventilation defects increase with increasing COPD severity<sup>259,284</sup> and are related to airflow obstruction.<sup>248,283</sup> In milder disease, ventilation defects are more predominant in the basal lung and the distribution becomes more homogeneous in more severe disease.<sup>285</sup> Repeatability of ventilation defects in COPD has been observed on same-day and 7-day evaluations,<sup>259</sup> which is in agreement with the understanding of persistent airflow obstruction in COPD. Regional and quantitative improvements in ventilation defects have however been observed following bronchodilation in the absence of spirometric improvement,<sup>286</sup> suggesting the increased sensitivity of MRI ventilation abnormalities to bronchodilation in COPD. Importantly, ventilation defects are related to COPD symptoms and exercise

limitation<sup>287</sup> and are predictive of COPD exacerbations.<sup>288</sup> Pathologically, ventilation defects are spatially and quantitatively related to CT measurements of emphysema<sup>289</sup> and comparison with CT parametric response maps revealed that ventilation defects in mild COPD are related to air trapping and small airways disease, whereas in severe COPD, defects are more related to emphysema.<sup>284</sup>

The sensitivity and safety of MRI provide a unique opportunity to evaluate the natural progression of lung diseases. The progressive nature of COPD was evaluated in a preliminary longitudinal study in 15 participants with COPD, which demonstrated that MRI ventilation significantly worsened after two years in the absence of FEV<sub>1</sub> changes.<sup>290</sup> In a larger cohort study evaluating spirometry, CT and MRI over three years, only MRI ventilation biomarkers significantly predicted disease worsening in mild-moderate COPD.<sup>291</sup> In comparison in asthma, MRI ventilation abnormalities have only been studied over a longitudinal period of up to 1.5 years.<sup>22,23</sup> With the novel understanding of a progressive phenotype of asthma and progression to COPD, longitudinal studies are required to better understand asthma disease progression, and previous results in COPD<sup>290,291</sup> suggest MRI ventilation biomarkers may be sensitive to early disease changes.

#### *Diffusion-weighted Imaging*

Diffusion-weighted hyperpolarized gas MRI leverages the self-diffusion of the inhaled gases to measure the lung microstructure.<sup>292</sup> The random Brownian motion of the noble gas atoms reflects the restricted diffusion of the gases within the airways and airspaces and is quantified as apparent diffusion coefficients (ADC). The diffusion time interval is a surrogate of airspace size or dimension such that increased ADC reflects a greater mean square displacement of the gas molecule, which typically occurs in enlarged airspaces in the case of emphysema. ADC were first evaluated using <sup>3</sup>He, which were validated against histology<sup>61</sup> and shown to be highly reproducible *in vivo*.<sup>259,293</sup> <sup>3</sup>He ADC were subsequently used to validate <sup>129</sup>Xe ADC.<sup>294</sup> Owing to the respective pathophysiologies, diffusion-weighted MRI is commonly evaluated in COPD but not asthma.

Limited studies in asthma show conflicting evidence; some studies have shown elevated ADC compared with healthy controls<sup>295,296</sup> whereas another observed no difference.<sup>265</sup> ADC has however been shown to increase following methacholine-induced

bronchoconstriction and subsequently decrease with bronchodilation.<sup>265</sup> The methacholine-induced increase in ADC was suggested to be due to gas trapping,<sup>265</sup> and a more recent study demonstrated direct relationships between elevated ADC in asthma and CT-measured gas trapping.<sup>296</sup>

In COPD, ADC are certainly elevated relative to healthy controls<sup>248,297,298</sup> and as expected, are related to CT measurements of emphysema.<sup>248,299,300</sup> ADC are also related to airflow obstruction<sup>297,299</sup> and diffusing capacity of the lung.<sup>294</sup> In a <sup>3</sup>He-<sup>129</sup>Xe comparative study, ADC were used to explain the differences between <sup>3</sup>He and <sup>129</sup>Xe ventilation defects, which was ultimately determined to be related to emphysema.<sup>289</sup> The use of ADC in COPD phenotyping has also been described in a preliminary investigation,<sup>301</sup> similar to that for CT described previously. It is important to acknowledge however that ADC measurements are limited to those regions that ventilate in a single breath-hold and therefore may be unable to probe the most diseased regions.

#### *Dissolved-phase Imaging*

<sup>129</sup>Xe is especially advantageous because, unlike <sup>3</sup>He, it is soluble in biological tissue and can probe the efficiency of gas exchange.<sup>302,303</sup> The so-called dissolved phase refers to xenon dissolved in the alveolar-capillary membrane and red blood cells within the pulmonary capillaries – once dissolved, <sup>129</sup>Xe exhibits a chemical shift from the gaseous state that can be resolved as three distinct nuclear MR peaks: 1) gas, 2) tissue barrier plus plasma, and 3) red blood cell. The gas state reflects the spin density imaging described previously and has the largest measurable signal. The tissue barrier plus plasma signal represents <sup>129</sup>Xe dissolved in the alveolar-capillary membrane and blood plasma. The tissue barrier and plasma themselves have indistinguishable chemical shifts and together combine for the second largest signal approximately 197 ppm from the gas state.<sup>304</sup> Once uptaken into the red blood cells, <sup>129</sup>Xe exhibits an additional chemical shift of approximately 20 ppm beyond the tissue-plasma peak, creating the third and smallest peak. All three compartments may be imaged simultaneously within a single breath-hold of <sup>129</sup>Xe<sup>303</sup> to quantify gas exchange on a regional level.<sup>305</sup> Each peak may be quantified as a defect percent on its own analogous to VDP, or ratios between the peaks may also be expressed, for example tissue-to-gas, red blood cell-to-gas, or red blood cell-to-tissue.<sup>306</sup>

The primary applications of dissolved-phase imaging have been in diseases of pulmonary fibrosis, with limited application to date in asthma and COPD. In the first evaluation of asthma and COPD using  $^{129}\text{Xe}$  dissolved-phase MRI, Qing and colleagues observed reduced red blood cell-to-tissue ratio in COPD and increased variance in the red blood cell-to-tissue ratio in asthma, both compared with healthy controls.<sup>306</sup> Additional preliminary work has observed greater improvements in  $^{129}\text{Xe}$  barrier and red blood cell biomarkers compared with ventilation following dual bronchodilator therapy<sup>307</sup> and also identified phenotypes of gas exchange in patients with COPD.<sup>308</sup> Although there are limited applications of dissolved phase imaging to date in obstructive lung disease, there is enormous opportunity for  $^{129}\text{Xe}$  dissolved phase to better understand pathophysiology, evaluate and determine new disease phenotypes, and evaluate treatment response. Similar to ADC, dissolved-phase measurements are also limited to those regions that ventilate in a single breath-hold.

#### 1.6.4.3 Functional $^1\text{H}$ MRI

Fourier decomposition MRI (FDMRI) is a free-breathing  $^1\text{H}$  approach that permits simultaneous ventilation and perfusion imaging of the lung.<sup>309</sup> As the patient tidally breathes, a time series of  $^1\text{H}$  images are acquired and subsequently deformably co-registered to a reference image frame. The reference image is usually chosen as one at mid-position between end-inspiration and end-expiration. In the registered image, the signal intensity oscillates over time due to the mechanical compression and expansion of the lung tissue during breathing. Fast Fourier transforms of the signal oscillations in each voxel generate the ‘signal intensity’ of the ventilation map using the first ventilation harmonic, which corresponds to the respiratory rate. Example FDMR ventilation images are shown in **Figure 1-11** for healthy, asthmatic and COPD participants. The same process may be performed at the cardiac rate to generate perfusion maps.<sup>309</sup>

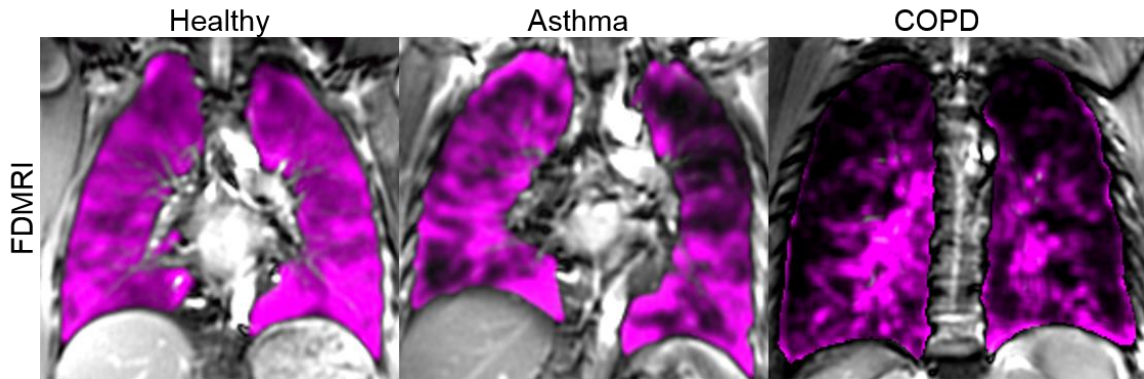


**Figure 1-11** Functional  $^1\text{H}$  FDMRI

FDMRI ventilation maps (magenta) generated from free-breathing  $^1\text{H}$  MRI co-registered to anatomical  $^1\text{H}$  (grey-scale) show homogeneous ventilation for healthy participant and ventilation heterogeneity for asthma and COPD participants.

FDMRI sensitively detects ventilation abnormalities in both asthma<sup>310</sup> and COPD<sup>311</sup> that show strong agreement with  $^3\text{He}$  static ventilation abnormalities. FDMRI may however exhibit a small bias towards smaller ventilation defect abnormalities than  $^3\text{He}$ , likely owing to the different time constants for lung filling during the image acquisition time (2 minutes FDMRI versus 12 seconds  $^3\text{He}$ ).<sup>310</sup> Kaireit and colleagues also demonstrated strong agreement between FDMRI and dynamic washout  $^{19}\text{F}$  MRI ventilation abnormalities in patients with COPD.<sup>312</sup> In a randomized control trial, a similar variation of FDMRI<sup>313</sup> showed ventilation improvements in patients with COPD following dual bronchodilator therapy.<sup>314</sup>

Although FDMRI requires advanced post-processing to generate functional maps, it eliminates the need for additional hardware and contrast agents, and enables functional ventilation maps on any MRI system using conventional  $^1\text{H}$  sequences and coils. A rapid, automated pipeline was recently developed<sup>315</sup> to facilitate wider translation of this technique.

## 1.7 Thesis Hypotheses and Objectives

The underlying structure-function determinants of ventilation heterogeneity in asthma are not well understood. *In silico* models suggest that asthmatic airway abnormalities are random, whereas early *in vivo* MRI results suggest airway abnormalities in asthma are not random. Instead, MRI findings reveal focal ventilation abnormalities that persist for up to

1.5 years.<sup>22,23</sup> There is enormous potential for pulmonary imaging to provide a better understanding of the mechanisms and physiological relevance of ventilation heterogeneity in asthma. Accordingly, the overarching objective of this thesis was to exploit sensitive pulmonary imaging measurements to better understand the structure and function of the asthmatic lung that drive ventilation heterogeneity and provide a foundation for imaging to guide disease phenotyping, predict disease worsening, and deliver personalized asthma treatment. The hypotheses and objectives specific to each chapter of this thesis are described below.

We first wanted to better understand the structural biomechanics of ventilation heterogeneity in asthma compared with that of COPD and if these differences could be explained by oscillometry and MRI ventilation defects. We hypothesized that oscillometry measurements of resistance and reactance exhibit different relationships with MRI ventilation defects in participants with asthma and COPD. The objective of **Chapter 2** was therefore to evaluate and compare hyperpolarized <sup>3</sup>He MRI and oscillometry in participants with asthma versus those with COPD, never-smokers without asthma and ex-smokers without COPD.

We next wanted to understand the long-term spatial and temporal nature of airway and ventilation abnormalities in asthma. Based on previous work that showed that ventilation abnormalities are spatially persistent for up to 1.5 years, we hypothesized that MRI ventilation defects and CT airway abnormalities in asthma are spatially and quantitatively persistent for longer than 1.5 years. In **Chapter 3**, our objective was to evaluate and compare CT airway and MRI ventilation abnormalities in nonidentical twins over a period 7 years.

Building on this, we further evaluated the long-term structure-function relationships in asthma in a group of unrelated asthma patients. We also wanted to determine the role for MRI in predicting disease worsening and we hypothesized that ventilation defects are predictive of future bronchodilator reversibility. In **Chapter 4**, we conducted a proof-of-concept study in 11 mild-to-moderate asthmatics over 6.5 years with the objective to

investigate the long-term pattern of ventilation defects and to identify predictors of longitudinal bronchodilator reversibility after 6.5 years.

Finally, based on previous work in COPD, we wondered whether the airway tree appears truncated on CT in patients with asthma. Due to the nature of airway remodeling in asthma, we hypothesized that CT airway count is reduced in patients with severe asthma compared to those with mild-to-moderate asthma, and that this reduction is associated with thickened airway walls and worse lung function. Accordingly, the objective of **Chapter 5** was to measure CT total airway count in patients with asthma across a range of severities and evaluate relationships with asthma severity, airway morphology, pulmonary function, and MRI ventilation.

In **Chapter 6**, I provide an overview and summary of the important observations and conclusions from **Chapters 2-5**. I also discuss the study specific and general limitations for these studies and suggest some potential solutions. I conclude my thesis with an outline of future studies that can build on the work presented here.

## 1.8 References

- 1 Masoli, M., Fabian, D., Holt, S. & Beasley, R. The global burden of asthma: Executive summary of the GINA dissemination committee report. *Allergy* **59**, 469-478 (2004).
- 2 Public Health Agency of Canada. Report from the Canadian chronic disease surveillance system: Asthma and chronic obstructive pulmonary disease in Canada. (2018).
- 3 Public Health Agency of Canada. Life and breath: Respiratory disease in Canada. (Public Health Agency of Canada,, Ottawa, 2007).
- 4 Public Health Agency of Canada. How healthy are Canadians? A trend analysis of the health of Canadians from a healthy living and chronic disease perspective. (Ottawa, 2016).
- 5 Canadian Institute for Health Information. Health indicators 2008. (CIHI, Ottawa, 2008).
- 6 Smetanin, P., Stiff, D., Briante, D., Ahmed, S., Wong, L. & Ler, A. Life and economic burden of lung disease in Ontario: 2011 to 2041. (RiskAnalytica, on behalf of the Ontario Lung Association, 2011).

- 7 GBD 2015 Chronic Respiratory Disease Collaborators. Global, regional, and national deaths, prevalence, disability-adjusted life years, and years lived with disability for chronic obstructive pulmonary disease and asthma, 1990-2015: A systematic analysis for the global burden of disease study 2015. *Lancet Respir Med* **5**, 691-706 (2017).
- 8 GBD 2017 Causes of Death Collaborators. Global, regional, and national age-sex-specific mortality for 282 causes of death in 195 countries and territories, 1980-2017: A systematic analysis for the global burden of disease study 2017. *Lancet* **392**, 1736-1788 (2018).
- 9 Silva, G. E., Sherrill, D. L., Guerra, S. & Barbee, R. A. Asthma as a risk factor for COPD in a longitudinal study. *Chest* **126**, 59-65 (2004).
- 10 Hayden, L. P. *et al.* Asthma is a risk factor for respiratory exacerbations without increased rate of lung function decline: Five-year follow-up in adult smokers from the COPDGene study. *Chest* **153**, 368-377 (2018).
- 11 To, T. *et al.* Progression from asthma to chronic obstructive pulmonary disease. Is air pollution a risk factor? *Am J Respir Crit Care Med* **194**, 429-438 (2016).
- 12 To, T. *et al.* Do community demographics, environmental characteristics and access to care affect risks of developing ACOS and mortality in people with asthma? *Eur Respir J* **50** (2017).
- 13 Sadatsafavi, M. *et al.* History of asthma in patients with chronic obstructive pulmonary disease. A comparative study of economic burden. *Ann Am Thorac Soc* **13**, 188-196 (2016).
- 14 Kendzerska, T. *et al.* The impact of a history of asthma on long-term outcomes of people with newly diagnosed chronic obstructive pulmonary disease: A population study. *J Allergy Clin Immunol* **139**, 835-843 (2017).
- 15 Marketos, S. G. & Ballas, C. N. Bronchial asthma in the medical literature of greek antiquity. *J Asthma* **19**, 263-269 (1982).
- 16 Becklake, M. R. A new index of the intrapulmonary mixture of inspired air. *Thorax* **7**, 111-116 (1952).
- 17 Ballester, E. *et al.* Ventilation-perfusion mismatching in acute severe asthma: Effects of salbutamol and 100% oxygen. *Thorax* **44**, 258-267 (1989).
- 18 Bentivoglio, L. G. *et al.* Regional pulmonary function studied with xenon in patients with bronchial asthma. *J Clin Invest* **42**, 1193-1200 (1963).
- 19 Heckscher, T. *et al.* Regional lung function in patients with bronchial asthma. *J Clin Invest* **47**, 1063-1070 (1968).

- 20 Venegas, J. G. *et al.* Self-organized patchiness in asthma as a prelude to catastrophic shifts. *Nature* **434**, 777-782 (2005).
- 21 Tgavalekos, N. T. *et al.* Relationship between airway narrowing, patchy ventilation and lung mechanics in asthmatics. *Eur Respir J* **29**, 1174-1181 (2007).
- 22 de Lange, E. E. *et al.* The variability of regional airflow obstruction within the lungs of patients with asthma: Assessment with hyperpolarized helium-3 magnetic resonance imaging. *J Allergy Clin Immunol* **119**, 1072-1078 (2007).
- 23 de Lange, E. E. *et al.* Changes in regional airflow obstruction over time in the lungs of patients with asthma: Evaluation with <sup>3</sup>He MR imaging. *Radiology* **250**, 567-575 (2009).
- 24 Vestbo, J. *et al.* Evaluation of COPD longitudinally to identify predictive surrogate end-points (ECLIPSE). *Eur Respir J* **31**, 869-873 (2008).
- 25 Regan, E. A. *et al.* Genetic epidemiology of COPD (COPDGene) study design. *COPD* **7**, 32-43 (2010).
- 26 Couper, D. *et al.* Design of the subpopulations and intermediate outcomes in COPD study (SPIROMICS). *Thorax* **69**, 491-494 (2014).
- 27 Bourbeau, J. *et al.* Canadian cohort obstructive lung disease (CanCOLD): Fulfilling the need for longitudinal observational studies in COPD. *COPD* **11**, 125-132 (2014).
- 28 Kirby, M. *et al.* Longitudinal computed tomography and magnetic resonance imaging of COPD: Thoracic imaging network of Canada (TINCan) study objectives. *Chronic Obstr Pulm Dis* **1**, 200-211 (2014).
- 29 Barnes, P. J., Drazen, J. M., Rennard, S. I. & Thomson, N. C. *Asthma and COPD: Basic mechanisms and clinical management.* (Elsevier, 2009).
- 30 West, J. B., Luks, A.M. *Respiratory physiology: The essentials.* 10th edn, (Lippincott Williams & Wilkins, 2016).
- 31 Lumb, A. B. *Nunn's applied respiratory physiology.* Eighth edn, (Elsevier Ltd., 2017).
- 32 Weibel, E. R., Cournand, A. F. & Richards, D. W. *Morphometry of the human lung.* Vol. 1 (Springer, 1963).
- 33 Boyden, E. A. *Segmental anatomy of the lung.* (New York: McGraw-Hill, 1955).
- 34 Tschirren, J., McLennan, G., Palagyi, K., Hoffman, E. A. & Sonka, M. Matching and anatomical labeling of human airway tree. *IEEE Trans Med Imaging* **24**, 1540-1547 (2005).

- 35 Ochs, M. *et al.* The number of alveoli in the human lung. *Am J Respir Crit Care Med* **169**, 120-124 (2004).
- 36 Gil, J., Bachofen, H., Gehr, P. & Weibel, E. R. Alveolar volume-surface area relation in air- and saline-filled lungs fixed by vascular perfusion. *J Appl Physiol Respir Environ Exerc Physiol* **47**, 990-1001 (1979).
- 37 Global Initiative for Asthma (GINA). Global strategy for asthma management and prevention: Updated 2019. (2019).
- 38 Saetta, M. & Turato, G. Airway pathology in asthma. *Eur Respir J Suppl* **34**, 18s-23s (2001).
- 39 Fahy, J. V. Goblet cell and mucin gene abnormalities in asthma. *Chest* **122**, 320S-326S (2002).
- 40 Roche, W. R., Beasley, R., Williams, J. H. & Holgate, S. T. Subepithelial fibrosis in the bronchi of asthmatics. *Lancet* **1**, 520-524 (1989).
- 41 Harkness, L. M., Ashton, A. W. & Burgess, J. K. Asthma is not only an airway disease, but also a vascular disease. *Pharmacol Ther* **148**, 17-33 (2015).
- 42 Dunnill, M. S., Massarella, G. R. & Anderson, J. A. A comparison of the quantitative anatomy of the bronchi in normal subjects, in status asthmaticus, in chronic bronchitis, and in emphysema. *Thorax* **24**, 176-179 (1969).
- 43 James, A. L. *et al.* Airway smooth muscle hypertrophy and hyperplasia in asthma. *Am J Respir Crit Care Med* **185**, 1058-1064 (2012).
- 44 Bousquet, J. *et al.* Eosinophilic inflammation in asthma. *N Engl J Med* **323**, 1033-1039 (1990).
- 45 Bergeron, C., Al-Ramli, W. & Hamid, Q. Remodeling in asthma. *Proc Am Thorac Soc* **6**, 301-305 (2009).
- 46 van der Wiel, E., ten Hacken, N. H., Postma, D. S. & van den Berge, M. Small-airways dysfunction associates with respiratory symptoms and clinical features of asthma: A systematic review. *J Allergy Clin Immunol* **131**, 646-657 (2013).
- 47 Jackson, D. J., Hartert, T. V., Martinez, F. D., Weiss, S. T. & Fahy, J. V. Asthma: NHLBI workshop on the primary prevention of chronic lung diseases. *Ann Am Thorac Soc* **11 Suppl 3**, S139-S145 (2014).
- 48 Moffatt, M. F. *et al.* A large-scale, consortium-based genomewide association study of asthma. *N Engl J Med* **363**, 1211-1221 (2010).

- 49 Litonjua, A. A., Carey, V. J., Burge, H. A., Weiss, S. T. & Gold, D. R. Parental history and the risk for childhood asthma. Does mother confer more risk than father? *Am J Respir Crit Care Med* **158**, 176-181 (1998).
- 50 Almqvist, C., Worm, M., Leynaert, B. & working group of, G. A. L. E. N. W. P. G. Impact of gender on asthma in childhood and adolescence: A GA2LEN review. *Allergy* **63**, 47-57 (2008).
- 51 Simpson, A. *et al.* Beyond atopy: Multiple patterns of sensitization in relation to asthma in a birth cohort study. *Am J Respir Crit Care Med* **181**, 1200-1206 (2010).
- 52 Jackson, D. J. The role of rhinovirus infections in the development of early childhood asthma. *Curr Opin Allergy Clin Immunol* **10**, 133-138 (2010).
- 53 Laumbach, R. J. & Kipen, H. M. Respiratory health effects of air pollution: Update on biomass smoke and traffic pollution. *J Allergy Clin Immunol* **129**, 3-13 (2012).
- 54 Global Initiative for Chronic Obstructive Lung Disease (GOLD). Global strategy for the diagnosis, management, and prevention of chronic obstructive pulmonary disease. 2019 report. (2019).
- 55 Barnes, P. J. Inflammatory mechanisms in patients with chronic obstructive pulmonary disease. *J Allergy Clin Immunol* **138**, 16-27 (2016).
- 56 Hogg, J. C., Macklem, P. T. & Thurlbeck, W. M. Site and nature of airway obstruction in chronic obstructive lung disease. *N Engl J Med* **278**, 1355-1360 (1968).
- 57 Yanai, M., Sekizawa, K., Ohru, T., Sasaki, H. & Takishima, T. Site of airway obstruction in pulmonary disease: Direct measurement of intrabronchial pressure. *J Appl Physiol* **72**, 1016-1023 (1992).
- 58 Mead, J., Turner, J. M., Macklem, P. T. & Little, J. B. Significance of the relationship between lung recoil and maximum expiratory flow. *J Appl Physiol* **22**, 95-108 (1967).
- 59 Hogg, J. C. Pathophysiology of airflow limitation in chronic obstructive pulmonary disease. *Lancet* **364**, 709-721 (2004).
- 60 Reid, L. Measurement of the bronchial mucous gland layer: A diagnostic yardstick in chronic bronchitis. *Thorax* **15**, 132-141 (1960).
- 61 Woods, J. C. *et al.* Hyperpolarized <sup>3</sup>He diffusion MRI and histology in pulmonary emphysema. *Magn Reson Med* **56**, 1293-1300 (2006).
- 62 The definition of emphysema. Report of a national heart, lung, and blood institute, division of lung diseases workshop. *Am Rev Respir Dis* **132**, 182-185 (1985).

- 63 Smith, B. M. *et al.* Pulmonary emphysema subtypes on computed tomography: The MESA COPD study. *Am J Med* **127**, 94.e97 (2014).
- 64 Hogg, J. C. *et al.* The nature of small-airway obstruction in chronic obstructive pulmonary disease. *N Engl J Med* **350**, 2645-2653 (2004).
- 65 Tan, W. C. *et al.* Characteristics of COPD in never-smokers and ever-smokers in the general population: Results from the CanCOLD study. *Thorax* **70**, 822-829 (2015).
- 66 Lamprecht, B. *et al.* COPD in never smokers: Results from the population-based burden of obstructive lung disease study. *Chest* **139**, 752-763 (2011).
- 67 Vogelmeier, C. F. *et al.* Global strategy for the diagnosis, management, and prevention of chronic obstructive lung disease 2017 report. GOLD executive summary. *Am J Respir Crit Care Med* **195**, 557-582 (2017).
- 68 Cho, M. H. *et al.* Variants in FAM13A are associated with chronic obstructive pulmonary disease. *Nat Genet* **42**, 200-202 (2010).
- 69 Pillai, S. G. *et al.* A genome-wide association study in chronic obstructive pulmonary disease (COPD): Identification of two major susceptibility loci. *PLoS Genet* **5**, e1000421-e1000421 (2009).
- 70 Stern, D. A., Morgan, W. J., Wright, A. L., Guerra, S. & Martinez, F. D. Poor airway function in early infancy and lung function by age 22 years: A non-selective longitudinal cohort study. *Lancet* **370**, 758-764 (2007).
- 71 Paulin, L. M. *et al.* Occupational exposures are associated with worse morbidity in patients with chronic obstructive pulmonary disease. *Am J Respir Crit Care Med* **191**, 557-565 (2015).
- 72 Gan, W. Q., FitzGerald, J. M., Carlsten, C., Sadatsafavi, M. & Brauer, M. Associations of ambient air pollution with chronic obstructive pulmonary disease hospitalization and mortality. *Am J Respir Crit Care Med* **187**, 721-727 (2013).
- 73 de Marco, R. *et al.* Risk factors for chronic obstructive pulmonary disease in a European cohort of young adults. *Am J Respir Crit Care Med* **183**, 891-897 (2011).
- 74 Vermeire, P. A. & Pride, N. B. A "splitting" look at chronic nonspecific lung disease (CNSLD): Common features but diverse pathogenesis. *Eur Respir J* **4**, 490-496 (1991).
- 75 *Bronchitis: An international symposium.* (eds N.G.M. Orie & H.J. Sluiter) (Springfield, 1961).
- 76 Gibson, P. G. & Simpson, J. L. The overlap syndrome of asthma and COPD: What are its features and how important is it? *Thorax* **64**, 728-735 (2009).

- 77 de Marco, R. *et al.* The coexistence of asthma and chronic obstructive pulmonary disease (COPD): Prevalence and risk factors in young, middle-aged and elderly people from the general population. *PLoS One* **8**, e62985 (2013).
- 78 Postma, D. S. & Rabe, K. F. The asthma-COPD overlap syndrome. *N Engl J Med* **373**, 1241-1249 (2015).
- 79 Sin, D. D. *et al.* What is asthma-COPD overlap syndrome? Towards a consensus definition from a round table discussion. *Eur Respir J* **48**, 664-673 (2016).
- 80 Miller, M. R. *et al.* Standardisation of spirometry. *Eur Respir J* **26**, 319-338 (2005).
- 81 Hankinson, J. L., Odencrantz, J. R. & Fedan, K. B. Spirometric reference values from a sample of the general U.S. Population. *Am J Respir Crit Care Med* **159**, 179-187 (1999).
- 82 Wanger, J. *et al.* Standardisation of the measurement of lung volumes. *Eur Respir J* **26**, 511-522 (2005).
- 83 Stocks, J. & Quanjer, P. H. Reference values for residual volume, functional residual capacity and total lung capacity. ATS workshop on lung volume measurements. Official statement of the European respiratory Society. *Eur Respir J* **8**, 492-506 (1995).
- 84 Quanjer, P. H. *et al.* Lung volumes and forced ventilatory flows. Report working party standardization of lung function tests, European community for steel and coal. Official statement of the European respiratory Society. *Eur Respir J Suppl* **16**, 5-40 (1993).
- 85 Koch, B. *et al.* Static lung volumes and airway resistance reference values in healthy adults. *Respirology* **18**, 170-178 (2013).
- 86 Graham, B. L. *et al.* 2017 ERS/ATS standards for single-breath carbon monoxide uptake in the lung. *Eur Respir J* **49** (2017).
- 87 DeCato, T. W. & Hegewald, M. J. Breathing red: Physiology of an elevated single-breath diffusing capacity of carbon monoxide. *Ann Am Thorac Soc* **13**, 2087-2092 (2016).
- 88 Stanojevic, S. *et al.* Official ERS technical standards: Global lung function initiative reference values for the carbon monoxide transfer factor for caucasians. *Eur Respir J* **50** (2017).
- 89 Dubois, A. B. & Ross, B. B. A new method for studying mechanics of breathing using cathode ray oscillograph. *Proc Soc Exp Biol Med* **78**, 546-549 (1951).
- 90 Dubois, A. B., Brody, A. W., Lewis, D. H. & Burgess, B. F., Jr. Oscillation mechanics of lungs and chest in man. *J Appl Physiol* **8**, 587-594 (1956).

- 91 Bates, J. H. *Lung mechanics: An inverse modeling approach*. (Cambridge University Press, 2009).
- 92 Goldman, M. D. Clinical application of forced oscillation. *Pulm Pharmacol Ther* **14**, 341-350 (2001).
- 93 Goldman, M. D., Saadeh, C. & Ross, D. Clinical applications of forced oscillation to assess peripheral airway function. *Respir Physiol Neurobiol* **148**, 179-194 (2005).
- 94 Oostveen, E. *et al.* Respiratory impedance in healthy subjects: Baseline values and bronchodilator response. *Eur Respir J* **42**, 1513-1523 (2013).
- 95 Pellegrino, R. *et al.* Interpretative strategies for lung function tests. *Eur Respir J* **26**, 948-968 (2005).
- 96 Guyatt, G. H. *et al.* Acute response to bronchodilator. An imperfect guide for bronchodilator therapy in chronic airflow limitation. *Arch Intern Med* **148**, 1949-1952 (1988).
- 97 Brand, P. L. *et al.* Interpretation of bronchodilator response in patients with obstructive airways disease. The Dutch chronic non-specific lung disease (CNSLD) study group. *Thorax* **47**, 429-436 (1992).
- 98 Cockcroft, D. W. & Hargreave, F. E. *Asthma: Its pathology and treatment* (eds M.A. Kaliner, P.J. Barnes, & C.G.A. Persson) (Marcel Dekker, 1991).
- 99 Crapo, R. O. *et al.* Guidelines for methacholine and exercise challenge testing-1999. This official statement of the American Thoracic Society was adopted by the ATS board of directors, July 1999. *Am J Respir Crit Care Med* **161**, 309-329 (2000).
- 100 Juniper, E. F., O'Byrne, P. M., Guyatt, G. H., Ferrie, P. J. & King, D. R. Development and validation of a questionnaire to measure asthma control. *Eur Respir J* **14**, 902-907 (1999).
- 101 Juniper, E. F., Svensson, K., Mork, A. C. & Stahl, E. Measurement properties and interpretation of three shortened versions of the asthma control questionnaire. *Respir Med* **99**, 553-558 (2005).
- 102 Reddel, H. K. *et al.* An official American Thoracic Society/European respiratory Society statement: Asthma control and exacerbations: Standardizing endpoints for clinical asthma trials and clinical practice. *Am J Respir Crit Care Med* **180**, 59-99 (2009).
- 103 Cox, G. *et al.* Asthma control during the year after bronchial thermoplasty. *N Engl J Med* **356**, 1327-1337 (2007).

- 104 FitzGerald, J. M. *et al.* Benralizumab, an anti-interleukin-5 receptor alpha monoclonal antibody, as add-on treatment for patients with severe, uncontrolled, eosinophilic asthma (CALIMA): A randomised, double-blind, placebo-controlled phase 3 trial. *Lancet* **388**, 2128-2141 (2016).
- 105 Juniper, E. F. *et al.* Evaluation of impairment of health related quality of life in asthma: Development of a questionnaire for use in clinical trials. *Thorax* **47**, 76-83 (1992).
- 106 Juniper, E. F., Guyatt, G. H., Willan, A. & Griffith, L. E. Determining a minimal important change in a disease-specific quality of life Questionnaire. *J Clin Epidemiol* **47**, 81-87 (1994).
- 107 Jones, P. W., Quirk, F. H., Baveystock, C. M. & Littlejohns, P. A self-complete measure of health status for chronic airflow limitation. The St. George's respiratory Questionnaire. *Am Rev Respir Dis* **145**, 1321-1327 (1992).
- 108 Celli, B. R. The importance of spirometry in COPD and asthma: Effect on approach to management. *Chest* **117**, 15S-19S (2000).
- 109 Busse, W. W. Asthma diagnosis and treatment: Filling in the information gaps. *J Allergy Clin Immunol* **128**, 740-750 (2011).
- 110 Cerveri, I. *et al.* Underestimation of airflow obstruction among young adults using FEV1/FVC <70% as a fixed cut-off: A longitudinal evaluation of clinical and functional outcomes. *Thorax* **63**, 1040-1045 (2008).
- 111 Macklem, P. T. & Mead, J. Resistance of central and peripheral airways measured by a retrograde catheter. *J Appl Physiol* **22**, 395-401 (1967).
- 112 Enright, P. L. & Kaminsky, D. A. Strategies for screening for chronic obstructive pulmonary disease. *Respir Care* **48**, 1194-1203 (2003).
- 113 Brenner, D. J. & Hall, E. J. Computed tomography--an increasing source of radiation exposure. *N Engl J Med* **357**, 2277-2284 (2007).
- 114 Canadian Nuclear Safety Commission. Natural background radiation. (Government of Canada, 2014).
- 115 Rebeck, A. S. Radiological aspects of severe asthma. *Australas Radiol* **14**, 264-268 (1970).
- 116 Hodson, M. E., Simon, G. & Batten, J. C. Radiology of uncomplicated asthma. *Thorax* **29**, 296-303 (1974).
- 117 Paganin, F. *et al.* Chest radiography and high resolution computed tomography of the lungs in asthma. *Am Rev Respir Dis* **146**, 1084-1087 (1992).

- 118 Pipavath, S. N. J., Schmidt, R. A., Takasugi, J. E. & Godwin, J. D. Chronic obstructive pulmonary disease: Radiology-pathology correlation. *J Thorac Imaging* **24**, 171-180 (2009).
- 119 Thurlbeck, W. M. & Simon, G. Radiographic appearance of the chest in emphysema. *Am J Roentgenol* **130**, 429-440 (1978).
- 120 Goldman, L. W. Principles of CT and CT technology. *J Nucl Med Technol* **35**, 115-130 (2007).
- 121 Hounsfield, G. N. Computerized transverse axial scanning (tomography). 1. Description of system. *Br J Radiol* **46**, 1016-1022 (1973).
- 122 Mettler, F. A., Jr., Huda, W., Yoshizumi, T. T. & Mahesh, M. Effective doses in radiology and diagnostic nuclear medicine: A catalog. *Radiology* **248**, 254-263 (2008).
- 123 Lambert, L., Banerjee, R., Votruba, J., El-Lababidi, N. & Zeman, J. Ultra-low-dose CT imaging of the thorax: Decreasing the radiation dose by one order of magnitude. *Indian J Pediatr* **83**, 1479-1481 (2016).
- 124 Kim, Y. *et al.* Ultra-low-dose CT of the thorax using iterative reconstruction: Evaluation of image quality and radiation dose reduction. *Am J Roentgenol* **204**, 1197-1202 (2015).
- 125 Willeminck, M. J. *et al.* Iterative reconstruction techniques for computed tomography part 2: Initial results in dose reduction and image quality. *Eur Radiol* **23**, 1632-1642 (2013).
- 126 Newell, J. D., Jr., Sieren, J. & Hoffman, E. A. Development of quantitative computed tomography lung protocols. *J Thorac Imaging* **28**, 266-271 (2013).
- 127 Tschirren, J., Hoffman, E. A., McLennan, G. & Sonka, M. Intrathoracic airway trees: Segmentation and airway morphology analysis from low-dose CT scans. *IEEE Trans Med Imaging* **24**, 1529-1539 (2005).
- 128 Okazawa, M. *et al.* Human airway narrowing measured using high resolution computed tomography. *Am J Respir Crit Care Med* **154**, 1557-1562 (1996).
- 129 Awadh, N., Muller, N. L., Park, C. S., Abboud, R. T. & FitzGerald, J. M. Airway wall thickness in patients with near fatal asthma and control groups: Assessment with high resolution computed tomographic scanning. *Thorax* **53**, 248-253 (1998).
- 130 Niimi, A. *et al.* Airway wall thickness in asthma assessed by computed tomography. Relation to clinical indices. *Am J Respir Crit Care Med* **162**, 1518-1523 (2000).

- 131 Kasahara, K., Shiba, K., Ozawa, T., Okuda, K. & Adachi, M. Correlation between the bronchial subepithelial layer and whole airway wall thickness in patients with asthma. *Thorax* **57**, 242-246 (2002).
- 132 Niimi, A. *et al.* Effect of short-term treatment with inhaled corticosteroid on airway wall thickening in asthma. *Am J Med* **116**, 725-731 (2004).
- 133 Siddiqui, S. *et al.* Airway wall geometry in asthma and nonasthmatic eosinophilic bronchitis. *Allergy* **64**, 951-958 (2009).
- 134 Gupta, S. *et al.* Quantitative analysis of high-resolution computed tomography scans in severe asthma subphenotypes. *Thorax* **65**, 775-781 (2010).
- 135 Little, S. A. *et al.* High resolution computed tomographic assessment of airway wall thickness in chronic asthma: Reproducibility and relationship with lung function and severity. *Thorax* **57**, 247-253 (2002).
- 136 Aysola, R. S. *et al.* Airway remodeling measured by multidetector CT is increased in severe asthma and correlates with pathology. *Chest* **134**, 1183-1191 (2008).
- 137 Berair, R. *et al.* Associations in asthma between quantitative computed tomography and bronchial biopsy-derived airway remodelling. *Eur Respir J* **49** (2017).
- 138 Gono, H., Fujimoto, K., Kawakami, S. & Kubo, K. Evaluation of airway wall thickness and air trapping by hrcr in asymptomatic asthma. *Eur Respir J* **22**, 965-971 (2003).
- 139 Niimi, A. *et al.* Relationship of airway wall thickness to airway sensitivity and airway reactivity in asthma. *Am J Respir Crit Care Med* **168**, 983-988 (2003).
- 140 Lee, Y. M. *et al.* High-resolution CT findings in patients with near-fatal asthma: Comparison of patients with mild-to-severe asthma and normal control subjects and changes in airway abnormalities following steroid treatment. *Chest* **126**, 1840-1848 (2004).
- 141 Kurashima, K. *et al.* Effect of early versus late intervention with inhaled corticosteroids on airway wall thickness in patients with asthma. *Respirology* **13**, 1008-1013 (2008).
- 142 Konietzke, P. *et al.* Quantitative CT detects changes in airway dimensions and air-trapping after bronchial thermoplasty for severe asthma. *Eur J Radiol* **107**, 33-38 (2018).
- 143 Dunican, E. M. *et al.* Mucus plugs in patients with asthma linked to eosinophilia and airflow obstruction. *J Clin Invest* **128**, 997-1009 (2018).
- 144 Berger, P. *et al.* Airway wall thickness in cigarette smokers: Quantitative thin-section CT assessment. *Radiology* **235**, 1055-1064 (2005).

- 145 Matsuoka, S., Kurihara, Y., Yagihashi, K., Hoshino, M. & Nakajima, Y. Airway dimensions at inspiratory and expiratory multisection CT in chronic obstructive pulmonary disease: Correlation with airflow limitation. *Radiology* **248**, 1042-1049 (2008).
- 146 Grydeland, T. B. *et al.* Quantitative computed tomography measures of emphysema and airway wall thickness are related to respiratory symptoms. *Am J Respir Crit Care Med* **181**, 353-359 (2010).
- 147 Nakano, Y. *et al.* Computed tomographic measurements of airway dimensions and emphysema in smokers. Correlation with lung function. *Am J Respir Crit Care Med* **162**, 1102-1108 (2000).
- 148 Hasegawa, M. *et al.* Airflow limitation and airway dimensions in chronic obstructive pulmonary disease. *Am J Respir Crit Care Med* **173**, 1309-1315 (2006).
- 149 Kim, W. J. *et al.* CT metrics of airway disease and emphysema in severe COPD. *Chest* **136**, 396-404 (2009).
- 150 Smith, B. M. *et al.* Comparison of spatially matched airways reveals thinner airway walls in COPD. The multi-ethnic study of atherosclerosis (MESA) COPD study and the subpopulations and intermediate outcomes in COPD study (SPIROMICS). *Thorax* **69**, 987-996 (2014).
- 151 Diaz, A. A. *et al.* Airway count and emphysema assessed by chest CT imaging predicts clinical outcome in smokers. *Chest* **138**, 880-887 (2010).
- 152 Kirby, M. *et al.* Total airway count on computed tomography and the risk of chronic obstructive pulmonary disease progression. Findings from a population-based study. *Am J Respir Crit Care Med* **197**, 56-65 (2018).
- 153 Kligerman, S. J., Henry, T., Lin, C. T., Franks, T. J. & Galvin, J. R. Mosaic attenuation: Etiology, methods of differentiation, and pitfalls. *Radiographics* **35**, 1360-1380 (2015).
- 154 Busacker, A. *et al.* A multivariate analysis of risk factors for the air-trapping asthmatic phenotype as measured by quantitative CT analysis. *Chest* **135**, 48-56 (2009).
- 155 Lynch, D. A. & Al-Qaisi, M. A. Quantitative computed tomography in chronic obstructive pulmonary disease. *J Thorac Imaging* **28**, 284-290 (2013).
- 156 Newman, K. B., Lynch, D. A., Newman, L. S., Ellegood, D. & Newell, J. D., Jr. Quantitative computed tomography detects air trapping due to asthma. *Chest* **106**, 105-109 (1994).

- 157 Beigelman-Aubry, C. *et al.* Mild intermittent asthma: CT assessment of bronchial cross-sectional area and lung attenuation at controlled lung volume. *Radiology* **223**, 181-187 (2002).
- 158 Mitsunobu, F. *et al.* Influence of age and disease severity on high resolution CT lung densitometry in asthma. *Thorax* **56**, 851-856 (2001).
- 159 Tunon-de-Lara, J. M. *et al.* Air trapping in mild and moderate asthma: Effect of inhaled corticosteroids. *J Allergy Clin Immunol* **119**, 583-590 (2007).
- 160 Goldin, J. G. *et al.* Comparative effects of hydrofluoroalkane and chlorofluorocarbon beclomethasone dipropionate inhalation on small airways: Assessment with functional helical thin-section computed tomography. *J Allergy Clin Immunol* **104**, S258-267 (1999).
- 161 Zeidler, M. R. *et al.* Montelukast improves regional air-trapping due to small airways obstruction in asthma. *Eur Respir J* **27**, 307-315 (2006).
- 162 Murphy, K. *et al.* Toward automatic regional analysis of pulmonary function using inspiration and expiration thoracic CT. *Med Phys* **39**, 1650-1662 (2012).
- 163 Schroeder, J. D. *et al.* Relationships between airflow obstruction and quantitative CT measurements of emphysema, air trapping, and airways in subjects with and without chronic obstructive pulmonary disease. *Am J Roentgenol* **201**, W460-W470 (2013).
- 164 Hayhurst, M. D. *et al.* Diagnosis of pulmonary emphysema by computerised tomography. *Lancet* **2**, 320-322 (1984).
- 165 Müller, N. L., Staples, C. A., Miller, R. R. & Abboud, R. T. "Density mask". An objective method to quantitate emphysema using computed tomography. *Chest* **94**, 782-787 (1988).
- 166 Madani, A., Zanen, J., de Maertelaer, V. & Gevenois, P. A. Pulmonary emphysema: Objective quantification at multi-detector row CT--comparison with macroscopic and microscopic morphometry. *Radiology* **238**, 1036-1043 (2006).
- 167 Gevenois, P. A. *et al.* Comparison of computed density and microscopic morphometry in pulmonary emphysema. *Am J Respir Crit Care Med* **154**, 187-192 (1996).
- 168 Heussel, C. P. *et al.* Fully automatic quantitative assessment of emphysema in computed tomography: Comparison with pulmonary function testing and normal values. *Eur Radiol* **19**, 2391-2402 (2009).
- 169 Bankier, A. A., De Maertelaer, V., Keyzer, C. & Gevenois, P. A. Pulmonary emphysema: Subjective visual grading versus objective quantification with

- macroscopic morphometry and thin-section CT densitometry. *Radiology* **211**, 851-858 (1999).
- 170 Park, K. J., Bergin, C. J. & Clausen, J. L. Quantitation of emphysema with three-dimensional CT densitometry: Comparison with two-dimensional analysis, visual emphysema scores, and pulmonary function test results. *Radiology* **211**, 541-547 (1999).
- 171 Galban, C. J. *et al.* Computed tomography-based biomarker provides unique signature for diagnosis of COPD phenotypes and disease progression. *Nat Med* **18**, 1711-1715 (2012).
- 172 Kirby, M. *et al.* A novel method of estimating small airway disease using inspiratory-to-expiratory computed tomography. *Respiration* **94**, 336-345 (2017).
- 173 Hoffman, E. A. *et al.* Pulmonary CT and MRI phenotypes that help explain chronic pulmonary obstruction disease pathophysiology and outcomes. *J Magn Reson Imaging* **43**, 544-557 (2016).
- 174 Ostridge, K. *et al.* Using novel computed tomography analysis to describe the contribution and distribution of emphysema and small airways disease in chronic obstructive pulmonary disease. *Ann Am Thorac Soc* **16**, 990-997 (2019).
- 175 Boes, J. L. *et al.* Parametric response mapping monitors temporal changes on lung CT scans in the subpopulations and intermediate outcome measures in COPD study (SPIROMICS). *Acad Radiol* **22**, 186-194 (2015).
- 176 Bhatt, S. P. *et al.* Association between functional small airway disease and FEV1 decline in chronic obstructive pulmonary disease. *Am J Respir Crit Care Med* **194**, 178-184 (2016).
- 177 Pompe, E. *et al.* Parametric response mapping on chest computed tomography associates with clinical and functional parameters in chronic obstructive pulmonary disease. *Respir Med* **123**, 48-55 (2017).
- 178 Vasilescu, D. M. *et al.* Noninvasive imaging biomarker identifies small airway damage in severe chronic obstructive pulmonary disease. *Am J Respir Crit Care Med* **200**, 575-581 (2019).
- 179 Zavaletta, V. *et al.* Characterizing patterns of fsad in asthma using an automated parametric response map algorithm [abstract]. *Am J Respir Crit Care Med* **193**, A2496 (2016).
- 180 Amelon, R. *et al.* Three-dimensional characterization of regional lung deformation. *J Biomech* **44**, 2489-2495 (2011).

- 181 Choi, S. *et al.* Registration-based assessment of regional lung function via volumetric CT images of normal subjects vs. Severe asthmatics. *J Appl Physiol* **115**, 730-742 (2013).
- 182 Choi, S. *et al.* Quantitative computed tomographic imaging-based clustering differentiates asthmatic subgroups with distinctive clinical phenotypes. *J Allergy Clin Immunol* (2017).
- 183 Choi, S. *et al.* Differentiation of quantitative CT imaging phenotypes in asthma versus COPD. *BMJ open respiratory research* **4**, e000252-e000252 (2017).
- 184 Murphy, D. M., Nicewicz, J. T., Zabbatino, S. M. & Moore, R. A. Local pulmonary ventilation using nonradioactive xenon-enhanced ultrafast computed tomography. *Chest* **96**, 799-804 (1989).
- 185 Chiro, G. D. *et al.* Tissue signatures with dual-energy computed tomography. *Radiology* **131**, 521-523 (1979).
- 186 Kong, X. *et al.* Xenon-enhanced dual-energy CT lung ventilation imaging: Techniques and clinical applications. *Am J Roentgenol* **202**, 309-317 (2014).
- 187 Remy-Jardin, M. *et al.* Thoracic applications of dual energy. *Semin Respir Crit Care Med* **35**, 64-73 (2014).
- 188 Chae, E. J. *et al.* Xenon ventilation CT with a dual-energy technique of dual-source CT: Initial experience. *Radiology* **248**, 615-624 (2008).
- 189 Chae, E. J. *et al.* Xenon ventilation imaging using dual-energy computed tomography in asthmatics: Initial experience. *Invest Radiol* **45**, 354-361 (2010).
- 190 Kim, W. W. *et al.* Xenon-enhanced dual-energy CT of patients with asthma: Dynamic ventilation changes after methacholine and salbutamol inhalation. *AJR Am J Roentgenol* **199**, 975-981 (2012).
- 191 Goo, H. W. & Yu, J. Redistributed regional ventilation after the administration of a bronchodilator demonstrated on xenon-inhaled dual-energy CT in a patient with asthma. *Korean J Radiol* **12**, 386-389 (2011).
- 192 Jung, J. W. *et al.* New insight into the assessment of asthma using xenon ventilation computed tomography. *Ann Allergy Asthma Immunol* **111**, 90-95 e92 (2013).
- 193 Park, H. W. *et al.* Xenon ventilation computed tomography and the management of asthma in the elderly. *Respirology* **19**, 389-395 (2014).
- 194 Park, E.-A. *et al.* Chronic obstructive pulmonary disease: Quantitative and visual ventilation pattern analysis at xenon ventilation CT performed by using a dual-energy technique. *Radiology* **256**, 985-997 (2010).

- 195 Lee, S. M. *et al.* Assessment of regional emphysema, air-trapping and xenon-ventilation using dual-energy computed tomography in chronic obstructive pulmonary disease patients. *Eur Radiol* **27**, 2818-2827 (2017).
- 196 Petersson, J., Sánchez-Crespo, A., Larsson, S. A. & Mure, M. Physiological imaging of the lung: Single-photon-emission computed tomography (SPECT). *J Appl Physiol* **102**, 468-476 (2007).
- 197 Amis, T. C., Crawford, A. B., Davison, A. & Engel, L. A. Distribution of inhaled <sup>99m</sup>technetium labelled ultrafine carbon particle aerosol (Technegas) in human lungs. *Eur Respir J* **3**, 679-685 (1990).
- 198 Parker, J. A. *et al.* SNM practice guideline for lung scintigraphy 4.0. *J Nucl Med Technol* **40**, 57-65 (2012).
- 199 Ramanna, L. *et al.* Radioaerosol lung imaging in chronic obstructive pulmonary disease: Comparison with pulmonary function tests and roentgenography. *Chest* **68**, 634-640 (1975).
- 200 Taplin, G. V. *et al.* Early detection of chronic obstructive pulmonary disease using radionuclide lung-imaging procedures. *Chest* **71**, 567-575 (1977).
- 201 Engel, L. A., Landau, L., Taussig, L., Martin, R. R. & Sybrecht, G. Influence of bronchomotor tone on regional ventilation distribution at residual volume. *J Appl Physiol* **40**, 411-416 (1976).
- 202 Clague, H., Ahmad, D., Chamberlain, M. J., Morgan, W. K. & Vinitzki, S. Histamine bronchial challenge: Effect on regional ventilation and aerosol deposition. *Thorax* **38**, 668-675 (1983).
- 203 Bybel, B. *et al.* SPECT/CT imaging: Clinical utility of an emerging technology. *Radiographics* **28**, 1097-1113 (2008).
- 204 King, G. G., Eberl, S., Salome, C. M., Meikle, S. R. & Woolcock, A. J. Airway closure measured by a technegas bolus and SPECT. *Am J Respir Crit Care Med* **155**, 682-688 (1997).
- 205 King, G. G., Eberl, S., Salome, C. M., Young, I. H. & Woolcock, A. J. Differences in airway closure between normal and asthmatic subjects measured with single-photon emission computed tomography and technegas. *Am J Respir Crit Care Med* **158**, 1900-1906 (1998).
- 206 Farrow, C. E. *et al.* Airway closure on imaging relates to airway hyperresponsiveness and peripheral airway disease in asthma. *J Appl Physiol* **113**, 958-966 (2012).
- 207 Norberg, P. *et al.* Quantitative lung SPECT applied on simulated early COPD and humans with advanced COPD. *EJNMMI research* **3**, 28-28 (2013).

- 208 Bajc, M. *et al.* Grading obstructive lung disease using tomographic pulmonary scintigraphy in patients with chronic obstructive pulmonary disease (COPD) and long-term smokers. *Ann Nucl Med* **29**, 91-99 (2015).
- 209 Suga, K., Iwanaga, H., Tokuda, O., Okada, M. & Matsunaga, N. Intrabullous ventilation in pulmonary emphysema: Assessment with dynamic xenon-133 gas SPECT. *Nucl Med Commun* **33**, 371-378 (2012).
- 210 Newman, S., Salmon, A., Nave, R. & Drollmann, A. High lung deposition of <sup>99m</sup>Tc-labeled ciclesonide administered via HFA-MDI to patients with asthma. *Respir Med* **100**, 375-384 (2006).
- 211 Leach, C. L. *et al.* Characterization of respiratory deposition of fluticasone-salmeterol hydrofluoroalkane-134a and hydrofluoroalkane-134a beclomethasone in asthmatic patients. *Ann Allergy Asthma Immunol* **108**, 195-200 (2012).
- 212 Musch, G. & Venegas, J. G. Positron emission tomography imaging of regional pulmonary perfusion and ventilation. *Proc Am Thorac Soc* **2**, 522-509 (2005).
- 213 Kapoor, V., McCook, B. M. & Torok, F. S. An introduction to PET-CT imaging. *Radiographics* **24**, 523-543 (2004).
- 214 Quick, H. H. Integrated PET/MR. *J Magn Reson Imaging* **39**, 243-258 (2014).
- 215 Harris, R. S. *et al.* Regional pulmonary perfusion, inflation, and ventilation defects in bronchoconstricted patients with asthma. *Am J Respir Crit Care Med* **174**, 245-253 (2006).
- 216 Brudin, L. H. *et al.* Regional structure-function correlations in chronic obstructive lung disease measured with positron emission tomography. *Thorax* **47**, 914-921 (1992).
- 217 Chen, D. L. & Schuster, D. P. Imaging pulmonary inflammation with positron emission tomography: A biomarker for drug development. *Mol Pharm* **3**, 488-495 (2006).
- 218 Harris, R. S. *et al.* <sup>18</sup>F-fdg uptake rate is a biomarker of eosinophilic inflammation and airway response in asthma. *J Nucl Med* **52**, 1713-1720 (2011).
- 219 Rinck, P. A. in *Magnetic Resonance in Medicine: A Critical Introduction* (BoD, Germany, 2018).
- 220 Bergin, C. J., Glover, G. M. & Pauly, J. Magnetic resonance imaging of lung parenchyma. *J Thorac Imaging* **8**, 12-17 (1993).
- 221 Parent, A. *Carpenter's human neuroanatomy*. (Williams & Wilkins, 1996).

- 222 Bergin, C. J., Glover, G. M. & Pauly, J. Magnetic resonance imaging of lung parenchyma. *J Thorac Imaging* **8**, 12-17 (1993).
- 223 Bergin, C. J., Noll, D. C., Pauly, J. M., Glover, G. H. & Macovski, A. MR imaging of lung parenchyma: A solution to susceptibility. *Radiology* **183**, 673-676 (1992).
- 224 Ohno, Y. *et al.* Pulmonary high-resolution ultrashort TE MR imaging: Comparison with thin-section standard- and low-dose computed tomography for the assessment of pulmonary parenchyma diseases. *J Magn Reson Imaging* **43**, 512-532 (2016).
- 225 Ma, W. *et al.* Ultra-short echo-time pulmonary MRI: Evaluation and reproducibility in COPD subjects with and without bronchiectasis. *J Magn Reson Imaging* **41**, 1465-1474 (2015).
- 226 Sheikh, K. *et al.* Ultrashort echo time MRI biomarkers of asthma. *J Magn Reson Imaging* **45**, 1204-1215 (2017).
- 227 Rinck, P. A., Petersen, S. B. & Lauterbur, P. C. NMR imaging of fluorine-containing substances. 19-fluorine ventilation and perfusion studies. *Rofo* **140**, 239-243 (1984).
- 228 Wolf, U. *et al.* Fluorine-19 MRI of the lung: First human experiment in *Proc Intl Soc Magn Reson Imaging*.
- 229 Couch, M. J. *et al.* Pulmonary ultrashort echo time 19F MR imaging with inhaled fluorinated gas mixtures in healthy volunteers: Feasibility. *Radiology* **269**, 903-909 (2013).
- 230 Halaweish, A. F. *et al.* Perfluoropropane gas as a magnetic resonance lung imaging contrast agent in humans. *Chest* **144**, 1300-1310 (2013).
- 231 Gutberlet, M. *et al.* Free-breathing dynamic (19)f gas MR imaging for mapping of regional lung ventilation in patients with COPD. *Radiology* **286**, 1040-1051 (2018).
- 232 Saam, B. T. Magnetic resonance imaging with laser-polarized noble gases. *Nat Med* **2**, 358-359 (1996).
- 233 Albert, M. S. *et al.* Biological magnetic resonance imaging using laser-polarized <sup>129</sup>Xe. *Nature* **370**, 199-201 (1994).
- 234 Walker, T. G. & Happer, W. Spin-exchange optical pumping of noble-gas nuclei. *Rev Mod Phys* **69**, 629 (1997).
- 235 Kauczor, H. U. *et al.* Normal and abnormal pulmonary ventilation: Visualization at hyperpolarized He-3 MR imaging. *Radiology* **201**, 564-568 (1996).
- 236 Shea, D. A. & Morgan, D. The helium-3 shortage: Supply, demand, and options for congress. (Congressional Research Service, Library of Congress, 2010).

- 237 Cho, A. Physics. Helium-3 shortage could put freeze on low-temperature research. *Science (New York, N.Y.)* **326**, 778-779 (2009).
- 238 Woods, J. C. Mine the moon for  $^3\text{He}$  MRI? Not yet. *J Appl Physiol* **114**, 705-706 (2013).
- 239 Hersman, F. W. *et al.* Large production system for hyperpolarized  $^{129}\text{Xe}$  for human lung imaging studies. *Acad Radiol* **15**, 683-692 (2008).
- 240 Nikolaou, P. *et al.* Near-unity nuclear polarization with an open-source  $^{129}\text{Xe}$  hyperpolarizer for NMR and MRI. *Proc Natl Acad Sci U S A* **110**, 14150-14155 (2013).
- 241 Norquay, G., Parnell, S. R., Xu, X., Parra-Robles, J. & Wild, J. M. Optimized production of hyperpolarized  $^{129}\text{Xe}$  at 2 bars for in vivo lung magnetic resonance imaging. *J Appl Phys* **113**, 044908 (2013).
- 242 Lutey, B. A. *et al.* Hyperpolarized  $^3\text{He}$  MR imaging: Physiologic monitoring observations and safety considerations in 100 consecutive subjects. *Radiology* **248**, 655-661 (2008).
- 243 Shukla, Y. *et al.* Hyperpolarized  $^{129}\text{Xe}$  magnetic resonance imaging: Tolerability in healthy volunteers and subjects with pulmonary disease. *Acad Radiol* **19**, 941-951 (2012).
- 244 Driehuys, B. *et al.* Chronic obstructive pulmonary disease: Safety and tolerability of hyperpolarized  $^{129}\text{Xe}$  MR imaging in healthy volunteers and patients. *Radiology* **262**, 279-289 (2012).
- 245 Polarean Imaging PLC. *Polarean imaging plc announces positive results from pivotal phase III clinical trials*, (2020).
- 246 Altes, T. A. *et al.* Ventilation imaging of the lung: Comparison of hyperpolarized helium-3 MR imaging with Xe-133 scintigraphy. *Acad Radiol* **11**, 729-734 (2004).
- 247 Svenningsen, S. *et al.* Hyperpolarized ( $^3\text{He}$  and ( $^{129}\text{Xe}$ ) MRI: Differences in asthma before bronchodilation. *J Magn Reson Imaging* **38**, 1521-1530 (2013).
- 248 Kirby, M. *et al.* Hyperpolarized  $^3\text{He}$  and  $^{129}\text{Xe}$  MR imaging in healthy volunteers and patients with chronic obstructive pulmonary disease. *Radiology* **265**, 600-610 (2012).
- 249 Stewart, N. J. *et al.* Comparison of ( $^3\text{He}$  and ( $^{129}\text{Xe}$ ) MRI for evaluation of lung microstructure and ventilation at 1.5t. *J Magn Reson Imaging* (2018).
- 250 Hamedani, H. *et al.* Regional fractional ventilation by using multibreath wash-in ( $^3\text{He}$ ) MR imaging. *Radiology* **279**, 917-924 (2016).

- 251 Horn, F. C., Rao, M., Stewart, N. J. & Wild, J. M. Multiple breath washout of hyperpolarized (129) Xe and (3) He in human lungs with three-dimensional balanced steady-state free-precession imaging. *Magn Reson Med* **77**, 2288-2295 (2017).
- 252 Kirby, M. *et al.* Hyperpolarized 3He magnetic resonance functional imaging semiautomated segmentation. *Acad Radiol* **19**, 141-152 (2012).
- 253 He, M. *et al.* Extending semiautomatic ventilation defect analysis for hyperpolarized (129)Xe ventilation MRI. *Acad Radiol* **21**, 1530-1541 (2014).
- 254 Zha, W. *et al.* Semiautomated ventilation defect quantification in exercise-induced bronchoconstriction using hyperpolarized helium-3 magnetic resonance imaging: A repeatability study. *Acad Radiol* **23**, 1104-1114 (2016).
- 255 Tustison, N. J. *et al.* Ventilation-based segmentation of the lungs using hyperpolarized (3)He MRI. *J Magn Reson Imaging* **34**, 831-841 (2011).
- 256 Guo, F. *et al.* Globally optimal co-segmentation of three-dimensional pulmonary 1H and hyperpolarized 3He MRI with spatial consistence prior. *Med Image Anal* **23**, 43-55 (2015).
- 257 Woodhouse, N. *et al.* Combined helium-3/proton magnetic resonance imaging measurement of ventilated lung volumes in smokers compared to never-smokers. *J Magn Reson Imaging* **21**, 365-369 (2005).
- 258 Tzeng, Y. S., Lutchen, K. & Albert, M. The difference in ventilation heterogeneity between asthmatic and healthy subjects quantified using hyperpolarized 3He MRI. *J Appl Physiol* **106**, 813-822 (2009).
- 259 Mathew, L. *et al.* Hyperpolarized 3He magnetic resonance imaging of chronic obstructive pulmonary disease: Reproducibility at 3.0 tesla. *Acad Radiol* **15**, 1298-1311 (2008).
- 260 Fain, S. B. *et al.* Evaluation of structure-function relationships in asthma using multidetector CT and hyperpolarized He-3 MRI. *Acad Radiol* **15**, 753-762 (2008).
- 261 He, M., Driehuys, B., Que, L. G. & Huang, Y. T. Using hyperpolarized 129Xe MRI to quantify the pulmonary ventilation distribution. *Acad Radiol* **23**, 1521-1531 (2016).
- 262 Zha, N. *et al.* Second-order texture measurements of (3)He ventilation MRI: Proof-of-concept evaluation of asthma bronchodilator response. *Acad Radiol* **23**, 176-185 (2016).
- 263 de Lange, E. E. *et al.* Evaluation of asthma with hyperpolarized helium-3 MRI: Correlation with clinical severity and spirometry. *Chest* **130**, 1055-1062 (2006).

- 264 Altes, T. A. *et al.* Hyperpolarized <sup>3</sup>He MR lung ventilation imaging in asthmatics: Preliminary findings. *J Magn Reson Imaging* **13**, 378-384 (2001).
- 265 Costella, S. *et al.* Regional pulmonary response to a methacholine challenge using hyperpolarized (<sup>3</sup>He) magnetic resonance imaging. *Respirology* **17**, 1237-1246 (2012).
- 266 Svenningsen, S. *et al.* What are ventilation defects in asthma? *Thorax* **69**, 63-71 (2014).
- 267 Zha, W. *et al.* Regional heterogeneity of lobar ventilation in asthma using hyperpolarized helium-3 MRI. *Acad Radiol* **25**, 169-178 (2018).
- 268 Samee, S. *et al.* Imaging the lungs in asthmatic patients by using hyperpolarized helium-3 magnetic resonance: Assessment of response to methacholine and exercise challenge. *J Allergy Clin Immunol* **111**, 1205-1211 (2003).
- 269 Niles, D. J. *et al.* Exercise-induced bronchoconstriction: Reproducibility of hyperpolarized <sup>3</sup>He MR imaging. *Radiology* **266**, 618-625 (2013).
- 270 Kruger, S. J. *et al.* Hyperpolarized helium-3 MRI of exercise-induced bronchoconstriction during challenge and therapy. *J Magn Reson Imaging* **39**, 1230-1237 (2014).
- 271 Svenningsen, S. *et al.* Pulmonary functional magnetic resonance imaging: Asthma temporal-spatial maps. *Acad Radiol* **21**, 1402-1410 (2014).
- 272 Teague, W. G., Tustison, N. J. & Altes, T. A. Ventilation heterogeneity in asthma. *J Asthma* **51**, 677-684 (2014).
- 273 Svenningsen, S., Nair, P., Guo, F., McCormack, D. G. & Parraga, G. Is ventilation heterogeneity related to asthma control? *Eur Respir J* **48**, 370-379 (2016).
- 274 Mummy, D. G. *et al.* Ventilation defect percent in helium-3 magnetic resonance imaging as a biomarker of severe outcomes in asthma. *J Allergy Clin Immunol* **141**, 1140-1141 e1144 (2018).
- 275 Svenningsen, S. *et al.* CT and functional MRI to evaluate airway mucus in severe asthma. *Chest* **155**, 1178-1189 (2019).
- 276 Young, H. M., Guo, F., Eddy, R. L., Maksym, G. & Parraga, G. Oscillometry and pulmonary MRI measurements of ventilation heterogeneity in obstructive lung disease: Relationship to quality of life and disease control. *J Appl Physiol (1985)* **125**, 73-85 (2018).
- 277 Mummy, D. *et al.* Image-guided bronchoscopy of regional ventilation heterogeneity in asthma as a means of assessing localized inflammatory response: Preliminary results [abstract]. *Am J Respir Crit Care Med* **197**, A2745 (2018).

- 278 Svenningsen, S. *et al.* Sputum eosinophilia and magnetic resonance imaging ventilation heterogeneity in severe asthma. *Am J Respir Crit Care Med* **197**, 876-884 (2018).
- 279 Thomen, R. P. *et al.* Regional ventilation changes in severe asthma after bronchial thermoplasty with (3)He MR imaging and CT. *Radiology* **274**, 250-259 (2015).
- 280 Svenningsen, S., Haider, E. A., Eddy, R. L., Parraga, G. & Nair, P. Normalisation of MRI ventilation heterogeneity in severe asthma by dupilumab. *Thorax* **74**, 1087-1088 (2019).
- 281 Hall, C. *et al.* Regional ventilation changes in severe asthma after bronchial thermoplasty [abstract]. *Am J Respir Crit Care Med* **197**, A6382 (2018).
- 282 Parraga, G. (NIH ClinicalTrials.gov, 2019).
- 283 Virgincar, R. S. *et al.* Quantitative analysis of hyperpolarized <sup>129</sup>Xe ventilation imaging in healthy volunteers and subjects with chronic obstructive pulmonary disease. *NMR Biomed* **26**, 424-435 (2013).
- 284 Capaldi, D. P. *et al.* Pulmonary imaging biomarkers of gas trapping and emphysema in COPD: (3)He MR imaging and CT parametric response maps. *Radiology* **279**, 597-608 (2016).
- 285 Pike, D. *et al.* Regional heterogeneity of chronic obstructive pulmonary disease phenotypes: Pulmonary (3)He magnetic resonance imaging and computed tomography. *COPD* **13**, 601-609 (2016).
- 286 Kirby, M. *et al.* Chronic obstructive pulmonary disease: Quantification of bronchodilator effects by using hyperpolarized (3)He MR imaging. *Radiology* **261**, 283-292 (2011).
- 287 Kirby, M. *et al.* COPD: Do imaging measurements of emphysema and airway disease explain symptoms and exercise capacity? *Radiology* **277**, 872-880 (2015).
- 288 Kirby, M., Pike, D., Coxson, H. O., McCormack, D. G. & Parraga, G. Hyperpolarized (3)He ventilation defects used to predict pulmonary exacerbations in mild to moderate chronic obstructive pulmonary disease. *Radiology* **273**, 887-896 (2014).
- 289 Kirby, M. *et al.* Pulmonary ventilation visualized using hyperpolarized helium-3 and xenon-129 magnetic resonance imaging: Differences in COPD and relationship to emphysema. *J Appl Physiol* **114**, 707-715 (2013).
- 290 Kirby, M. *et al.* Chronic obstructive pulmonary disease: Longitudinal hyperpolarized (3)He MR imaging. *Radiology* **256**, 280-289 (2010).

- 291 Kirby, M. *et al.* MRI ventilation abnormalities predict quality-of-life and lung function changes in mild-to-moderate COPD: Longitudinal TINCan study. *Thorax* **72**, 475-477 (2017).
- 292 Saam, B. T. *et al.* MR imaging of diffusion of (3)He gas in healthy and diseased lungs. *Magn Reson Med* **44**, 174-179 (2000).
- 293 Diaz, S. *et al.* Hyperpolarized 3He apparent diffusion coefficient MRI of the lung: Reproducibility and volume dependency in healthy volunteers and patients with emphysema. *J Magn Reson Imaging* **27**, 763-770 (2008).
- 294 Kirby, M. *et al.* Hyperpolarized 3He and 129Xe magnetic resonance imaging apparent diffusion coefficients: Physiological relevance in older never- and ex-smokers. *Physiol Rep* **2** (2014).
- 295 Wang, C. *et al.* Assessment of the lung microstructure in patients with asthma using hyperpolarized 3He diffusion MRI at two time scales: Comparison with healthy subjects and patients with COPD. *J Magn Reson Imaging* **28**, 80-88 (2008).
- 296 Gonem, S. *et al.* Characterization of acinar airspace involvement in asthmatic patients by using inert gas washout and hyperpolarized (3)helium magnetic resonance. *J Allergy Clin Immunol* **137**, 417-425 (2016).
- 297 Salerno, M. *et al.* Emphysema: Hyperpolarized helium 3 diffusion MR imaging of the lungs compared with spirometric indexes--initial experience. *Radiology* **222**, 252-260 (2002).
- 298 Kaushik, S. S. *et al.* Diffusion-weighted hyperpolarized 129Xe MRI in healthy volunteers and subjects with chronic obstructive pulmonary disease. *Magn Reson Med* **65**, 1154-1165 (2011).
- 299 Ley, S. *et al.* Functional evaluation of emphysema using diffusion-weighted 3helium-magnetic resonance imaging, high-resolution computed tomography, and lung function tests. *Invest Radiol* **39**, 427-434 (2004).
- 300 Diaz, S. *et al.* Validity of apparent diffusion coefficient hyperpolarized 3He-MRI using msct and pulmonary function tests as references. *Eur J Radiol* **71**, 257-263 (2009).
- 301 Mathew, L. *et al.* Hyperpolarized 3He magnetic resonance imaging: Preliminary evaluation of phenotyping potential in chronic obstructive pulmonary disease. *Eur J Radiol* **79**, 140-146 (2011).
- 302 Qing, K. *et al.* Regional mapping of gas uptake by blood and tissue in the human lung using hyperpolarized xenon-129 MRI. *J Magn Reson Imaging* **39**, 346-359 (2014).

- 303 Kaushik, S. S. *et al.* Single-breath clinical imaging of hyperpolarized (129)Xe in the airspaces, barrier, and red blood cells using an interleaved 3D radial 1-point dixon acquisition. *Magn Reson Med* **75**, 1434-1443 (2016).
- 304 Mugler, J. P., 3rd *et al.* MR imaging and spectroscopy using hyperpolarized 129Xe gas: Preliminary human results. *Magn Reson Med* **37**, 809-815 (1997).
- 305 Kaushik, S. S. *et al.* Probing the regional distribution of pulmonary gas exchange through single-breath gas- and dissolved-phase 129Xe MR imaging. *J Appl Physiol* **115**, 850-860 (2013).
- 306 Qing, K. *et al.* Assessment of lung function in asthma and COPD using hyperpolarized 129Xe chemical shift saturation recovery spectroscopy and dissolved-phase MRI. *NMR Biomed* **27**, 1490-1501 (2014).
- 307 Coleman, E. *et al.* Regional gas exchange function before and after glycopyrrolate/formoterol fumarate measured by hyperpolarized 129Xe MRI in chronic obstructive lung disease [abstract]. *Am J Respir Crit Care Med* **199**, A1122 (2019).
- 308 Mammarappallil, J. *et al.* Identification of gas exchange phenotypes using hyperpolarized 129Xe MRI in patients with chronic obstructive pulmonary disease (COPD) [abstract]. *Am J Respir Crit Care Med* **199**, A2406 (2019).
- 309 Bauman, G. *et al.* Non-contrast-enhanced perfusion and ventilation assessment of the human lung by means of fourier decomposition in proton MRI. *Magn Reson Med* **62**, 656-664 (2009).
- 310 Capaldi, D. P. I. *et al.* Free-breathing functional pulmonary MRI: Response to bronchodilator and bronchoprovocation in severe asthma. *Acad Radiol* (2017).
- 311 Capaldi, D. P. *et al.* Free-breathing pulmonary 1H and hyperpolarized 3He MRI: Comparison in COPD and bronchiectasis. *Acad Radiol* **22**, 320-329 (2015).
- 312 Kaireit, T. F. *et al.* Comparison of quantitative regional ventilation-weighted fourier decomposition MRI with dynamic fluorinated gas washout MRI and lung function testing in COPD patients. *J Magn Reson Imaging* **47**, 1534-1541 (2018).
- 313 Voskrebenev, A. *et al.* Feasibility of quantitative regional ventilation and perfusion mapping with phase-resolved functional lung (PREFUL) MRI in healthy volunteers and COPD, CTEPH, and CF patients. *Magn Reson Med* **79**, 2306-2314 (2018).
- 314 Vogel-Claussen, J. *et al.* Effect of indacaterol/glycopyrronium on pulmonary perfusion and ventilation in hyperinflated patients with chronic obstructive pulmonary disease (CLAIM). A double-blind, randomized, crossover trial. *Am J Respir Crit Care Med* **199**, 1086-1096 (2019).

- 315 Guo, F., Capaldi, D. P. I., McCormack, D. G., Fenster, A. & Parraga, G. A framework for Fourier-decomposition free-breathing pulmonary (1)h MRI ventilation measurements. *Magn Reson Med* **81**, 2135-2146 (2019).

## CHAPTER 2

### 2 OSCILLOMETRY AND PULMONARY MAGNETIC RESONANCE IMAGING IN ASTHMA AND COPD

*To better understand the biomechanical impacts of asthma and how this compares to COPD, we evaluated and compared oscillometry and MRI ventilation defects in participants with asthma and COPD as well as never-smokers without asthma and ex-smokers without COPD.*

*The contents of this chapter were previously published in the journal Physiological Reports: RL Eddy, A Westcott, GN Maksym, G Parraga, RJ Dandurand. Oscillometry and Pulmonary Magnetic Resonance Imaging in Asthma and COPD. Physiol Rep. 2019;7(1):e13955. This article is available under the terms of the Creative Commons Attribution License.*

#### 2.1 Introduction

First developed over 60 years ago,<sup>1</sup> oscillometry has re-emerged as a way to generate clinical measurements in patients with obstructive lung disease because minimal coaching and patient effort is required. Moreover, oscillometry is well-tolerated in young and old patients across disease severities<sup>2</sup> and is sensitive to small airway abnormalities.<sup>3</sup> Oscillometry also provides a non-invasive way<sup>4</sup> to reveal lung pathologies that result in ventilation heterogeneity<sup>5-7</sup> by directly measuring resistance and reactance as functions of frequency. It is well established that in asthma, respiratory-system resistance responds to bronchodilator inhalation<sup>8-11</sup> and is frequency-dependent.<sup>12-14</sup> The frequency dependence of resistance has also been observed in patients with chronic obstructive pulmonary disease (COPD),<sup>15</sup> in whom low frequency resistance also diminishes after bronchodilation.<sup>8,9</sup>

In patients with asthma and COPD, reactance is more negative at low frequencies.<sup>16</sup> The area under the reactance curve can be quantified as the reactance area ( $A_x$ )<sup>17</sup> which is determined by the reactance value measured at the lowest frequency, the resonant frequency, and the shape of the low frequency reactance curve.  $A_x$  measurements correlate strongly with the frequency dependence of resistance<sup>18</sup> and in asthmatics,  $A_x$  detects bronchodilator<sup>8</sup> and bronchial challenge<sup>19</sup> responses in the absence of low frequency reactance changes. Furthermore,  $A_x$  has been suggested as a useful tool for early disease

screening and monitoring in COPD, and may be more sensitive to therapy response than the frequency dependence of resistance.<sup>20</sup>

X-ray computed tomography (CT) airway measurements were previously shown to be related to oscillometry measurements of resistance in asthma<sup>21</sup> and COPD.<sup>22</sup> Quantitative CT measurements of emphysema have also been shown to be related to oscillometry-measured reactance in COPD<sup>22</sup> and there are differences in the relationships between CT measurements and respiratory impedance in different COPD phenotypes.<sup>23</sup> Magnetic resonance imaging (MRI) using inhaled noble gases was also recently used to discern the relationships between low frequency resistance and elastance as well as the frequency dependence of resistance with MRI signal intensity coefficients of variation.<sup>24</sup> Another study showed a relationship between MRI ventilation defect percent (VDP) and the frequency-dependence of resistance in COPD patients.<sup>25</sup>

While these previous results are intriguing, no large-scale, controlled study has investigated a diversity of patients across a spectrum of disease severities to ascertain the relationships between experimental oscillometry measurements and imaging biomarkers of airway and parenchymal disease. This is important because in patients with asthma and COPD, airway and parenchymal abnormalities both contribute to symptomatic derangements in lung function and poor exercise capacity. In recent years, there has been modest clinical support for experimental impedance measurements as a way to evaluate patients.<sup>20,26</sup> Accordingly, our objective was to investigate the relationships between oscillometry measurements including resistance, reactance and the frequency dependence of resistance as well as  $A_x$  with MRI ventilation defect measurements across a wide variety of patients. In contrast with previous investigations,<sup>24,25,27</sup> here we evaluated participants with asthma and those with COPD (with and without emphysema) as well as control groups of never-smokers without asthma and ex-smokers without COPD.

## 2.2 Materials and Methods

### 2.2.1 Study Participants and Design

We evaluated never-smokers aged 60 to 90 years, asthmatics aged 18 to 70 years and ex-smokers with and without COPD aged 50 to 90 years who provided written informed consent to study protocols approved by the local research ethics board and Health Canada and registered (NCT02483403, NCT02279329, NCT02351141 <https://clinicaltrials.gov>). All subjects underwent a single three-hour study visit including spirometry, plethysmography, oscillometry and MRI. Some of these subjects were previously evaluated and results published.<sup>25</sup> Never-smokers performed all testing without administration of a short-acting bronchodilator. Participants with asthma and all ex-smokers performed all testing after administration of a short-acting bronchodilator. In addition, all ex-smokers underwent post-bronchodilator thoracic CT. Post-bronchodilator testing was performed 20 minutes after administration of four inhaled doses of 100 µg Novo-Salbutamol HFA (Teva Novopharm Ltd., Toronto, ON, Canada) through a pressurized metered-dose inhaler using an *AeroChamber Plus* spacer (Trudell Medical International, London, ON, Canada).

### 2.2.2 Pulmonary Function Tests

Spirometry and plethysmography were performed using a *MedGraphics Elite Series* plethysmograph (MGC Diagnostics Corporation, St. Paul, MN, USA). Spirometry was performed according to American Thoracic Society (ATS)/European Respiratory Society (ERS) guidelines<sup>28</sup> to measure the forced expiratory volume in one second (FEV<sub>1</sub>), forced vital capacity (FVC) and FEV<sub>1</sub>/FVC, while plethysmography was performed to measure lung volumes and airways resistance (R<sub>aw</sub>). For never-smokers and all ex-smokers, the diffusing capacity of the lung for carbon monoxide (DL<sub>CO</sub>) was also measured using a stand-alone gas analyzer attached to the plethysmograph. For post-bronchodilator testing in asthma, ex-smoker and COPD subgroups, participants withheld short-acting β-agonists for 6 hours, long-acting β-agonists for 12 hours and long-acting muscarinic antagonists for 24 hours before their study visit.

### 2.2.3 Oscillometry

Oscillometry was performed using the *tremoFlo C-100* Airwave Oscillometry System (Thorasys, Montreal, QC, Canada) with the non-harmonic composite airwaves in the adult frequency range consisting of 5, 11, 13, 17, 19, 23, 29, 31 and 37 Hz to measure total respiratory system resistance at 5 Hz ( $R_5$ ), frequency-dependence of resistance as  $R$  at 5 Hz minus  $R$  at 19 Hz ( $R_{5-19}$ ), reactance at 5 Hz ( $X_5$ ), resonant frequency ( $f_{res}$ ) and  $A_X$ .  $A_X$  was calculated by integrating the reactance curve from 5 Hz to  $f_{res}$  and when  $f_{res}$  was greater than 37 Hz, the reactance curve was truncated at 37 Hz and integrated up to that point. Participants were seated comfortably with legs uncrossed and supported their chin and cheeks with their hands to limit upper airway shunt. Oscillometry measurements were acquired over 16 seconds and repeated for three acceptable and repeatable tests, as judged by a coefficient of variation in resistance at 5 Hz ( $CV_{R5}$ ) of  $< 15\%$ . Artefacts were automatically identified and removed by the manufacturer's automated algorithms. Calibration of the oscillometry unit was performed daily using the vendor-provided nominal 2 cmH<sub>2</sub>O·s/L reference test load.

### 2.2.4 Image Acquisition and Analysis

All subjects underwent anatomical proton ( $^1\text{H}$ ) followed by hyperpolarized  $^3\text{He}$  static ventilation MRI (within five minutes) using a whole body 3T system (MR750 Discovery, General Electric Healthcare, Milwaukee, WI) with broadband imaging capability as previously described.<sup>29</sup>  $^3\text{He}$  gas was polarized to 30-40% polarization (HeliSpin; Polarean Inc., Durham, NC, USA) and diluted with  $\text{N}_2$  gas to 25%  $^3\text{He}$  by volume. Subjects were positioned supine in the scanner with their arms above their head and instructed to inhale 1.0 L of gas (100%  $\text{N}_2$  for  $^1\text{H}$  MRI,  $^3\text{He}/\text{N}_2$  mixture for  $^3\text{He}$  MRI) from functional residual capacity (FRC) and coronal images were acquired in 8-15 seconds under breath-hold conditions. For all image acquisition, FRC was assumed to be the lung volume at end tidal expiration.

Hyperpolarized  $^3\text{He}$  MR images were analyzed using in-house segmentation software as previously described.<sup>30</sup> Briefly, a single user placed seeds on the  $^1\text{H}$  and  $^3\text{He}$  images to

label the lung and the surrounding background tissue and image registration and segmentation were completed automatically.  $^3\text{He}$  images were segmented into five clusters of signal intensity using three-dimensional k-means clustering,<sup>31</sup> and the ventilation defect percent (VDP) was quantified as the ventilation defect volume normalized to the thoracic cavity volume.

Ex-smoker participants were transported from the MRI suite to the CT suite by wheelchair to avoid exercise-induced dilatation of the airways. Thoracic CT volumes were acquired within ten minutes of completion of MRI using a 64-slice LightSpeed VCT system (General Electric Healthcare) as previously described<sup>32</sup> under breath-hold conditions after full inspiration. The total effective dose for each CT scan was 1.8 mSv as calculated using the manufacturer's settings and the ImPACT patient dosimetry calculator (based on the UK Health Protection Agency NRPB-SR250 software).

Thoracic CT images were analyzed using Pulmonary Workstation 2.0 (VIDA Diagnostics Inc., Coralville, IA, USA) to quantify emphysema using the relative area of the lung < -950 Hounsfield units ( $\text{RA}_{950}$ ). An  $\text{RA}_{950}$  threshold of 6.8% was used to stratify COPD subjects with and without CT evidence of emphysema.<sup>33</sup>

### 2.2.5 Statistical Analysis

Data were tested for normality using the Shapiro-Wilk test using IBM SPSS Statistics 25.0 (IBM Corporation, Armonk, NY, USA) and when not normally distributed, non-parametric statistics were performed. One-way ANOVA and Kruskal-Wallis H test were performed for group-wise differences with post-hoc least significant difference and Holm-Bonferroni correction to adjust for multiple comparisons and Fisher's exact test was used for categorical variables using SPSS. Univariate relationships were evaluated using Pearson correlations ( $r$ ) for normally distributed data and Spearman correlations ( $\rho$ ) when the data were not normally distributed using GraphPad Prism 7.00 (GraphPad Software, La Jolla, CA, USA). Multivariable models were generated in SPSS using the enter approach to determine the contributions of  $R_5$ ,  $R_{5-19}$ ,  $X_5$  and  $A_X$  to VDP using age, sex and body mass index (BMI) as covariates for four separate models: (1) all subjects, (2) never-smokers and ex-smokers with and without COPD, (3) ex-smokers with and without COPD, and (4)

asthmatics only. Results were considered statistically significant when the probability of making a Type I error was less than 5% ( $p < 0.05$ ).

## 2.3 Results

We evaluated 175 participants including 42 elderly never-smokers ( $74 \pm 7$  years), 49 participants with asthma ( $48 \pm 12$  years;  $n=14$  treatment steps 1-2,  $n=35$  treatment steps 3-4 as per the Global Initiative for Asthma [GINA] guidelines<sup>34</sup>), 28 ex-smokers without COPD ( $70 \pm 9$  years) and 56 ex-smokers with COPD ( $73 \pm 9$  years;  $n=18$  mild [GOLD I],  $n=22$  moderate [GOLD II],  $n=16$  severe [GOLD III-IV]). **Table 2-1** shows demographic, pulmonary function test and imaging measurements for never-smokers, asthma participants, ex-smokers and COPD participants and between-group differences are shown in **Figure 2-1** for select data. We note that for 10 participants,  $f_{res}$  was greater than 37 Hz ( $n=1$  asthma,  $n=9$  COPD). Participants with COPD had significantly worse post-bronchodilator pulmonary function than never-smoker and ex-smoker participants, whereas participants with asthma did not have significantly different post-bronchodilator oscillometry measurements than never-smokers and ex-smokers. There were no significant differences between never-smoker and ex-smoker subgroups.

**Table 2-1** Participant demographics

<b>Parameter</b>	<b>Never-smokers</b>	<b>Asthma</b>	<b>Ex-smokers</b>	<b>COPD</b>	<b>Sig diff*</b>
<b>Mean (±SD)</b>	<b>(n=42)</b>	<b>(n=49)</b>	<b>(n=28)</b>	<b>(n=56)</b>	<b>(p)</b>
Age years	74 (7)	48 (13)	70 (9)	73 (9)	< <b>0.0001</b>
Male n (%)	21 (50)	19 (39)	16 (57)	36 (64)	0.1
BMI kg/m <sup>2</sup>	27 (4)	28 (5)	31 (4)	26 (4)	< <b>0.0001</b>
FEV <sub>1</sub> % <sub>pred</sub>	107 (18)	77 (21)	102 (19)	68 (27)	< <b>0.0001</b>
FVC % <sub>pred</sub>	103 (15)	88 (15)	95 (19)	92 (21)	<b>0.002</b>
FEV <sub>1</sub> /FVC %	77 (6)	69 (13)	80 (6)	53 (12)	< <b>0.0001</b>
RV % <sub>pred</sub>	98 (22)	121 (33)	100 (21)	148 (47)	< <b>0.0001</b>
TLC % <sub>pred</sub>	100 (13)	102 (15)	96 (13)	113 (18)	< <b>0.0001</b>
RV/TLC % <sub>pred</sub>	96 (17)	118 (23)	104 (16)	129 (26)	< <b>0.0001</b>
DL <sub>CO</sub> % <sub>pred</sub>	90 (16)	-	87 (17)	61 (23)	< <b>0.0001</b>
R <sub>aw</sub> % <sub>pred</sub>	83 (38)	105 (51)	65 (24)	117 (49)	< <b>0.0001</b>
R <sub>5</sub> cmH <sub>2</sub> O·s/L	3.59 (1.68)	4.25 (1.49)	3.32 (1.12)	3.64 (1.23)	0.7
R <sub>5-19</sub> cmH <sub>2</sub> O·s/L	0.54 (0.76)	0.82 (0.87)	0.36 (0.54)	0.96 (0.79)	<b>0.001</b>
X <sub>5</sub> cmH <sub>2</sub> O·s/L	-1.41 (0.88)	-1.86 (1.26)	-1.42 (0.72)	-2.41 (1.57)	<b>0.001</b>
f <sub>res</sub> Hz <sup>†</sup>	19.77 (7.40)	19.53 (6.86)	20.20 (5.78)	23.66 (7.67)	<b>0.001</b>
A <sub>X</sub> cmH <sub>2</sub> O/L	12.94 (14.94)	14.38 (14.90)	9.79 (7.57)	23.30 (19.96)	<b>0.008</b>
VDP %	3 (2)	5 (6)	5 (4)	19 (12)	< <b>0.0001</b>

SD=standard deviation; Sig diff=significance of difference; BMI=body mass index; FEV<sub>1</sub>=forced expiratory volume in one second; %<sub>pred</sub>=percent predicted; FVC=forced vital capacity; RV=residual volume; TLC=total lung capacity; DL<sub>CO</sub>=diffusing capacity of the lung for carbon monoxide; R<sub>aw</sub>=airways resistance; R<sub>5</sub>=respiratory system resistance at 5 Hz; R<sub>5-19</sub>=frequency dependence of resistance; X<sub>5</sub>=respiratory system reactance at 5 Hz; f<sub>res</sub>=resonant frequency; A<sub>X</sub>=reactance area; VDP=ventilation defect percent.

Pre-bronchodilator values shown for never-smokers and post-bronchodilator values shown for asthmatics, ex-smokers and COPD subjects.

\*Significance of difference calculated using one-way ANOVA for parametric variables and Kruskal-Wallis H test for non-parametric variables; significant values are bolded.

<sup>†</sup>n=42 for never-smokers, n=48 for asthma, n=28 for ex-smokers, n=47 for COPD; f<sub>res</sub>> 37 Hz for remaining subjects.

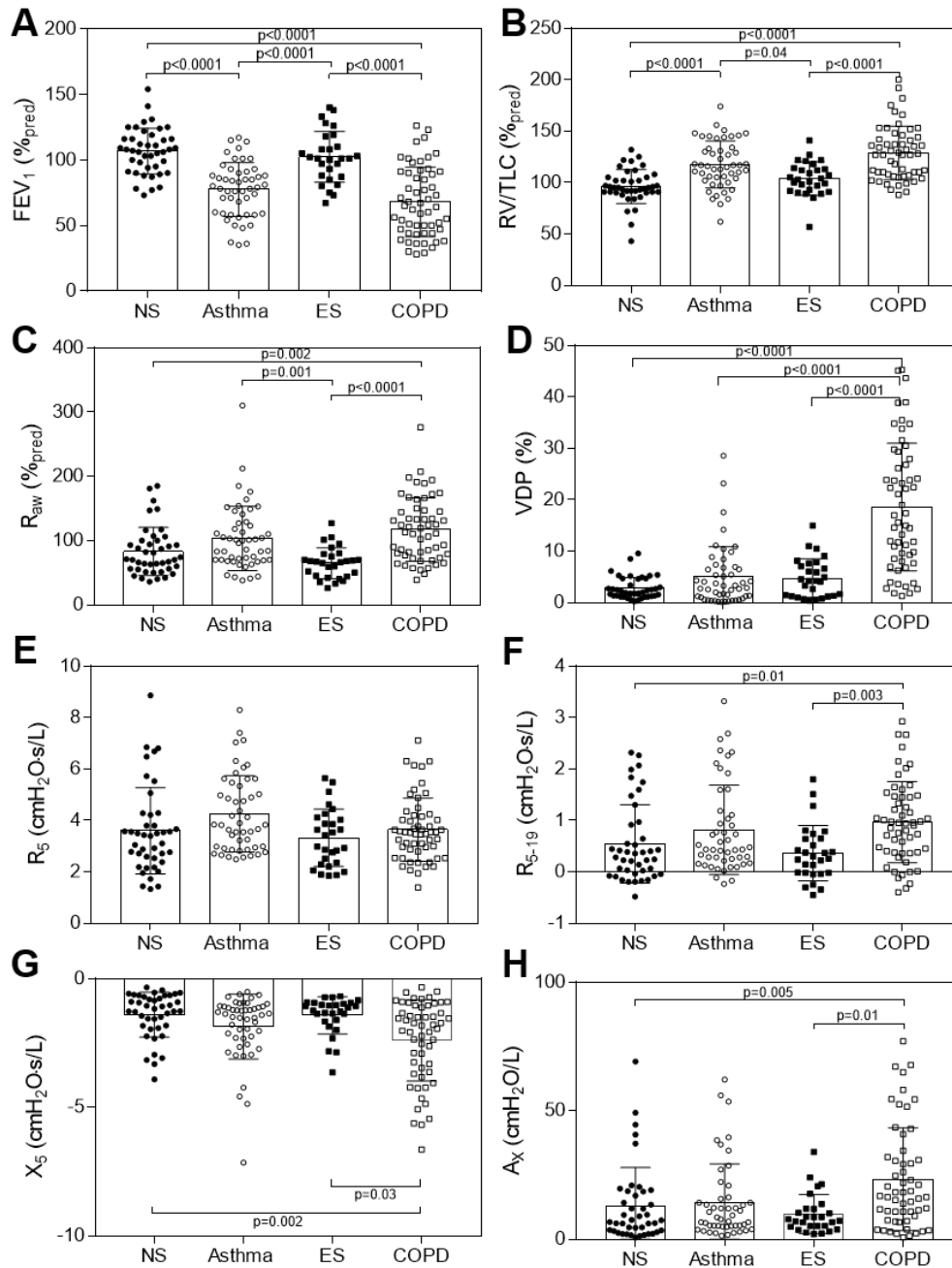


**Figure 2-1** Pulmonary function test and MRI VDP measurements

A) Significantly lower FEV<sub>1</sub> in asthma and COPD compared to never-smokers and ex-smokers. B) Significantly greater RV/TLC in asthma and COPD compared to never-smokers and ex-smokers. C) Significantly greater R<sub>aw</sub> in asthma as compared to ex-smokers and COPD subjects and significantly greater R<sub>aw</sub> in COPD as compared to never and ex-smokers. D) Significantly greater VDP in COPD as compared to all other subgroups. E) R<sub>5</sub> not significantly different between all subgroups. F) Significantly greater R<sub>5-19</sub>, and, G) Significantly more negative X<sub>5</sub>, and, H) significantly greater A<sub>x</sub> in COPD as compared to never- and ex-smokers.

**Figure 2-2** shows  $^3\text{He}$  MRI ventilation defects and oscillometry plots for two representative participants in each group: one with low (normal) VDP and one with greater (abnormal) VDP. For participants with asthma and COPD, worse ventilation heterogeneity qualitatively reflected increased frequency dependence of resistance and reactance as well as greater  $A_X$ . Increased ventilation heterogeneity in never-smokers and ex-smokers without COPD, however, did not reflect qualitatively apparent changes in oscillometry. As shown quantitatively in **Figure 2-3**, in asthma and COPD participants, post-bronchodilator VDP was significantly related to  $R_{5-19}$ ,  $X_5$  and  $A_X$ , but not  $R_5$ . For never-smokers, VDP was significantly negatively related to  $R_5$  only and there were no relationships in ex-smokers (not shown).

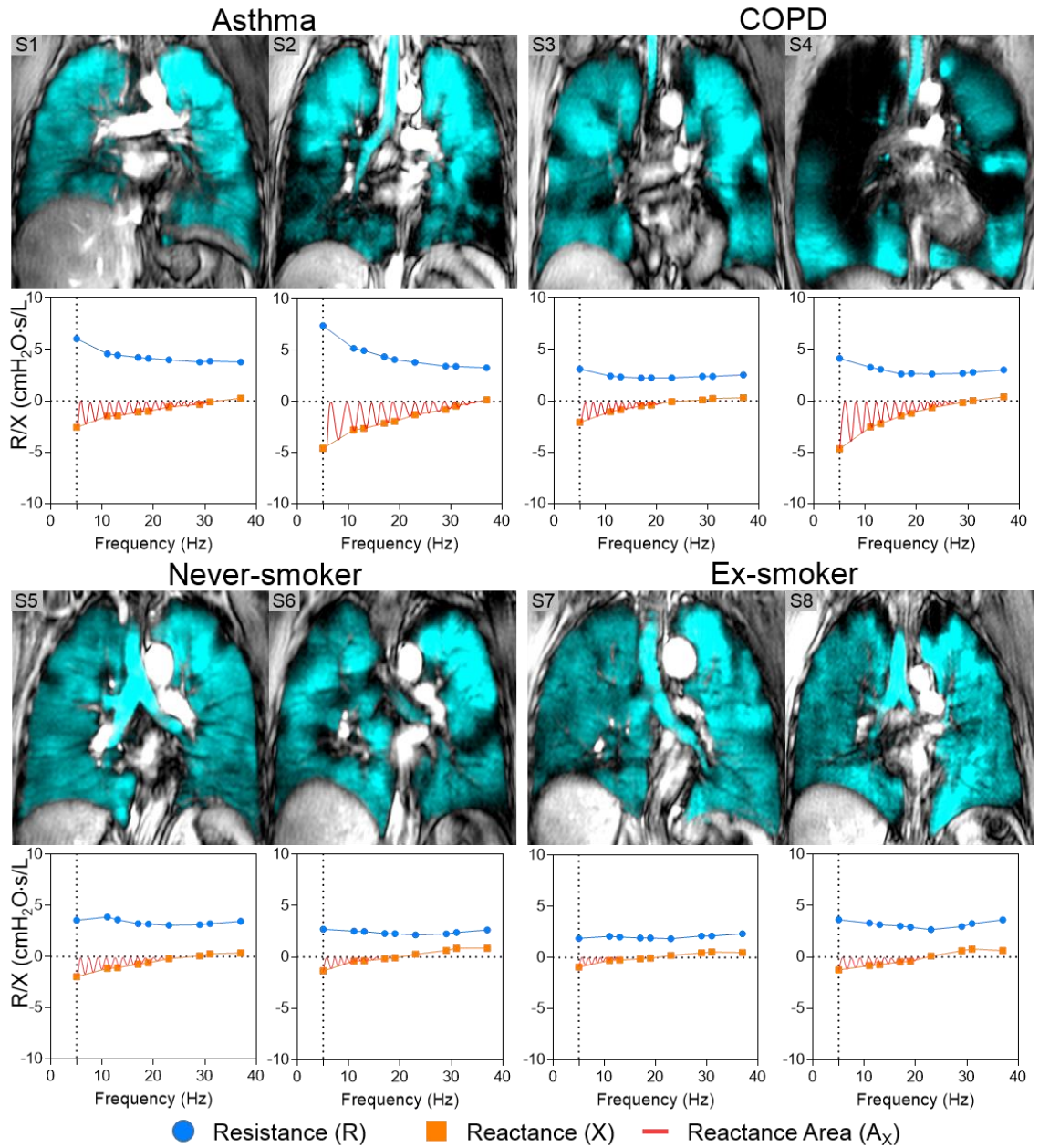


**Figure 2-2** Relationships between MRI ventilation heterogeneity and impedance measurements in representative subjects  
 Centre slice coronal static ventilation  $^3\text{He}$  MRI (cyan) co-registered to anatomical  $^1\text{H}$  (grey-scale) and corresponding oscillometry plots for two representative asthma, COPD, never-smokers and ex-smokers.

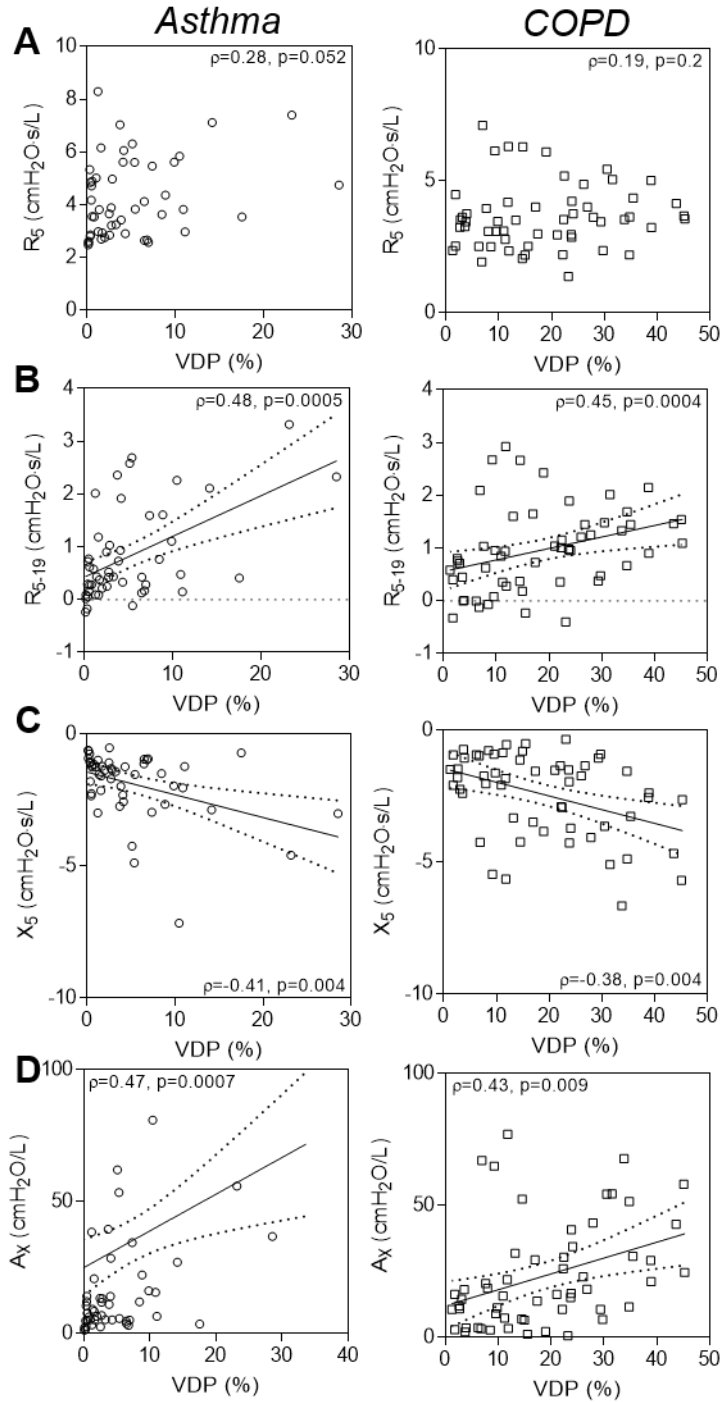


**Figure 2-3** Quantitative relationships between MRI VDP and impedance measurements  
 A) VDP was not significantly related to  $R_5$  in asthma nor in COPD subjects. B) VDP was significantly related to  $R_{5-19}$ , and, C)  $X_5$  and, D)  $A_x$  in asthma and COPD participants.

**Table 2-2** shows multivariable models that predict VDP from oscillometric parameters  $R_5$ ,  $R_{5-19}$ ,  $X_5$  and  $A_X$ .  $R_5$  ( $\beta=-0.22$ ,  $p=0.01$ ) and  $X_5$  ( $\beta=-0.34$ ,  $p=0.03$ ) significantly added to the prediction of VDP for all subjects (Model 1:  $R=0.63$ ,  $R^2=0.39$ ,  $p<0.0001$ ). For never-smokers and ex-smokers with and without COPD,  $R_5$  ( $\beta=-0.48$ ,  $p=0.001$ ),  $R_{5-19}$  ( $\beta=0.35$ ,  $p=0.03$ ) and  $X_5$  ( $\beta=-0.41$ ,  $p=0.03$ ) significantly added to the prediction of VDP (Model 2:  $R=0.66$ ,  $R^2=0.44$ ,  $p<0.0001$ ), whereas for only ex-smokers with and without COPD, the overall model was significant (Model 3:  $R=0.62$ ,  $R^2=0.38$ ,  $p<0.0001$ ) but none of the oscillometry parameters significantly added to the model. The overall model was also significant for asthmatic participants only (Model 4:  $R=0.65$ ,  $R^2=0.43$ ,  $p=0.001$ ) but none of the oscillometry parameters significantly added to the model.

**Table 2-2** Multivariable models to predict VDP from oscillometry

Variable	Unstandardized		Standardized	p
	B	Standard Error	$\beta$	
<b>MODEL 1: All subjects, n=175</b> ( $R=0.63$ ; $R^2=0.39$ , $p<0.0001$ )				
$R_5$	-1.98	0.77	-0.22	<b>0.01</b>
$R_{5-19}$	1.81	1.61	0.15	0.3
$X_5$	-2.75	1.26	-0.34	<b>0.03</b>
$A_X$	0.13	0.11	0.21	0.2
<b>MODEL 2: Never-smokers, ex-smokers with and without COPD, n=126</b> ( $R=0.66$ , $R^2=0.44$ , $p<0.0001$ )				
$R_5$	-3.96	1.17	-0.48	<b>0.001</b>
$R_{5-19}$	5.14	2.35	0.35	<b>0.03</b>
$X_5$	-3.55	1.63	-0.41	<b>0.03</b>
$A_X$	0.10	0.13	0.15	0.5
<b>MODEL 3: Ex-smokers with and without COPD, n=84</b> ( $R=0.62$ ; $R^2=0.38$ , $p<0.0001$ )				
$R_5$	-2.95	1.93	-0.29	0.1
$R_{5-19}$	6.24	3.41	0.39	0.07
$X_5$	-1.16	2.20	-0.14	0.6
$A_X$	0.18	0.17	0.27	0.3
<b>MODEL 4: Asthma only, n=49</b> ( $R=0.65$ , $R^2=0.43$ , $p=0.001$ )				
$R_5$	-1.28	0.84	-0.20	0.1
$R_{5-19}$	3.33	1.85	0.49	0.08
$X_5$	1.15	1.36	0.24	0.4
$A_X$	0.14	0.13	0.36	0.3

VDP=ventilation defect percent;  $R_5$ =resistance at 5 Hz;  $R_{5-19}$ =resistance at 5 Hz minus resistance at 19 Hz;  $X_5$ =reactance at 5 Hz;  $A_X$ =reactance area.

Covariates: age, sex, BMI

Of the 56 COPD participants evaluated, 33 had CT evidence of emphysema ( $RA_{950} \geq 6.8\%$ <sup>33</sup>) and 23 had no CT evidence of emphysema ( $RA_{950} < 6.8\%$ ). VDP was not significantly related to  $R_5$  regardless of the presence of emphysema, but VDP was related to  $A_x$  in COPD with ( $\rho=0.39$ ,  $p=0.02$ ) and without emphysema ( $\rho=0.43$ ,  $p=0.04$ ). VDP and  $R_{5-19}$  were significantly related in COPD subjects without emphysema only ( $\rho=0.54$ ,  $p=0.008$ ), and significantly related to  $X_5$  in COPD subjects with emphysema only ( $\rho=-0.36$ ,  $p=0.04$ ). There was no CT evidence of emphysema (all  $RA_{950} < 6.8\%$ ) in ex-smokers without spirometry evidence of airflow limitation based on GOLD criteria of  $FEV_1/FVC < 0.7$ .<sup>35</sup>

## 2.4 Discussion

We evaluated oscillometry and hyperpolarized  $^3\text{He}$  MRI measurements in a relatively large group of patients with asthma and COPD as well as two control groups and made four important observations: 1) in asthma and COPD participants, VDP was significantly but weakly correlated with  $R_{5-19}$ ,  $X_5$  and  $A_x$ , but not  $R_5$ , 2) in COPD patients without emphysema, VDP was related only to  $R_{5-19}$  and  $A_x$ , and only  $X_5$  and  $A_x$  in COPD patients with emphysema, 3) in an ex-smoker control group, there were no significant relationships while in never-smokers, only VDP and  $R_5$  were related, and, 4)  $A_x$  was weakly related to VDP in all subgroups with airflow obstruction, demonstrating its sensitivity to airflow obstruction but not specificity to type of obstruction.

The relationship between oscillometry and MRI VDP with quality-of-life measurements was previously investigated in 100 patients<sup>25</sup> and this previous work was in agreement with our observations. The fact that there were no significant relationships between VDP and oscillometry in the control subgroups except for  $R_5$  and VDP in never-smokers is also congruent with previous results.<sup>25</sup> Based on this previous work, our results were not unexpected.  $R_5$  reflects the resistance of the entire respiratory system including all airways (and not just the small airways or the larger airways) and this may explain why significant relationships with VDP were not present.  $R_5$  was also not significantly different between the four subgroups, whereas  $R_{5-19}$ ,  $X_5$ ,  $A_x$  as well as plethysmography-measured airways resistance ( $R_{aw}$ ) were. This suggests that  $R_5$  is not sensitive to the differences in

resistance in our patient population and this could be because much of the resistance in these patients may be due to the peripheral airways and this effect is overshadowed in the  $R_5$  signal. Oscillometry measurements that reflect the heterogeneity of airway narrowing ( $R_{5-19}$ ) as well as  $X_5$  and  $A_X$ <sup>36,37</sup> were all related to VDP in asthma and all COPD patients, and none of these relationships were detected in never- or ex-smokers. Notably, ventilation defects in severe COPD were previously shown to be related to both emphysema and small airways disease<sup>38,39</sup> so the negative relationship between VDP and  $X_5$  in COPD was not surprising. This was not previously observed<sup>25</sup> perhaps due to the current study's larger sample size across all grades of COPD severity. It has been shown in experimental studies in humans and animals however, that the major influence of heterogeneity is its impact on resistance and elastance between 0.1 – 5 Hz,<sup>40-42</sup> whereas our system is limited to 5 Hz and above. We are thus only capturing the 'tail-end' of the impact of heterogeneities using  $R_{5-19}$  and this may explain the weak correlations observed.

To better understand how oscillometry and MRI VDP measurements are related and may explain the biomechanical impact of obstructive lung disease in patients, we generated multivariable models. We were surprised to observe that  $R_5$  significantly contributed to the models with all subjects (Model 1) and in never-smokers and ex-smokers with and without COPD (Model 2).  $R_5$  did not significantly contribute to the models in ex-smokers with and without COPD (Model 3) or in asthmatics (Model 4). Based on these differences it is possible that the  $R_5$  results were being driven by the never-smoker subgroup in whom there is no airflow obstruction. There were no significant coefficients in Model 3 and 4 which may be due to the smaller subgroup sizes which limited power to detect significant contributions. However,  $R_{5-19}$  has the greatest relative influence on VDP in Models 3 and 4 which did not include the never-smoker group.

COPD patients can be phenotyped based on the presence of airways disease and emphysema<sup>43</sup> and these phenotypes also reflect differences in lung biomechanics and function.<sup>23</sup> We observed differences in the relationships between VDP and oscillometry measurements in COPD patients with and without emphysema, although it is likely that all COPD patients had airways disease too. The fact that  $X_5$  and  $A_X$  were related to VDP in emphysematous COPD patients suggests that  $X_5$  and  $A_X$  may reflect parenchymal stiffness

or derecruitment, resulting in ventilation defects. In contrast, in COPD patients with little or no emphysema, VDP was related to  $A_x$  and  $R_{5-19}$  indicative of heterogeneous airway narrowing largely in the periphery, which was in agreement with previous work.<sup>2</sup> The different behaviours of  $R_{5-19}$  and  $X_5$  in COPD patients with and without emphysema suggests that  $X_5$  measures a different component that is independent of heterogeneous airway obstruction associated with  $R_{5-19}$ .<sup>5</sup> However,  $A_x$  was weakly significantly related to VDP in patients with and without emphysema, and this suggests that it is non-specific to the type of obstruction (either airways disease or emphysema) in COPD patients. Emphysematous and airways disease phenotypes may be best identified by appropriate use of  $R_{5-19}$  and  $X_5$ . In COPD patients, it is also important to acknowledge that airways disease and emphysema phenotypes are typically observed in combination,<sup>44</sup> so future examinations should also evaluate mixed phenotypes which were not evaluated here.

$A_x$  was originally developed to improve the signal-to-noise ratio of respiratory system reactance compared to reactance values at a single frequency.<sup>17</sup> **Table 2-3** provides an overview of the advantages and limitations of oscillometry measurements of obstructive lung disease including  $A_x$ . It is clear that  $A_x$  is sensitive to airflow obstruction, however it is non-specific to the type of obstruction and cannot distinguish airway constriction from lung recruitment or parenchymal stiffening.  $R_{5-19}$  on the other hand is known to reflect obstruction in the distal airways<sup>12</sup> whereas  $X_5$  is known to reflect elastic components of the lung. Moreover,  $A_x$  and the frequency dependence of resistance may depend on the number and choice of harmonics in the forcing waveform making them variable in different settings. For  $A_x$ , the largest influence is the first harmonic since this is where the most of the area is located, and different commercially available devices start at different frequencies anywhere from 4 Hz for adults up to 8 Hz for children. Our data also demonstrated that for COPD participants with markedly abnormal  $A_x$  greater than 50 cmH<sub>2</sub>O/L, VDP values ranged from 5% to 45% (Figure 3D) and this suggests that  $A_x$  is weakly related to inter-subject VDP differences. We note that  $A_x$  did not significantly contribute to VDP in any of the multivariable models. The multiple correlation coefficients ranged from 0.62-0.66 with  $R^2=0.39-0.44$ , so together, the oscillometry parameters contributed to no more than 44% of the variability in VDP regardless of subgroup.

**Table 2-3** Advantages and limitations of oscillometry measurements

<b>Advantages</b>	<b>Limitations</b>
<i>Frequency Dependence of Resistance (<math>R_{5-19}</math>)</i>	
+ Signal averaging minimizes noise and potential artefacts	- Variable in different settings
+ Differentiates proximal from distal obstruction	
+ Detects mild/early obstruction	
<i>Reactance at 5 Hz (<math>X_5</math>)</i>	
+ Reflects elastic components	- More noise
+ Reflects peripheral airway disease	- Non-specific to obstruction versus restriction
<i>Reactance Area (<math>A_x</math>)</i>	
+ Sensitive to obstruction	- Non-specific to type of obstruction
+ Signal averaging minimizes noise and potential artefacts	- Variable in different settings
+ Units of cmH <sub>2</sub> O/L, similar to compliance	- When $f_{res}$ is undefined, $A_x$ value is user-defined (hence variable between different devices)
+ Sensitive to intra-subject response to therapy or provocation	- Weakly related to inter-subject differences

We also recognize a number of other study limitations. Hyperpolarized  $^3\text{He}$  MRI is unlikely to be clinically used because of the vanishing global quantities and exorbitant cost of  $^3\text{He}$ .<sup>45</sup>  $^{129}\text{Xe}$  MRI is more sensitive to airway obstruction,<sup>38,46</sup> less costly and therefore, more feasible for clinical examinations so it will be important to compare oscillometry and  $^{129}\text{Xe}$  MRI measurements in patients. Moreover, shunting of the oscillatory waves to the upper airways reduces sensitivity to obstruction despite firm cheek-holding.<sup>47</sup> This means that in patients with obstruction, impedance may be underestimated, which may have also limited the correlation strengths observed here. We note that the never-smoker control group studied here underwent testing without inhaled bronchodilators whereas asthmatics, ex-smokers and COPD ex-smokers were evaluated post-bronchodilator. We previously showed that there was no post-bronchodilator MRI ventilation response in elderly never-smokers<sup>48</sup> with ventilation abnormalities, so we expect no confounding effects due to the lack of post-bronchodilator measurements in this subgroup. Finally, we also acknowledge positional differences in the oscillometry (seated upright) and MRI measurements (supine). Respiratory system resistance is increased in the supine position compared to upright<sup>49,50</sup>

and the presence of emphysema also causes large upright to supine  $A_x$  variability,<sup>51</sup> which may also explain why the relationships observed here were weak to moderate.

To our knowledge, this is the largest controlled evaluation of oscillometry and functional MRI undertaken in patients and healthy volunteers. The pattern of significant relationships for VDP with  $R_{5-19}$  and  $X_5$  was different between the different disease subgroups (i.e., COPD with and without emphysema, asthma). On the other hand, the relationship of  $A_x$  with VDP was similar across disease subgroups, suggesting that  $A_x$  is a sensitive but not specific measurement of obstruction. The different relationships for MRI VDP with  $R_{5-19}$  and  $X_5$  may reflect airway and parenchymal disease-specific biomechanical abnormalities that lead to ventilation defects.

## 2.5 References

- 1 Dubois, A. B., Brody, A. W., Lewis, D. H. & Burgess, B. F., Jr. Oscillation mechanics of lungs and chest in man. *J Appl Physiol* **8**, 587-594 (1956).
- 2 Smith, H., Reinhold, P. & Goldman, M. Forced oscillation technique and impulse oscillometry. *European Respiratory Monograph* **31**, 72 (2005).
- 3 Peslin, R. & Fredberg, J. J. Vol. 3 145-178 (Am. Physiol. Soc. Bethesda, MD, 1986).
- 4 Oostveen, E. *et al.* The forced oscillation technique in clinical practice: Methodology, recommendations and future developments. *Eur Respir J* **22**, 1026-1041 (2003).
- 5 Otis, A. B. *et al.* Mechanical factors in distribution of pulmonary ventilation. *J Appl Physiol* **8**, 427-443 (1956).
- 6 Lutchen, K. R. & Gillis, H. Relationship between heterogeneous changes in airway morphometry and lung resistance and elastance. *J Appl Physiol* **83**, 1192-1201 (1997).
- 7 Kaczka, D. W., Lutchen, K. R. & Hantos, Z. Emergent behavior of regional heterogeneity in the lung and its effects on respiratory impedance. *J Appl Physiol* **110**, 1473-1481 (2011).
- 8 Van Noord, J. A., Smeets, J., Clement, J., Van de Woestijne, K. P. & Demedts, M. Assessment of reversibility of airflow obstruction. *Am J Respir Crit Care Med* **150**, 551-554 (1994).

- 9 Zerah, F., Lorino, A. M., Lorino, H., Harf, A. & Macquin-Mavier, I. Forced oscillation technique vs spirometry to assess bronchodilatation in patients with asthma and COPD. *Chest* **108**, 41-47 (1995).
- 10 Kaczka, D. W., Ingenito, E. P., Israel, E. & Lutchen, K. R. Airway and lung tissue mechanics in asthma. Effects of albuterol. *Am J Respir Crit Care Med* **159**, 169-178 (1999).
- 11 Delacourt, C. *et al.* Use of the forced oscillation technique to assess airway obstruction and reversibility in children. *Am J Respir Crit Care Med* **161**, 730-736 (2000).
- 12 Grimby, G., Takishima, T., Graham, W., Macklem, P. & Mead, J. Frequency dependence of flow resistance in patients with obstructive lung disease. *J Clin Invest* **47**, 1455-1465 (1968).
- 13 Bhansali, P. V., Irvin, C. G., Dempsey, J. A., Bush, R. & Webster, J. G. Human pulmonary resistance: Effect of frequency and gas physical properties. *J Appl Physiol Respir Environ Exerc Physiol* **47**, 161-168 (1979).
- 14 Brochard, L. *et al.* Density and frequency dependence of resistance in early airway obstruction. *Am Rev Respir Dis* **135**, 579-584 (1987).
- 15 Di Mango, A. M., Lopes, A. J., Jansen, J. M. & Melo, P. L. Changes in respiratory mechanics with increasing degrees of airway obstruction in COPD: Detection by forced oscillation technique. *Respir Med* **100**, 399-410 (2006).
- 16 Clement, J., Landser, F. J. & Van de Woestijne, K. P. Total resistance and reactance in patients with respiratory complaints with and without airways obstruction. *Chest* **83**, 215-220 (1983).
- 17 Goldman, M. D. Clinical application of forced oscillation. *Pulm Pharmacol Ther* **14**, 341-350 (2001).
- 18 Skloot, G. *et al.* Respiratory symptoms and physiologic assessment of ironworkers at the world trade center disaster site. *Chest* **125**, 1248-1255 (2004).
- 19 Van Noord, J., Clement, J., Van de Woestijne, K. & Demedts, M. Total respiratory resistance and reactance as a measurement of response to bronchial challenge with histamine. *Am Rev Respir Dis* **139**, 921-926 (1989).
- 20 Lipworth, B. J. & Jabbal, S. What can we learn about COPD from impulse oscillometry? *Respir Med* **139**, 106-109 (2018).
- 21 Karayama, M. *et al.* Respiratory impedance is correlated with airway narrowing in asthma using three-dimensional computed tomography. *Clin Exp Allergy* **48**, 278-287 (2018).

- 22 Karayama, M. *et al.* Respiratory impedance is correlated with morphological changes in the lungs on three-dimensional CT in patients with COPD. *Sci Rep* **7**, 41709 (2017).
- 23 Wada, Y. *et al.* Diversity of respiratory impedance based on quantitative computed tomography in patients with COPD. *Int J Chron Obstruct Pulmon Dis* **13**, 1841-1849 (2018).
- 24 Lui, J. K., Parameswaran, H., Albert, M. S. & Lutchen, K. R. Linking ventilation heterogeneity quantified via hyperpolarized 3He MRI to dynamic lung mechanics and airway hyperresponsiveness. *PLoS One* **10**, e0142738 (2015).
- 25 Young, H. M., Guo, F., Eddy, R. L., Maksym, G. & Parraga, G. Oscillometry and pulmonary MRI measurements of ventilation heterogeneity in obstructive lung disease: Relationship to quality of life and disease control. *J Appl Physiol* **125**, 73-85 (2018).
- 26 Shi, Y. *et al.* Relating small airways to asthma control by using impulse oscillometry in children. *J Allergy Clin Immunol* **129**, 671-678 (2012).
- 27 Young, H. M., Guo, F., Eddy, R. L., Maksym, G. & Parraga, G. Oscillometry and pulmonary MRI measurements of ventilation heterogeneity in obstructive lung disease: Relationship to quality of life and disease control. *J Appl Physiol* (1985) **125**, 73-85 (2018).
- 28 Miller, M. R. *et al.* Standardisation of spirometry. *Eur Respir J* **26**, 319-338 (2005).
- 29 Parraga, G. *et al.* Hyperpolarized 3He ventilation defects and apparent diffusion coefficients in chronic obstructive pulmonary disease: Preliminary results at 3.0 tesla. *Invest Radiol* **42**, 384-391 (2007).
- 30 Guo, F. *et al.* Globally optimal co-segmentation of three-dimensional pulmonary 1H and hyperpolarized 3He MRI with spatial consistence prior. *Med Image Anal* **23**, 43-55 (2015).
- 31 Kirby, M. *et al.* Hyperpolarized 3He magnetic resonance functional imaging semiautomated segmentation. *Acad Radiol* **19**, 141-152 (2012).
- 32 Owangi, A. M., Etemad-Rezai, R., McCormack, D. G., Cunningham, I. A. & Parraga, G. Computed tomography density histogram analysis to evaluate pulmonary emphysema in ex-smokers. *Acad Radiol* **20**, 537-545 (2013).
- 33 Gevenois, P. A. *et al.* Comparison of computed density and microscopic morphometry in pulmonary emphysema. *Am J Respir Crit Care Med* **154**, 187-192 (1996).
- 34 Global Initiative for Asthma (GINA). Global strategy for asthma management and prevention: Updated 2017. (2017).

- 35 Global Initiative for Chronic Obstructive Lung Disease (GOLD). Global strategy for the diagnosis, management and prevention of chronic obstructive pulmonary disease. (2017).
- 36 Dellaca, R. L. *et al.* Lung recruitment assessed by total respiratory system input reactance. *Intensive Care Med* **35**, 2164-2172 (2009).
- 37 Tgavalekos, N. T. *et al.* Relationship between airway narrowing, patchy ventilation and lung mechanics in asthmatics. *Eur Respir J* **29**, 1174-1181 (2007).
- 38 Kirby, M. *et al.* Pulmonary ventilation visualized using hyperpolarized helium-3 and xenon-129 magnetic resonance imaging: Differences in COPD and relationship to emphysema. *J Appl Physiol* **114**, 707-715 (2013).
- 39 Capaldi, D. P. *et al.* Pulmonary imaging biomarkers of gas trapping and emphysema in COPD: (3)He MR imaging and CT parametric response maps. *Radiology* **279**, 597-608 (2016).
- 40 Hantos, Z., Daroczy, B., Suki, B., Galgoczy, G. & Csendes, T. Forced oscillatory impedance of the respiratory system at low frequencies. *J Appl Physiol* **60**, 123-132 (1986).
- 41 Hantos, Z., Daroczy, B., Csendes, T., Suki, B. & Nagy, S. Modeling of low-frequency pulmonary impedance in dogs. *J Appl Physiol* **68**, 849-860 (1990).
- 42 Tepper, R., Sato, J., Suki, B., Martin, J. G. & Bates, J. H. Low-frequency pulmonary impedance in rabbits and its response to inhaled methacholine. *J Appl Physiol* **73**, 290-295 (1992).
- 43 Hogg, J. C. *et al.* The nature of small-airway obstruction in chronic obstructive pulmonary disease. *N Engl J Med* **350**, 2645-2653 (2004).
- 44 Nakano, Y. *et al.* Computed tomographic measurements of airway dimensions and emphysema in smokers. Correlation with lung function. *Am J Respir Crit Care Med* **162**, 1102-1108 (2000).
- 45 Shea, D. A. & Morgan, D. The helium-3 shortage: Supply, demand, and options for congress. (Congressional Research Service, Library of Congress, 2010).
- 46 Svenningsen, S. *et al.* Hyperpolarized (3) He and (129) Xe MRI: Differences in asthma before bronchodilation. *J Magn Reson Imaging* **38**, 1521-1530 (2013).
- 47 Cauberghs, M. & Van de Woestijne, K. P. Effect of upper airway shunt and series properties on respiratory impedance measurements. *J Appl Physiol* **66**, 2274-2279 (1989).
- 48 Sheikh, K. *et al.* Pulmonary ventilation defects in older never-smokers. *J Appl Physiol* **117**, 297-306 (2014).

- 49 Lorino, A. M., Atlan, G., Lorino, H., Zanditenas, D. & Harf, A. Influence of posture on mechanical parameters derived from respiratory impedance. *Eur Respir J* **5**, 1118-1122 (1992).
- 50 Gonzales, P. A., Pearson, D. J., Haislip, G. D., Morris, M. J. & Skabelund, A. J. Effect of body position on impulse oscillometry in healthy volunteers: A pilot study [abstract]. *Am J Respir Crit Care Med* **195**, A2605 (2017).
- 51 Dandurand, R. J. *et al.* Oscillometry changes with body position and correlates with tlc and lung density. *Eur Respir J* **46**, PA2277 (2015).

## CHAPTER 3

### 3 NONIDENTICAL TWINS WITH ASTHMA: SPATIALLY-MATCHED CT AIRWAY AND MRI VENTILATION ABNORMALITIES

*To better understand the long-term spatial and temporal nature of ventilation heterogeneity in asthma, we evaluated and compared CT airway and MRI ventilation abnormalities in nonidentical twins. We compared these measurements between the twins over two visits separated by seven years and estimated the probability of the twins having the same MRI ventilation abnormality.*

*The contents of this chapter were previously published in the journal Chest: RL Eddy, AM Matheson, S Svenningsen, D Knipping, C Licskai, DG McCormack, G Parraga. Nonidentical Twins with Asthma: Spatially-matched CT Airway and MRI Ventilation Abnormalities. Chest. 2019;156(6):e111-6. This article is available under the terms of the Creative Commons CC-BY-NC-ND License.*

#### 3.1 Introduction

We report magnetic resonance (MR) and x-ray computed tomography (CT) imaging findings for female adult non-identical twins with moderate asthma who recounted a similar clinical history and symptoms of asthma since childhood, or about 40 years. In both 48-year-old women, there were spatially identical MRI ventilation defects and the same abnormal subsegmental airway, both of which remained persistently abnormal in the same spatial location over a period of seven years.

In patients with asthma, chronic cough, dyspnea and wheeze as well as acute bronchoconstrictive worsening can be directly related to abnormal airway smooth muscle,<sup>1</sup> luminal inflammation and mucus plugging,<sup>2</sup> and airway wall remodeling.<sup>3</sup> Pulmonary functional MRI has recently revealed that asthma may be expressed in a spatially heterogeneous manner, leading to MRI quantifiable ventilation heterogeneity<sup>4,5</sup> and ventilation defects that are both spatially and temporally persistent.<sup>6,7</sup> Importantly and across a number of different research centres, pulmonary functional MRI has shown that in patients with asthma, ventilation abnormalities do not appear to be stochastic, nor diffusely homogeneous.<sup>6</sup> Such MRI findings contradict *in silico* modeling studies that predict randomly distributed ventilation defects in patients with asthma.<sup>8,9</sup>

### 3.2 Case

As part of a longitudinal asthma study (clinicaltrials.gov NCT02351141, ethics board# 103516), we prospectively followed female twins for two study visits between January 2010 and March 2017 using hyperpolarized  $^3\text{He}$  MRI, thoracic CT and pulmonary function tests. Both twins were never-smokers (tobacco and cannabis) and attended separate baseline visits, each reporting a longstanding diagnosis of moderate asthma according to the Global Initiative for Asthma (GINA) treatment step criteria.<sup>10</sup> Their clinical histories were similar; they reported that both parents were heavy tobacco smokers within the family home and both father and mother had a clinical history of airways disease. They both lived within 25 km of each other and their original family home during their lifetime. Neither twin reported occupational exposures or risk; they worked as healthcare (Twin1) and daycare (Twin2) providers for most of their working lives. The twins had been independently prescribed 400 mcg daily dose budesonide combined with formoterol (Twin1, 200/6 mcg 2-puffs od; Twin2, 200/6 mcg 1-puff bid), by different asthma specialist care providers for the past decade. During the seven-year follow-up period, asthma medications remained the same and there were no asthma exacerbations reported. They both reported weak-to-moderate controller medication adherence, although both exhibited audible wheeze, shortness of breath and reported significant exercise limitation. Both twins had airways hyperreactivity, with a provocative concentration of methacholine resulting in a 20% decrease in  $\text{FEV}_1$  ( $\text{PC}_{20}$ ) of 0.08 mg/mL for Twin1 and 0.07 mg/mL for Twin2 at the baseline visit. They also demonstrated bronchodilator reversibility according to ATS/ERS guidelines<sup>11</sup> over the follow-up period (Twin1,  $\Delta\text{FEV}_1=260$  mL, 14%; Twin2,  $\Delta\text{FEV}_1=220$  mL, 15%).  $\text{FEV}_1$  did not change over the follow-up period for both twins (+30 mL for Twin1, +130 mL for Twin2; less than the minimal clinically important difference for  $\text{FEV}_1$  in asthma<sup>12,13</sup>) and they both reported adequate asthma control (asthma control questionnaire score [ACQ] <1.0).

Figure 1 shows pre-bronchodilator hyperpolarized  $^3\text{He}$  MRI at baseline (V1) and follow-up (V2), seven-years later. MR ventilation images provided in Figure 1 shows that for both twins there was a spatially identical, focal ventilation defect at baseline; the same left upper lobe ventilation abnormality also persisted at follow-up in both twins. We co-registered

the follow-up MRI ventilation to the patient's thoracic CT and generated three-dimensional airway trees (Figure 1, right panel) in order to reveal the specific airways that corresponded to the persistent MRI ventilation defects in each patient. The posterior branch of the left upper lobe apico-posterior bronchopulmonary segment (LB2) was abnormally remodeled and at follow-up, the subsegmental airway wall-area-percent was 71% for Twin1 and 75% for Twin 2 (both of which are markedly abnormal based on the literature<sup>14,15</sup>). Inset panels provide two-dimensional coronal CT airway subsegments which show that LB2 was not visible distally (due to airway termination or closure) to the same extent in Twin2 as in Twin1.

We also co-registered the airway trees to directly compare the twins' overall tree, as shown in Figure 2. The bulk airway anatomy was similar, with differences mainly in branching angles. Notably, Twin2 had less airways overall than Twin1 (total airway count 166 versus 202), and this is reflected in the number of airways by airway tree generation distal to LB2 and RB1. Wall-area-percent at the generation of the LB2 airway spatially-related to the persistent ventilation defect (indicated by \* in Figure 2), was increased relative to RB1 (as a comparator) in both twins.

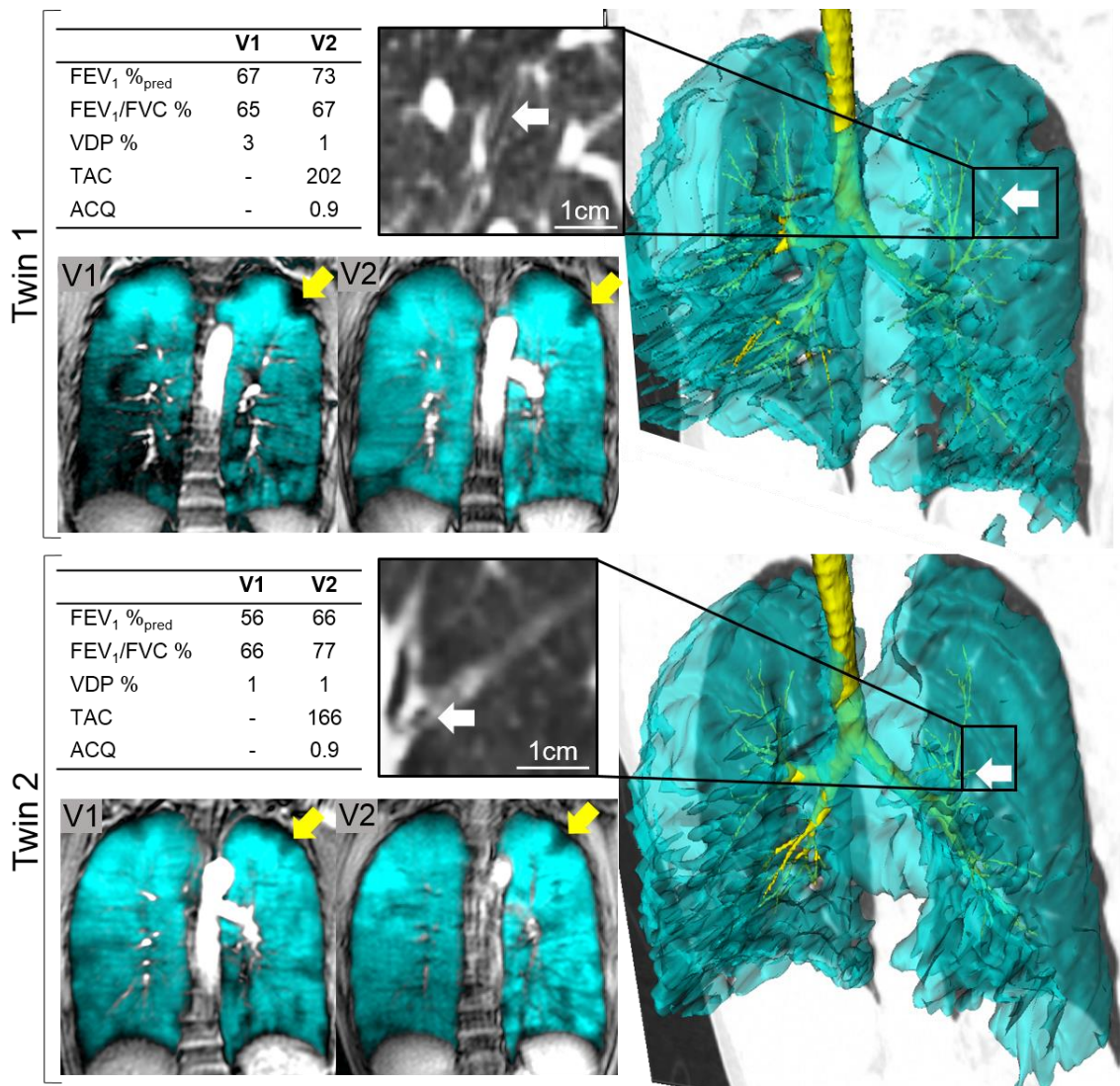


**Figure 3-1** Spatially-matched MRI ventilation defects and CT airways for twins with asthma

Tables show spirometry and MRI ventilation defect percent (VDP) at both visits, as well as CT total airway count (TAC) and asthma control questionnaire (ACQ-7) score at visit 2. <sup>3</sup>He MRI ventilation (cyan) co-registered to anatomical <sup>1</sup>H (grey-scale) for the twins at two study visits with yellow arrows showing spatially similar ventilation defects between the twins and over time. Follow-up 3D MRI ventilation on right co-registered to CT and 3D airway tree shows spatial relationship between left upper lobe apico-posterior segmental airway leading to similar defect, with inset showing airway segment on CT. White arrows show spatially persistent airways in 3D and in 2D CT inset.

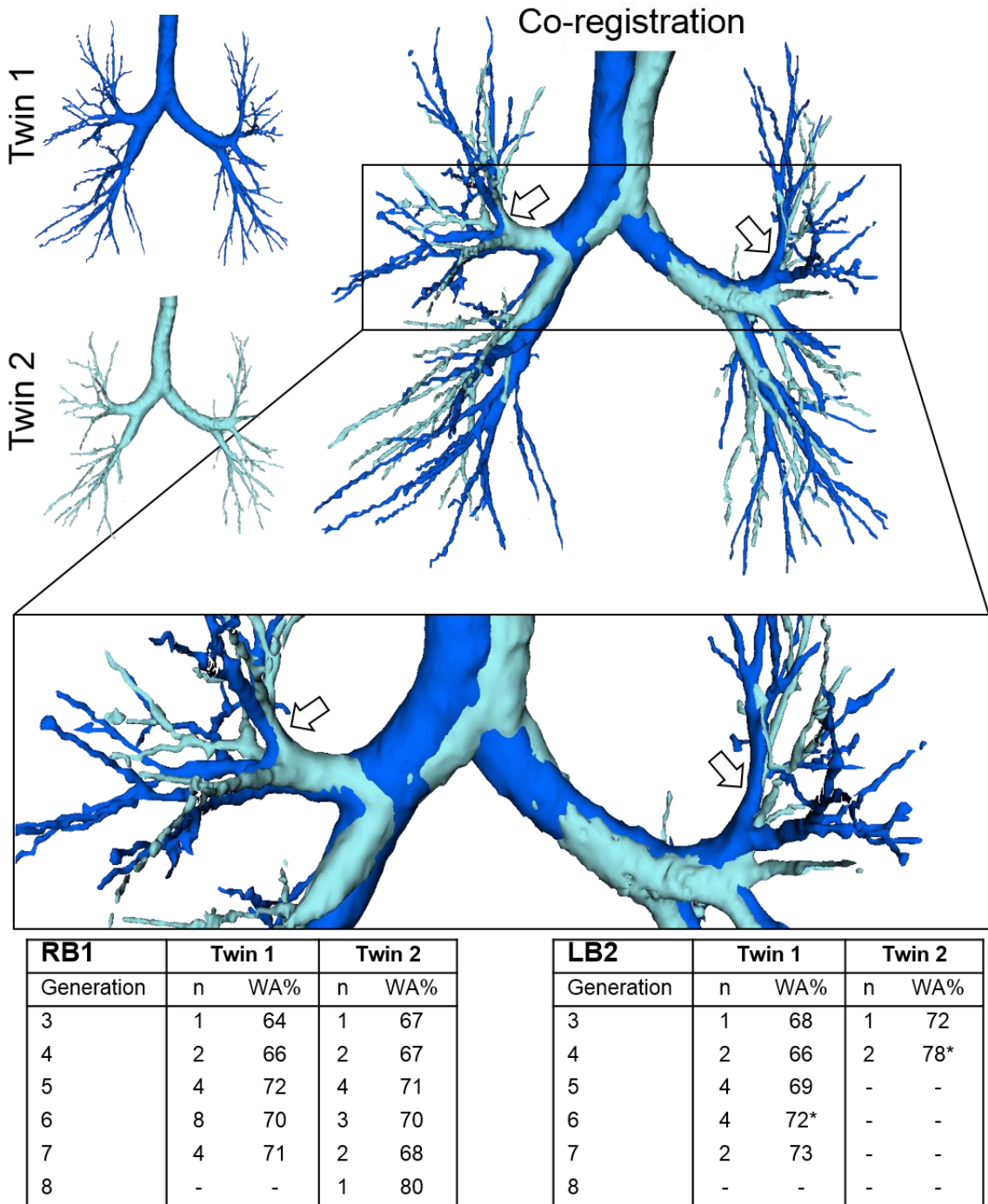


**Figure 3-2** Co-registered CT airway trees

Co-registered airway trees for Twin1 (dark blue) and Twin2 (light blue) show similar bulk airway anatomy. Airway trees were registered to align LB2 and comparator RB1 (zoomed, white arrows) and corresponding number of airway branches (n) and mean wall area percent (WA%) by airway tree generation are shown for both segments. Stars (\*) in the table indicate generation of abnormally remodeled LB2 airway that corresponds to the spatially persistent defect between the twins.

### 3.3 Discussion

A number of MRI investigations of asthma point to gas distribution abnormalities that are spatially and temporally persistent, suggestive of ventilation heterogeneity that is spatially non-random and preserved over time. We wondered about the likelihood of twins with asthma having identical MRI ventilation defects that could be identified as related to abnormal airways measured using CT; we also wondered if such abnormalities might also persist after a long-period of time in asthma patients with relatively stable disease.

If we assume that ventilation abnormalities are randomly distributed, to estimate the probability of two participants with asthma having the same segmental ventilation defect over a relatively long period of time, we considered the 19 anatomically and functionally distinct bronchopulmonary segments and made the following assumptions: 1) both patients with asthma would report at least one ventilation defect and no more than one defect per bronchopulmonary segment (ie.,  $>0$  and  $<19$  ventilation defects),<sup>16</sup> and, 2) there was an equivalent probability for each of the 19 bronchopulmonary segments to express a ventilation defect. We assumed that each of the twins would have at least one ventilation defect because of their longstanding clinical asthma diagnosis of asthma and their age.<sup>16</sup> Asthma patients with MRI ventilation defects are typically older than asthma patients without defects<sup>5</sup> and these twins were older than the mean age of participants in this previously reported investigation ( $35 \pm 11$ -years<sup>5</sup>). We first observed one ventilation defect in the apico-posterior left upper lobe segment in Twin1, and the probability for this single defect in this single bronchopulmonary segment was 1 in 19. Following this estimate, the probability that Twin2 would have exactly one defect in *the same bronchopulmonary segment* was 1 in  $19^2$  or 1 in 361.

Mathematical models of asthmatic airways predict that ventilation or gas distribution abnormalities would be random or stochastic.<sup>8,9,17</sup> If we assume that the occurrence of ventilation defects in asthma was random over time such that the presence and spatial locations of ventilation abnormalities appeared in different lung segments over time, we could also determine the probability that two patients have the same single segmental ventilation defect at baseline and again at seven-year follow-up to be 1 in  $19^4$  or 1 in 130,321. These odds are less likely than a single individual's risk of being struck by

lightning (~1 in 10,000 lifetime, 1 in 100,000 annual risk) and suggests that MRI ventilation defects may not be randomly distributed. While MRI studies have shown that the presence and size of specific ventilation defects may fluctuate modestly over time,<sup>7,18</sup> MRI ventilation defects in participants with asthma are mainly spatially persistent. In both twins, there was evidence of airways hyperreactivity and bronchodilator reversibility through the follow-up period, so the abnormal remodeling of the apico-posterior left upper lobe airway may stem from increased airway smooth muscle mass. However, we cannot comment on the contribution of airway inflammation because it was not evaluated. Longitudinal MRI and CT studies in patients with asthma have demonstrated persistent and dynamic disease components,<sup>7,18-20</sup> whereas here we focused on persistently abnormal regions. For example, Twin1 exhibited ventilation heterogeneity in the right lung base that was not present at follow-up, nor in Twin2. These regions of abnormal ventilation were associated with abnormally remodeled airways (Twin1 RB9 and RB10 most distal branches mean WA%=68% generation 5 versus LB2 WA%=71% generation 6). We think that intermittent ventilation abnormalities may be due to transient inflammation in combination with airway remodeling, although inflammatory status was not evaluated.

Limitations of our case study and analysis include the fact that the twins were only evaluated twice and the assumption we made that there was an equal probability of ventilation defects appearing in any of the 19 bronchopulmonary segments. In other words, we did not take into consideration that, in twins, there might be a bias for airway and ventilation abnormalities in specific lung regions. In addition, we did not make any assumptions about a potential upper limit for ventilation defect number, less than the 19 potential segmental airways. However, in our experience in over 200 asthmatic patients, there are typically fewer than five ventilation defects in participants with moderate disease, which is consistent with previous investigations.<sup>16</sup> Therefore, the probability of repeated defects in space and time as we observed would be lower, so our estimates are conservative. A more rigorous analysis could include the probability of multiple ventilation defects, the probability of twins having asthma, or the probability of subsegmental (38 subsegments) or sub-subsegmental (76 sub-subsegments) ventilation defects, all of which would serve to lower the probabilities estimated here. Finally, we have assumed the persistent ventilation defect in these patients to be related to asthma pathophysiology and/or abnormal airway

structure. These findings could also be explained to some extent by shared genetics, epigenetics or *in utero* events, which we did not evaluate here and cannot rule out.

In twins with asthma, we observed a single spatially-identical MRI ventilation defect related to abnormal airway remodeling which persisted in the same spatial location after seven years. If ventilation defects occur randomly in asthmatics, the probability of this occurring in both patients in the same location, twice over seven years is ~1 in 130,000.

### 3.4 References

- 1 Dunnill, M. S., Massarella, G. R. & Anderson, J. A. A comparison of the quantitative anatomy of the bronchi in normal subjects, in status asthmaticus, in chronic bronchitis, and in emphysema. *Thorax* **24**, 176-179 (1969).
- 2 Hargreave, F. E. & Nair, P. The definition and diagnosis of asthma. *Clin Exp Allergy* **39**, 1652-1658 (2009).
- 3 Postma, D. S. & Timens, W. Remodeling in asthma and chronic obstructive pulmonary disease. *Proc Am Thorac Soc* **3**, 434-439 (2006).
- 4 Altes, T. A. *et al.* Hyperpolarized 3He MR lung ventilation imaging in asthmatics: Preliminary findings. *J Magn Reson Imaging* **13**, 378-384 (2001).
- 5 Svenningsen, S. *et al.* What are ventilation defects in asthma? *Thorax* **69**, 63-71 (2014).
- 6 de Lange, E. E. *et al.* The variability of regional airflow obstruction within the lungs of patients with asthma: Assessment with hyperpolarized helium-3 magnetic resonance imaging. *J Allergy Clin Immunol* **119**, 1072-1078 (2007).
- 7 de Lange, E. E. *et al.* Changes in regional airflow obstruction over time in the lungs of patients with asthma: Evaluation with 3He MR imaging. *Radiology* **250**, 567-575 (2009).
- 8 Venegas, J. G. *et al.* Self-organized patchiness in asthma as a prelude to catastrophic shifts. *Nature* **434**, 777-782 (2005).
- 9 Tgavalekos, N. T. *et al.* Relationship between airway narrowing, patchy ventilation and lung mechanics in asthmatics. *Eur Respir J* **29**, 1174-1181 (2007).
- 10 Global Initiative for Asthma (GINA). Global strategy for asthma management and prevention: Updated 2018. (2018).
- 11 Miller, M. R. *et al.* Standardisation of spirometry. *Eur Respir J* **26**, 319-338 (2005).

- 12 Santanello, N. C., Zhang, J., Seidenberg, B., Reiss, T. F. & Barber, B. L. What are minimal important changes for asthma measures in a clinical trial? *Eur Respir J* **14**, 23-27 (1999).
- 13 Tepper, R. S. *et al.* Asthma outcomes: Pulmonary physiology. *J Allergy Clin Immunol* **129**, S65-87 (2012).
- 14 Awadh, N., Muller, N. L., Park, C. S., Abboud, R. T. & FitzGerald, J. M. Airway wall thickness in patients with near fatal asthma and control groups: Assessment with high resolution computed tomographic scanning. *Thorax* **53**, 248-253 (1998).
- 15 Gupta, S. *et al.* Quantitative analysis of high-resolution computed tomography scans in severe asthma subphenotypes. *Thorax* **65**, 775-781 (2010).
- 16 de Lange, E. E. *et al.* Evaluation of asthma with hyperpolarized helium-3 MRI: Correlation with clinical severity and spirometry. *Chest* **130**, 1055-1062 (2006).
- 17 Tgavalekos, N. T. *et al.* Identifying airways responsible for heterogeneous ventilation and mechanical dysfunction in asthma: An image functional modeling approach. *J Appl Physiol* **99**, 2388-2397 (2005).
- 18 Svenningsen, S. *et al.* Pulmonary functional magnetic resonance imaging: Asthma temporal-spatial maps. *Acad Radiol* **21**, 1402-1410 (2014).
- 19 Witt, C. A. *et al.* Longitudinal changes in airway remodeling and air trapping in severe asthma. *Acad Radiol* **21**, 986-993 (2014).
- 20 Dunican, E. M. *et al.* Mucus plugs in patients with asthma linked to eosinophilia and airflow obstruction. *J Clin Invest* **128**, 997-1009 (2018).

## CHAPTER 4

### 4 HYPERPOLARIZED HELIUM 3 MRI IN MILD-TO-MODERATE ASTHMA: PREDICTION OF POSTBRONCHODILATOR REVERSIBILITY

*Building on the evidence of spatially and temporally persistent regional lung abnormalities in twins with asthma from **Chapter 3**, we wanted to evaluate the long-term structure-function relationships in unrelated asthma patients and determine the role for MRI ventilation abnormalities in predicting longitudinal disease worsening.*

*In order to quantitatively evaluate ventilation abnormalities over time, we first determined the minimal clinically important difference for MRI ventilation defects; this work is provided in **Appendix A**.*

*The contents of this chapter were previously published in the journal *Radiology*: RL Eddy, S Svenningsen, C Licskai, DG McCormack, G Parraga. *Hyperpolarized Helium 3 MRI in Mild-to-Moderate Asthma: Prediction of Postbronchodilator Reversibility*. *Radiology*. 2019;293(1):212-20. Permission to reproduce this article was granted by the Radiological Society of North America (RSNA) and is provided in **Appendix B**.*

#### 4.1 Introduction

In patients who have asthma, chronic airways disease typically results in variable airflow obstruction that may be partially or completely reversed using bronchodilators.<sup>1</sup> Many people with asthma maintain stable lung function and bronchodilator reversibility over time, while a subset of patients may experience accelerated lung function decline and eventually lose post-bronchodilator reversibility.<sup>2-4</sup> Recent epidemiological studies have revealed that in up to 10% of people with asthma, airways disease may lead to chronic, persistent airflow obstruction and chronic obstructive pulmonary disease<sup>5,6</sup> but the mechanisms underlying these changes are not fully understood.

Airway remodeling caused by chronic inflammation has been suggested to mediate changes that result in airflow obstruction that is not bronchodilator-reversible.<sup>7</sup> Asthma involves both the small and large airways and it is difficult to measure small airway dysfunction using spirometry measurements of the forced expiratory volume in one second (FEV<sub>1</sub>) because it is insensitive to peripheral airway changes.

The morphologic structure of remodeled and inflamed airways can be directly measured using thoracic radiographic CT<sup>8-10</sup> and airway function may also be viewed by using expiratory CT lucency of gas trapping<sup>11,12</sup> or parametric response mapping.<sup>13,14</sup> Parametric response map gas trapping was shown<sup>14</sup> to be increased in participants with severe asthma as compared with participants with non-severe asthma and control participants. Inhaled hyperpolarized gas MRI directly probes ventilation as a consequence of both central and peripheral airway function and has revealed the presence of non-random ventilation defects<sup>15</sup> that are the functional consequences of airway remodeling, inflammation and/or intraluminal plugging.<sup>16-18</sup> In patients with asthma, MRI ventilation defects are spatially-related to abnormally remodeled airways,<sup>16,17</sup> positively correlated with disease severity<sup>19</sup> and improved in response to bronchodilators,<sup>15,20</sup> The size and spatial locations of MRI ventilation abnormalities persist over time<sup>21,22</sup> and are related to asthma exacerbations<sup>23</sup> and asthma control/quality-of-life.<sup>24</sup>

Although epidemiological studies<sup>5,6,25</sup> suggest that asthma progression to chronic obstructive pulmonary disease may be relatively common, it is difficult to identify patients who are at-risk. Because hyperpolarized helium 3 (<sup>3</sup>He) and xenon 129 (<sup>129</sup>Xe) MRI provide sensitive tools to simultaneously measure both small and large airway function, we hypothesized that MRI ventilation abnormalities would be predictive of future FEV<sub>1</sub> bronchodilator reversibility and, at the same time, ventilation defects would remain spatially-persistent during follow-up. Accordingly, the purpose of this study was to investigate six-year longitudinal changes in hyperpolarized <sup>3</sup>He MRI ventilation defects in study participants with mild-moderate asthma and identify predictors of longitudinal changes in post-bronchodilator FEV<sub>1</sub> reversibility.

## **4.2 Materials and Methods**

### **4.2.1 Study Participants and Design**

Between January 2010 and April 2011, we consecutively recruited study participants from a tertiary care pulmonary clinic who had mild-to-moderate asthma (ie, prescribed medium-high dose inhaled corticosteroid with long-acting beta-agonist LABA or less treatment for asthma controller medication) according to the Global Initiative for Asthma treatment step

criteria,<sup>1</sup> and were aged 18–70 years with less than 1 pack-year smoking history. Participants provided written informed consent to an ethics-board-approved, Health Insurance Portability and Accountability Act-compliant, registered (ClinicalTrials.gov: NCT02351141) protocol for baseline and 6-year follow-up visits (November 2016–June 2017). Exclusion criteria included the following: FEV<sub>1</sub> greater than 80%<sub>pred</sub> and concentration of methacholine required to decrease FEV<sub>1</sub> by 20% from baseline (PC<sub>20</sub>) greater than 8 mg/mL, claustrophobia, inability to undergo spirometry, body mass index greater than 40 kg/m<sup>2</sup>, and contraindications to MRI (ie, metal, electronic, or magnetic implants). Baseline measurements were previously reported<sup>17</sup> and focused on the cross-sectional analyses; in our study, we reported the longitudinal follow-up measurements after 6 years and compared them with baseline measurements. Data generated during our study are available from the corresponding author.

Spirometry, plethysmography, CT and MRI were performed at both study visits. At baseline, participants underwent a methacholine challenge, with MRI and spirometry performed before methacholine, after methacholine and after bronchodilator recovery, and plethysmography and CT before methacholine. At follow-up, participants underwent all tests before and after bronchodilator only (no methacholine challenge at follow-up), with CT performed after bronchodilator. We used electronic health records and participant self-reports to measure exacerbations and changes in medication during the study visit interval.<sup>26</sup>

#### 4.2.2 Pulmonary Function Tests and Methacholine Challenge

Spirometry was performed according to American Thoracic Society guidelines<sup>27</sup> by using a spirometer (*ndd EasyOne*; ndd Medizintechnik AG, Zurich, Switzerland). Plethysmography was performed by using a plethysmograph (*MedGraphics Elite Series*; MGC Diagnostics Corporation, St. Paul, MN) to measure lung volumes and airways resistance. Methacholine challenge was performed according to American Thoracic Society guidelines<sup>28</sup> with the two-minute tidal breathing method up to and including PC<sub>20</sub> by using a breath-actuated nebulizer (*AeroEclipse II*; Trudell Medical International, London, ON, Canada). Bronchodilation was achieved following four separate doses of 100 µg of novo-salbutamol hydrofluoroalkane (Teva Novopharm Ltd., Toronto, ON,

Canada) through a pressurized metered-dose inhaler using a spacer (*AeroChamber Plus*; Trudell Medical International). Bronchodilator reversibility of FEV<sub>1</sub> was defined as a post-bronchodilator increase of 200 mL and 12%<sup>29</sup>; participants were dichotomized as reversible or not reversible FEV<sub>1</sub> at follow-up. The minimal clinically important difference for FEV<sub>1</sub> was used to determine changes in FEV<sub>1</sub> between visits as previously described.<sup>29,30</sup> Participants withheld asthma medications according to American Thoracic Society guidelines<sup>28</sup> before both visits as follows: short-acting  $\beta$ -agonists were withheld for 8 hours, long-acting  $\beta$ -agonists were withheld for 48 hours and long-acting muscarinic agents were withheld for 24 hours.

#### 4.2.3 MRI Parameters and Analysis

We performed anatomical proton (hydrogen 1 [<sup>1</sup>H]) and <sup>3</sup>He static ventilation MRI at the coronal plane within 5 minutes by using a whole-body 3.0-T imager (Discovery MR750; General Electric Healthcare, Milwaukee, WI) with broadband capability as previously described.<sup>31</sup> Participants were instructed to inhale a gas mixture from a 1.0-L bag (Tedlar<sup>®</sup>; Jensen Inert Products, Coral Springs, FL) from functional residual capacity, and 15 coronal sections were acquired in 8-15 seconds at breath-hold. We performed <sup>1</sup>H MRI before hyperpolarized <sup>3</sup>He during 1.0-L breath-hold of high purity, medical-grade nitrogen (N<sub>2</sub>; Spectra Gases, Alpha, NJ) by using the whole-body radiofrequency coil and a fast-spoiled gradient-recalled echo sequence (partial echo acquisition; total acquisition time, 8 seconds; repetition time msec/echo time msec, 4.7/1.2; flip angle, 30°; field of view, 40x40cm<sup>2</sup>; bandwidth, 24.4kHz; 128x80 matrix zero-padded to 128x128; partial echo percentage, 62.5%, 15-17 sections; slice section thickness, 15mm; no gap). <sup>3</sup>He gas was polarized to 30–40% by using a commercial turn-key polarizer (HeliSpin; Polarean, Durham, NC). We performed <sup>3</sup>He static ventilation MRI during 1.0-L breath-hold of hyperpolarized <sup>3</sup>He diluted to 25% by volume with N<sub>2</sub> by using a single-channel rigid elliptical transmit-receive chest coil (RAPID Biomedical, Wuerzburg, Germany) and a two-dimensional multisection fast-gradient-recalled echo sequence (partial echo acquisition; total acquisition time, 11 seconds; repetition time msec/echo time msec, 3.8/1.0; flip angle, 7°; field of view, 40x40cm<sup>2</sup>; bandwidth, 48.8kHz; 128x80 matrix zero-padded to 128x128; partial echo percentage, 62.5%, 15-17 sections; section thickness, 15mm; no gap).

Quantitative MRI analysis was performed by a single observer (R.L.E., with four-years experience) who was blinded to baseline and follow-up visits by using in-house segmentation software (smallest detectable difference<sup>32</sup> and minimal clinically important difference<sup>33</sup>) in MATLAB R2016a (Mathworks, Natick, MA) as previously described.<sup>32</sup> Static ventilation images were segmented by using three-dimensional k-means clustering that classified voxel intensities into five clusters ranging from signal void or ventilation defects (cluster 1) to hyperintense signal (cluster 5; all ventilated volume clusters 2-5). Ventilation abnormalities were quantified as the ventilation defect volume (VDV) and as the ventilation defect percent (VDV normalized to the MRI-measured volume of the thoracic cavity). Repeatability of MRI VDV and ventilation defect percent in this study was evaluated by a single observer (R.L.E., blinded for segmentation) in five randomly selected participants. Blinded participant selection and randomization between repeated segmentation rounds was provided by an additional observer who did not participate in the data analysis. Quantitative, clinically-relevant MRI changes were evaluated by using the following equation:  $\Delta VDV > |110| \text{ mL}$ , which is the published minimal clinically important difference for VDV,<sup>33</sup> where  $\Delta VDV$  is the change in VDV. The spatial locations of ventilation defects were visually and qualitatively compared between visits (R.L.E.).

#### 4.2.4 CT Parameters and Analysis

Thoracic CT was performed within 10 minutes of MRI using a 64-section system (LightSpeed VCT; GE Healthcare) at breath-hold after inhalation of 1.0 L of N<sub>2</sub> from functional residual capacity to volume match to MRI. Participants were transported from MRI to CT by wheelchair to avoid exercise-induced changes. At baseline, CT was performed in a 4–10 cm axial region of interest with visually obvious ventilation defects as previously described<sup>17</sup> to reduce radiation dose. At follow-up, a full CT image of the thorax was acquired by using a low-dose protocol as previously described.<sup>34</sup>

Thoracic CT images were analyzed by using a commercial workstation (Pulmonary Workstation 2.0; VIDA Diagnostics Inc., Coralville, IA) to segment and measure the three-dimensional airway tree. The measurements between visits were compared within the region of the partial CT acquired at baseline.

#### 4.2.5 Statistical Analysis

Data were tested for normality by using Shapiro-Wilk tests with commercially-available software (SPSS Statistics 25.0; IBM Corporation, Armonk, NJ). When data were not normally distributed, they were log transformed. Measurements for each visit were compared by using paired t-tests, and bronchodilator-reversible and bronchodilator-not-reversible subgroup measurements were compared by using unpaired t-tests (SPSS; IBM). MRI VDV and ventilation defect percent repeatability were determined by using the coefficient of variation and two-way mixed effects intraclass correlation coefficient (SPSS; IBM). Univariable relationships were evaluated by using Pearson correlation coefficients ( $r$ ) in commercially-available software (GraphPad Prism 7.00; GraphPad Software, La Jolla, CA) for follow-up post-bronchodilator change in FEV<sub>1</sub> with baseline measurements related to the methacholine challenge. These included FEV<sub>1</sub> and VDV before methacholine with differences between challenge states (ie, post-methacholine minus pre-methacholine) and PC<sub>20</sub>. On the basis of univariable relationships, multivariable models were generated (SPSS; IBM) by using the enter approach to determine the largest influence for predicting FEV<sub>1</sub> bronchodilator reversibility (post-bronchodilator change in FEV<sub>1</sub> in milliliters) at follow-up for the following two models: a) baseline variables that had significant univariable relationships with post-bronchodilator change in FEV<sub>1</sub> at follow-up, and b) age, FEV<sub>1</sub>, and PC<sub>20</sub> at baseline which have been shown<sup>2,4,35</sup> to predict future bronchodilator reversibility, along with baseline VDV. The regression coefficients for the variables in the multivariable models were expressed as standardized  $\beta$ . Results were considered statistically significant when the probability of making a Type I error was less than 5% ( $p < 0.05$ ).

### 4.3 Results

#### 4.3.1 Study Participants

The study flow chart is provided in **Figure 4-1**; 26 participants were enrolled<sup>17</sup> but two participants (2/26, 8%) did not have asthma and were excluded. Of 24 participants who completed the baseline visit, nine participants (35%) were lost to follow-up because they moved farther than 500 km away or could not be contacted, and four participants (15%)

participants declined the follow-up visit. In total, 11 participants (seven men and 4 women) with mild-moderate asthma (Global Initiative for Asthma treatment steps 1-4<sup>1</sup>) were evaluated twice within mean 78 months  $\pm$  7 (standard deviation; median, 79 months; range, 68-87). Mean participant age was 42 years  $\pm$  9 at baseline (men, 41 years  $\pm$  10; women, 44 years  $\pm$  6,  $p=.63$ ) and 49 years  $\pm$  9 at follow-up (men, 48 years  $\pm$  10; women, 51 years  $\pm$  7,  $p=.62$ ). **Table 4-5** in the supplement shows the baseline measurements for participants who completed longitudinal follow-up (11 participants; 42%) and those who were lost to follow-up (15 participants, 58%). Participants who completed longitudinal follow-up were older (mean age 42 years  $\pm$  9 vs 28 years  $\pm$  9, respectively;  $p<.01$ ) with worse lung function overall (all  $p<.05$  except forced vital capacity and total lung capacity) and ventilation defect percent (5%  $\pm$  4 vs 2%  $\pm$  1, respectively;  $p<.01$ ).

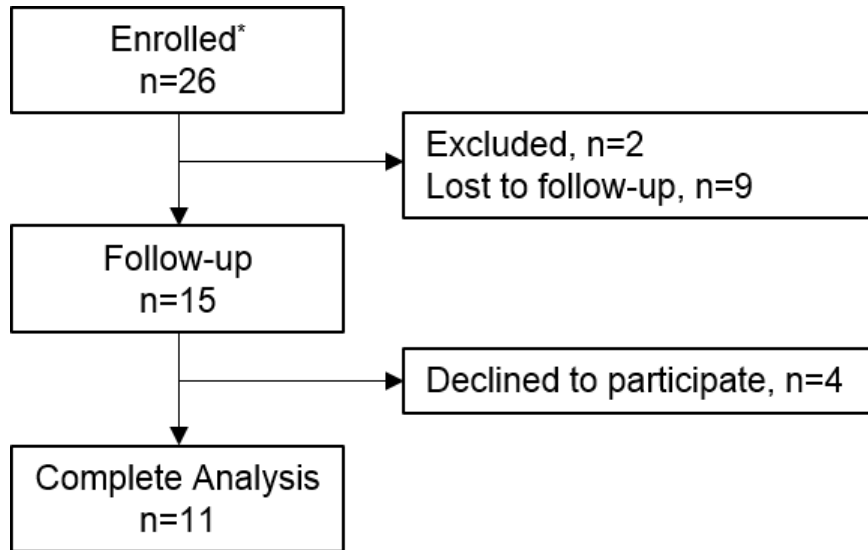


**Figure 4-1** Study flowchart of patient inclusion and exclusion  
Two participants were excluded because they did not have current asthma.  
\*Enrolled per Svenningsen et al<sup>17</sup>

**Table 4-1** provides demographic, pulmonary function test, and MRI measurements. A participant listing is provided in **Table 4-6** and a detailed list of asthma medications is provided in **Table 4-7**, both in the supplement. Between the baseline and follow-up visits, mean body mass index (27 kg/m<sup>2</sup>  $\pm$  4 vs 28 kg/m<sup>2</sup>  $\pm$  4, respectively;  $p=.03$ ) and mean residual volume (126%<sub>pred</sub>  $\pm$  20 vs 136%<sub>pred</sub>  $\pm$  26, respectively;  $p=.02$ ) were different; all other measurements were not different ( $p>.05$ ). All participants were never-smokers (0 pack-year) and none reported an asthma exacerbation between study visits. All participants

except one (participant S06) were prescribed inhaled corticosteroids and/or inhaled corticosteroids with long-acting  $\beta$ -agonist at baseline. During the interval between visits, nine participants (82%) remained on the same type and dose of medication whereas a single participant (participant S03) changed the type of inhaled corticosteroid and long-acting  $\beta$ -agonist controller while administered the same daily inhaled corticosteroid dose. Against medical advice, a single participant (participant S11) refused to self-administer prescribed asthma medications during the interval between the baseline and follow-up visits.

**Table 4-1** Participant and MRI measurements at baseline and follow-up

Parameter ( $\pm$ SD)	Baseline			Follow-up*			Baseline vs. follow-up p-value (all n=11)	
	ALL (n=11)	Stable VDV (n=8)	Worse VDV (n=3)	p-value	ALL (n=11)	Stable VDV (n=8)		Worse VDV (n=3)
Age years	42 (9)	42 (10)	43 (6)	.92	49 (9)	49 (10)	49 (7)	>.99
Women n	4	2	2	-	4	2	2	-
BMI kg/m <sup>2</sup>	27 (4)	26 (4)	29 (2)	.33	28 (4)	27 (5)	29 (2)	.48
FVC % <sub>pred</sub>	87 (13)	88 (13)	85 (14)	.78	85 (14)	87 (15)	79 (5)	.39
FEV <sub>1</sub> L	2.80 (0.86)	2.89 (1.00)	2.56 (0.37)	.60	2.65 (0.85)	2.76 (0.92)	2.35 (0.69)	.51
FEV <sub>1</sub> % <sub>pred</sub>	76 (12)	76 (14)	75 (7)	.94	76 (12)	78 (12)	72 (11)	.53
FEV <sub>1</sub> /FVC %	70 (7)	69 (7)	72 (6)	.52	73 (8)	72 (7)	74 (11)	.69
RV % <sub>pred</sub>	126 (20)	127 (14)	124 (26)	.85	136 (26)	136 (18)	135 (48)	.96
TLC % <sub>pred</sub>	103 (9)	104 (7)	101 (13)	.55	104 (11)	105 (9)	102 (15)	.71
RV/TLC % <sub>pred</sub>	123 (18)	123 (16)	122 (24)	.98	129 (17)	129 (15)	128 (27)	.96
R <sub>aw</sub> % <sub>pred</sub>	172 (68)	177 (70)	160 (75)	.75	178 (44)	159 (35)	230 (6)	.01
VDV mL	240 (180)	290 (180)	120 (130)	.19	250 (210)	180 (110)	440 (330)	.06
VDP %	5 (3)	5 (3)	3 (2)	.27	5 (4)	3 (2)	8 (6)	.31
ICS dose $\mu$ g/day <sup>†</sup>	400 (0-1600)	400 (0-800)	600 (400-1600)	.19	400 (0-1600)	400 (0-800)	800 (0-1600)	.50
OCS dose mg/day	0	0	0	-	0	0	0	-

SD=standard deviation; BMI=body mass index; FVC=forced vital capacity; %<sub>pred</sub>=percent predicted; FEV<sub>1</sub>=forced expiratory volume in one second; RV=residual volume; TLC=total lung capacity; R<sub>aw</sub>=airways resistance; VDV=ventilation defect volume; VDP=ventilation defect percent; ICS=inhaled corticosteroids; OCS=oral corticosteroids; \*Follow-up mean $\pm$ SD, 78 $\pm$ 7 months, (median 79, range 68-87) from baseline. <sup>†</sup>Median (range), shown as budesonide equivalent; n=10 participants prescribed ICS and/or ICS/long-acting  $\beta$ -agonist (LABA).

### 4.3.2 <sup>3</sup>He MRI Ventilation at Baseline and Follow-up

MRI measurements were highly repeatable with coefficient of variation of 5% (95% confidence interval: 3%, 7%) and intraclass correlation coefficient of 1.00 (95% confidence interval 0.98, 1.00) for both VDV and ventilation defect percent. For eight study participants (of 11 participants, 73%), MRI ventilation defects remained in the same location at the 6-year follow-up MRI and were similar in size (change in VDV between visits, <110 mL). **Figure 4-2** shows <sup>3</sup>He MRI ventilation at baseline and follow-up and airway corresponding to a persistent defect for a representative participant with stable VDV (participant S03). A subsegmental bifurcation in the RB8 bronchus showed narrowing in the inferior daughter branch compared with the superior daughter branch. For the remaining three participants (of 11; 27%), follow-up pre-bronchodilator ventilation defects were visually and quantitatively larger than baseline defects (change in VDV between visits, ≥110 mL) and were in the same lung regions as baseline post-methacholine ventilation defects. **Figure 4-3** shows <sup>3</sup>He MRI ventilation and airway corresponding to worsened follow-up defect for a representative participant with worse VDV at follow-up (participant S01). The LB8 bronchus leading to the worsened follow-up defect was abruptly truncated.

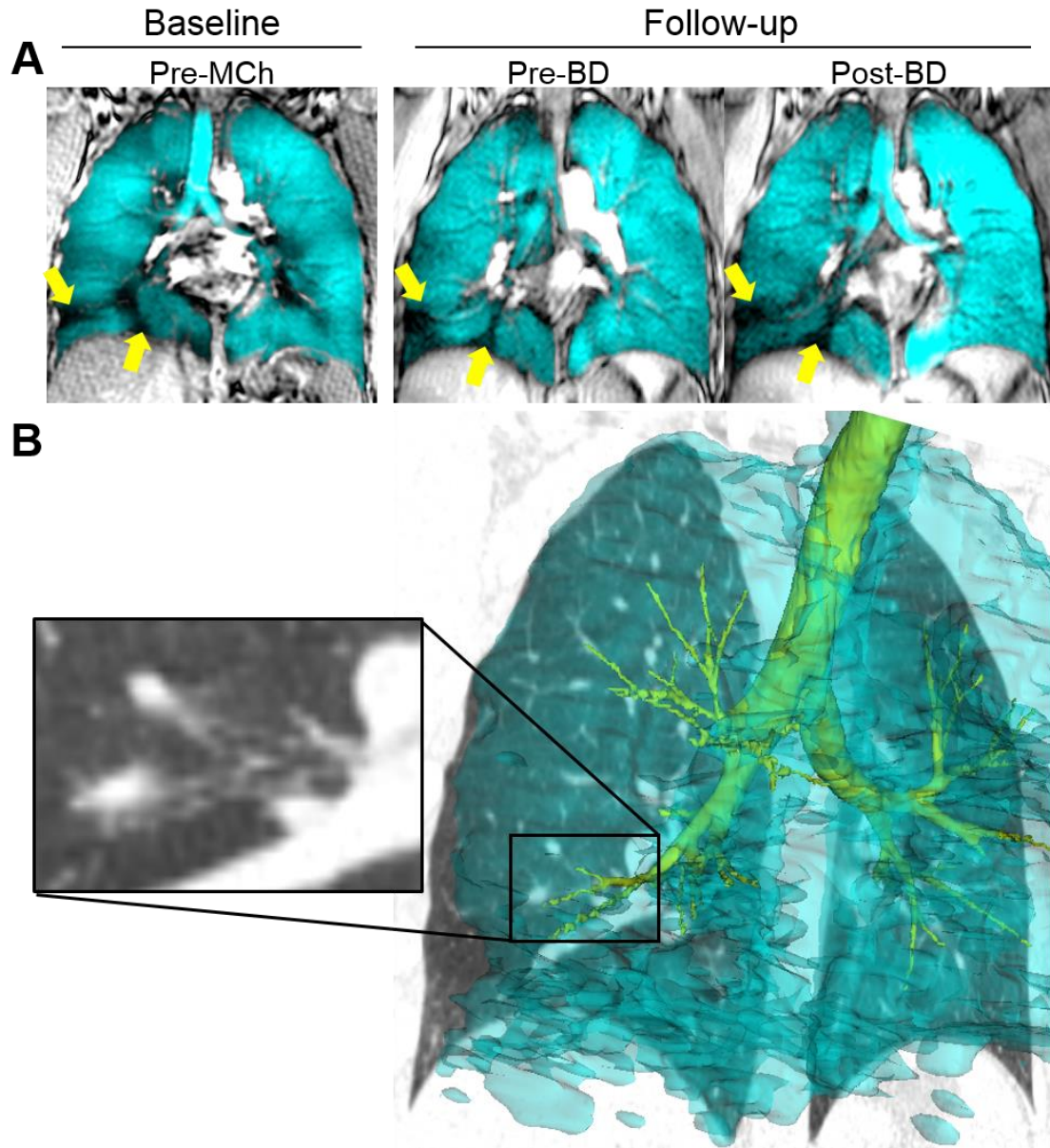


**Figure 4-2**  $^3\text{He}$  MRI ventilation in a representative participant with stable ventilation between baseline and follow-up

A, Centre coronal section  $^3\text{He}$  ventilation MRI (cyan, administered as an inhaled contrast agent) coregistered to anatomic hydrogen 1 ( $^1\text{H}$ ) MRI (gray scale) for baseline pre-methacholine challenge (pre-MCh) and follow-up before and after bronchodilator (pre-BD and post-BD, respectively). Persistent defects between visits are shown (arrows).

B, Follow-up three-dimensional  $^3\text{He}$  MRI shows ventilation coregistered to CT with three-dimensional airway tree at oblique angle. Inset (coronal view) shows RB8 bronchus subsegmental bifurcation. Inferior daughter branch leading to persistent defect between baseline and follow-up appears narrowed compared with superior daughter branch. Participant S03 was a man with mild-to-moderate asthma (baseline and follow-up, respectively: age, 28 years and 35 years; forced expiratory volume in 1 second, 3.97 L and 4.19 L; ventilation defect volume, 340 mL and 260 mL).

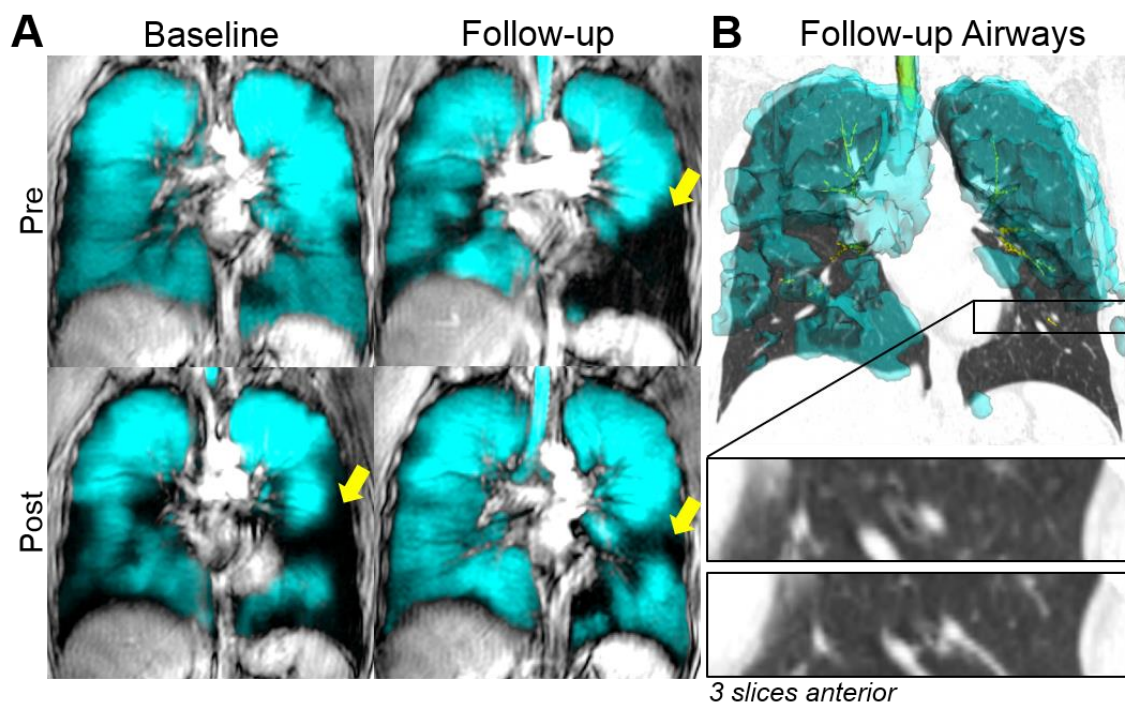


**Figure 4-3**  $^3\text{He}$  MRI ventilation in a representative participant with worse ventilation at 6-year follow-up

A, Centre coronal section  $^3\text{He}$  ventilation MRI (cyan, administered as an inhaled contrast agent) coregistered anatomic hydrogen 1 MRI (gray scale) for baseline premethacholine challenge (pre) and after methacholine challenge (post), and follow-up before (pre) and after (post) bronchodilator. Worsened defects were shown between visits (arrows).

B, Follow-up three-dimensional  $^3\text{He}$  MRI shows ventilation coregistered to CT with three-dimensional airway tree at oblique angle. Inset on top (coronal view) shows LB8 bronchus leading to worsened follow-up defect. Lumen appears clear and open but is abruptly truncated within three sections anteriorly (inset on bottom). Participant S01 was a woman with mild-to-moderate asthma (baseline and follow-up, respectively: age, 36 and 41 years; forced expiratory volume in 1 second, 2.28 L and 1.71 L; ventilation defect volume, 270 mL and 780 mL).

**Table 4-2** shows CT airway measurements including airway wall area percent, lumen area, wall thickness, and number of mucus plugs at baseline and follow-up, and total airway count at follow-up. For all participants at baseline versus follow-up, mean wall area percent ( $70\% \pm 2$  vs  $69\% \pm 1$ , respectively;  $p=.14$ ) and wall thickness ( $28.3 \text{ mm} \pm 2.1$  vs  $27.8 \text{ mm} \pm 3.3$ , respectively;  $p=.66$ ) were not different, whereas mean lumen area was greater at follow-up (baseline vs follow-up,  $5.4 \text{ mm}^2 \pm 1.9$  vs  $6.9 \text{ mm}^2 \pm 1.6$ , respectively;  $p<.001$ ). Airway measurements were not different between subgroups ( $p>.05$ ). One

participant (participant S01) had three subsegmental mucus plugs at follow-up in the LB4, RB2 and RB10 bronchi, which did not correspond to ventilation defects.

**Table 4-2** CT measurements

Participant	Baseline (n=11)				Follow-up (n=11)				TAC
	WA%	LA (mm <sup>2</sup> )	WT (mm)	M	WA%	LA (mm <sup>2</sup> )	WT (mm)	M	
<i>Stable VDV at follow-up (n=8)</i>									
S02	69	6.7	28.3	0	69	8.8	24.5	0/0	170
S03	72	4.8	28.5	0	70	5.9	27.2	0/0	130
S04	72	3.5	25.7	0	69	6.0	25.3	0/0	166
S06	72	5.7	28.7	0	67	7.8	23.6	0/0	145
S07	72	4.9	27.0	0	69	7.1	27.3	0/0	180
S08	69	3.0	24.5	0	69	4.5	25.3	0/0	202
S09	74	4.3	31.6	0	71	6.5	29.3	0/0	165
S10	69	6.7	28.3	0	68	7.8	29.7	0/0	141
Mean (±SD)	71 (2)	5.0 (1.4)	27.8 (2.1)	-	69 (1)	6.8 (1.4)	26.5 (2.2)	-	162 (23)
<i>Worse VDV at follow-up (n=3)</i>									
S01	70	3.4	27.6	0	72	4.5	26.3	1/3	114
S05	66	3.8	29.3	0	71	5.7	31.5	0/0	224
S11	69	6.8	28.6	0	67	8.2	31.1	0/0	196
Mean (±SD)	68 (2)	4.7 (1.9)	28.5 (0.9)	-	70 (3)	6.1 (1.9)	29.7 (2.9)	-	178 (57)
<i>Group differences (n=11)</i>									
p	.12	.87	.72	-	.66	.30	.59	-	.51
<b>ALL (±SD)</b> (n=11)	70 (2)	5.4 (1.9)	28.3 (2.1)	-	69 (1)	6.9 (1.6)	27.8 (3.3)	-	167 (33)
<i>Difference from baseline (p)</i>					.14	<.001	.66	-	-

WA%=wall area percent; LA=lumen area; WT=wall thickness; M=mucus; TAC=total airway count; VDV=ventilation defect volume; SD=standard deviation.

Mucus indicates mucus plugging.

Measurements are matched for segments within partial CT images acquired at baseline, except mucus plugging at follow-up shown as matched partial CT/whole thoracic CT.

### 4.3.3 FEV<sub>1</sub> and Ventilation Defect Postbronchodilator Reversibility Measurements

**Table 4-3** shows FEV<sub>1</sub> and ventilation defect post-bronchodilator reversibility measurements for each participant by groups with stable and worse VDV at follow-up. At follow-up, six participants were not FEV<sub>1</sub> bronchodilator reversible and eight participants had marginal MRI ventilation defect (change in VDV was greater than -110 mL) bronchodilator reversibility (grey-shaded cells). We compared measurements between FEV<sub>1</sub> reversible and not reversible participant groups and, as shown in **Figure 4-4**, PC<sub>20</sub> was greater (ie, more normal) in participants who were not reversible (**Figure 4-4A**;  $p=.01$ ), whereas the ratio of residual volume to total lung capacity (RV/TLC) was greater in participants who were bronchodilator reversible (**Figure 4-4B**;  $p<.001$ ). All other measurements were not different between reversible and not reversible participant groups (supplement **Table 4-8**;  $p>.05$ ). We also plotted baseline measurements against post-bronchodilator  $\Delta$ FEV<sub>1</sub> at follow-up and univariable relationships are shown in **Figure 4-4C** and **D**. PC<sub>20</sub> ( $r=-.61$ ,  $p=.049$ ), and pre-methacholine challenge VDV ( $r=.67$ ,  $p=.02$ ) at baseline were related to post-bronchodilator change in FEV<sub>1</sub>. All other measurements were not correlated with post-bronchodilator change in FEV<sub>1</sub> (supplement **Table 4-9**,  $p>.05$ ).

**Table 4-3** Changes in forced expiratory volume in 1 second and ventilation defects

	Baseline		Baseline		Follow-up	
	PostBD–PreMCh		PostBD–PostMCh		PostBD–PreBD	
	$\Delta$ FEV <sub>1</sub> (mL, %)	$\Delta$ VD (mL, %)	$\Delta$ FEV <sub>1</sub> (mL, %)	$\Delta$ VD (mL, %)	$\Delta$ FEV <sub>1</sub> (mL, %)	$\Delta$ VD (mL, %)
<i>Stable VDV at follow-up (n=8)</i>						
S02	-520, -15	-190, -3	+780, +35	-420, -7	+680, +24	-200, -4
S03	+380, +10	-120, -2	+1360, +45	-1710, -25	+220, +5	-90, -2
S04	+30, +2	-10, 0	+360, +37	-80, -2	+220, +15	-20, 0
S06	+70, +3	+10, 0	+810, +43	-1150, -19	+150, +5	-10, 0
S07	-90, -2	-210, -4	+1080, +53	-870, -11	+950, +37	-250, -2
S08	+470, +26	-30, -1	+1010, +81	-230, -4	+260, +14	-10, 0
S09	-350, -9	-70, -2	+650, +21	-340, -5	+400, +11	-50, -2
S10	-30, -1	+10, 0	+580, +29	-630, -9	+60, +2	+20, 0
Mean	-10, +2	-80, -1	+830, +43	-680, -10	+370, +14	-80, -1
SD	330, 12	120, 3	310, 18	480, 7	300, 11	100, 2
<i>Worse VDV at follow-up (n=3)</i>						
S01	-110, -5	+190, +5	+800, +58	-1040, -19	+1030, +60	-580, -11
S05	+200, +7	-60, 0	+600, +23	-430, -6	+160, +5	-100, -1
S11	-140, -6	+40, +1	+740, +48	-340, -7	+110, +5	-40, -1
Mean	-20, -1	+60, +2	+710, +42	-600, -10	+430, +23	-240, -4
SD	190, 7	130, 3	100, 18	380, 7	520, 32	300, 6
<i>ALL (n=11)</i>						
Mean	-10, +1	-30, 0	+760, +40	-570, -9	+300, +14	-100, -2
SD	270, 10	100, 2	270, 18	500, 8	370, 18	160, 3

BD=bronchodilator; MCh=methacholine challenge; FEV<sub>1</sub>=forced expiratory volume in one second; VD=ventilation defects; VDV=ventilation defect volume; SD=standard deviation.

$\Delta$ FEV<sub>1</sub> shown as absolute difference in mL and as a percent of baseline.

$\Delta$ VD shown as absolute ventilation defect volume (VDV) difference in mL and as absolute ventilation defect percent (VDP) difference.

Grey shaded cells indicate not reversible FEV<sub>1</sub> and VDV (n=6 not reversible FEV<sub>1</sub>, n=8 not reversible VDV).

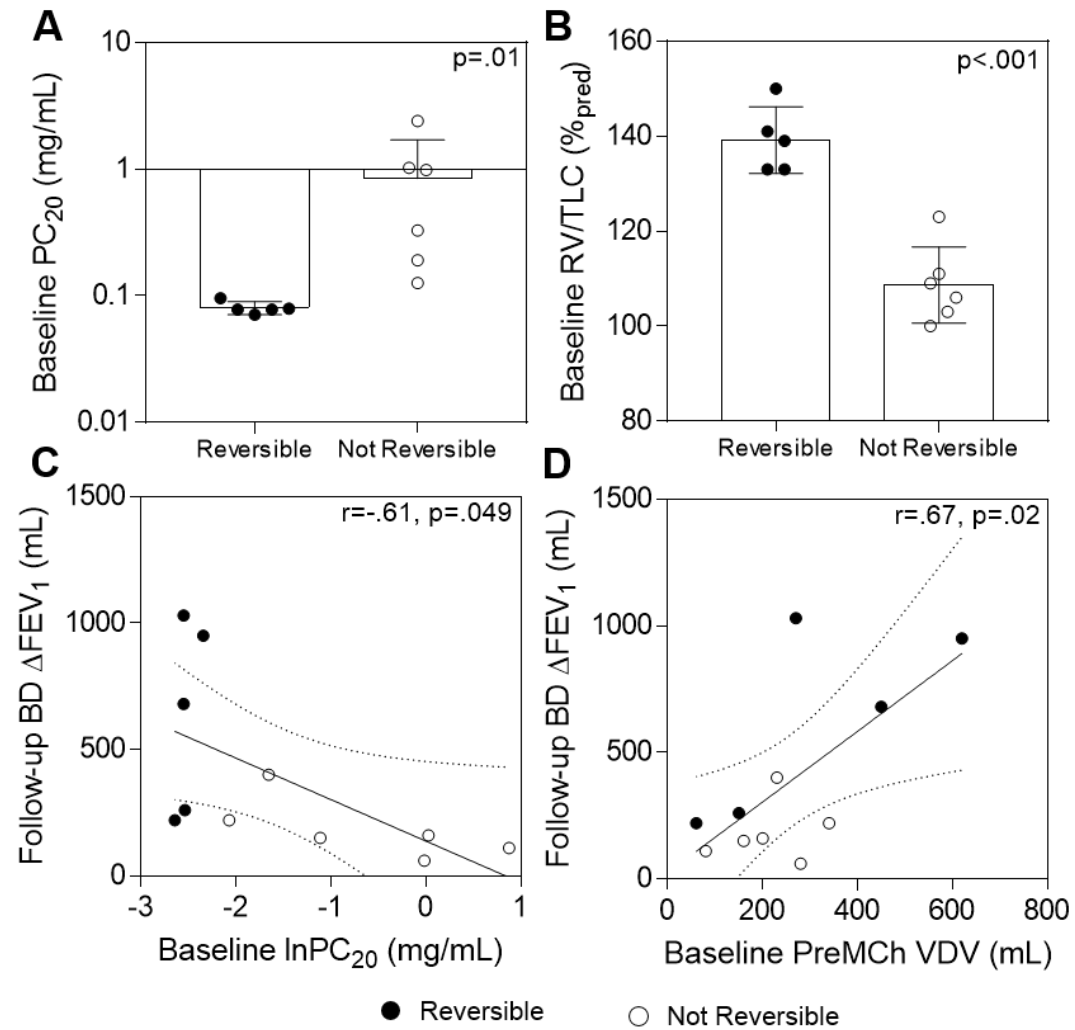


**Figure 4-4** Group differences and univariable relationships for postBD FEV<sub>1</sub> reversibility. *A*, Baseline concentration of methacholine required to decrease FEV<sub>1</sub> by 20% (PC<sub>20</sub>; log scale) was lower (ie, worse) in FEV<sub>1</sub>-reversible participants ( $p=.01$ ) and, *B*, baseline residual volume (RV)-to-total lung capacity (TLC) ratio (RV/TLC) was greater in reversible participants ( $p<.001$ ). *C*, Natural logarithm of PC<sub>20</sub> ( $\ln PC_{20}$ ;  $r=-0.61$ ;  $p=.049$ ) and, *D*, premethacholine challenge (preMCh) VDV ( $r=0.67$ ;  $p=.02$ ) were related to BD change in FEV<sub>1</sub> ( $\Delta FEV_1$ ) at follow-up.

#### 4.3.4 Multivariable Analysis

We generated multivariable models to explore potential predictors of post-bronchodilator FEV<sub>1</sub> reversibility at follow-up (**Table 4-4**). Baseline pre-methacholine challenge VDV (standardized  $\beta=0.89$ ;  $p=.01$ ) and pre-methacholine challenge to post-bronchodilator change in VDV (standardized  $\beta=0.58$ ;  $p=.03$ ) predicted post-bronchodilator change in FEV<sub>1</sub> (model 1:  $R^2=.80$ ;  $p=.01$ ). A second model including FEV<sub>1</sub>, age and PC<sub>20</sub> did not predict post-bronchodilator change in FEV<sub>1</sub> (model 2:  $R^2=.63$ ;  $p=.15$ ).

**Table 4-4** Multivariable model to predict bronchodilator reversibility

Parameter	Unstandardized		Standardized	p
	B	Standard Error	$\beta$	
<b>MODEL 1: FEV<sub>1</sub> reversibility at follow-up, n=11 (<math>R^2=.80, p&lt;.01</math>)</b>				
Baseline PreMCh VDV <sup>†</sup>	1.86	0.47	0.89	.01
Baseline PostBD–PreMCh $\Delta$ VDV <sup>†</sup>	1.80	0.67	0.58	.03
PC <sub>20</sub> mL <sup>2</sup> /mg*	-0.11	0.05	-0.41	.052
<b>MODEL 2: FEV<sub>1</sub> reversibility at follow-up n=11 (<math>R^2=.63, p=.15</math>)</b>				
Baseline PreMCh VDV <sup>†</sup>	1.15	0.67	0.55	.14
Baseline PreMCh FEV <sub>1</sub> <sup>†</sup>	-0.01	0.01	-0.14	.72
Age mL/year	-0.01	0.02	-0.26	.54
PC <sub>20</sub> mL <sup>2</sup> /mg*	-0.08	0.10	-0.29	.48

B=regression coefficient;  $\beta$ =standardized regression coefficient; FEV<sub>1</sub>=forced expiratory volume in one second; MCh=methacholine challenge; VDV=ventilation defect volume; BD= bronchodilator; PC<sub>20</sub>=concentration of methacholine causing 20% decrease in FEV<sub>1</sub>. \*log transformed PC<sub>20</sub>. For all models, dependent variable being predicted was bronchodilator  $\Delta$ FEV<sub>1</sub> in mL at follow-up (FEV<sub>1,post</sub>-FEV<sub>1,pre</sub>). Percent predicted (%<sub>pred</sub>) was used for pre-MCh FEV<sub>1</sub> to account for age, sex, height and race differences, and absolute differences in mL were used for  $\Delta$ FEV<sub>1</sub>.

<sup>†</sup>Unitless because independent and dependent variables have the same units.

## 4.4 Discussion

Recent epidemiological studies have revealed that in up to 10% of asthmatics, airways disease may lead to chronic, persistent airflow obstruction and chronic obstructive pulmonary disease, but the mechanisms underlying these changes are not fully understood. In this study, we investigated six-year longitudinal changes in hyperpolarized  $^3\text{He}$  MRI ventilation defects in individuals with mild-to-moderate asthma and sought to identify predictors of longitudinal changes in post-bronchodilator FEV<sub>1</sub>-reversibility. We showed that MRI ventilation predicts long-term post-bronchodilator FEV<sub>1</sub> reversibility in mild-to-moderate asthma. We observed: 1) negligible post-bronchodilator reversibility in six of 11 participants at follow-up, 2) baseline MRI ventilation defects predicted follow-up post-bronchodilator reversibility ( $R^2=.80$ ,  $p=.01$ ), 3) MRI ventilation defects persisted in the same spatial locations 6.5-years later, and, 4) ventilation defects worsened in three of 11 participants, in the same lung regions they previously worsened during methacholine challenge, 6.5-years prior.

MRI ventilation defects persisted in the same spatial locations at follow-up. For three participants (S01, S05, S11), ventilation defects also worsened in the same spatial regions that worsened during a methacholine challenge, approximately 6.5 years prior. Previous studies have evaluated MRI ventilation defects for up to approximately 1.5 years<sup>21,22</sup> and revealed spatially persistent defects,<sup>21</sup> suggesting that fixed asthma airway abnormalities are spatially heterogeneous. We also evaluated CT airway measurements to investigate the underlying pathophysiology of persistent and worsening ventilation defects which revealed inter-individual differences and mucus plugs in a single participant who worsened. However, there was no spatial relationship between ventilation worsening and mucus plugs in this participant with mild-moderate asthma.

The prevalence of negligible bronchodilator reversibility in our participant cohort (6/11, 55%) was higher than previously reported in epidemiological studies.<sup>5,6</sup> In all but one of these participants, there were no changes in medication (except for S11 who refused prescribed ICS/LABA) or exacerbations. Moreover, at follow-up, two participants in this subgroup (S06, S10) met the criteria for fixed airflow obstruction consistent with COPD<sup>36</sup> and two others (S05, S11) had worse VDV at follow-up. Airway remodeling caused by

chronic inflammation has been suggested to mediate changes that result in airflow obstruction not reversed by bronchodilators<sup>7</sup> and patients with asthma not using regular treatment may progress to irreversible obstruction.<sup>4</sup> We did not test for airway inflammation, so it is possible that inadequately controlled inflammation was responsible for the lack of reversibility which is consistent with the CT finding here of mucus plugs in only one participant.

For two participants (S04, S08) there was poorly reversible post-bronchodilator VDV alongside physiologically-relevant FEV<sub>1</sub> reversibility, and in participant S11 who apparently stopped all asthma medications, there was neither FEV<sub>1</sub> nor VDV post-bronchodilator reversibility and ventilation defects worsened at follow-up. These findings are consistent with unresolved small airway abnormalities or mucus plugs<sup>37</sup> leading to persistent ventilation defects that are not reversed using salbutamol, which mainly has receptors in the central airways. This could also be consistent with airway inflammation<sup>18</sup> and suggests that irreversible FEV<sub>1</sub> and worsening ventilation defects may result from inadequate treatment and/or poor adherence to prescribed asthma medication.

MRI ventilation defect volume at baseline predicted bronchodilator reversibility at follow-up whereas age, PC<sub>20</sub> and FEV<sub>1</sub> did not predict bronchodilator reversibility. Although baseline VDV had the greatest relative influence, the difference between pre-methacholine and post-challenge recovery ventilation defects (PostBD–PreMCh  $\Delta$ VDV) also significantly contributed. Abnormal FEV<sub>1</sub> and reduced post-bronchodilator FEV<sub>1</sub> reversibility were previously shown to predict post-bronchodilator FEV<sub>1</sub> reversibility.<sup>4</sup> Both diminished<sup>4</sup> and augmented<sup>2,35</sup> airway hyper-responsiveness were also shown to predict FEV<sub>1</sub> decline and irreversible airflow obstruction in asthmatics. Severe airway hyper-responsiveness was previously suggested to have a protective effect on the airways by preventing airway narrowing, thereby preserving bronchodilator reversibility.<sup>4</sup> Whilst post-bronchodilator FEV<sub>1</sub> changes following methacholine have been evaluated,<sup>38</sup> to our knowledge, this is the first exploration of the potential longitudinal consequence of ventilation defects induced using methacholine. It is somewhat counterintuitive that diminished ventilation at baseline predicted post-bronchodilator reversibility six years later. MRI ventilation defects can be due to large and small airway abnormalities,

inflammation and/or intraluminal mucus plugging;<sup>17,18,37</sup> the fact that baseline ventilation defects *and* the post-bronchodilator change in ventilation defects following a methacholine challenge predict future FEV<sub>1</sub> reversibility suggests that it is airway abnormalities and not inflammation or mucus plugging that drive MRI predictions of future post-bronchodilator reversibility. However, the near complete lack of mucus plugs in the participants studied here means we cannot test the role of mucus in our longitudinal findings. Nevertheless, we think these results highlight the utility and sensitivity of MRI ventilation measurements for hypothesis-driven, mechanistic studies, especially when combined with pulmonary function tests and thoracic CT. We think it is important to point out that MRI and CT are highly complementary. In other words, MRI in combination with CT provides a way to discern the airway structural and luminal determinants of ventilation abnormalities in asthma.

We acknowledge the small sample size and the fact that this study was limited to two time points, both of which limit the generalizability of the multivariable models. Baseline and follow-up MRI evaluations were also different, but this allowed us to explore different relationships between airway hyper-responsiveness, ventilation defects and bronchodilator reversibility. Finally, we recognize that compared to <sup>3</sup>He MRI, <sup>129</sup>Xe MRI offers a much less costly and highly sensitive alternative to measure small airway function,<sup>20</sup> so with <sup>129</sup>Xe MRI, we would expect similar if not more sensitive detection of ventilation defects.

In study participants with mild to moderate asthma, MRI ventilation defect volume predicted reversibility of post-bronchodilator FEV<sub>1</sub>, six years later, suggesting that pulmonary functional MRI may help identify patients at risk for the transition from asthma to fixed airflow obstruction and chronic obstructive pulmonary disease.

## 4.5 References

- 1 Global Initiative for Asthma (GINA). Global strategy for asthma management and prevention: Updated 2018. (2018).
- 2 Peat, J. K., Woolcock, A. J. & Cullen, K. Rate of decline of lung function in subjects with asthma. *Eur J Respir Dis* **70**, 171-179 (1987).

- 3 Brown, P. J., Greville, H. W. & Finucane, K. E. Asthma and irreversible airflow obstruction. *Thorax* **39**, 131-136 (1984).
- 4 Vonk, J. M. *et al.* Risk factors associated with the presence of irreversible airflow limitation and reduced transfer coefficient in patients with asthma after 26 years of follow up. *Thorax* **58**, 322-327 (2003).
- 5 To, T. *et al.* Do community demographics, environmental characteristics and access to care affect risks of developing ACOS and mortality in people with asthma? *Eur Respir J* **50** (2017).
- 6 To, T. *et al.* Progression from asthma to chronic obstructive pulmonary disease. Is air pollution a risk factor? *Am J Respir Crit Care Med* **194**, 429-438 (2016).
- 7 Elias, J. A. Airway remodeling in asthma. Unanswered questions. *Am J Respir Crit Care Med* **161**, S168-171 (2000).
- 8 Awadh, N., Muller, N. L., Park, C. S., Abboud, R. T. & FitzGerald, J. M. Airway wall thickness in patients with near fatal asthma and control groups: Assessment with high resolution computed tomographic scanning. *Thorax* **53**, 248-253 (1998).
- 9 Siddiqui, S. *et al.* Airway wall geometry in asthma and nonasthmatic eosinophilic bronchitis. *Allergy* **64**, 951-958 (2009).
- 10 Witt, C. A. *et al.* Longitudinal changes in airway remodeling and air trapping in severe asthma. *Acad Radiol* **21**, 986-993 (2014).
- 11 Newman, K. B., Lynch, D. A., Newman, L. S., Ellegood, D. & Newell, J. D., Jr. Quantitative computed tomography detects air trapping due to asthma. *Chest* **106**, 105-109 (1994).
- 12 Busacker, A. *et al.* A multivariate analysis of risk factors for the air-trapping asthmatic phenotype as measured by quantitative CT analysis. *Chest* **135**, 48-56 (2009).
- 13 Galban, C. J. *et al.* Computed tomography-based biomarker provides unique signature for diagnosis of COPD phenotypes and disease progression. *Nat Med* **18**, 1711-1715 (2012).
- 14 Zavaletta, V. *et al.* Characterizing patterns of fsad in asthma using an automated parametric response map algorithm [abstract]. *Am J Respir Crit Care Med* **193**, A2496 (2016).
- 15 Altes, T. A. *et al.* Hyperpolarized <sup>3</sup>He MR lung ventilation imaging in asthmatics: Preliminary findings. *J Magn Reson Imaging* **13**, 378-384 (2001).
- 16 Fain, S. B. *et al.* Evaluation of structure-function relationships in asthma using multidetector CT and hyperpolarized He-3 MRI. *Acad Radiol* **15**, 753-762 (2008).

- 17 Svenningsen, S. *et al.* What are ventilation defects in asthma? *Thorax* **69**, 63-71 (2014).
- 18 Svenningsen, S. *et al.* Sputum eosinophilia and magnetic resonance imaging ventilation heterogeneity in severe asthma. *Am J Respir Crit Care Med* **197**, 876-884 (2018).
- 19 de Lange, E. E. *et al.* Evaluation of asthma with hyperpolarized helium-3 MRI: Correlation with clinical severity and spirometry. *Chest* **130**, 1055-1062 (2006).
- 20 Svenningsen, S. *et al.* Hyperpolarized (<sup>3</sup>He and (<sup>129</sup>Xe MRI: Differences in asthma before bronchodilation. *J Magn Reson Imaging* **38**, 1521-1530 (2013).
- 21 de Lange, E. E. *et al.* The variability of regional airflow obstruction within the lungs of patients with asthma: Assessment with hyperpolarized helium-3 magnetic resonance imaging. *J Allergy Clin Immunol* **119**, 1072-1078 (2007).
- 22 de Lange, E. E. *et al.* Changes in regional airflow obstruction over time in the lungs of patients with asthma: Evaluation with <sup>3</sup>He MR imaging. *Radiology* **250**, 567-575 (2009).
- 23 Mummy, D. G. *et al.* Ventilation defect percent in helium-3 magnetic resonance imaging as a biomarker of severe outcomes in asthma. *J Allergy Clin Immunol* **141**, 1140-1141 e1144 (2018).
- 24 Svenningsen, S., Nair, P., Guo, F., McCormack, D. G. & Parraga, G. Is ventilation heterogeneity related to asthma control? *Eur Respir J* **48**, 370-379 (2016).
- 25 Kendzerska, T. *et al.* The impact of a history of asthma on long-term outcomes of people with newly diagnosed chronic obstructive pulmonary disease: A population study. *J Allergy Clin Immunol* **139**, 835-843 (2017).
- 26 Reddel, H. K. *et al.* An official American Thoracic Society/European respiratory Society statement: Asthma control and exacerbations: Standardizing endpoints for clinical asthma trials and clinical practice. *Am J Respir Crit Care Med* **180**, 59-99 (2009).
- 27 Miller, M. R. *et al.* Standardisation of spirometry. *Eur Respir J* **26**, 319-338 (2005).
- 28 Crapo, R. O. *et al.* Guidelines for methacholine and exercise challenge testing-1999. This official statement of the American Thoracic Society was adopted by the ATS board of directors, July 1999. *Am J Respir Crit Care Med* **161**, 309-329 (2000).
- 29 Pellegrino, R. *et al.* Interpretative strategies for lung function tests. *Eur Respir J* **26**, 948-968 (2005).

- 30 Tepper, R. S. *et al.* Asthma outcomes: Pulmonary physiology. *J Allergy Clin Immunol* **129**, S65-87 (2012).
- 31 Parraga, G. *et al.* Hyperpolarized <sup>3</sup>He ventilation defects and apparent diffusion coefficients in chronic obstructive pulmonary disease: Preliminary results at 3.0 tesla. *Invest Radiol* **42**, 384-391 (2007).
- 32 Kirby, M. *et al.* Hyperpolarized <sup>3</sup>He magnetic resonance functional imaging semiautomated segmentation. *Acad Radiol* **19**, 141-152 (2012).
- 33 Eddy, R. L., Svenningsen, S., McCormack, D. G. & Parraga, G. What is the minimal clinically important difference for helium-3 magnetic resonance imaging ventilation defects? *Eur Respir J* **51** (2018).
- 34 Kirby, M. *et al.* Pulmonary ventilation visualized using hyperpolarized helium-3 and xenon-129 magnetic resonance imaging: Differences in COPD and relationship to emphysema. *J Appl Physiol* **114**, 707-715 (2013).
- 35 Van Schayck, C. P., Dompeling, E., Van Herwaarden, C. L., Wever, A. M. & Van Weel, C. Interacting effects of atopy and bronchial hyperresponsiveness on the annual decline in lung function and the exacerbation rate in asthma. *Am Rev Respir Dis* **144**, 1297-1301 (1991).
- 36 Global Initiative for Chronic Obstructive Lung Disease (GOLD). Global strategy for the diagnosis, management, and prevention of chronic obstructive pulmonary disease. 2019 report. (2019).
- 37 Dunican, E. M. *et al.* Mucus plugs in patients with asthma linked to eosinophilia and airflow obstruction. *J Clin Invest* **128**, 997-1009 (2018).
- 38 Park, H. W. *et al.* Bronchodilator response following methacholine-induced bronchoconstriction predicts acute asthma exacerbations. *Eur Respir J* **48**, 104-114 (2016).

## 4.6 Supplement

**Table 4-5** Baseline measurements for participants who completed longitudinal follow-up and lost to follow-up

<b>Parameter (±SD)</b>	<b>All (n=26)</b>	<b>Completed Follow-up (n=11)</b>	<b>Lost to Follow-up (n=15)</b>	<b>Sig Diff* (p)</b>
Age years	35 (11)	42 (9)	28 (9)	<.01
Female Sex n	14	4	10	.23
BMI kg/m <sup>2</sup>	25 (5)	27 (4)	25 (5)	.32
FVC % <sub>pred</sub>	93 (11)	87 (13)	96 (10)	.06
FEV <sub>1</sub> % <sub>pred</sub>	84 (15)	76 (12)	93 (12)	<.01
FEV <sub>1</sub> /FVC %	74 (11)	70 (7)	81 (10)	<.01
RV % <sub>pred</sub>	113 (24)	126 (20)	104 (24)	.02
TLC % <sub>pred</sub>	101 (9)	103 (9)	100 (9)	.28
RV/TLC % <sub>pred</sub>	113 (20)	123 (18)	106 (19)	.03
R <sub>aw</sub> % <sub>pred</sub>	124 (69)	172 (68)	91 (49)	<.01
PC <sub>20</sub> mg/mL	5.87 (12.28)	0.50 (0.72)	9.80 (15.15)	<.01
VDP %	3 (3)	5 (4)	2 (1)	<.01

SD=standard deviation; BMI=body mass index; FVC=forced vital capacity; %<sub>pred</sub>=percent predicted; FEV<sub>1</sub>=forced expiratory volume in one second; RV=residual volume; TLC=total lung capacity; R<sub>aw</sub>=airways resistance; PC<sub>20</sub>=concentration of methacholine causing a 20% decrease in FEV<sub>1</sub>; VDP=ventilation defect percent. \*Significance of difference between participants included and excluded for longitudinal follow-up.

**Table 4-6** Participant listing of demographic characteristics and pulmonary function and MRI measurements at baseline and follow-up

Participant	Age (yrs)	Sex	FVC (%pred)	FEV <sub>1</sub> (L)	FEV <sub>1</sub> (%pred)	FEV <sub>1</sub> /FVC (%)	RV (%pred)	TLC (%pred)	RV/TLC (%pred)	R <sub>aw</sub> (%pred)	VDV (mL)	VDP (%)	PC <sub>20</sub> (mg/mL)
<i>Baseline (pre-MCh OR pre-MCh/post-MCh/post-BD)</i>													
S01	36	F	94	2.28(1.37/2.17)	74/55/71	66	165	113	150	247	270/1500/460	5/29/10	0.08
S02	37	M	86	3.52/2.22/3.00	86/54/73	80	135	97	141	202	450/680/260	9/13/6	0.08
S03	28	M	102	3.97/2.99/4.35	86/65/94	69	115	111	103	300	340/1930/220	6/29/4	0.1
S04	48	F	68	1.31/0.98/1.34	56/42/58	66	130	96	139	-	60/130/50	1/3/1	0.07
S05	48	M	69	2.98/2.58/3.18	69/59/73	78	98	87	111	122	200/570/140	3/8/2	1.03
S06	46	M	74	2.63/1.89/2.70	60/43/62	64	115	94	123	113	160/1320/170	3/22/3	0.3
S07	42	M	87	3.19/2.02/3.10	79/50/77	72	144	108	133	225	620/1280/410	11/19/7	0.1
S08	48	F	82	1.78/1.24/2.25	67/46/84	65	144	110	133	163	150/350/120	3/6/2	0.08
S09	30	M	103	4.09/3.09/3.74	97/73/89	77	108	109	100	104	230/500/160	5/8/3	0.2
S10	57	M	102	2.60/1.99/2.57	77/59/76	58	121	110	109	132	280/920/290	5/14/5	1.0
S11	44	F	93	2.42/1.54/2.28	83/53/78	72	108	102	106	112	80/460/120	2/9/2	2.4
Mean (±SD)	38 (9)	-	88 (13)	2.91 (0.85)/ 2.13 (0.73)/ 2.90 (0.81)	79 (16)/ 59 (14)/ 79 (15)	73 (10)	128 (22)	104 (10)	123 (17)	157 (72)	230 (170)/ 770 (580)/ 200 (120)	5 (4)/ 13 (9)/ 4 (3)	0.3 (9.8)
<i>Follow-up (pre-BD/post-BD)</i>													
S01	41	F	79/111	1.71/2.74	60/96	62/71	190/94	120/111	158/84	223/75	780/200	15/4	-
S02	43	M	76/84	2.88/3.56	72/90	75/84	131/86	100/87	128/98	202/62	250/50	5/1	-
S03	35	M	109/110	4.29/4.51	100/105	74/77	132/124	115/117	114/106	143/70	260/170	6/3	-
S04	55	F	67/76	1.44/1.66	66/76	77/79	131/122	96/98	142/128	157/113	60/40	1/1	-
S05	54	M	74/78	3.08/3.24	76/80	79/79	115/121	94/102	120/117	234/185	430/330	8/7	-
S06	52	M	87/88	2.87/3.02	71/75	63/65	109/101	93/93	116/108	133/83	90/80	2/1	-
S07	48	M	74/88	2.57/3.52	66/91	70/80	162/112	103/100	157/111	186/69	360/110	6/2	-
S08	55	F	86/86	1.81/2.07	73/83	67/76	157/125	117/108	134/115	143/102	70/60	1/1	-
S09	37	M	92/98	3.69/4.09	91/101	79/82	122/136	102/109	118/123	200/86	150/100	3/2	-
S10	64	M	108/106	2.53/2.59	82/84	57/59	143/113	116/107	123/105	105/72	170/190	3/4	-
S11	51	F	84/82	2.26/2.37	81/85	76/82	100/102	93/94	107/109	232/74	120/80	2/2	-
Mean (±SD)	45(9)	-	87 (14)/ 92 (12)	2.81 (0.87)/ 3.05 (0.79)	81 (16)/ 88 (9)	74 (10)/ 77 (8)	134 (27)/ 118 (23)	105 (11)/ 104 (10)	126 (18)/ 113 (15)	163 (55)/ 88 (35)	220 (210)/ 110 (90)	4 (4)/ 2 (2)	-

MCh=methacholine challenge; BD=bronchodilator; M=male; F=female; FVC=forced vital capacity; %<sub>pred</sub>=percent predicted; FEV<sub>1</sub>=forced expiratory volume in one second; RV=residual volume; TLC=total lung capacity; R<sub>aw</sub>=airways resistance; VDV=ventilation defect volume; VDP=ventilation defect percent; PC<sub>20</sub>=concentration of methacholine causing a 20% decrease in FEV<sub>1</sub>.

**Table 4-7** Medication use at both visits

	<b>Baseline</b>	<b>Follow-up</b>
<i>Corticosteroid use, n (%)</i>		
None	1 (9)	2 (18)
Low-medium dose ICS	10 (91)	9 (82)
High-dose ICS	0	0
OCS	0	0
<i>Types of controllers, n (%)</i>		
ICS only	1 (10)	1 (11)
ICS/LABA only	8 (80)	7 (78)
ICS/LABA + ICS	1 (10)	1 (11)

ICS=inhaled corticosteroid; OCS=oral corticosteroid; LABA=long-acting  $\beta$ -agonist. Participants were prescribed budesonide alone or in combination with formoterol, except for one participant prescribed fluticasone furoate in combination with vilanterol and another prescribed budesonide alone and in combination with formoterol. No participants were prescribed leukotriene receptor antagonists (LTRA) or tiotropium.

**Table 4-8** Baseline measurement differences between reversible and not reversible participant groups

<b>Parameter (±SD)</b>	<b>Reversible (n=5)</b>	<b>Not Reversible (n=6)</b>	<b>Sig Diff (p)</b>
Age years	42 (6)	42 (11)	>.99
Female Sex n	3	1	.24
BMI kg/m <sup>2</sup>	26 (4)	27 (4)	.89
FVC % <sub>pred</sub>	83 (10)	91 (15)	.39
FEV <sub>1</sub> % <sub>pred</sub>	72 (12)	79 (13)	.43
PostMCh–PreMCh ΔFEV <sub>1</sub> L	-0.85 (0.41)	-0.77 (0.23)	.69
PostBD–PreMCh ΔFEV <sub>1</sub> L	-0.04 (0.35)	0.02 (0.26)	.73
PostBD–PostMCh ΔFEV <sub>1</sub> L	0.81 (0.28)	0.79 (0.29)	.93
FEV <sub>1</sub> /FVC %	70 (6)	70 (8)	.98
RV % <sub>pred</sub>	144 (13)	111 (8)	<.01*
TLC % <sub>pred</sub>	105 (8)	102 (10)	.64
RV/TLC % <sub>pred</sub>	139 (7)	109 (8)	<.001
R <sub>aw</sub> % <sub>pred</sub>	209 (36)	109 (8)	.17
PC <sub>20</sub> mg/mL	0.08 (0.01)	0.84 (0.86)	.01
VDV mL	310 (230)	190 (120)	.27
PostMCh–PreMCh ΔVDV mL	0.48 (0.48)	0.74 (0.53)	.42
PostBD–PreMCh ΔVDV mL	-0.05 (0.16)	-0.04 (0.06)	.80
PostBD–PostMCh ΔVDV mL	-0.53 (0.41)	-0.77 (0.55)	.45
VDP %	6 (4)	4 (2)	.36

SD=standard deviation; BMI=body mass index; FVC=forced vital capacity; %<sub>pred</sub>=percent predicted; FEV<sub>1</sub>=forced expiratory volume in one second; MCh=methacholine challenge; VD=bronchodilator; RV=residual volume; TLC=total lung capacity; R<sub>aw</sub>=airways resistance; PC<sub>20</sub>=concentration of methacholine causing a 20% decrease in FEV<sub>1</sub>; VDV=ventilation defect volume; VDP=ventilation defect percent. \*Highly collinear with RV/TLC therefore only reported RV.

NOTE: subgroups defined by bronchodilator reversibility at follow-up.

**Table 4-9** Correlation coefficients for univariable relationships with post-bronchodilator  $\Delta$ FEV<sub>1</sub> at follow-up

<b>Parameter</b>	<b>Pearson Coeff (r)</b>	<b>Sig (p)</b>
FEV <sub>1</sub> % <sub>pred</sub>	.23	.50
PostMCh–PreMCh $\Delta$ FEV <sub>1</sub> L	.16	.65
PostBD–PreMCh $\Delta$ FEV <sub>1</sub> L	-.08	.81
PostBD–PostMCh $\Delta$ FEV <sub>1</sub> L	-.18	.60
VDV mL	.67	.02
PostMCh–PreMCh $\Delta$ VDV mL	-.61	.048
PostBD–PreMCh $\Delta$ VDV mL	-.42	.20
PostBD–PostMCh $\Delta$ VDV mL	.25	.46
lnPC <sub>20</sub> mg/mL	-.61	.049

FEV<sub>1</sub>=forced expiratory volume in one second; %<sub>pred</sub>=percent predicted; MCh=methacholine challenge; BD=bronchodilator; VDV=ventilation defect volume; PC<sub>20</sub>=concentration of methacholine causing a 20% decrease in FEV<sub>1</sub>; VDV=ventilation defect volume.

## CHAPTER 5

### 5 IS COMPUTED TOMOGRAPHY TOTAL AIRWAY COUNT RELATED TO ASTHMA SEVERITY AND AIRWAY STRUCTURE-FUNCTION?

*To better understand regional and whole-lung airway abnormalities in asthma, we evaluated CT total airway count in participants with asthma over a range of severities and compared these results with previously published results for COPD. We determined the relationship between CT total airway count with airway morphology, pulmonary function and MRI ventilation.*

*The contents of this chapter were previously published in the journal American Journal of Respiratory and Critical Care Medicine: RL Eddy, S Svenningsen, M Kirby, D Knipping, DG McCormack, C Licskai, P Nair, G Parraga. Is Computed Tomography Total Airway Count Related to Asthma Severity and Airway Structure-function? Am J Respir Crit Care Med. 2020. [Epub ahead of print] Permission to reproduce this article was granted by the American Thoracic Society (ATS) and is provided in **Appendix B**.*

#### 5.1 Introduction

In asthma, airways disease caused by smooth muscle abnormalities, inflammation and/or mucus hypersecretion leads to variable airflow obstruction that is reversible or improves post-bronchodilator.<sup>1</sup> Airway abnormalities in asthma are believed to encompass the entire tracheobronchial tree from the large to the small airways<sup>2</sup> and small airways disease is recognized as a distinct phenotype of asthma.<sup>2-4</sup> While small airway abnormalities remain difficult to directly measure, the large airways have been extensively investigated *in vivo*, using x-ray computed tomography (CT). Airway walls in asthmatics are thicker as compared to healthy controls<sup>5-12</sup> and this thickening tends to worsen with increasing asthma severity. Until now, CT studies of asthma have focused on morphological airway measurements and their relationships with clinical measurements, however the total number of CT-visible airways in patients with asthma has not been investigated.

Landmark studies of airways disease in COPD were performed using micro-CT<sup>13-15</sup> and more recently, *in vivo* CT total airway count (TAC) revealed missing distal airways that were associated with thinning airway walls in patients with mild COPD.<sup>16</sup> We think this finding may have implications for airways disease in asthma and hypothesized that in

severe asthma, thickened airways are concomitant with airway obstruction and/or occlusion, which could be quantified using TAC.

Accordingly, our objective was to measure and evaluate CT total airway count in patients with asthma across a range of severities and explore potential relationships of TAC with asthma severity, airway measurements, pulmonary function and pulmonary functional magnetic resonance imaging (MRI). A preliminary description of these results was previously reported in abstract form.<sup>17</sup>

## **5.2 Materials and Methods**

### **5.2.1 Study Participants and Design**

Study participants with asthma according to the Global Initiative for Asthma (GINA) treatment step criteria<sup>1</sup> were recruited as a convenience sample between ages 18 to 70 years with <1 pack year smoking history from two tertiary care respirology clinics (Asthma Centre, St Joseph's Health Care London, Western University, London, Ontario, Canada; Firestone Institute for Respiratory Health, St Joseph's Health Care Hamilton, McMaster University, Hamilton, Ontario, Canada). Participants provided written informed consent to an ethics board and Health Canada-approved, registered ([www.clinicaltrials.gov](http://www.clinicaltrials.gov), NCT02351141) protocol for a single study visit (Robarts Research Institute, Western University, London Canada). Participants performed spirometry, plethysmography and MRI before and after bronchodilator and completed a single post-bronchodilator thoracic CT as well as the asthma control (ACQ-6)<sup>18</sup> and quality of life questionnaires (AQLQ).<sup>19</sup> Participants were stratified by asthma severity according to GINA treatment steps<sup>1</sup> as: GINA1-3, GINA4, and GINA5.

### **5.2.2 Pulmonary Function Tests**

Spirometry and plethysmography were performed using a *MedGraphics Elite Series* plethysmograph (MGC Diagnostics Corporation, St. Paul, MN, USA). Spirometry was performed according to ATS guidelines<sup>20</sup> to measure FEV<sub>1</sub> and FVC, and plethysmography was performed to measure lung volumes and airways resistance. Post-bronchodilator measurements were acquired after four separate doses of 100 µg of Novo-Salbutamol HFA (Teva Novopharm Ltd., Toronto, ON, Canada) through a pressurized metered-dose inhaler

using an *AeroChamber Plus* spacer (Trudell Medical International, London, ON, Canada). Participants withheld asthma medications before the study visit according to ATS guidelines<sup>20</sup>: short-acting  $\beta$ -agonists for  $\geq 6$  hours, long-acting  $\beta$ -agonists for  $\geq 12$  hours and long-acting muscarinic agents for  $\geq 24$  hours.

### 5.2.3 CT

Thoracic CT was acquired post-bronchodilator using a 64-slice LightSpeed VCT system (General Electric Healthcare, Milwaukee, WI, USA) as previously described<sup>21</sup> from apex to base under breath-hold conditions after inhalation of 1.0 L of N<sub>2</sub> gas from functional residual capacity. CT parameters were as follows: 64 x 0.625 collimation, 120 kVp, 100 mA, tube rotation time 500 ms, pitch 1.25, standard reconstruction kernel, 1.25 mm slice thickness and field of view (FOV) 36-40 cm<sup>2</sup>. The total effective dose for each CT scan was 1.8 mSv, calculated using the manufacturer's settings and the ImPACT patient dosimetry calculator (based on the UK Health Protection Agency NRPB-SR250 software).

Thoracic CT images were analyzed by a single observer with four-years experience (RLE) using Pulmonary Workstation 2.0 (VIDA Diagnostics Inc., Coralville, IA, USA) to segment and label the airway tree and lung lobes. All airway segments in the segmented tree were summed to quantify total airway count (TAC),<sup>16</sup> and airway counts were also generated by tree generation from the trachea (generation 0) to generation 11.

We utilized a combination of automated airway segmentation and manual segmentation in the presence of complete airway lumen occlusions (possible mucus, cellular debris or its combination<sup>22</sup>). These were also recorded by manual inspection during airway segmentation as follows: 1) if there was completely visible lumen on both proximal and distal sides of an occlusion, the airway was manually segmented to its terminus and TAC was recorded at the distal terminus beyond the occlusion, and, 2) if there was lumen visible only on the proximal side of an occlusion which terminated the airway, TAC was recorded at the proximal end of the occlusion and not beyond the occlusion. Anatomically equivalent segmental, subsegmental and sub-subsegmental airways for five airway paths (RB1, RB4, RB10, LB1, LB10; third to fifth generation)<sup>23</sup> were used to generate airway wall area percent (WA%) and lumen area (LA). We determined if subsegmental and sub-

subsegmental daughter branches were missing for the five airway paths using the output file exported from Pulmonary Workstation 2.0. All airway segments were assigned a unique identifier that linked each parent airway to its corresponding daughter branches, and we defined participants with missing subsegments (generation 4) and sub-subsegments (generation 5) if one or more daughter branches were missing in the report. Airways were qualitatively assessed for segmental branch variants similar to previously published results.<sup>24</sup>

#### 5.2.4 MRI

Anatomical proton ( $^1\text{H}$ ) and  $^3\text{He}$  static ventilation MRI were acquired within five minutes of each other using a whole-body 3.0 T Discovery MR750 (General Electric Healthcare, Milwaukee, WI, USA) system with broadband imaging capability as previously described.<sup>25</sup> Participants were instructed to inhale a gas mixture from a 1.0 L Tedlar<sup>®</sup> bag (Jensen Inert Products, Coral Springs, FL, USA) from functional residual capacity, and 15 coronal slices were acquired in 8-15 seconds under breath-hold conditions.  $^1\text{H}$  MRI was performed before hyperpolarized  $^3\text{He}$  during 1.0 L breath-hold of ultra-high purity, medical-grade nitrogen ( $\text{N}_2$ ; Spectra Gases, Alpha, NJ, USA).  $^3\text{He}$  gas was polarized to 30–40% (HeliSpin; Polarean, Durham, NC, USA) and static ventilation imaging was performed during 1.0 L breath-hold of hyperpolarized  $^3\text{He}$  diluted to 25% by volume with  $\text{N}_2$ .

Quantitative MRI analysis was performed by a single observer with four-years experience (RLE) using in-house segmentation software as previously described<sup>26</sup> and MRI ventilation abnormalities were quantified as the ventilation defect percent (VDP; ventilation defect volume normalized to the MRI-measured thoracic cavity volume). VDP was also generated for each lung lobe by registering MRI to CT and normalizing the ventilation defect volume within each lobe to the corresponding lobe volume.<sup>27</sup>

#### 5.2.5 Statistical Analysis

All statistical analysis was performed using SPSS Statistics 25.0 (IBM Corporation, Armonk, NJ, USA). Data were tested for normality using Shapiro-Wilk tests and when not normally distributed, non-parametric tests were performed. Demographic, pulmonary

function test and imaging measurements between treatment step groups were compared using one-way analysis of variance (ANOVA) or Kruskal-Wallis tests with post-hoc Holm-Bonferroni correction for multiple comparisons. An analysis of covariance (ANCOVA) was used to compare TAC by treatment step group adjusted by age, sex and body mass index (BMI) as potential covariates, with post-hoc Holm-Bonferroni correction for multiple comparisons. The number of participants with missing sub-subsegmental branches was plotted in a histogram for the number of missing sub-subsegments, and the mode from the histogram was used to dichotomize participants; groups were compared using unpaired t-tests. Receiver operator characteristic (ROC) curves were generated to determine thresholds for TAC and the number of missing sub-subsegments for differentiating mild (GINA1-3) from severe asthma (GINA4-5). Univariate relationships were evaluated using Pearson (r) or Spearman ( $\rho$ ) correlation coefficients. Multivariable models were generated using the enter approach to determine the relative influence of significant univariate parameters on FEV<sub>1</sub> and WA%, with age, sex and BMI entered in the first step as potential covariates. All results were considered statistically significant when the probability of making a Type I error was less than 5% ( $p < 0.05$ ).

## 5.3 Results

### 5.3.1 Participant Demographics, Pulmonary Function and Imaging Measurements

We evaluated 70 participants with a clinical diagnosis of asthma as shown in **Table 5-1**. There were 15 participants in the GINA1-3 subgroup (6 females/9 males, 45±12 years), 19 participants in the GINA4 subgroup (10 females/9 males, 51±12 years) and 36 participants in the GINA5 subgroup (24 females/12 males, 48±13 years). Participants in the GINA4 group had worse FEV<sub>1</sub> (64±19%<sub>pred</sub> vs. 88±20%<sub>pred</sub>,  $p=0.003$ ) and FEV<sub>1</sub>/FVC (58±17% vs. 74±11%,  $p=0.006$ ) as compared to participants in the GINA1-3 subgroup. Participants in the GINA5 subgroup had worse FEV<sub>1</sub> (65±22%<sub>pred</sub> vs. 88±20%<sub>pred</sub>,  $p=0.004$ ) and FVC (80±18%<sub>pred</sub> vs. 94±14%<sub>pred</sub>,  $p=0.03$ ), WA% (68.2±1.7% vs. 66.7±1.5%,  $p=0.006$ ) and VDP (10±8% vs. 3±2%,  $p=0.02$ ) compared with participants in the GINA1-3 subgroup. There were no differences between the GINA4 and GINA5 subgroups. CT FOV differed to a small extent among study participants such that FOV=36x36 cm<sup>2</sup> for 47 participants,

FOV=40x40 cm<sup>2</sup> for 20 participants, FOV=39x39 cm<sup>2</sup> for 2 participants and FOV=41x41 cm<sup>2</sup> for a single participant. Importantly, TAC was not significantly different between subgroups based on FOV (p=0.7) and FOV was not significantly different between GINA subgroups (p=0.1).

**Table 5-1** Participant demographics, pulmonary function and imaging measurements

Parameter (±SD)	ALL (n=70)	GINA1-3 (n=15)	GINA4 (n=19)	GINA5 (n=36)
Age years	48 (12)	45 (12)	51 (12)	48 (13)
Female n (%)	40 (57)	6 (40)	10 (53)	24 (67)
BMI kg/m <sup>2</sup>	29 (5)	28 (5)	28 (6)	30 (5)
ACQ-6 Score	1.6 (1.2)	1.6 (0.9)	1.3 (1.3)	1.7 (1.3)
AQLQ Score	5.0 (1.4)	5.1 (1.1)	5.5 (1.3)	4.7 (1.4)
FEV <sub>1</sub> % <sub>pred</sub>	70 (22)	88 (20)	64 (19)*	65 (22)*
BD ΔFEV <sub>1</sub> %	17 (20)	8 (11)	16 (21)	20 (22)
FVC % <sub>pred</sub>	85 (17)	94 (14)	86 (14)	80 (18)*
FEV <sub>1</sub> /FVC %	65 (14)	74 (11)	58 (17)*	64 (12)
RV L	2.41 (0.67)	2.29 (0.55)	2.67 (0.53)	2.32 (0.77)
RV % <sub>pred</sub>	131 (35)	125 (35)	144 (24)	128 (39)
TLC L	5.98 (1.18)	6.47 (0.89)	6.19 (1.10)	5.63 (1.27)
TLC % <sub>pred</sub>	104 (14)	105 (11)	110 (10)*	100 (15)
RV/TLC % <sub>pred</sub>	127 (26)	118 (25)	131 (19)	128 (30)
R <sub>aw</sub> % <sub>pred</sub>	195 (118)	167 (93)	190 (80)	210 (244)
CT FOV cm <sup>2</sup>	37 (2)	37 (2)	38 (2)	37 (2)
TAC n	154 (45)	183 (49)	148 (36)*	146 (47)*
WA%	67.7 (1.6)	66.7 (1.5)	67.5 (1.1)	68.2 (1.7)*
LA mm <sup>2</sup>	10.5 (2.4)	11.5 (2.0)	10.4 (2.4)	9.7 (2.7)
VDP % <sup>†</sup>	9 (8)	3 (2)	10 (10)	10 (8)*

ACQ=asthma control questionnaire; AQLQ=asthma quality of life questionnaire; BD=bronchodilator; BMI=body mass index; FEV<sub>1</sub>=forced expiratory volume in one second; FOV=field of view; FVC=forced vital capacity; GINA=Global Initiative for Asthma; LA=lumen area; R<sub>aw</sub>=airways resistance; RV=residual volume; SD=standard deviation; TAC=total airway count; TLC=total lung capacity; VDP=ventilation defect percent; WA%=wall area percent; %<sub>pred</sub>=percent predicted.

\*Significantly different from GINA Steps 1-3 (p<0.05) using one-way ANOVA for parametric variables or Kruskal Wallis tests for non-parametric variables, both with post-hoc Holm Bonferroni corrections. <sup>†</sup>n=60

### 5.3.2 Is TAC Reduced with Increasing Asthma Severity?

In **Figure 5-1**, representative 3D reconstructed CT airway trees show that with greater asthma severity, the airway tree has fewer segmented airways. TAC was significantly lower in the GINA4 (145±10, p=0.03) and GINA5 (148±7, p=0.045) subgroups as

compared to GINA1-3 subgroup ( $182 \pm 11$ ) when adjusting for covariates (age, sex, BMI). BMI was the only significant covariate ( $p=0.003$ ), whereas age and sex were not significant ( $p=0.05$  and  $p=0.06$ , respectively). We performed an additional ANCOVA to include RV/TLC as a covariate, however RV/TLC was not significant ( $p=0.07$ ) and TAC and GINA subgroup remained a significant interaction ( $p=0.03$ ). TAC was not different between males and females (males TAC= $155 \pm 42$  vs. females TAC= $155 \pm 50$ ,  $p=1.0$ ), and there was no significant interaction between sex and GINA status for TAC ( $p=0.2$ ). **Figure 5-1** also shows that TAC was significantly reduced for generations 6 ( $p=0.04$ ) and 7 ( $p=0.01$ ) for the GINA4 subgroup and generations 6 ( $p=0.04$ ), 7 ( $p=0.01$ ), 10 ( $p=0.01$ ) and 11 ( $p=0.02$ ) for the GINA5 subgroup as compared to the GINA1-3 subgroup. The values for airway count by generation are shown in supplementary **Table 5-6**, as well as those previously published for healthy never-smokers<sup>16</sup> for comparison.

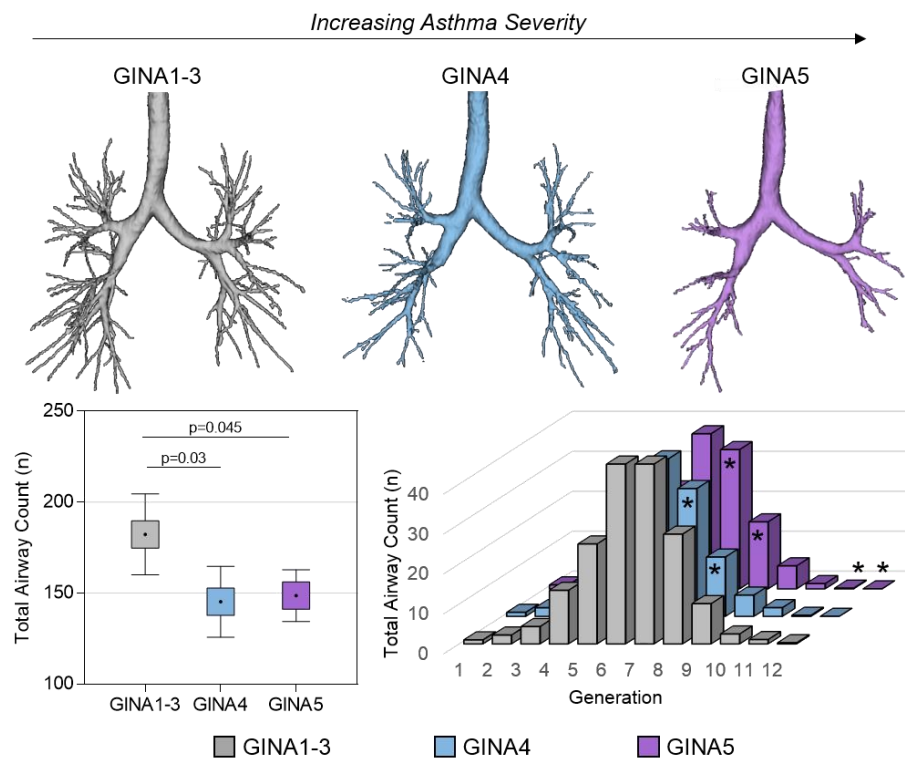


**Figure 5-1** CT airway count by airway tree generation

Three-dimensional reconstruction of the segmented airway tree for representative participants with asthma by Global Initiative for Asthma (GINA) treatment steps for asthma severity shows reduced airways as asthma severity increases (top). Total airway count was significantly less for GINA4 ( $p=0.03$ ) and GINA5 ( $p=0.045$ ) participants compared with GINA1-3 participants. GINA4 participants had significantly less airways at airway tree generations 6 and 7 compared with GINA1-3, whereas GINA5 participants

had significantly less airways at generations 6, 7, 10 and 11 compared with GINA1-3. Stars (\*) indicate significantly different from GINA1-3.

### 5.3.3 Is TAC Associated with Abnormal Airway Structure and Function?

**Table 5-2** shows the number of participants with CT invisible or missing subsegmental (generation 4) and sub-subsegmental (generation 5) daughter branches. A total of 19 participants (27%) were missing subsegmental branches, which was most common in the right middle lobe (RB4; 13/19). A total of 69 participants (99%) were missing sub-subsegmental branches, and this was most common in the left lower lobe (LB10; 54/69) and right middle lobe (RB4; 48/69). The distribution of participants with missing sub-subsegments provided in **Figure 5-2** shows that the most common number of missing sub-subsegments (mode) was 10; 34/70 participants or 49% were missing  $\geq 10$  (or  $\geq 50\%$ ) of 20 potential total sub-subsegmental airways. **Figure 5-2** also shows that asthma participants with  $\geq 10$  missing sub-subsegments (n=34) had increased WA% ( $68.6 \pm 1.4\%$  vs.  $66.8 \pm 1.3\%$ ,  $p < 0.0001$ ) and reduced LA ( $9.1 \pm 1.9 \text{ mm}^2$  vs.  $11.8 \pm 2.2 \text{ mm}^2$ ,  $p < 0.0001$ ) compared with participants with  $< 10$  missing sub-subsegments (n=36). Participants with  $\geq 10$  missing sub-subsegments also had greater pre-bronchodilator VDP compared with participants with  $< 10$  missing sub-subsegments ( $7 \pm 7\%$  vs.  $11 \pm 9\%$ ,  $p = 0.03$ ), but not post-bronchodilator VDP ( $5 \pm 7\%$  vs.  $7 \pm 6\%$ ,  $p = 0.053$ ). VDP improved post-bronchodilator in both subgroups dichotomized by missing sub-subsegments (both  $p < 0.001$ ). ROC curves showed an area under the curve of 0.71 ( $p = 0.01$ ) for TAC. A TAC threshold of 165 discriminated between subgroups with a sensitivity of 60% and specificity of 67%.

**Table 5-2** Participants with missing subsegmental and sub-subsegmental daughter branches by whole-lung and lung lobe

Parameter n (%)	Number of Participants n=70	
	Subsegments	Sub-subsegments
Whole-lung	19 (27)	69 (99)
RUL (RB1)	2 (3)	21 (30)
RML (RB4)	13 (19)	48 (69)
RLL (RB10)	2 (3)	45 (64)
LUL (LB1)	5 (7)	42 (60)
LLL (LB10)	4 (6)	54 (77)

LLL=left lower lobe; LUL=left upper lobe; RLL=right lower lobe; RML=right middle lobe; RUL=right upper lobe. All percentages shown as fraction of total n=70.

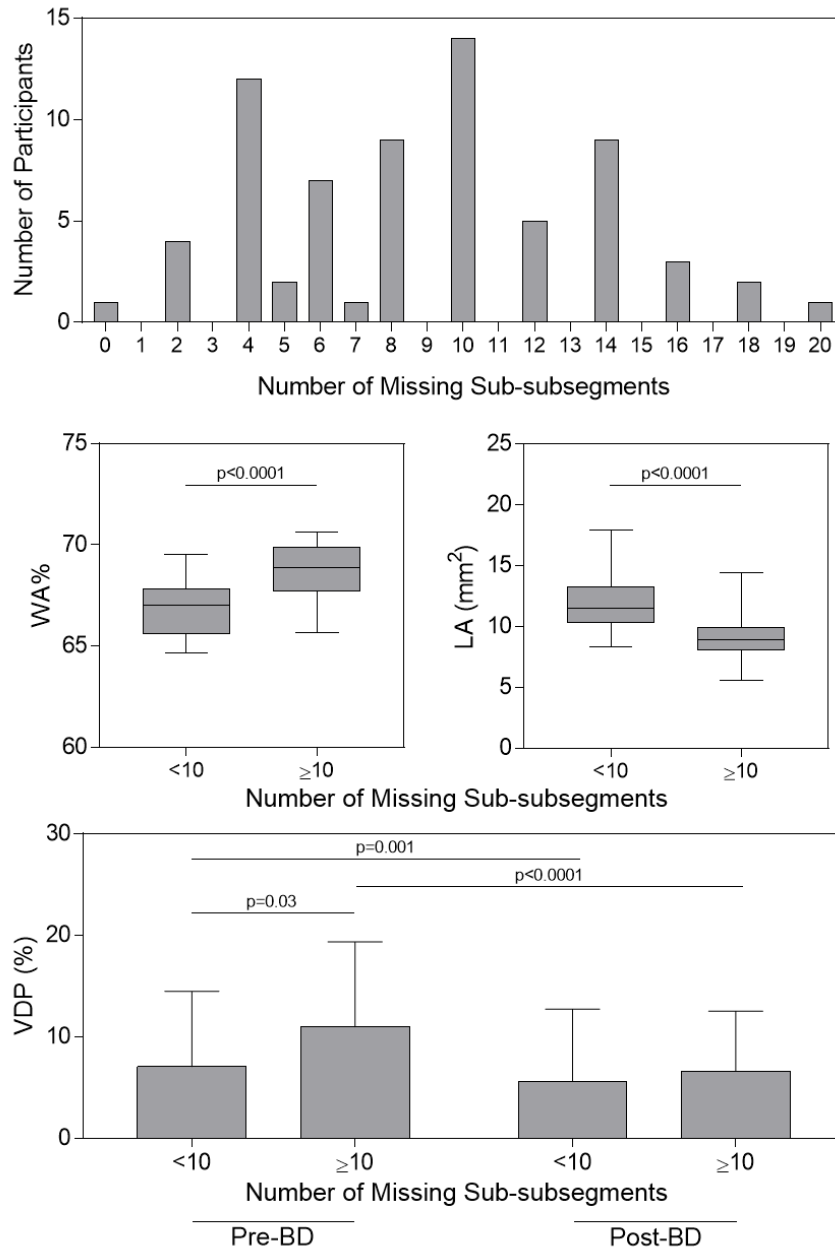


**Figure 5-2** Airway morphology and VDP by number of missing sub-subsegmental airways. Participants were dichotomized by the number of missing sub-subsegmental airways less than and greater than the mode of the number of missing sub-subsegmental airways (mode=10); 36 participants had <10 missing sub-subsegmental airways and 34 had  $\geq 10$  missing sub-subsegmental airways. For participants with  $\geq 10$  missing sub-subsegmental airways, wall area percent (WA%) was significantly greater and lumen area (LA) was significantly less (both  $p < 0.0001$ ), compared with participants with  $\geq 10$  missing sub-subsegmental airways. Pre-bronchodilator (BD) ventilation defect percent (VDP) was significantly worse in participants with  $\geq 10$  missing sub-subsegments ( $p = 0.03$ ) but post-BD VDP was not different ( $p = 0.053$ ).

The relationship between missing sub-subsegmental airways and VDP on a lobar level is shown in **Figure 5-3**. MRI ventilation defect percent (VDP) was significantly greater in the right middle lobe (RML,  $p=0.04$ ), right lower lobe (RLL,  $p<0.0001$ ) and left lower lobe (LLL,  $p<0.0001$ ) as compared to the right upper lobe (RUL), and VDP was significantly greater in the RLL ( $p<0.0001$ ) and LLL ( $p<0.0001$ ) as compared to the left upper lobe (LUL). We also classified participants by the number of missing sub-subsegments on each of the five airway paths; as compared to participants with 0 missing sub-subsegments, participants with 3-4 missing on RB10 and LB1 had significantly greater VDP in the RLL and LUL, respectively (both  $p=0.04$ ), whereas participants with 1-2 missing had significantly greater VDP in the LUL ( $p=0.02$ ). Groups were not different for the RML ( $p=0.7$ ), LLL ( $p=0.3$ ), nor RUL ( $p=0.5$ ; not shown).

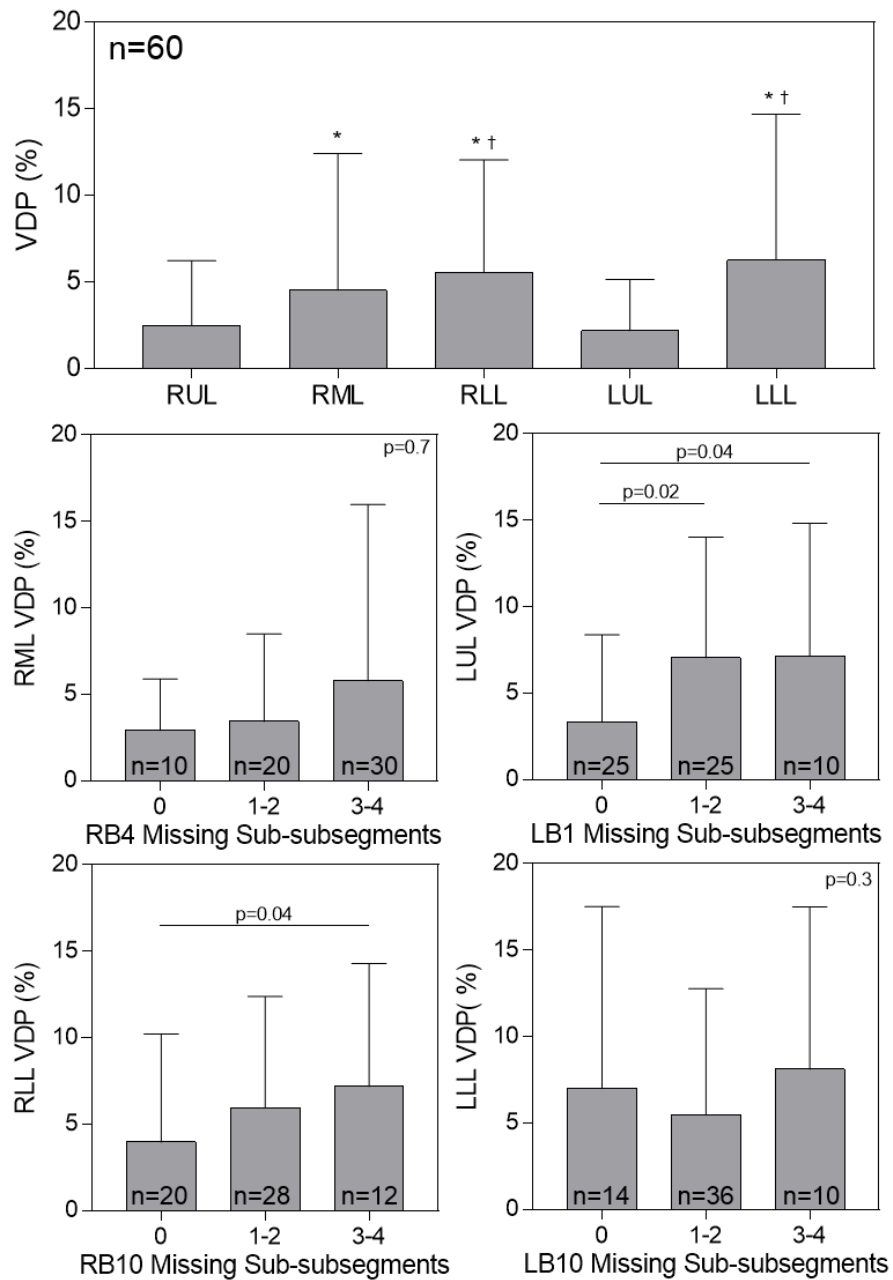


**Figure 5-3 MRI VDP by lung lobe**

MRI ventilation defect percent (VDP) was significantly greater in the right middle lobe (RML), right lower lobe (RLL) and left lower lobe (LLL) as compared to the right upper lobe (RUL; \* $p < 0.05$ ); VDP was significantly greater in the RLL and LLL as compared to the left upper lobe (LUL; † $p < 0.05$ ). As compared to participants with 0 missing sub-segments, participants with 3-4 missing sub-segments on RB10 and LB1 had significantly greater VDP in the RLL and LUL, respectively (both  $p = 0.04$ ), whereas participants with 1-2 missing sub-segments had significantly greater VDP in the LUL ( $p = 0.02$ ). Groups were not different for the RML nor LLL.

As shown in **Table 5-3**, we also investigated airway branch variants at the segmental level. Airway branch variants were observed in 18 of 70 participants (26%). The most common branch variants were the accessory sub-superior segment (n=10, 14%) and the accessory left-medial basal segment (n=4, 6%). Other variants included an absent right-medial basal, accessory right anterior, accessory right-medial basal and accessory airway off the left main bronchus, before the left upper lobe bronchus. Participants with airway variants had significantly diminished pre-bronchodilator RV ( $117 \pm 28\%_{\text{pred}}$  vs.  $137 \pm 36\%_{\text{pred}}$ ,  $p=0.03$ ), TLC ( $99 \pm 14\%_{\text{pred}}$  vs.  $105 \pm 13\%_{\text{pred}}$ ,  $p=0.04$ ) and RV/TLC ( $117 \pm 24\%_{\text{pred}}$  vs.  $130 \pm 26\%_{\text{pred}}$ ,  $p=0.050$ ), significantly diminished post-bronchodilator MRI VDP ( $5 \pm 6\%$  vs.  $7 \pm 7\%$ ,  $p=0.048$ ), and significantly greater LA ( $11.6 \pm 2.4 \text{ mm}^2$  vs.  $10.1 \pm 2.4 \text{ mm}^2$ ), compared with participants without airway variants. TAC was not significantly different between participants with and without airway variants ( $164 \pm 33$  vs.  $152 \pm 50$ ,  $p=0.4$ ).

**Table 5-3** Segmental airway branch variants

<b>Parameter n (%)</b>	<b>Number of Participants n=70</b>
None	52 (74)
Any	18 (26)
Accessory sub-superior (RB6)*	10 (14)
Absent right-medial basal (RB7)	1 (1)
Accessory left-medial basal (LB7)	4 (6)
Accessory right anterior (RB3)	1 (1)
Accessory right-medial basal (RB7)	1 (1)
Accessory left main bronchus <sup>†</sup>	1 (1)

\*Accessory right sub-superior (RB6) observed in 10 of 70 participants, 2 of which also had accessory left sub-superior (LB6), and 1 of which also had absent right-medial basal (RB7).

<sup>†</sup>Accessory branch off left main bronchus, before left upper lobe bronchus.

**Table 5-4** summarizes the number of participants with CT evidence of airway occlusions that either terminated or did not terminate airways and the total number of airway occlusions observed during the segmentation process. Intraluminal airway occlusions were identified in 20 of the 70 (29%) participants; five (7%) participants had occlusions that terminated the airway (11 total occlusions) and 15 participants (22%) had occlusions that did not terminate the airway segmentation distal to the plug (31 total occlusions). Of the five participants with occlusions terminating airways, two were GINA4 (2/19, 11%) and three were GINA5 (3/36, 8%). Of the 15 participants with occlusions that did not terminate the airways, one was GINA3 (1/15, 7%), four were GINA4 (4/19, 21%) and ten were GINA5 (10/36, 28%).

**Table 5-4** CT airway count and airway occlusion

<b>Parameter</b>	<b>ALL (n=70)</b>	<b>GINA1-3 (n=15)</b>	<b>GINA4 (n=19)</b>	<b>GINA5 (n=36)</b>
<i>Occlusions terminating airways</i>				
Participants n (%)	5 (7)	0	2 (11)	3 (8)
Occlusions n	11	0	3	8
<i>Occlusions not terminating airway</i>				
Participants n (%)	15 (22)	1 (7)	4 (21)	10 (28)
Occlusions n	31	1	10	20
<i>No occlusions</i>				
Participants n (%)	50 (71)	14 (93)	13 (68)	23 (64)

GINA=Global Initiative for Asthma.

#### 5.3.4 Is TAC Related to FEV<sub>1</sub> and Airway Wall Area?

**Figure 5-4** shows that TAC was moderately related to post-bronchodilator FEV<sub>1</sub> ( $r=0.39$ ,  $p=0.001$ ; post-bronchodilator  $\Delta$ FEV<sub>1</sub>  $r=-0.38$ ,  $p=0.002$  [not shown]), WA% ( $r=-0.55$ ,  $p<0.0001$ ) and LA ( $r=0.52$ ,  $p<0.0001$ ). In a subset of 60 participants who underwent hyperpolarized <sup>3</sup>He MRI (two did not fit the MRI coil and eight were consented to <sup>129</sup>Xe MRI only), TAC was also related to post-bronchodilator VDP ( $\rho=-0.34$ ,  $p=0.008$ ). TAC was weakly related to RV/TLC ( $r=-0.28$ ,  $p=0.02$ ), but not FVC ( $r=0.24$ ,  $p=0.051$ ), RV ( $r=-0.21$ ,  $p=0.09$ ), TLC ( $r=-0.02$ ,  $p=0.9$ ) nor FOV ( $r=0.03$ ,  $p=0.8$ ; data not shown).

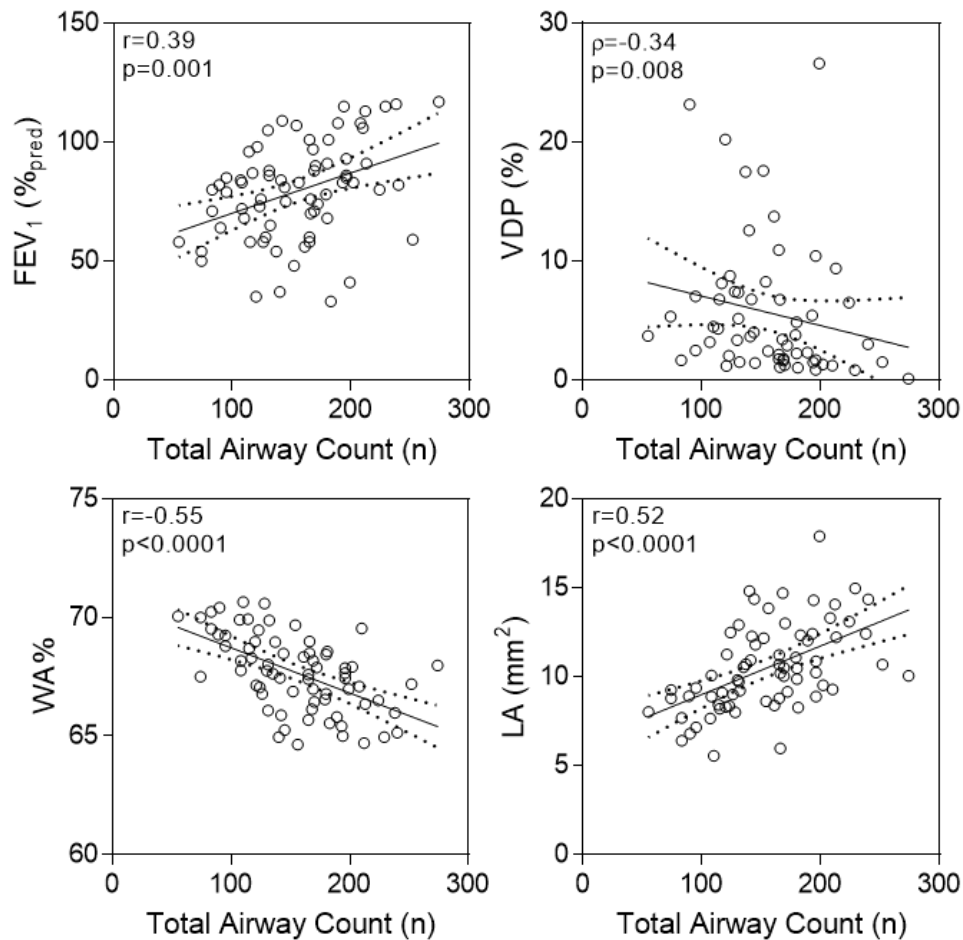


**Figure 5-4** CT total airway count relationships

Total airway count was significantly related to post-bronchodilator FEV<sub>1</sub> ( $r=0.39$ ,  $p=0.001$ ) and MRI ventilation defect percent (VDP;  $\rho=-0.34$ ,  $p=0.008$ ), as well as CT wall area percent (WA%;  $r=-0.55$ ,  $p<0.0001$ ) and lumen area (LA;  $r=0.52$ ,  $p<0.0001$ ).

Multivariable models to determine the relative influence of TAC on FEV<sub>1</sub> and WA%, adjusted for covariates, are shown in **Table 5-5**. First, we determined the relative influence of CT imaging measurements on FEV<sub>1</sub> (Model 1:  $R^2=0.27$ ,  $p=0.003$ ), for which TAC was the only predictor ( $\beta=0.50$ ,  $p=0.001$ ). Next, we determined the relative influence of CT and MRI on FEV<sub>1</sub> (Model 2:  $R^2=0.49$ ,  $p<0.0001$ ), and both CT TAC ( $\beta=0.27$ ,  $p=0.03$ ) and MRI VDP ( $\beta=-0.53$ ,  $p<0.0001$ ) significantly contributed. Finally, in a model for WA% (Model 3:  $R^2=0.32$ ,  $p=0.0001$ ), only TAC was a significant predictor ( $\beta=-0.53$ ,  $p<0.0001$ ). Some of these important relationships can be demonstrated in **Figure 5-5** where 3D reconstructed airway trees are shown co-registered to <sup>3</sup>He MRI static ventilation.

**Table 5-5** Multivariable models

Parameter	Unstandardized		Standardized	p
	B	Standard Error	$\beta$	
<b>MODEL 1: FEV<sub>1</sub> %<sub>pred</sub> (<math>R^2=0.27</math>, <math>p=0.003</math>)</b>				
TAC	0.22	0.07	0.50	0.001
WA%	-0.58	2.44	-0.05	0.8
LA	-0.62	1.62	-0.07	0.7
<b>MODEL 2: FEV<sub>1</sub> %<sub>pred</sub> (<math>R^2=0.49</math>, <math>p&lt;0.0001</math>)</b>				
TAC	0.13	0.06	0.27	0.03
WA%	-0.25	2.25	-0.02	0.9
LA	-0.18	1.45	-0.02	0.9
VDP	-1.34	0.28	-0.53	<0.0001
<b>MODEL 3: WA% (<math>R^2=0.32</math>, <math>p=0.0001</math>)</b>				
TAC	-0.02	0.01	-0.53	<0.0001
FEV <sub>1</sub>	-0.01	0.01	-0.07	0.7
VDP	-0.02	0.04	-0.09	0.5

B=regression coefficient;  $\beta$ =standardized regression coefficient; FEV<sub>1</sub>=forced expiratory volume in one second; LA=lumen area; TAC=total airway count; VDP=ventilation defect percent; WA%=wall area percent; %<sub>pred</sub>=percent predicted.

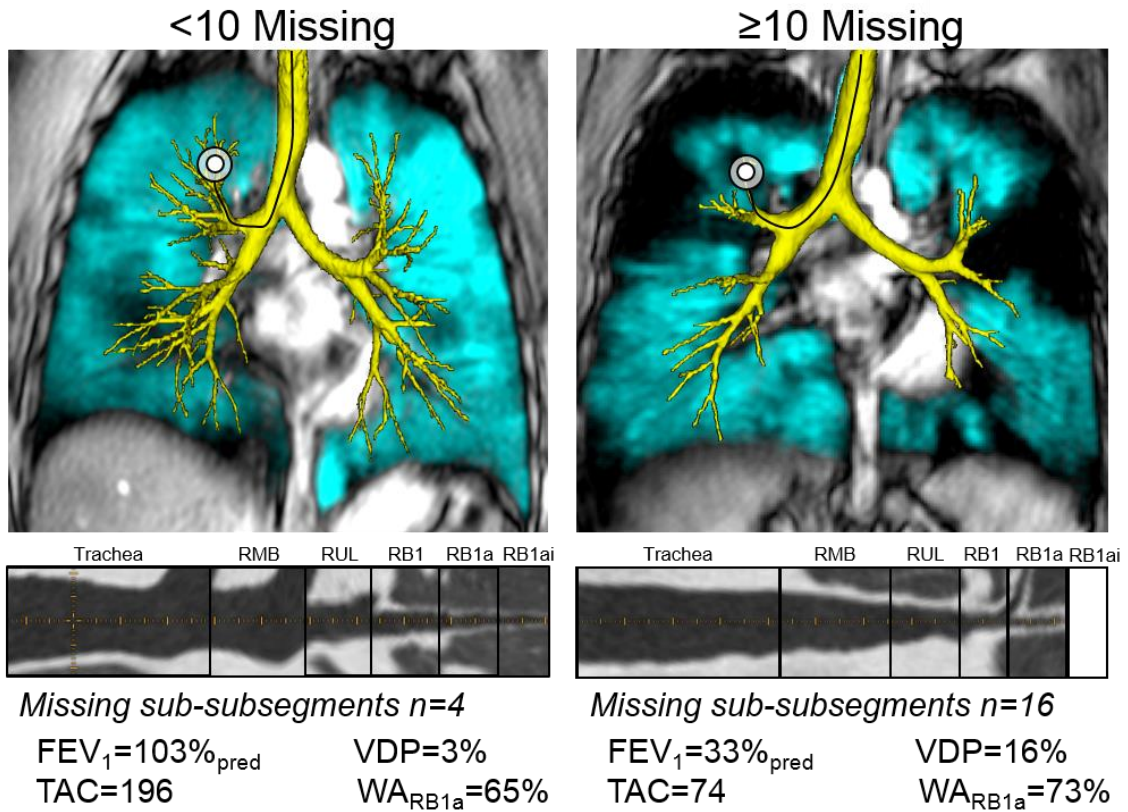


**Figure 5-5** Airway count and wall area relationship with MRI ventilation defects and FEV<sub>1</sub>. Three-dimensional reconstruction of the segmented airway tree co-registered to two-dimensional coronal centre slice <sup>3</sup>He MRI static ventilation (cyan) and anatomical <sup>1</sup>H (grey-scale) for participants with <10 (left) and ≥10 (right) missing sub-subsegments. The participant with <10 missing sub-subsegments (45-year-old female) has greater TAC, less MRI ventilation defects and greater FEV<sub>1</sub> than the participant with ≥10 missing sub-subsegments (31-year-old female). The two-dimensional airway paths to RB1 (below) show the CT-visible sub-subsegmental daughter branch (RB1ai) with less abnormal airway wall thickening at the subsegmental level (RB1a) for the participant with <10 missing sub-subsegments, versus the missing sub-segmental daughter branch with marked airway wall thickening at the segmental level for a participant with ≥10 missing sub-subsegments.

## 5.4 Discussion

Recent work has shown that CT total airway count decreases with increasing severity in COPD<sup>16</sup> and based on these findings, we wondered whether airways also appear missing on CT in asthma and about the potential relationship of CT TAC with asthma severity. We evaluated 70 participants with asthma and made the following observations: 1) TAC was diminished in GINA4 and GINA5 participants compared with GINA1-3, 2) asthma participants with  $\geq 10$  missing sub-subsegmental airways had thicker airway walls, narrower airway lumens and worse MRI ventilation defects than asthma participants with  $< 10$  missing sub-subsegmental airways, and 3) TAC was moderately related to FEV<sub>1</sub>, MRI VDP, airway wall thickness and lumen area, and in multivariate models, TAC independently predicted FEV<sub>1</sub> and WA%.

### 5.4.1 TAC is Reduced with Increasing Asthma Severity

To our knowledge, this is the first time the relationship between CT airway count and asthma severity has been directly measured and we were surprised to observe that the total number of CT-visible airways was reduced in GINA4-5 participants. Moreover, mean TAC for all asthma participants in this study ( $154 \pm 45$ ) was less than mean TAC previously reported for never-smoker healthy participants in the CanCOLD cohort ( $221 \pm 73$ ),<sup>16</sup> suggesting the reduced number of airways may be linked to asthma susceptibility or pathogenesis. In fact, TAC reported for GINA1-3 ( $183 \pm 49$ ) and GINA4-5 ( $148 \pm 36$ ,  $146 \pm 47$ , respectively) were qualitatively similar to TAC measurements previously reported in GOLD 1 ( $190 \pm 66$ ) and GOLD II COPD ( $152 \pm 53$ ), respectively.<sup>16</sup> We note that BMI was the only significant covariate when comparing TAC between treatment steps; age, sex and RV/TLC were not significant covariates. To the best of our knowledge, there are no previously published TAC values for patients with asthma. Missing or CT-invisible airways started to be obvious at generation 6 in asthma which is similar to previous findings (generation 5) in COPD<sup>16</sup> and could be due to airway narrowing, obstruction and/or obliteration. We note that four participants with the lowest FEV<sub>1</sub>/FVC were GINA4, which may dictate a need for treatment step-up.<sup>1</sup> The GINA4 subgroup sample size was about half the GINA5 subgroup and the small sample size may have also influenced this result.

#### 5.4.2 TAC is Associated with Abnormal Airway Structure and Function

For asthmatics with  $\geq 10$  missing sub-subsegmental airways, airway walls were thicker and airway lumens were narrower; this is in agreement with extensive CT studies demonstrating thickened airway walls in patients with asthma.<sup>5-12</sup> COPD participants were previously dichotomized using the presence or absence of sub-subsegmental branches.<sup>16</sup> However, we were alarmed that all but one participant had missing sub-subsegments and the dichotomization scheme previously described was not possible. In fact, approximately 50% of the 70 participants we evaluated were missing half or more ( $\geq 10$ ) of the total 20 possible sub-subsegmental airways. We note that the mean number of missing sub-subsegments was 9, the median=8, and the mode=10 and that using any of these thresholds resulted in the same subgroup composition. Similar to previous work in COPD,<sup>16</sup> our results suggest that in asthma, CT-invisible airways may be related to abnormal airway structure, which may be a combination of airway remodeling<sup>28</sup> and/or intraluminal occlusion.<sup>22</sup> Intraluminal airway occlusion (mucus, cellular debris or their combination) was identified in 20 participants, although such occlusions terminated the airways in a quarter of those with occlusions (5 of 20) which is 7% (5 of 70) of all participants evaluated. All but one participant with occlusions reported severe asthma, which is similar to previous reports,<sup>22</sup> although we observed fewer occlusions or plugs in fewer participants overall than previously reported. Together, this suggests that intraluminal occlusions did not have a large impact on TAC in this study. The presence of thicker airway walls and narrowed lumens in subsegmental airways that were missing daughter branches suggest that it is obstruction (via airway wall remodeling or collapse), rather than airway destruction that is responsible for our findings in participants with asthma. Quantitative CT phenotypes have been identified in patients with asthma<sup>29</sup> largely based on proximal airway morphology including airway luminal narrowing and wall thickness. TAC provides a complementary quantitative CT measurement that reflects the architecture of the airway tree and may help to further enrich imaging-based phenotypes of asthma. We also investigated the functional consequences of reduced TAC and observed worse MRI ventilation defects in participants with more missing sub-subsegments on the whole-lung level and worse MRI VDP in lung lobes with greater prevalence of missing sub-subsegments. Previous work<sup>30</sup> demonstrated a relationship between thickened airway walls and MRI ventilation defects in asthma,

which is congruent with our finding that TAC and abnormal airway structure contribute to abnormal MRI ventilation on whole-lung and regional lobar levels.

Similar to recently published findings in COPD,<sup>24</sup> we observed airway variants in 18 of 70 or 26% of participants. The most common variant was an accessory sub-superior segment which was observed 14% of participants. These results are in good agreement with published results in 3,000 COPD participants,<sup>24</sup> with very similar prevalence of airway variants and the presence of the accessory sub-superior segment. Interestingly, MRI VDP was worse in participants with conventional segmental airway anatomy compared with participants with airway variants, which may be explained by the smaller airway lumens also observed in participants with conventional airway tree architecture. We were not powered to investigate relationships for individual airway variants which should be investigated in larger-scale studies.

#### 5.4.3 TAC is Related to FEV<sub>1</sub> and Airway Wall Area

TAC was significantly, albeit weakly to moderately, related to FEV<sub>1</sub>, VDP, WA% and LA. In addition, TAC was inversely and positively correlated with WA% and LA, respectively. This suggests that thickened airway walls and narrow airway lumens help explain diminished TAC in asthma, in contrast to COPD where missing airways were related to thinning airway walls.<sup>16</sup> The relationship between TAC and VDP was especially weak, possibly because a large proportion of participants reported VDP<5%. We note that VDP values here were similar to previously reported values in mild-moderate (3-4%<sup>30,31</sup>) and severe asthma (6-10%<sup>31,32</sup>). Univariate relationships were used to drive multivariable models to investigate these relationships and showed that among the CT measurements investigated, TAC was the only independent predictor of FEV<sub>1</sub>. In a separate model, CT TAC and MRI VDP together explained a greater proportion of FEV<sub>1</sub> variability. Hence, CT airway count provided unique information related to FEV<sub>1</sub>, independent of airway morphology. Previous work in COPD<sup>16</sup> also showed that TAC and lumen area both helped to explain FEV<sub>1</sub>. To more deeply explore this finding and our own results, we generated an additional multivariable model using only CT wall area percent ( $\beta=-0.24$ ,  $p=0.2$ ) and CT lumen area ( $\beta=0.04$ ,  $p=0.8$ ), neither of which was significant (model  $R^2=0.13$ ,  $p=0.1$ ).

It is important to note that airway wall and lumen measurements were generated for anatomically equivalent segmental, subsegmental and sub-subsegmental airways in five airway paths.<sup>23</sup> BMI was a significant covariate in the multivariable models (participant age and sex were not) which may help explain the weak to moderate univariate relationships. CT in combination with MRI offers highly complementary information about lung structure and function in patients with asthma and generates an understanding of the functional consequences of structural abnormalities. TAC also uniquely explained airway wall morphology (WA%) which suggests there is some form of interaction between airway thickening and apparently lost/missing or CT invisible airways.

#### 5.4.4 Limitations and Unanswered Questions

Limitations of our study include the fact that the study was based on a convenience sample dominated by more severe disease, such that we were underpowered to individually evaluate GINA1-3 (GINA1 n=4, GINA2 n=2 and GINA3 n=9). A population-based sample would provide more participants with milder disease which would allow for the detection of differences between all GINA subgroups. It is important to note that CT images were acquired at functional residual capacity plus 1.0 L to volume-match CT and MRI datasets. We pondered the relationship between CT/MRI lung volume and airway count and the fact that most studies acquire CT close to TLC.<sup>16</sup> CT lung volume acquisition differences could impact participants with larger lung volumes because at a lower fraction of vital capacity, the elastic forces tethering the airways open would also be lowered which would impact lumen diameters and potentially contribute to reduced TAC. We note however that TAC was not significantly related to the fraction of lung volume for imaging normalized to vital capacity ( $r=0.04$ ,  $p=0.7$ ) or total lung capacity ( $r=0.045$ ,  $p=0.7$ ). We did not acquire expiratory CT and therefore we have no CT measurements of air trapping<sup>33,34</sup> so it is not possible to compare parametric response map or expiratory CT lucency measures with TAC in this study. Although CT FOV differed to a small extent among study participants, we confirmed that CT FOV was not different between treatment step groups and was not correlated with TAC, nor was TAC different between participant groups with different FOV. We also acknowledge the lack of repeat and longitudinal follow-up CT imaging at this time. Future work will be needed evaluate the reproducibility

of TAC in participants with asthma and potential changes in TAC over time. Whereas repeat and sometimes longitudinal CT in patients with asthma is not common due to radiation burden, MRI allows for repeat evaluations without added risk to patients. Missing airways on CT were related to worse MRI ventilation defects on whole-lung and lobar levels, and previous work has demonstrated spatial relationships between focal ventilation defects and abnormally remodeled airways.<sup>30,35</sup> Although MRI and CT measure different but complimentary information, this supports the notion that ventilation defects are indicative of abnormal airways in severe asthma and can be used to guide treatment decisions or localized therapies with the goal of resolving ventilation defects and thus, airway abnormalities and asthma control.

This study raises more questions than it answers. What are the underlying pathophysiological processes that drive airway drop-out in severe asthma? Do mucus or other types of occlusions play a role and were these more dominant at airway termini at a timepoint prior to our evaluation? In other words, is the relative lack of mucus at most airway termini definitive for the process underlying missing airways? Are some patients preprogrammed for low TAC which may be coincident to, or predictive of the development of asthma? Is TAC a missing link between asthma-COPD overlap or the asthma transition to loss of post-bronchodilator reversibility and COPD? How does TAC change over time, with and without treatment? Future studies ought to investigate histologic airway wall remodeling,<sup>28</sup> inflammatory markers including sputum cell counts or exhaled nitric oxide<sup>32,36</sup> and/or CT scores for intraluminal obstructions<sup>22,37</sup> to elucidate the underlying mechanisms for missing airways. Integration of TAC with ‘omic investigations or genome-wide association studies (GWAS)<sup>38,39</sup> may help determine possible predispositions for reduced TAC and development of obstructive lung disease. Finally, longitudinal studies are also required to understand the stability of TAC over time and how it may help monitor disease progression or changes in response to therapy.

### 5.4.5 Conclusions

Whilst chronic airflow obstruction and airway obliteration have been described in COPD,<sup>13-15</sup> airways disease in asthma is regarded as temporally variable and reversible within an entire tracheobronchial tree. Here we show that the airway tree is truncated in patients with severe asthma and the reduced number of terminal airways is similar in magnitude to what was previously reported in moderate COPD.<sup>16</sup> The reduced number of airways detected using CT in asthma may be related to airway obstruction (luminal plugging, airway collapse or wall thickening) rather than destruction or obliteration. How TAC may change with treatment or over time in patients with asthma remains to be determined. In severe asthma, MRI ventilation heterogeneity was recently likened to a canary in the coal mine<sup>40</sup> because MRI ventilation abnormalities uniquely explained asthma control<sup>40</sup> and also predicted the transition of asthma to fixed obstruction.<sup>41</sup> In a similar manner, the airway tree may represent the tunneling shafts that support the coal mining operation; once blocked or destroyed, the entire enterprise is threatened and sometimes doomed.

## 5.5 References

- 1 Global Initiative for Asthma (GINA). Global strategy for asthma management and prevention: Updated 2019. (2019).
- 2 van der Wiel, E., ten Hacken, N. H., Postma, D. S. & van den Berge, M. Small-airways dysfunction associates with respiratory symptoms and clinical features of asthma: A systematic review. *J Allergy Clin Immunol* **131**, 646-657 (2013).
- 3 Lipworth, B., Manoharan, A. & Anderson, W. Unlocking the quiet zone: The small airway asthma phenotype. *Lancet Respir Med* **2**, 497-506 (2014).
- 4 Postma, D. S. *et al.* Exploring the relevance and extent of small airways dysfunction in asthma (ATLANTIS): Baseline data from a prospective cohort study. *Lancet Respir Med* **7**, 402-416 (2019).
- 5 Grenier, P. *et al.* Abnormalities of the airways and lung parenchyma in asthmatics: CT observations in 50 patients and inter- and intraobserver variability. *Eur Radiol* **6**, 199-206 (1996).
- 6 Okazawa, M. *et al.* Human airway narrowing measured using high resolution computed tomography. *Am J Respir Crit Care Med* **154**, 1557-1562 (1996).

- 7 Awadh, N., Muller, N. L., Park, C. S., Abboud, R. T. & FitzGerald, J. M. Airway wall thickness in patients with near fatal asthma and control groups: Assessment with high resolution computed tomographic scanning. *Thorax* **53**, 248-253 (1998).
- 8 Niimi, A. *et al.* Airway wall thickness in asthma assessed by computed tomography. Relation to clinical indices. *Am J Respir Crit Care Med* **162**, 1518-1523 (2000).
- 9 Kasahara, K., Shiba, K., Ozawa, T., Okuda, K. & Adachi, M. Correlation between the bronchial subepithelial layer and whole airway wall thickness in patients with asthma. *Thorax* **57**, 242-246 (2002).
- 10 Siddiqui, S. *et al.* Airway wall geometry in asthma and nonasthmatic eosinophilic bronchitis. *Allergy* **64**, 951-958 (2009).
- 11 Gupta, S. *et al.* Qualitative analysis of high-resolution CT scans in severe asthma. *Chest* **136**, 1521-1528 (2009).
- 12 Gupta, S. *et al.* Quantitative analysis of high-resolution computed tomography scans in severe asthma subphenotypes. *Thorax* **65**, 775-781 (2010).
- 13 Hogg, J. C., Macklem, P. T. & Thurlbeck, W. M. Site and nature of airway obstruction in chronic obstructive lung disease. *N Engl J Med* **278**, 1355-1360 (1968).
- 14 Hogg, J. C. *et al.* The nature of small-airway obstruction in chronic obstructive pulmonary disease. *N Engl J Med* **350**, 2645-2653 (2004).
- 15 McDonough, J. E. *et al.* Small-airway obstruction and emphysema in chronic obstructive pulmonary disease. *N Engl J Med* **365**, 1567-1575 (2011).
- 16 Kirby, M. *et al.* Total airway count on computed tomography and the risk of chronic obstructive pulmonary disease progression. Findings from a population-based study. *Am J Respir Crit Care Med* **197**, 56-65 (2018).
- 17 Eddy, R. L., McCormack, D. G., Kirby, M. & Parraga, G. CT airway count as a biomarker of asthma pathogenesis: Severe asthma and ACOS in never-smokers [abstract]. *Am J Respir Crit Care Med* **199**, A5769 (2019).
- 18 Juniper, E. F., O'Byrne, P. M., Guyatt, G. H., Ferrie, P. J. & King, D. R. Development and validation of a questionnaire to measure asthma control. *Eur Respir J* **14**, 902-907 (1999).
- 19 Juniper, E. F. *et al.* Evaluation of impairment of health related quality of life in asthma: Development of a questionnaire for use in clinical trials. *Thorax* **47**, 76-83 (1992).
- 20 Miller, M. R. *et al.* Standardisation of spirometry. *Eur Respir J* **26**, 319-338 (2005).

- 21 Owrangi, A. M., Etemad-Rezai, R., McCormack, D. G., Cunningham, I. A. & Parraga, G. Computed tomography density histogram analysis to evaluate pulmonary emphysema in ex-smokers. *Acad Radiol* **20**, 537-545 (2013).
- 22 Dunican, E. M. *et al.* Mucus plugs in patients with asthma linked to eosinophilia and airflow obstruction. *J Clin Invest* **128**, 997-1009 (2018).
- 23 Smith, B. M. *et al.* Comparison of spatially matched airways reveals thinner airway walls in COPD. The multi-ethnic study of atherosclerosis (MESA) COPD study and the subpopulations and intermediate outcomes in COPD study (SPIROMICS). *Thorax* **69**, 987-996 (2014).
- 24 Smith, B. M. *et al.* Human airway branch variation and chronic obstructive pulmonary disease. *Proc Natl Acad Sci U S A* **115**, E974-E981 (2018).
- 25 Parraga, G. *et al.* Hyperpolarized <sup>3</sup>He ventilation defects and apparent diffusion coefficients in chronic obstructive pulmonary disease: Preliminary results at 3.0 tesla. *Invest Radiol* **42**, 384-391 (2007).
- 26 Kirby, M. *et al.* Hyperpolarized <sup>3</sup>He magnetic resonance functional imaging semiautomated segmentation. *Acad Radiol* **19**, 141-152 (2012).
- 27 Adams, C. J., Capaldi, D. P. I., Di Cesare, R., McCormack, D. G. & Parraga, G. On the potential role of MRI biomarkers of COPD to guide bronchoscopic lung volume reduction. *Acad Radiol* **25**, 159-168 (2018).
- 28 Berair, R. *et al.* Associations in asthma between quantitative computed tomography and bronchial biopsy-derived airway remodelling. *Eur Respir J* **49** (2017).
- 29 Choi, S. *et al.* Quantitative computed tomographic imaging-based clustering differentiates asthmatic subgroups with distinctive clinical phenotypes. *J Allergy Clin Immunol* (2017).
- 30 Svenningsen, S. *et al.* What are ventilation defects in asthma? *Thorax* **69**, 63-71 (2014).
- 31 Zha, W. *et al.* Regional heterogeneity of lobar ventilation in asthma using hyperpolarized helium-3 MRI. *Acad Radiol* **25**, 169-178 (2018).
- 32 Svenningsen, S. *et al.* Sputum eosinophilia and magnetic resonance imaging ventilation heterogeneity in severe asthma. *Am J Respir Crit Care Med* **197**, 876-884 (2018).
- 33 Galban, C. J. *et al.* Computed tomography-based biomarker provides unique signature for diagnosis of COPD phenotypes and disease progression. *Nat Med* **18**, 1711-1715 (2012).

- 34 Kirby, M. *et al.* A novel method of estimating small airway disease using inspiratory-to-expiratory computed tomography. *Respiration* **94**, 336-345 (2017).
- 35 Fain, S. B. *et al.* Evaluation of structure-function relationships in asthma using multidetector CT and hyperpolarized He-3 MRI. *Acad Radiol* **15**, 753-762 (2008).
- 36 Inoue, H. *et al.* CT-assessed large airway involvement and lung function decline in eosinophilic asthma: The association between induced sputum eosinophil differential counts and airway remodeling. *J Asthma* **53**, 914-921 (2016).
- 37 Svenningsen, S. *et al.* CT and functional MRI to evaluate airway mucus in severe asthma. *Chest* **155**, 1178-1189 (2019).
- 38 Hersh, C. P. *et al.* SOX5 is a candidate gene for chronic obstructive pulmonary disease susceptibility and is necessary for lung development. *Am J Respir Crit Care Med* **183**, 1482-1489 (2011).
- 39 Hobbs, B. D. *et al.* Genetic loci associated with chronic obstructive pulmonary disease overlap with loci for lung function and pulmonary fibrosis. *Nat Genet* **49**, 426-432 (2017).
- 40 Svenningsen, S., Nair, P., Guo, F., McCormack, D. G. & Parraga, G. Is ventilation heterogeneity related to asthma control? *Eur Respir J* **48**, 370-379 (2016).
- 41 Eddy, R. L., Svenningsen, S., Licskai, C., McCormack, D. G. & Parraga, G. Hyperpolarized helium 3 MRI in mild-to-moderate asthma: Prediction of postbronchodilator reversibility. *Radiology* **293**, 212-220 (2019).

## 5.6 Supplement

**Table 5-6** Total airway count by airway generation

<b>Generation</b> Count ( $\pm$ SD)	<b>Never-smokers<sup>1</sup></b>	<b>GINA1-3</b> <b>(n=15)</b>	<b>GINA4</b> <b>(n=19)</b>	<b>GINA5</b> <b>(n=36)</b>
0	1.0 (0.0)	1.0 (0.0)	1.0 (0.0)	1.0 (0.0)
1	2.0 (0.1)	2.0 (0.0)	2.0 (0.0)	2.0 (0.0)
2	4.0 (0.1)	4.3 (0.8)	4.5 (1.4)	4.2 (0.5)
3	13.0 (0.8)	13.4 (0.6)	13.9 (1.1)	13.5 (1.0)
4	24.2 (1.3)	25.0 (2.2)	24.9 (1.7)	25.0 (2.5)
5	43.5 (6.2)	45.3 (6.2)	39.4 (7.3)	38.8 (10.1)
6	52.3 (17.4)	46.9 (16.3)	32.0 (15.4)*	34.9 (17.3)
7	42.1 (22.9)	27.5 (16.3)	14.8 (8.8)*	13.8 (12.1)*
8	23.3 (16.4)	10.1 (10.5)	5.3 (4.7)	5.8 (5.5)
9	10.8 (9.8)	2.5 (3.3)	2.2 (2.7)	1.3 (2.0)
10	3.8 (4.6)	1.1 (1.8)	0.3 (0.6)	0.2 (0.6)*
11	-	0.3 (0.7)	0.0 (0.0)	0.0 (0.0)*

GINA=Global Initiative for Asthma. <sup>1</sup>From Kirby et al., 2018. \*Significantly different from treatment steps 1-3, p<0.05.

## CHAPTER 6

### 6 CONCLUSIONS AND FUTURE DIRECTIONS

*In this final chapter, I provide a summary and overview of the important findings and conclusions presented in **Chapters 2-5**. The limitations specific to each study and general limitations are also provided with some potential solutions. Finally, I end my thesis with future directions based on what we observed using hyperpolarized  $^3\text{He}$  MRI, CT and oscillometry.*

#### 6.1 Overview and Research Questions

Asthma has long been idealized as a diffuse airways disease with variable symptoms and airflow limitation despite evidence of ventilation heterogeneity that was first identified over six decades ago.<sup>1-4</sup> Structure and function of asthma are still clinically characterized using the forced expiratory volume in one second ( $\text{FEV}_1$ ) – although  $\text{FEV}_1$  is a simple and inexpensive measurement, it only provides a global measurement of lung function that cannot capture the regional heterogeneity of airway abnormalities that may be responsible for symptoms and disease worsening. In an effort to better understand the mechanisms of ventilation heterogeneity, computational models have been generated and suggest that the regional heterogeneity observed in asthma can only be described by randomly distributed airway abnormalities throughout the whole lung.<sup>5,6</sup> The *in vivo* mechanisms however have been challenging to measure using current clinical tools such as  $\text{FEV}_1$ . As a result, asthma is still regarded as a random disease and treatments are geared towards all airways and not individualized.

Quantitative pulmonary imaging methods have been developed to directly visualize and quantify regional abnormalities in patients with lung disease. In particular, hyperpolarized gas MRI provides *in vivo* images of regional gas distribution in high resolution. As expected, MRI ventilation in young healthy volunteers is homogeneously distributed,<sup>7,8</sup> whereas in asthmatics, characteristic ventilation heterogeneity is observed.<sup>9,10</sup> In conjunction with CT and oscillometry, the underlying structure of ventilation heterogeneity may be ascertained; focal ventilation abnormalities, known as ventilation defects, are spatially and quantitatively related to abnormal large<sup>11</sup> and small airways.<sup>12,13</sup> The physiological relevance of ventilation defects has been anchored to important clinical

measures including FEV<sub>1</sub>,<sup>11,12,14,15</sup> asthma control<sup>16</sup> and airway inflammation.<sup>17</sup> Preliminary longitudinal studies in asthma demonstrate that defects are spatially and temporally persistent for up to 1.5 years,<sup>15,18</sup> importantly contradicting *in silico* results. These early disruptive MRI results suggest that asthmatic airway and corresponding ventilation abnormalities are not random. Despite this evidence and support for clinical use, pulmonary imaging has played a limited role in asthma research and clinical care because the physiological mechanisms, long-term nature and clinical relevance of regional ventilation heterogeneity in asthma are poorly understood.

The overarching objective of this thesis was to exploit sensitive pulmonary imaging measurements to better understand the structure and function of the asthmatic lung that drive ventilation heterogeneity and provide a foundation for imaging to guide disease phenotyping for personalized asthma treatment and predict disease worsening.

The specific research questions addressed were: 1) Are the biomechanical impacts of ventilation heterogeneity in asthma different from those of COPD and can these differences be explained using oscillometry and MRI ventilation defects? (**Chapter 2**); 2) Are ventilation defects similar between twins with asthma and spatially and temporally persistent over long periods of time? (**Chapter 3**); 3) Are ventilation defects spatially and quantitatively persistent over long periods of time in unrelated asthma patients, and can ventilation defects predict future bronchodilator reversibility? (**Chapter 4**); and 4) Is the airway tree truncated in severe asthma and are truncated airways to thickened airway walls and worse airway function? (**Chapter 5**)

## 6.2 Summary and Conclusions

In **Chapter 2**, we evaluated the relationships between hyperpolarized <sup>3</sup>He MRI ventilation defects and oscillometry measurements of lung biomechanics in a total of 175 participants including 49 with asthma, 56 with COPD, 28 ex-smokers without COPD and 42 never-smokers without lung disease. In both asthma and COPD, VDP was significantly related to R<sub>5-19</sub> (asthma:  $\rho=0.48$ ,  $p=0.0005$ ; COPD:  $\rho=0.45$ ,  $p=0.0004$ ), X<sub>5</sub> (asthma:  $\rho=-0.41$ ,  $p=0.004$ ; COPD:  $\rho=-0.38$ ,  $p=0.004$ ) and A<sub>x</sub> (asthma:  $\rho=0.47$ ,  $p=0.0007$ ; COPD:  $\rho=0.43$ ,  $p=0.0009$ ). When COPD participants were dichotomized by the presence of emphysema

( $RA_{950} \geq 6.8\%$ ), VDP was significantly related to  $X_5$  in those with emphysema ( $\rho = -0.36$ ,  $p = 0.04$ ) whereas in those without emphysema, VDP was related to  $R_{5-19}$  ( $\rho = 0.54$ ,  $p = 0.008$ ). VDP was significantly related to  $A_X$  in participants with ( $\rho = 0.39$ ,  $p = 0.02$ ) and without ( $\rho = 0.43$ ,  $p = 0.04$ ) emphysema. These results suggest that MRI VDP and oscillometry-measured  $R_{5-19}$  and  $X_5$  may reflect disease-specific airway and parenchymal biomechanical abnormalities that lead to ventilation defects.

In **Chapter 3**, we evaluated the spatial and temporal nature of CT airway and hyperpolarized  $^3\text{He}$  MRI ventilation abnormalities over the course of seven years in adult female nonidentical twins with asthma. Both twins showed a spatially-matched subsegmental MRI ventilation defect in the left upper lobe corresponding to the LB2 apicoposterior bronchopulmonary segment. At 7-year follow-up, the LB2 WA% was 71% and 75% for twin 1 and twin 2, respectively. Based on the 19 anatomically and functionally distinct bronchopulmonary segments, and under the assumptions of no more than one defect per segment and an equivalent probability for each of the 19 segments to express a defect, we estimated the probability that two patients have the same single defect at two timepoints to be 1 in 130,321. These findings suggest that ventilation abnormalities may not be randomly distributed within patients with asthma and persist distal to airway abnormalities for long periods of time.

In **Chapter 4**, we investigated 6-year longitudinal changes in hyperpolarized  $^3\text{He}$  ventilation defects in 11 participants with mild-to-moderate and aimed to determine predictors of longitudinal post-bronchodilator  $FEV_1$  reversibility. There were no differences between  $FEV_1$  ( $76\%_{\text{pred}}$  vs  $76\%_{\text{pred}}$ ,  $p = 0.9$ ) and MRI VDV (240 mL vs 250 mL,  $p = 0.9$ ) between baseline and follow-up and no participants experienced any medication changes or exacerbations during the time between study visits. For 8 of 11 participants, MRI ventilation defects were spatially and quantitatively persistent between study visits. For the remaining 3 participants, ventilation defects worsened in the same locations previously induced by methacholine at the baseline visit. At follow-up,  $FEV_1$  was not reversible in 6 of 11 participants; baseline  $PC_{20}$  was significantly worse in  $FEV_1$ -reversible compared with nonreversible participants ( $0.08 \pm 0.01$  mg/mL vs  $0.84 \pm 0.86$  mg/mL,  $p = 0.01$ ). No other measurements were significantly different between  $FEV_1$  reversible and

FEV<sub>1</sub> non-reversible groups. In multivariable models including MRI VDV, FEV<sub>1</sub>, PC<sub>20</sub> and participant age, only VDV significantly predicted post-bronchodilator FEV<sub>1</sub> reversibility at follow-up ( $R^2=0.80$ ,  $p<0.01$ ). These results suggest that MRI ventilation defects are spatially persistent over 6.5 years, and are uniquely predictive of future bronchodilator reversibility in patients with asthma.

In **Chapter 5**, we measured CT TAC in 70 participants with asthma across a range of severities including 15 GINA1-3, 19 GINA4 and 36 GINA5, and evaluated relationships for TAC with asthma severity, airway morphology, pulmonary function and MRI ventilation. TAC was significantly diminished in GINA4 ( $145\pm 10$ ,  $p=0.03$ ) and GINA5 ( $148\pm 7$ ,  $p=0.045$ ) compared with GINA1-3 ( $182\pm 11$ ). Sub-subsegmental airways were CT-invisible or missing in 69 of 70 participants. The most common number of missing sub-subsegments was 10, and participants with  $\geq 10$  missing sub-subsegments had worse WA% ( $68.6\pm 1.4\%$  vs  $66.8\pm 1.3\%$ ,  $p<0.0001$ ), LA ( $9.1\pm 1.9$  mm<sup>2</sup> vs  $11.8\pm 2.2$  mm<sup>2</sup>,  $p<0.0001$ ) and VDP ( $7\pm 7\%$  vs  $11\pm 9\%$ ,  $p=0.03$ ) than those with  $<10$  missing sub-subsegments. In a multivariable model including all CT parameters, TAC ( $\beta=0.50$ ,  $p=0.001$ ) independently predicted FEV<sub>1</sub> ( $R^2=0.27$ ,  $p=0.003$ ). In a separate model including VDP, TAC ( $\beta=0.27$ ,  $p=0.03$ ) and VDP ( $\beta=-0.53$ ,  $p<0.0001$ ) combined to explain FEV<sub>1</sub> ( $R^2=0.49$ ,  $p<0.0001$ ). In severe asthma, TAC was reduced to a similar degree as previously published results in moderate COPD, and these results challenge our understanding of airways disease in asthma as temporally variable and reversible.

In summary, we have provided: 1) an understanding of biomechanical lung abnormalities specifically related to asthma compared with COPD with and without emphysema; 2) evidence of a spatially-matched MRI ventilation defect in twins with asthma that is spatially and temporally persistent for seven years; 3) evidence that MRI ventilation defects are spatially and temporally persistent for over six years in a group of participants with mild-to-moderate asthma, and that ventilation defects are predictive of future bronchodilator reversibility; 4) evidence that airway wall thickening is related to reduced total number of CT-visible airways in severe asthma that is similar in magnitude to moderate COPD and related to worse MRI VDP.

## 6.3 Limitations

The most significant limitations from **Chapters 2-5** are presented here. The study specific limitations are also provided within the Discussion section of each respective chapter. Following the study specific limitations, general limitations common to all chapters are addressed.

### 6.3.1 Study Specific Limitations

#### **Chapter 2:** *Oscillometry and Pulmonary Magnetic Resonance Imaging in Asthma and COPD*

In the study presented in **Chapter 2**, the oscillometry-derived results were limited by the use of raw values without correction for age or anthropometric factors. It is well-established that pulmonary function measurements vary with age, sex, height and ethnicity.<sup>19</sup> Although our participant cohort was well-matched for sex and consisted only of Caucasian adults, impedance differences between groups, or lack of differences, may have been influenced by participant age and height. This may also partially explain the weak correlations observed between oscillometry measurements and MRI VDP. Diverse, global reference equations are currently under development for oscillometry, and future investigations should employ normalized values where possible.

Another limitation of this study derives from the fact  $R_{5-19}$  may not capture the largest influence of ventilation heterogeneity on the frequency dependence of resistance. Experimental studies in animal models and humans have shown that heterogeneity has the largest influence on respiratory system resistance between 0.1-5 Hz.<sup>20-22</sup> We therefore only captured a small portion of the impact of heterogeneities using  $R_{5-19}$  and this may explain the weak correlations observed. It is important to note though that all commercially available oscillometry devices approved for use in humans employ broadband signals with lower bounds of 4-5 Hz.<sup>23</sup> Future studies could investigate the relationships between respiratory system resistance at frequencies <5 Hz and MRI ventilation heterogeneity, however this would require custom-built oscillometry systems.

As a technical limitation, shunting of the oscillatory waves to the upper airways reduces sensitivity of oscillometry measurements to obstruction.<sup>24</sup> This means that in patients with

severe airflow obstruction, impedance may be underestimated and this may also have influenced correlation strengths observed in this study. To mitigate the effects of upper airway shunt, we perform extensive coaching and instruct participants to firmly hold their cheeks with their hands.

Finally, we acknowledge that oscillometry and MRI measurements were acquired in different positions, introducing the potential for postural effects. Oscillometry was performed in the upright position whereas MRI was performed supine and this may have had an additional impact on the strength of the relationships between MRI and oscillometry measurements of ventilation heterogeneity. Previous work has demonstrated that  $R_5$  is increased in the supine position compared to upright<sup>25,26</sup> and the presence of emphysema may also cause large upright-to-supine  $A_x$  variability.<sup>27</sup> Regardless, we took steps to mitigate and minimize potential postural effects in this study by completing imaging within five minutes to limit the time that patients are supine, which has been shown to minimize atelectasis.<sup>28</sup>

### **Chapter 3:** *Nonidentical Twins with Asthma: Spatially-matched CT Airway and MRI Ventilation Abnormalities*

In the study presented in **Chapter 3**, we only evaluated one set of twins. Our results are thus difficult to generalize to all patients or twins with asthma. We assumed the persistent ventilation defect in these participants to be related to asthma pathophysiology and/or abnormal airway structure. It is possible that these findings could also be explained to some extent by shared genetics, epi-genetics or *in utero* events, which we did not evaluate here and could not rule out. Future investigations would benefit from a more complete clinical history incorporating these factors.

Based on the assumptions we made, our probability estimate for a repeated ventilation abnormality in space and time was conservative. In twins, there may be a bias for airway and ventilation abnormalities in specific lung regions which we did not account for. Moreover, we did not make any assumptions about an upper limit of number of ventilation defects that might be less than one for each of the 19 potential segmental airways. In the literature, participants with moderate disease typically have fewer than five ventilation

defects.<sup>14</sup> A more rigorous analysis could include the probability of twins having asthma, the probability of multiple ventilation defects, or the probability of subsegmental (38 subsegments) or sub-subsegmental (76 sub-subsegments) ventilation defects. However, accounting for these factors would only serve to lower the estimated probability and would likely more strongly support our conclusions.

**Chapter 4:** *Hyperpolarized Helium 3 MRI in Mild-to-Moderate Asthma: Prediction of Postbronchodilator Reversibility*

The longitudinal study presented in **Chapter 4** was limited by the small sample size of only mild-to-moderate participants and this limits the generalizability of the multivariable model results to the broader asthma population. Importantly however, hyperpolarized gas MRI measurements are extremely sensitive; as demonstrated in this study and others in the literature, significant group differences and relationships may be detected using small sample sizes. Nonetheless, this study generated pilot data that can motivate large imaging cohort studies of asthma over a range of asthma severities to further confirm the results observed here.

Another limitation of this study was the partial thoracic CT images that were acquired at the baseline timepoint which limited the regional airway comparisons between study visits. Low-dose research CT protocols similar to that used at the time of follow-up are now widely available and may be employed in future studies to longitudinally investigate morphological airway changes. Further development of ultra-low dose CT methods<sup>29,30</sup> may also facilitate the broader use of longitudinal CT imaging in patients with asthma. In spite of the partial CT volume, we were able to demonstrate persistent structure-function relationships in specific lung regions.

**Chapter 5:** *Is Computed Tomography Total Airway Count Related to Asthma Severity and Airway Structure-function?*

The study presented in **Chapter 5** was based on a convenience sample of asthmatics recruited from local tertiary care centres, thus our participant population was dominated by more severe disease. We were underpowered to individually compare GINA treatment steps 1-3 to tease out differences between all levels of asthma severity. The strength of the

study could have been improved using a population-based sample which would have better facilitated recruitment of participants with milder disease.

Another limitation was the acquisition of CT images at FRC+1.0 L. While this facilitates comparison and registration to MRI by volume-matching the acquisitions, most studies acquire CT close to TLC and this may limit our comparisons to previous work.<sup>31</sup> The lung volume acquisition differences could especially impact participants with larger lung volumes because at a lower fraction of vital capacity, the elastic forces tethering the airways open would be reduced; this would impact lumen diameters and potentially contribute to decreased TAC. We determined that TAC was however not significantly related to the CT lung volume normalized to vital capacity ( $r=0.04$ ,  $p=0.7$ ) or total lung capacity ( $r=0.05$ ,  $p=0.7$ ), therefore we suspect lung inflation at imaging to have minimally impacted our results. We also did not acquire expiratory CT and therefore could not evaluate the regional nor whole-lung relationships between imaging measurements of gas trapping<sup>32,33</sup> and TAC. Future large cohort studies could benefit from paired inspiratory-expiratory CT imaging to contemporaneously evaluate and compare TAC and gas trapping.

### 6.3.2 General Limitations

A general limitation to the studies presented in **Chapters 2-5** is the lack of measurements of airway inflammation. Asthma is characterized by chronic airway inflammation, however we were unable to ascertain the role of inflammation within our findings. Previous work has demonstrated a direct relationship between MRI VDP and sputum eosinophils and suggested that ventilation defects which persist following bronchodilator are indicative of unresolved airway inflammation.<sup>17</sup> To our advantage in the absence of inflammatory biomarkers in **Chapters 4 and 5**, we used pre- and post-bronchodilator MRI evaluations to infer the role of smooth muscle dysfunction. In future work, direct comparison of oscillometry, CT airway and MRI ventilation abnormalities to airways inflammation will be important towards guiding clinical treatment decisions and for personalized therapy. Ongoing studies at our centre are now prospectively evaluating non-invasive biomarkers of inflammation from exhaled breath, sputum and blood in conjunction with MRI study visits.

Another general limitation to all chapters was our focus only on ventilation defects (as a volume and percent of total lung volume), though it is obvious that hyperpolarized gas MRI ventilation is not binary. In addition to ventilation defects, four distinct intensities of MR gas signal can be visualized by expert readers ranging from hypo- to hyper-intense signal.<sup>34</sup> The heterogeneity of the gas signal itself is evident in **Figure 1-10** in the introduction for both  $^3\text{He}$  and  $^{129}\text{Xe}$  in asthma and COPD. The well-established clinical relevance of ventilation defects in asthma supported their investigation in this thesis,<sup>11,16</sup> however the clinical relevance of the MRI signal distribution and its spatial and temporal behaviour are unknown. The semi-automated MR image segmentation method employed in this thesis quantifies each of the four respective intensities<sup>34</sup> that can subsequently be investigated individually to determine their underlying mechanisms and clinical relevance. Alternatively, coefficients of variation<sup>35</sup> or texture features<sup>36</sup> of the signal intensity may be investigated to directly probe heterogeneity. Oscillometry-MRI comparisons like those in **Chapter 2** may particularly benefit from direct comparison of signal intensity measurements because these are likely the regions actually probed by the oscillatory waves. In future work, it will be important to evaluate the signal intensity and its heterogeneity in space and time in conjunction with ventilation defects.

Pertinent to **Chapters 3-4**, we acknowledge the limited longitudinal analysis of two timepoints. Including a third timepoint, especially one at an interim point between the two study visits would add strength to these studies as well as to our conclusions of non-random, spatially and temporally persistent CT airway and MRI ventilation abnormalities. Moreover, we acknowledge the lack of longitudinal timepoints altogether in **Chapters 2** and **5**. We think that reduced CT TAC in severe has important implications for airways disease in asthma, however future work will be needed evaluate the reproducibility of TAC in participants with asthma and potential changes in TAC over time. Moreover, oscillometry has excellent intra-patient reproducibility<sup>37</sup> that could make it a sensitive tool for detecting changes in ventilation heterogeneity over long periods of time.

An important limitation through **Chapters 2-5** is the limited worldwide supply and subsequent high cost of  $^3\text{He}$  that has inhibited its clinical translation.<sup>38</sup>  $^3\text{He}$  MRI has played an important role in our developing understanding of asthma in previous work and the work

presented in this thesis, however novel prospective research studies using  $^3\text{He}$  are unlikely. In contrast,  $^{129}\text{Xe}$  is less costly and poised for clinical translation; clinical approval currently exists in the United Kingdom and approval is pending in the United States.  $^{129}\text{Xe}$  MRI is more sensitive to airway obstruction and exhibits significantly greater ventilation defects than  $^3\text{He}$  in both asthma<sup>39</sup> and COPD.<sup>40</sup> This increased sensitivity will be advantageous in future research and clinical studies, but could have implications for the conclusions in this thesis. For example, only 27% of participants in **Chapter 4** showed spatially persistent but quantitatively larger or worsened ventilation defects at follow-up. If this study were repeated using  $^{129}\text{Xe}$  MRI, it is plausible that more participants would show worsening defects that were undetected with  $^3\text{He}$ . Moreover, one might hypothesize that there are stronger relationships between  $^{129}\text{Xe}$  VDP and oscillometry measurements compared to those in **Chapter 2** due to systematically greater VDP or possible wider dynamic range of VDP compared with  $^3\text{He}$ . Speculations aside, future  $^{129}\text{Xe}$  MRI studies are required to validate the results presented here using  $^3\text{He}$  MRI.  $^{129}\text{Xe}$  is additionally advantageous because it can provide regional measurements of gas exchange. All prospective studies currently ongoing or upcoming at Western University in London, Canada are now employing  $^{129}\text{Xe}$  for ventilation and gas exchange measurements in patients with asthma and COPD.

## 6.4 Future Directions

### 6.4.1 Between-participant Probability Maps of MRI Ventilation Defects in Asthma

The work presented in **Chapters 3** and **4** of this thesis demonstrated spatially and temporally persistent CT airway abnormalities and MRI ventilation defects within participants with mild-to-moderate asthma. The results in **Chapter 3** also demonstrated a spatially-matched ventilation abnormality between twins with asthma, and this promotes speculation about a spatial preference for airway and ventilation abnormalities between participants with asthma. As a result, we now pose the following research questions:

- 1) *Are there more likely regional locations for airway and ventilation abnormalities between different participants with asthma?*

2) *Does inhaled methacholine act on particular airways between different participants with asthma?*

To answer these questions, we retrospectively evaluated 31 participants with asthma, including 12 with mild-to-moderate and 19 with severe asthma, to describe a proof-of-concept spatial probability distribution of MRI ventilation defects between patients with asthma. Participants underwent hyperpolarized  $^3\text{He}$  MRI before and after methacholine and images were segmented using a semi-automated method.<sup>34</sup> Each image in the respective groups of mild-to-moderate and severe asthma, before and after methacholine, were deformably co-registered using the modality-independent neighbourhood descriptor method (MIND)<sup>41</sup> in MATLAB R2015a (Mathworks, Natick, MA, USA) as previously described.<sup>42</sup> The ventilation mask for one participant was selected as the fixed reference image and the  $^3\text{He}$  images for all participants in each group were registered to the one mask to enable direct comparisons.

**Figure 6-1** shows preliminary probability maps for mild-to-moderate and severe asthma participants at baseline and post-methacholine. These maps describe the probability that a voxel was ventilated across the group of asthma patients included in each model; brighter blue regions represent higher likelihood of that voxel being ventilated whereas dark blue regions represent lower likelihood of that voxel being ventilated (ie, ventilation defects). Qualitatively comparing baseline and post-methacholine maps, the ventilation distribution is visually more heterogeneous following methacholine for both mild-moderate and severe asthmatics. At baseline, there is a visual superior-inferior gradient in both mild-moderate and severe participants, such that superior regions showed a greater likelihood of being ventilated. Post-methacholine, a posterior-anterior ventilation gradient becomes more evident. In severe asthma specifically, two locations can be visually identified in the post-methacholine posterior slice that appear as ventilation defects in roughly 50% or more of the sample, in the upper left and right lung lobes.

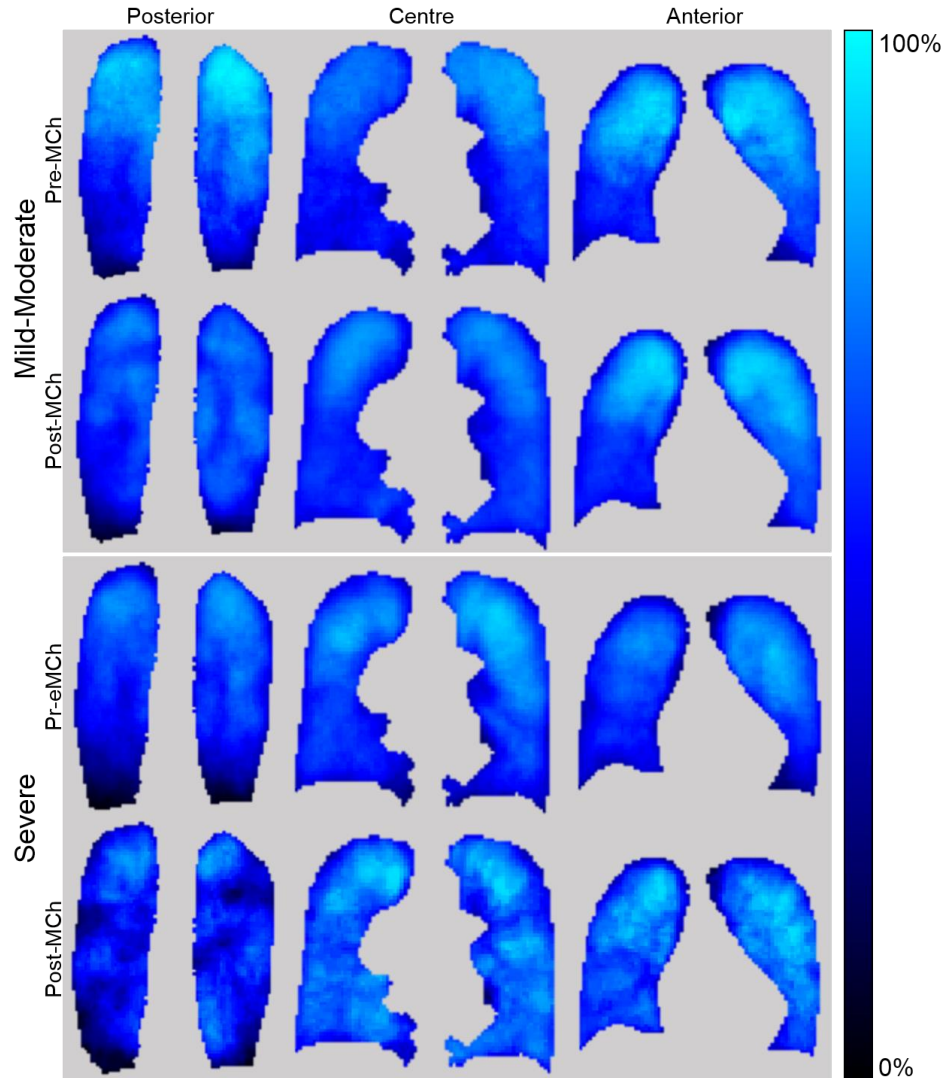


**Figure 6-1** Ventilation defect probability maps for mild-moderate and severe asthma. Posterior, centre and anterior slices pre- and post-methacholine showing regional probability of ventilation defects between participants with asthma. Colour map represents no ventilation in black (0%) to complete ventilation in cyan (100%) throughout the patients included in the model.

These results point towards a regional preference for the location of ventilation defects and abnormally remodeled airways between participants with asthma. These results may be important for the development of novel therapies that can be targeted towards regions with the highest likelihood to be abnormal. The registration pipeline and maps generated here provide a framework for development and application of a probability model of the distribution of ventilation in patients with asthma. Towards generating a functional atlas of the asthmatic lung that is generalizable to the broader asthma population, it will be

important to continue to build this model by continuously including data from more research participants.

#### 6.4.2 Contributions of Large versus Small Airways to Ventilation Heterogeneity in Asthma

With the understanding that ventilation defects in asthma are spatially persistent for long periods of time, ventilation defects may serve as important targets for novel asthma therapies, including image-guided and targeted small airway approaches. Ventilation defects in asthma may be driven by large<sup>11</sup> or small<sup>12</sup> airway abnormalities, however the relative contribution of large versus small airway obstruction to ventilation heterogeneity in a given patient is not well-understood.

With this in mind, we hypothesize that CT airway tree geometries can be used to differentiate the contributions of large versus small airways to ventilation heterogeneity in a patient-specific approach using CT airway tree geometries. In a preliminary study, we aimed to develop a pipeline to calculate VDP related to the small or large airways using paired MRI ventilation and CT image sets. MR ventilation images were segmented using a semi-automated method<sup>34</sup> and CT airway trees were segmented up to the 10<sup>th</sup> generation using commercial software (Pulmonary Workstation 2.0; VIDA Diagnostics Inc., Coralville, IA, USA). Airways that could be segmented were assumed to be all large airways, and those that could not be segmented were considered the small airways. MR static ventilation images were co-registered to the thoracic CT volume and airway tree using the MIND method<sup>41</sup> in MATLAB R2015a (Mathworks, Natick, MA, USA). The trachea was manually removed from the airway tree and the remaining airways were dilated on a voxel-wise basis using a 20x3 ellipsoid in order to account for the volume around the large airways. This volume was subsequently used to separate the <sup>3</sup>He ventilation into relative contributions of the small and large airways, and VDP was calculated as the volume of defects within each region normalized to the total volume of that region. This pipeline is outlined in **Figure 6-2**.

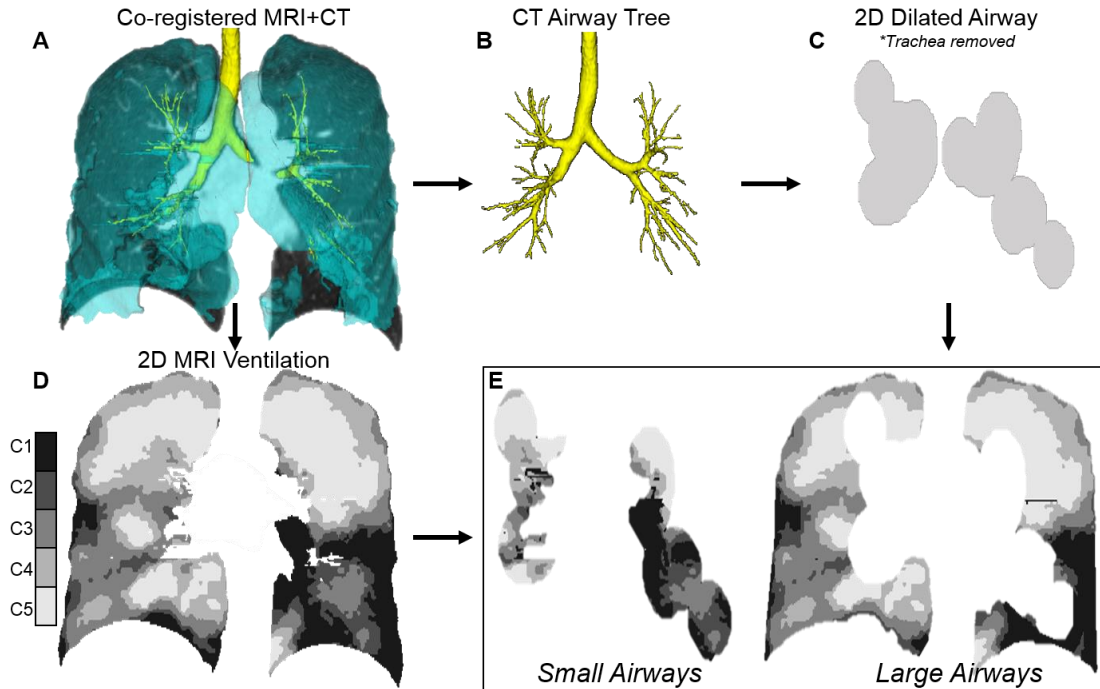


**Figure 6-2** Small versus large airways image analysis pipeline

MRI ventilation was deformably co-registered to the thoracic CT and airway tree volumes (A) and the registered airway tree (B) was dilated in 3D on a voxel-wise basis (C). The dilated airway tree volume was registered to the segmented ventilation clusters (D) to generate the ventilation volume corresponding to the large and small airways.

As a proof-of-concept, the pipeline was evaluated in 20 participants with asthma, 10 each with mild-to-moderate and severe asthma. Whole-lung ( $5 \pm 4\%$  vs  $8 \pm 4\%$ ,  $p=0.1$ ), large airway ( $2 \pm 2\%$  vs  $3 \pm 3\%$ ,  $p=0.3$ ) and small airway VDP ( $6 \pm 5\%$  vs  $10 \pm 3\%$ ,  $p=0.055$ ) were not significantly different between mild-to-moderate and severe asthma groups. In both mild-to-moderate and severe asthma, small airways VDP was significantly greater than large airways VDP ( $p=0.002$  and  $p=0.0001$ , respectively). Relationships for  $FEV_1$  with whole-lung and large and small airway VDP are shown in **Figure 6-3**. Whole-lung ( $r=-0.6$ ,  $p=0.008$ ) and large airway ( $r=-0.6$ ,  $p=0.01$ ) VDP were significantly related to  $FEV_1$ , whereas small airway VDP was not ( $r=-0.3$ ,  $p=0.2$ ). Because  $FEV_1$  is known to be dominated by airflow in the large airways,<sup>43</sup> the relationship between  $FEV_1$  and large airways VDP provides initial validation of our pipeline. This pipeline provides a first step towards distinguishing the large versus small airway contributions to ventilation heterogeneity in asthma.

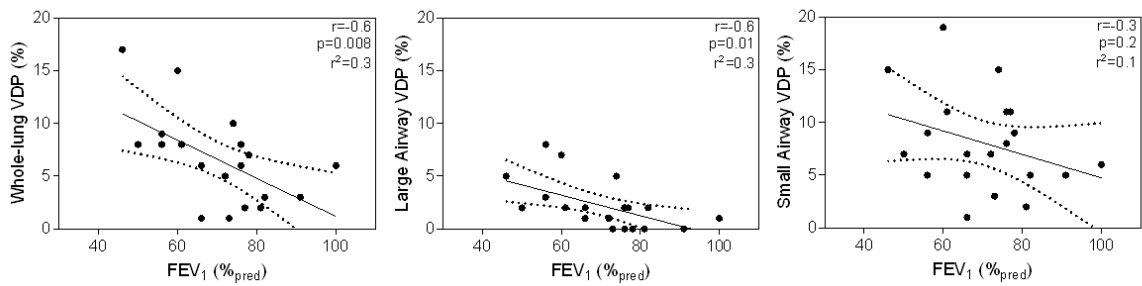


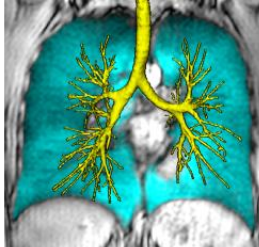
**Figure 6-3** Relationships between FEV<sub>1</sub> and whole-lung, large and small airway VDP  
 In 20 participants with asthma, whole-lung and large airway VDP were significantly related to FEV<sub>1</sub> whereas small airways VDP was not.

Our results in **Chapter 5** however suggest that the assumption that the airways in the segmented tree represent all large airways may be invalid, especially in severe asthma. This pipeline can be extended to account for *a priori* spatial relationships between large airways and ventilation defects. Alternatively, a computational three-dimensional airway tree model consisting of 64,895 airways<sup>44</sup> could be used to simulate large versus small airway narrowing in asthma related to ventilation defects. Although this approach is not patient-specific, it provides a controlled environment to model both the large and small airways and eliminates the impact of airways that appear missing on CT. Previous work has generated image-functional models using this airway tree in conjunction with MRI ventilation in participants with asthma to simulate respiratory system impedance by narrowing the small airways that were spatially related to ventilation defects.<sup>13,45</sup> When directly compared with experimental oscillometry impedance measurements, the simulated results did not completely explain the experimental impedance,<sup>13</sup> which may suggest an interplay between both large and small airways to generate ventilation defects that differs between patients. In contrast to the previous computational models with promote random airway abnormalities using a model of a single terminus,<sup>5,46</sup> models generated using a three-dimensional airway tree with patient-specific MRI ventilation and experimental oscillometry measurements can provide a way to generate models of the large versus small airways abnormalities in patients with asthma.

### 6.4.3 Imaging Phenotypes of Asthma

Quantitative imaging biomarkers provide novel ways to generate imaging-based phenotyping or clustering of patients with respiratory disease. Imaging plays a large role in COPD clinical care owing to multiple large cohort studies that have established imaging phenotypes of COPD<sup>47,48</sup> using x-ray computed tomography (CT)<sup>49-52</sup> and inhaled gas MRI.<sup>53</sup> In contrast, pulmonary imaging has played a limited role in asthma research and clinical care because the mechanisms and physiological relevance of regional ventilation heterogeneity have been poorly understood. In the Severe Asthma Research Program cohort, one study used CT measurements of proximal airway structure, tissue biomechanics and gas trapping to identify for the first time imaging phenotypes of asthma.<sup>54</sup> Pulmonary functional MRI measurements have never been evaluated independently or in conjunction with CT for the generation of imaging phenotypes of asthma. The results in this thesis have provided an understanding of the pulmonary imaging structure-function determinants of ventilation heterogeneity in asthma and support the use of MRI results to phenotype asthma.

The AIM-IT cohort study at Western University in London, Canada is the largest known cohort study with paired CT and inhaled gas MRI in participants with asthma and provides a unique platform to explore imaging phenotypes of asthma using both CT and MRI. As a first step, we used MRI VDP and CT airway measurements to drive imaging-based clusters of asthma in 60 participants with asthma, including 16 mild-moderate and 44 severe. CT TAC and morphological airway measurements were generated as they were in **Chapter 5**. Univariate relationships were assessed between VDP and CT TAC, WA%, WT, LA and Pi10, with age, sex and BMI included as covariates. These relationships suggested VDP, TAC, Pi10, age and BMI sufficiently explained the variability in the data. Based on these five parameters, k-means clustering was used to generate clusters of participants with similar parameters in MATLAB R2018a (Mathworks, USA). K-means clustering and corresponding Dunn's coefficients were used to determine the quality of the clustering method and were evaluated for 3-6 clusters; Dunn's coefficient was greatest for 6 clusters (3, 4, 5, 6: 0.05, 0.11, 0.16, 0.18), and the resultant 6 clusters are described in **Figure 6-4**.

CLUSTER 1	<p>Younger Lower BMI Normal MRI ventilation Normal airway count No wall thickening</p>	<p>Age 35±17 years BMI 26±7 kg/m<sup>2</sup> VDP 1±1% TAC 248±23 Pi10 3.83±0.08 mm</p>	
CLUSTER 2	<p>Older Moderate BMI Moderate MRI heterogeneity Normal airway count Moderate wall thickening</p>	<p>Age 47±14 years BMI 27±4 kg/m<sup>2</sup> VDP 8±9% TAC 200±11 Pi10 3.88±0.15 mm</p>	
CLUSTER 3	<p>Younger Higher BMI Moderate MRI heterogeneity Significantly reduced airway count Significant wall thickening</p>	<p>Age 34±9 years BMI 32±4 kg/m<sup>2</sup> VDP 9±6% TAC 71±14 Pi10 4.08±0.14 mm</p>	
CLUSTER 4	<p>Older Moderate BMI Moderate MRI heterogeneity Moderately reduced airway count Moderate wall thickening</p>	<p>Age 51±10 years BMI 28±4 kg/m<sup>2</sup> VDP 9±8% TAC 168±9 Pi10 3.86±0.09 mm</p>	
CLUSTER 5	<p>Older Moderate BMI Moderate MRI heterogeneity Significantly reduced airway count Moderate wall thickening</p>	<p>Age 50±10 years BMI 28±4 kg/m<sup>2</sup> VDP 7±5% TAC 134±7 Pi10 3.90±0.10 mm</p>	
CLUSTER 6	<p>Older Moderate BMI Significant MRI heterogeneity Significantly reduced airway count Significant wall thickening</p>	<p>Age 49±14 years BMI 28±4 kg/m<sup>2</sup> VDP 17±10% TAC 106±11 Pi10 3.95±0.06 mm</p>	

**Figure 6-4** MR and CT imaging-based clusters of asthma

Description of 6 imaging-based clusters of asthma with values for each variable included in the clustering. Representative <sup>3</sup>He MR (cyan) ventilation images co-registered to anatomical <sup>1</sup>H (grey-scale) and CT airway tree (yellow) are shown for each cluster.

These results provide a first MRI-driven approach to phenotype asthma as a proof-of-concept, however for MRI phenotypes to be clinically translated they must be driven by  $^{129}\text{Xe}$  MRI. As previously addressed,  $^{129}\text{Xe}$  MRI is more sensitive to airway abnormalities than  $^3\text{He}$  and it follows that  $^{129}\text{Xe}$  MRI may more sensitively detect different phenotypes. Moreover,  $^{129}\text{Xe}$  MRI measurements of signal intensity heterogeneity may also be included to further develop MRI phenotypes of asthma. As a final step, it will be critical for these MRI phenotypes to be anchored to important clinical characteristics of asthma<sup>54</sup> such as age at onset, sex, obesity, severity, disease control, presence and nature of inflammation, and bronchodilator reversibility. We expect that MRI phenotypes of asthma will be related to well-established clinical phenotypes and subsequently can be used to guide clinical treatment decisions, regional therapies and development of novel therapies.

## **6.5 Significance and Impact**

Even though the regional heterogeneity of asthma has been understood for over 60 years and early MRI results suggested focal abnormalities in patients were not random, pulmonary structure and function are still clinically characterized by FEV<sub>1</sub> and underlying regional structure-function abnormalities and their variation over time remained uncertain. Today, asthma is still regarded as random and treatments are geared towards all airways and not individualized. A better understanding of the mechanisms and physiological relevance of regional ventilation heterogeneity in asthma is critical at this time as the number of people in Canada and worldwide with asthma is continuously growing<sup>55,56</sup> and 10% of these patients will progressively worsen to develop COPD.<sup>57,58</sup>

This thesis advances our understanding of asthma the spatially heterogeneous nature of asthma. The studies presented in this thesis provide strong evidence that airway abnormalities and corresponding ventilation defects in asthma are not random, but are spatially and temporally persistent for up to 7 years. We have provided for the first time, evidence that disease worsening occurs in previously abnormal airways and that MRI ventilation abnormalities sensitively predict longitudinal disease worsening towards development of COPD. Ventilation abnormalities have a specific biomechanical impact in asthma compared with COPD, however in severe asthma, the airway tree becomes truncated to a similar degree as moderate COPD.

The long-term spatial and temporal persistence of airway and ventilation abnormalities in asthma makes them ideally suited for personalized treatment targets as well as targets for novel therapy development. Although there are often differences between asthma and COPD, a similar truncation of the airway tree in asthma and airways-disease predominant COPD challenges our understanding of these differences. MRI ventilation abnormalities may be the ‘red flag’ to identify patients at risk for asthma worsening to COPD and provide a means to stratify these patients for more rigorous treatment. Armed with these understandings of regional airway and ventilation abnormalities in asthma, there is increased potential to guide treatment decisions and regional therapies, predict disease worsening and ultimately, improve patient outcomes.

## 6.6 References

- 1 Becklake, M. R. A new index of the intrapulmonary mixture of inspired air. *Thorax* **7**, 111-116 (1952).
- 2 Ballester, E. *et al.* Ventilation-perfusion mismatching in acute severe asthma: Effects of salbutamol and 100% oxygen. *Thorax* **44**, 258-267 (1989).
- 3 Bentivoglio, L. G. *et al.* Regional pulmonary function studied with xenon in patients with bronchial asthma. *J Clin Invest* **42**, 1193-1200 (1963).
- 4 Heckscher, T. *et al.* Regional lung function in patients with bronchial asthma. *J Clin Invest* **47**, 1063-1070 (1968).
- 5 Venegas, J. G. *et al.* Self-organized patchiness in asthma as a prelude to catastrophic shifts. *Nature* **434**, 777-782 (2005).
- 6 Tgavalekos, N. T. *et al.* Relationship between airway narrowing, patchy ventilation and lung mechanics in asthmatics. *Eur Respir J* **29**, 1174-1181 (2007).
- 7 Kauczor, H. U. *et al.* Normal and abnormal pulmonary ventilation: Visualization at hyperpolarized He-3 MR imaging. *Radiology* **201**, 564-568 (1996).
- 8 Parraga, G. *et al.* Hyperpolarized <sup>3</sup>He ventilation defects and apparent diffusion coefficients in chronic obstructive pulmonary disease: Preliminary results at 3.0 tesla. *Invest Radiol* **42**, 384-391 (2007).
- 9 Altes, T. A. *et al.* Hyperpolarized <sup>3</sup>He MR lung ventilation imaging in asthmatics: Preliminary findings. *J Magn Reson Imaging* **13**, 378-384 (2001).
- 10 Teague, W. G., Tustison, N. J. & Altes, T. A. Ventilation heterogeneity in asthma. *J Asthma* **51**, 677-684 (2014).

- 11 Svenningsen, S. *et al.* What are ventilation defects in asthma? *Thorax* **69**, 63-71 (2014).
- 12 Fain, S. B. *et al.* Evaluation of structure-function relationships in asthma using multidetector CT and hyperpolarized He-3 MRI. *Acad Radiol* **15**, 753-762 (2008).
- 13 Young, H. M., Guo, F., Eddy, R. L., Maksym, G. & Parraga, G. Oscillometry and pulmonary MRI measurements of ventilation heterogeneity in obstructive lung disease: Relationship to quality of life and disease control. *J Appl Physiol* **125**, 73-85 (2018).
- 14 de Lange, E. E. *et al.* Evaluation of asthma with hyperpolarized helium-3 MRI: Correlation with clinical severity and spirometry. *Chest* **130**, 1055-1062 (2006).
- 15 de Lange, E. E. *et al.* The variability of regional airflow obstruction within the lungs of patients with asthma: Assessment with hyperpolarized helium-3 magnetic resonance imaging. *J Allergy Clin Immunol* **119**, 1072-1078 (2007).
- 16 Svenningsen, S., Nair, P., Guo, F., McCormack, D. G. & Parraga, G. Is ventilation heterogeneity related to asthma control? *Eur Respir J* **48**, 370-379 (2016).
- 17 Svenningsen, S. *et al.* Sputum eosinophilia and magnetic resonance imaging ventilation heterogeneity in severe asthma. *Am J Respir Crit Care Med* **197**, 876-884 (2018).
- 18 de Lange, E. E. *et al.* Changes in regional airflow obstruction over time in the lungs of patients with asthma: Evaluation with <sup>3</sup>He MR imaging. *Radiology* **250**, 567-575 (2009).
- 19 Pellegrino, R. *et al.* Interpretative strategies for lung function tests. *Eur Respir J* **26**, 948-968 (2005).
- 20 Hantos, Z., Daroczy, B., Suki, B., Galgoczy, G. & Csendes, T. Forced oscillatory impedance of the respiratory system at low frequencies. *J Appl Physiol* **60**, 123-132 (1986).
- 21 Hantos, Z., Daroczy, B., Csendes, T., Suki, B. & Nagy, S. Modeling of low-frequency pulmonary impedance in dogs. *J Appl Physiol* **68**, 849-860 (1990).
- 22 Tepper, R., Sato, J., Suki, B., Martin, J. G. & Bates, J. H. Low-frequency pulmonary impedance in rabbits and its response to inhaled methacholine. *J Appl Physiol* **73**, 290-295 (1992).
- 23 Dandurand, R. J., Lavoie, J.-P., Lands, L. C., Hantos, Z. & Oscillometry Harmonisation Study, G. Comparison of oscillometry devices using active mechanical test loads. *ERJ Open Res* **5**, 00160-02019 (2019).

- 24 Cauberghs, M. & Van de Woestijne, K. P. Effect of upper airway shunt and series properties on respiratory impedance measurements. *J Appl Physiol* **66**, 2274-2279 (1989).
- 25 Lorino, A. M., Atlan, G., Lorino, H., Zanditenas, D. & Harf, A. Influence of posture on mechanical parameters derived from respiratory impedance. *Eur Respir J* **5**, 1118-1122 (1992).
- 26 Gonzales, P. A., Pearson, D. J., Haislip, G. D., Morris, M. J. & Skabelund, A. J. Effect of body position on impulse oscillometry in healthy volunteers: A pilot study [abstract]. *Am J Respir Crit Care Med* **195**, A2605 (2017).
- 27 Dandurand, R. J. *et al.* Oscillometry changes with body position and correlates with tlc and lung density. *Eur Respir J* **46**, PA2277 (2015).
- 28 Mata, J. *et al.* Hyperpolarized <sup>3</sup>He MR imaging of the lung: Effect of subject immobilization on the occurrence of ventilation defects. *Acad Radiol* **15**, 260-264 (2008).
- 29 Lambert, L., Banerjee, R., Votruba, J., El-Lababidi, N. & Zeman, J. Ultra-low-dose CT imaging of the thorax: Decreasing the radiation dose by one order of magnitude. *Indian J Pediatr* **83**, 1479-1481 (2016).
- 30 Kim, Y. *et al.* Ultra-low-dose CT of the thorax using iterative reconstruction: Evaluation of image quality and radiation dose reduction. *Am J Roentgenol* **204**, 1197-1202 (2015).
- 31 Kirby, M. *et al.* Total airway count on computed tomography and the risk of chronic obstructive pulmonary disease progression. Findings from a population-based study. *Am J Respir Crit Care Med* **197**, 56-65 (2018).
- 32 Galban, C. J. *et al.* Computed tomography-based biomarker provides unique signature for diagnosis of COPD phenotypes and disease progression. *Nat Med* **18**, 1711-1715 (2012).
- 33 Kirby, M. *et al.* A novel method of estimating small airway disease using inspiratory-to-expiratory computed tomography. *Respiration* **94**, 336-345 (2017).
- 34 Kirby, M. *et al.* Hyperpolarized <sup>3</sup>He magnetic resonance functional imaging semiautomated segmentation. *Acad Radiol* **19**, 141-152 (2012).
- 35 Tzeng, Y. S., Lutchen, K. & Albert, M. The difference in ventilation heterogeneity between asthmatic and healthy subjects quantified using hyperpolarized <sup>3</sup>He MRI. *J Appl Physiol* **106**, 813-822 (2009).
- 36 Zha, N. *et al.* Second-order texture measurements of (<sup>3</sup>)He ventilation MRI: Proof-of-concept evaluation of asthma bronchodilator response. *Acad Radiol* **23**, 176-185 (2016).

- 37 Oostveen, E. *et al.* The forced oscillation technique in clinical practice: Methodology, recommendations and future developments. *Eur Respir J* **22**, 1026-1041 (2003).
- 38 Shea, D. A. & Morgan, D. The helium-3 shortage: Supply, demand, and options for congress. (Congressional Research Service, Library of Congress, 2010).
- 39 Svenningsen, S. *et al.* Hyperpolarized (3) He and (129) Xe MRI: Differences in asthma before bronchodilation. *J Magn Reson Imaging* **38**, 1521-1530 (2013).
- 40 Kirby, M. *et al.* Hyperpolarized 3He and 129Xe MR imaging in healthy volunteers and patients with chronic obstructive pulmonary disease. *Radiology* **265**, 600-610 (2012).
- 41 Heinrich, M. P. *et al.* MIND: Modality independent neighbourhood descriptor for multi-modal deformable registration. *Med Image Anal* **16**, 1423-1435 (2012).
- 42 Capaldi, D. P. *et al.* Pulmonary imaging biomarkers of gas trapping and emphysema in COPD: (3)He MR imaging and CT parametric response maps. *Radiology* **279**, 597-608 (2016).
- 43 Macklem, P. T. & Mead, J. Resistance of central and peripheral airways measured by a retrograde catheter. *J Appl Physiol* **22**, 395-401 (1967).
- 44 Tawhai, M. H. *et al.* CT-based geometry analysis and finite element models of the human and ovine bronchial tree. *J Appl Physiol* **97**, 2310-2321 (2004).
- 45 Leary, D. *et al.* Hyperpolarized 3He magnetic resonance imaging ventilation defects in asthma: Relationship to airway mechanics. *Physiol Rep* **4** (2016).
- 46 Frey, U. *et al.* Risk of severe asthma episodes predicted from fluctuation analysis of airway function. *Nature* **438**, 667-670 (2005).
- 47 Lynch, D. A. & Al-Qaisi, M. A. Quantitative computed tomography in chronic obstructive pulmonary disease. *J Thorac Imaging* **28**, 284-290 (2013).
- 48 Hoffman, E. A. *et al.* Pulmonary CT and MRI phenotypes that help explain chronic pulmonary obstruction disease pathophysiology and outcomes. *J Magn Reson Imaging* **43**, 544-557 (2016).
- 49 Vestbo, J. *et al.* Evaluation of COPD longitudinally to identify predictive surrogate end-points (ECLIPSE). *Eur Respir J* **31**, 869-873 (2008).
- 50 Regan, E. A. *et al.* Genetic epidemiology of COPD (COPDGene) study design. *COPD* **7**, 32-43 (2010).
- 51 Couper, D. *et al.* Design of the subpopulations and intermediate outcomes in COPD study (SPIROMICS). *Thorax* **69**, 491-494 (2014).

- 52 Bourbeau, J. *et al.* Canadian cohort obstructive lung disease (CanCOLD): Fulfilling the need for longitudinal observational studies in COPD. *COPD* **11**, 125-132 (2014).
- 53 Kirby, M. *et al.* Longitudinal computed tomography and magnetic resonance imaging of COPD: Thoracic imaging network of Canada (TINCan) study objectives. *Chronic Obstr Pulm Dis* **1**, 200-211 (2014).
- 54 Choi, S. *et al.* Quantitative computed tomographic imaging-based clustering differentiates asthmatic subgroups with distinctive clinical phenotypes. *J Allergy Clin Immunol* (2017).
- 55 Masoli, M., Fabian, D., Holt, S. & Beasley, R. The global burden of asthma: Executive summary of the GINA dissemination committee report. *Allergy* **59**, 469-478 (2004).
- 56 Public Health Agency of Canada. Report from the Canadian chronic disease surveillance system: Asthma and chronic obstructive pulmonary disease in Canada. (2018).
- 57 To, T. *et al.* Do community demographics, environmental characteristics and access to care affect risks of developing ACOS and mortality in people with asthma? *Eur Respir J* **50** (2017).
- 58 To, T. *et al.* Progression from asthma to chronic obstructive pulmonary disease. Is air pollution a risk factor? *Am J Respir Crit Care Med* **194**, 429-438 (2016).

## APPENDICES

### **Appendix A – What is the Minimal Clinically Important Difference for Helium-3 Magnetic Resonance Imaging Ventilation Defects?**

*In this article, we determined the minimal clinically important difference for MRI ventilation defects which accounts for both patient-reported asthma control and the ventilation defect measurement error. This work was a necessary first step in order to evaluate longitudinal changes in ventilation defects in **Chapter 4**.*

*The contents of this appendix were previously published in the European Respiratory Journal as a research letter: RL Eddy, S Svenningsen, DG McCormack, G Parraga. What is the minimal clinically important difference for helium-3 magnetic resonance imaging ventilation defects? Eur Respir J. 2018;51(6). Permission to reproduce this article was granted by the European Respiratory Society (ERS) and is provided in **Appendix B**.*

#### ***To the Editor:***

Pulmonary magnetic resonance imaging (MRI) using inhaled polarised gases provides a way to directly visualise and sensitively measure lung ventilation abnormalities or ventilation defects;<sup>1</sup> the burden in individual patients may be directly quantified as the percent ventilation volume,<sup>2</sup> ventilation defect volume (VDV)<sup>3</sup> or ventilation defect percent (VDP)<sup>4</sup> which is VDV normalised to the total lung volume. In patients with asthma, MRI ventilation defects worsen during methacholine<sup>5</sup> and exercise challenge<sup>5,6</sup> and respond to bronchodilation.<sup>5,6</sup> However, it is still unknown if quantitative changes in MRI ventilation abnormalities directly reflect changes in patient-related outcomes like symptoms; this is important when considering MRI for clinical and research studies in asthma patients which requires an understanding of the minimal clinically important difference (MCID).

First described in 1989,<sup>7</sup> the MCID reflects the smallest measurement difference that patients perceive as beneficial. MCID estimations typically involve patient perception but up to nine methods have been reported,<sup>8</sup> and no standard for calculating MCID has been established. For example, changes in clinical parameters provide the foundation for the so-called anchor-based MCID approach,<sup>9</sup> in which patient- or clinician-reported metrics serve as ‘anchors’. On the other hand, distribution-based or data-driven approaches reflect

instrument error and precision, including the standard error of measurement (SEM)<sup>10</sup> which has been validated as a proxy for the MCID.

Here we estimate the MCID of MRI VDV and VDP using distribution- and anchor-based approaches. We used both approaches because MRI VDV and VDP measurement precision are heavily dependent on the algorithm used and the reproducibility of the quantification. First, we used the SEM to estimate the distribution-based MCID for VDV based on algorithm precision previously published.<sup>3</sup> As previously described,<sup>3</sup> pulmonary MRI VDV is quantified using a semi-automated algorithm in units of mL while VDP is measured as a percentage of the thoracic cavity volume in units of %. Based on five repeated segmentation rounds in 15 subjects, the SEM for VDP was calculated as the square root of the repeated measures intra-observer VDP variance and was 40 mL.<sup>3</sup> We also consider the smallest detectable difference (SDD) which generates confidence about measurement uncertainty. The previously calculated SDD for VDV was 110 mL,<sup>3</sup> and because this is larger than the SEM, it is possible that an observed change less than the SEM would be due to measurement error. In contrast, if the SDD is smaller than the MCID, it is possible to distinguish a clinically important change with adequate measurement precision. To be certain that a clinically important change is not due to measurement error, we propose to conservatively use the MCID of 110 mL which reflects measurement precision, instead of 40 mL which was the measured SEM.

For the anchor-based method, we used the patient-reported and validated asthma control questionnaire (ACQ) score<sup>11</sup> as the anchor and the significant relationship between ACQ score and MRI VDP previously published in 18 asthmatic patients.<sup>12</sup> In these asthmatics, the relationship between ACQ score and VDP was determined by equation of their linear relationship as  $VDP = 7.5ACQ - 5.0$ .<sup>12</sup> The MCID for ACQ score was previously determined to be 0.5<sup>11</sup> and therefore based on the linear relationship, a 0.5 change in ACQ would result in a 4% VDP difference. Therefore, using ACQ score as an anchor, the VDP MCID is 4%.

While ACQ score and exacerbations may be used in asthma clinical trials, the most commonly-used objective endpoint is the forced expiratory volume in one second (FEV<sub>1</sub>);

the MCID for FEV<sub>1</sub> is often described as a range which for asthmatics is 100–200 mL.<sup>13</sup> In contrast with FEV<sub>1</sub> which is dominated by the large airways,<sup>14</sup> MRI is sensitive to all airways and the MCID is 110 mL for VDV (distribution-based) and 4% for VDP (anchor-based). The 4% VDP MCID can be translated to a VDV of 200 mL based on the mean thoracic cavity volume segmented from MRI which was reported to be 5.0 L.<sup>3</sup> In a similar manner, the VDV MCID of 110 mL is equivalent to approximately 2%. Thus, we report a range of 110–200 mL for VDV and 2–4% for VDP as MCID ranges. To illustrate the quantitative meaning of the MCID of VDP in individual patients, Figure 1 shows MRI for three patients with asthma with visually and quantitatively improved ventilation following bronchodilation (increasing VDP improvement shown from left to right). For subject S1 there was a change in VDV/VDP equivalent to the distribution-based MCID or SDD. For subjects S2 and S3, there were post-bronchodilator changes in VDV/VDP that were similar in magnitude to the anchor-based MCID estimate. Notably, S1 and S3 showed clinically significant post-bronchodilator FEV<sub>1</sub> changes ( $\geq 200$  mL and  $\geq 12\%$ ), while S2 did not. The sensitivity of MRI to post-bronchodilator changes highlights a unique opportunity for pulmonary MRI to help explain subjective or patient-perceived improvements (i.e. ACQ or quality of life improvements) that are not reflected by FEV<sub>1</sub>. The number of experts using hyperpolarised gas MRI in asthma clinical trials is still very small so it is important to consider the MRI VDP MCID in the context of the MCID of other established asthma biomarkers. The MCID we calculated for MRI VDP is similar to the MCID for FEV<sub>1</sub> in asthma at 110-200 mL. Moreover, we have used the ACQ MCID of 0.5<sup>11</sup> to determine the upper limit of this range at 200 mL and therefore these are already intrinsically related. The MCID for the asthma quality of life questionnaire (AQLQ) is also 0.5<sup>15</sup> and though the relationship between VDP and AQLQ has not been directly established, we previously showed that VDP is significantly worse in patients with lower quality of life (AQLQ<5).<sup>12</sup> MRI VDP directly detects early changes in clinically important pathologies with high reproducibility.<sup>16</sup> Taken together, this means that MRI has both the sensitivity and precision needed for clinical studies, although the complexity and cost of the acquisition of these measurements compared to other tests is still a limitation.

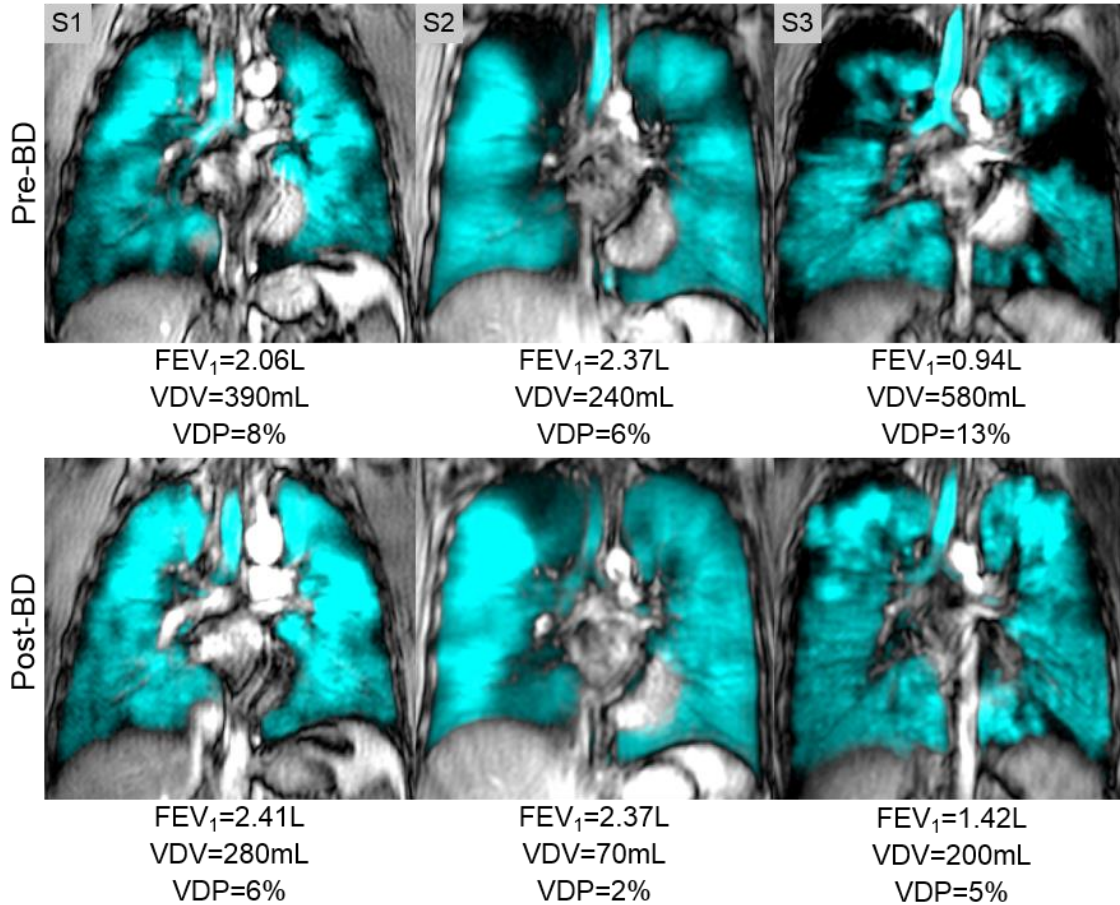


**Figure 1.** Change in asthmatic magnetic resonance imaging (MRI) ventilation after bronchodilator (BD) for three representative subjects. Three asthmatic subjects exhibited visual changes in MR ventilation post-BD. A 45-year-old male (S1) underwent an improvement in ventilation equal to the smallest detectable difference and distribution-based minimal clinically important difference (MCID), while a 28-year-old-female (S2) and a 31-year-old female (S3) underwent improvements at least as large as the anchor-based MCID. Notably, S1 and S3 also exhibited clinically significant changes in forced expiratory volume in 1 s (FEV<sub>1</sub>) ( $\geq 200$  mL and 12%) but S2 did not. VDV: ventilation defect volume; VDP: ventilation defect percent.

It is important to consider the <sup>3</sup>He MRI results in the context of future development of <sup>129</sup>Xe MRI which is much less costly to acquire. In this regard, we previously directly compared <sup>3</sup>He and <sup>129</sup>Xe MRI and showed that <sup>129</sup>Xe VDP was greater than <sup>3</sup>He VDP in asthmatics;<sup>17</sup> this suggested that there was enhanced sensitivity to airway abnormalities using <sup>129</sup>Xe gas which we speculated was due to the viscosity and diffusivity of the gas, so that <sup>129</sup>Xe VDP was systematically larger than <sup>3</sup>He VDP in asthmatics. Based on this important information, we speculate that the slope of the linear relationship between ACQ

and  $^{129}\text{Xe}$  VDP, and thus the MCID, would be similar to  $^3\text{He}$  MRI VDP, but these calculations still need to be undertaken in a prospective  $^{129}\text{Xe}$  MRI study. It is also important to note that, though there is no standard for calculating MCID values, the anchor-based estimation we generated here was based on cross-sectional data and did not reflect within-subject variability or response to therapy. Considering the original definition of MCID,<sup>7</sup> “within-subject” differences in response to therapy will be important to investigate in prospectively designed clinical trials.

In summary, pulmonary MRI biomarkers of ventilation have already provided some intriguing results in patients with asthma, but to our knowledge, MRI biomarkers have not been used in large-scale clinical trials of potential new therapies. Other considerations aside (i.e. technological and financial), this lack of uptake may reflect the lack of a deep understanding of the relationship between MRI biomarkers with how patients perceive symptoms. We provide calculations of MCID for  $^3\text{He}$  MRI VDV and VDP to support the use of MRI in the research and development of novel therapies, as well as therapy decisions or n=1 trials, towards more precise decision making in individual patients.

## REFEERENCES

- 1 Kauczor, H.-U. *et al.* Imaging of the lungs using  $^3\text{He}$  MRI: Preliminary clinical experience in 18 patients with and without lung disease. *J Magn Reson Imaging* **7**, 538-543 (1997).
- 2 Woodhouse, N. *et al.* Combined helium-3/proton magnetic resonance imaging measurement of ventilated lung volumes in smokers compared to never-smokers. *J Magn Reson Imaging* **21**, 365-369 (2005).
- 3 Kirby, M. *et al.* Hyperpolarized  $^3\text{He}$  magnetic resonance functional imaging semiautomated segmentation. *Acad Radiol* **19**, 141-152 (2012).
- 4 Fain, S. B. *et al.* Evaluation of structure-function relationships in asthma using multidetector CT and hyperpolarized He-3 MRI. *Acad Radiol* **15**, 753-762 (2008).
- 5 Samee, S. *et al.* Imaging the lungs in asthmatic patients by using hyperpolarized helium-3 magnetic resonance: Assessment of response to methacholine and exercise challenge. *J Allergy Clin Immunol* **111**, 1205-1211 (2003).
- 6 Kruger, S. J. *et al.* Hyperpolarized helium-3 MRI of exercise-induced bronchoconstriction during challenge and therapy. *J Magn Reson Imaging* **39**, 1230-1237 (2014).

- 7 Jaeschke, R., Singer, J. & Guyatt, G. H. Measurement of health status. Ascertaining the minimal clinically important difference. *Control Clin Trials* **10**, 407-415 (1989).
- 8 Wells, G. *et al.* Minimal clinically important differences: Review of methods. *J Rheumatol* **28**, 406-412 (2001).
- 9 Copay, A. G., Subach, B. R., Glassman, S. D., Polly, D. W., Jr. & Schuler, T. C. Understanding the minimum clinically important difference: A review of concepts and methods. *Spine J* **7**, 541-546 (2007).
- 10 Wyrwich, K. W., Nienaber, N. A., Tierney, W. M. & Wolinsky, F. D. Linking clinical relevance and statistical significance in evaluating intra-individual changes in health-related quality of life. *Med Care* **37**, 469-478 (1999).
- 11 Juniper, E. F., Svensson, K., Mork, A. C. & Stahl, E. Measurement properties and interpretation of three shortened versions of the asthma control questionnaire. *Respir Med* **99**, 553-558 (2005).
- 12 Svenningsen, S., Nair, P., Guo, F., McCormack, D. G. & Parraga, G. Is ventilation heterogeneity related to asthma control? *Eur Respir J* **48**, 370-379 (2016).
- 13 Jones, P. W. *et al.* Minimal clinically important differences in pharmacological trials. *Am J Respir Crit Care Med* **189**, 250-255 (2014).
- 14 Macklem, P. T. & Mead, J. Resistance of central and peripheral airways measured by a retrograde catheter. *J Appl Physiol* **22**, 395-401 (1967).
- 15 Juniper, E. F., Guyatt, G. H., Willan, A. & Griffith, L. E. Determining a minimal important change in a disease-specific quality of life Questionnaire. *J Clin Epidemiol* **47**, 81-87 (1994).
- 16 de Lange, E. E. *et al.* Changes in regional airflow obstruction over time in the lungs of patients with asthma: Evaluation with 3He MR imaging. *Radiology* **250**, 567-575 (2009).
- 17 Svenningsen, S. *et al.* Hyperpolarized (3) He and (129) Xe MRI: Differences in asthma before bronchodilation. *J Magn Reson Imaging* **38**, 1521-1530 (2013).

## Appendix B – Permission for Reproduction of Scientific Articles and Figures

**Pathophysiology of airflow limitation in chronic obstructive pulmonary disease**

**Author:** James C Hogg  
**Publication:** The Lancet  
**Publisher:** Elsevier  
**Date:** 21–27 August 2004

Copyright © 2004 Elsevier Ltd. All rights reserved.

### Order Completed

Thank you for your order.

This Agreement between Rachel Eddy ("You") and Elsevier ("Elsevier") consists of your license details and the terms and conditions provided by Elsevier and Copyright Clearance Center.

Your confirmation email will contain your order number for future reference.

**License Number** 4755491226617

[Printable Details](#)

**License date** Jan 24, 2020

#### Licensed Content

#### Order Details

**Licensed Content Publisher** Elsevier

**Licensed Content Publication** The Lancet

**Licensed Content Title** Pathophysiology of airflow limitation in chronic obstructive pulmonary disease

**Licensed Content Author** James C Hogg

**Licensed Content Date** 21–27 August 2004

**Licensed Content Volume** 364

**Licensed Content Issue** 9435

**Licensed Content Pages** 13

**Journal Type** HS

**Type of Use** reuse in a thesis/dissertation

**Portion** figures/tables/illustrations

**Number of figures/tables/illustrations** 1

**Format** both print and electronic

**Are you the author of this Elsevier article?** No

**Will you be translating?** No

#### About Your Work

#### Additional Data

**Title** Structure-function Determinants of Asthma Using Pulmonary Imaging

**Institution name** University of Western Ontario

**Expected presentation date** Apr 2020

**Portions** Figure 4

#### Requestor Location

#### Tax Details

Rachel Eddy  
Robarts Research Institute

**Publisher Tax ID** GB 494 6272 12

#### Requestor Location

-----  
Attn: Rachel Eddy

#### Airway pathology in asthma

M. Saetta, G. Turato

*European Respiratory Journal* 18 (34 suppl) 18s-23s; DOI: 10.1183/09031936.01.00229501 Published 1 January 2001

Material: Figure 1

Acknowledgement Wording: Reproduced with permission of the © ERS 2020: *European Respiratory Journal* 18 (34 suppl) 18s-23s; DOI: 10.1183/09031936.01.00229501 Published 1 January 2001

European Respiratory Society hereby grants you permission to reproduce the material as requested in your thesis and full acknowledgement must be given.

Copyright remains with © ERS 2020. These publications are copyrighted material and must not be copied, reproduced, transferred, distributed, leased, licensed, placed in a storage retrieval system or publicly performed or used in any way except as specifically permitted in writing by the publishers (European Respiratory Society), as allowed under the terms and conditions of which it was purchased or as strictly permitted by applicable copyright law. Reproduction of this material is confined to the purpose and/or media for which permission is hereby given. Altering/Modifying Material: This is not permitted, however figures and illustrations maybe altered/adapted minimally to serve your work. Please be aware that the permission fee for the requested use of this material is waived in this instance but please be advised that your future requests for materials may attract a fee. This agreement is personal to you and may not be sublicense, assigned or transferred by you to any other person without our written permission. Any unauthorised distribution or use of this text may be a direct infringement of the publisher's rights and those responsible may be liable in law accordingly

#### **"Green" open access and author archiving (where applicable)**

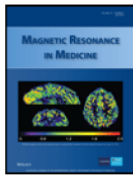
Authors who do not wish to pay for their article to be published open access in the *ERJ* will still have their manuscripts made free to access via the *ERJ* online archive following the journal's 18-month embargo period. Authors also have licence to make their manuscripts available in an institutional (or similar) repository for public archiving, 12 months after final publication, provided the following requirements are met:

- 1) The final, peer-reviewed, author-submitted version that was accepted for publication is used (before copy-editing and publication).
- 2) A permanent link is provided to the version of the article published in the *ERJ*, through the dx.doi.org platform. For example, if your manuscript has the DOI 10.1183/13993003.06543-2018, then the link you provide must be <https://doi.org/10.1183/13993003.06543-2018>
- 3) The repository on which the manuscript is deposited is not used for systematic distribution or commercial sales purposes.
- 4) The following required archiving statement appears on the title page of the archived manuscript: "This is an author-submitted, peer-reviewed version of a manuscript that has been accepted for publication in the *European Respiratory Journal*, prior to copy-editing, formatting and typesetting. This version of the manuscript may not be duplicated or reproduced without prior permission from the copyright owner, the European Respiratory Society. The publisher is not responsible or liable for any errors or omissions in this version of the manuscript or in any version derived from it by any other parties. The final, copy-edited, published article, which is the version of record, is available without a subscription 18 months after the date of issue publication."

For manuscripts with Europe PMC funding, the journal acknowledges that the author retains the right to provide a copy of the final, peer-reviewed author-supplied manuscript (before copy-editing and publication) for public archiving in compliance with the requirements of the funder, i.e. 6 months after final publication for authors with funding from Europe PubMed Central Funders Group members.

Kind regards,

Kay



## Hyperpolarized 3He diffusion MRI and histology in pulmonary emphysema

**Author:** James C. Hogg, Mark S. Conradi, Peter T. Macklem, et al

**Publication:** Magnetic Resonance in Medicine

**Publisher:** John Wiley and Sons

**Date:** Oct 20, 2006

Copyright © 2006 Wiley-Liss, Inc.

### Order Completed

Thank you for your order.

This Agreement between Rachel Eddy ("You") and John Wiley and Sons ("John Wiley and Sons") consists of your license details and the terms and conditions provided by John Wiley and Sons and Copyright Clearance Center.

Your confirmation email will contain your order number for future reference.

**License Number** 4755500063866

[Printable Details](#)

**License date** Jan 24, 2020

#### Licensed Content

#### Order Details

**Licensed Content Publisher** John Wiley and Sons

**Licensed Content Publication** Magnetic Resonance in Medicine

**Licensed Content Title** Hyperpolarized 3He diffusion MRI and histology in pulmonary emphysema

**Licensed Content Author** James C. Hogg, Mark S. Conradi, Peter T. Macklem, et al

**Licensed Content Date** Oct 20, 2006

**Licensed Content Volume** 56

**Licensed Content Issue** 6

**Licensed Content Pages** 8

**Type of use** Dissertation/Thesis

**Requestor type** University/Academic

**Format** Print and electronic

**Portion** Figure/table

**Number of figures/tables** 1

**Will you be translating?** No

#### About Your Work

#### Additional Data

**Title of your thesis / dissertation** Structure-function Determinants of Asthma Using Pulmonary Imaging

**Expected completion date** Apr 2020

**Expected size (number of pages)** 1

**Original Wiley figure/table number(s)** Figure 2

#### Requestor Location

#### Tax Details

Rachel Eddy

**Publisher Tax ID** EU826007151

#### Requestor Location

Attn: Rachel Eddy



November 19, 2019

Rachel L. Eddy  
Western University

Dear Rachel L. Eddy:

The Radiological Society of North America (RSNA®) is pleased to grant you permission to reproduce the following article in print and electronic formats for use in your Doctoral thesis and for use by Library and Archive Canada/ProQuest/UMI (post 1-year embargo), provided you give full credit to the authors of the original publication.

Full Article

Eddy R L, Svenningsen S, Licskai C, et al. Hyperpolarized helium 3 MRI in mild-to-moderate asthma: Prediction of postbronchodilator reversibility. *Radiology* 2019;293:212-220.

This permission is a one-time, non-exclusive grant for English-language use and is exclusively limited to the usage stated and underlined above. The requestor guarantees to reproduce the material as originally published. Permission is granted under the condition that a full credit line is prominently placed (i.e. author name(s), journal name, copyright year, volume #, inclusive pages and copyright holder).

This permission becomes effective upon receipt of this signed contract. Please sign a copy of this agreement, return a signed copy to me and retain a copy for your files. Thank you for your interest in our publication.

[Print Name]: \_\_\_\_\_

SIGNATURE: \_\_\_\_\_ Date: \_\_\_\_\_

Sincerely,

Ashley E. Daly  
Senior Manager, Journal Rights & Communications  
Publications

**From:** ATS Permission Requests  
**Sent:** Thursday, February 20, 2020 10:50 AM  
**To:** Rachel Lynn Eddy  
**Subject:** RE: Permission to Use AJRCCM Copyrighted Material in a Doctoral Thesis

Hello Rachel:

Thank you for your request. Permission is granted at no charge. Please complete the below and use it beneath the material. Thank you.

Reprinted with permission of the American Thoracic Society. Copyright © 2020 American Thoracic Society.  
Cite: Author(s)/Year/Title/Journal title/Volume/Pages.  
The American Journal of Respiratory and Critical Care Medicine is an official journal of the American Thoracic Society.

Best regards,

Megan Murphy

**From:** Rachel Lynn Eddy  
**Sent:** Wednesday, February 19, 2020 5:27 AM  
**To:** ATS Permission Requests  
**Subject:** Re: Permission to Use AJRCCM Copyrighted Material in a Doctoral Thesis

Hello Meagan,

I would like to reproduce the entire article with all tables and figures in my thesis.

Thank you, and please let me know if you need anything else.

Rachel

---

**From:** ATS Permission Requests  
**Sent:** Wednesday, February 19, 2020 5:25 AM  
**To:** Rachel Lynn Eddy  
**Subject:** RE: Permission to Use AJRCCM Copyrighted Material in a Doctoral Thesis

Dear Rachel,

Thank you for your interest in ATS. Can you please clarify what you will be using from our article?

Best regards,

Megan Murphy

**From:** Rachel Lynn Eddy  
**Sent:** Monday, February 17, 2020 8:25 AM  
**To:** ATS Permission Requests  
**Subject:** Permission to Use AJRCCM Copyrighted Material in a Doctoral Thesis

Hello,

I am a Western University (London, Ontario, Canada) graduate student completing my Doctoral thesis entitled "Structure-function Determinants of Asthma Using Pulmonary Imaging". My thesis will be available April 2020 in full-text on the internet for reference, study and / or copy. Except in situations where a thesis is under embargo or restriction, the electronic version will be accessible through the Western Libraries web pages, the Library's web catalogue, and also through web search engines. I will also be granting Library and Archives Canada and ProQuest/UMI a non-exclusive license to reproduce, loan, distribute, or sell single copies of my thesis by any means and in any form or format. These rights will in no way restrict republication of the material in any other form by you or by others authorized by you.

I would like permission to allow inclusion of the following material in my thesis which has been published in the American Journal of Respiratory and Critical Care Medicine (epub ahead of print):

RL Eddy, S Svenningsen, M Kirby, D Knipping, DG McCormack, C Liciskai, P Nair, G Parraga. Is Computed Tomography Airway Count Related to Asthma Severity and Airway Structure-function? American Journal of Respiratory and Critical Care Medicine. 2020 Jan 2[Online ahead of print] doi.org/10.1164/rccm.201908-1552oc  
<https://www.atsjournals.org/doi/abs/10.1164/rccm.201908-1552OC>

The material will be attributed through a citation.

Please confirm in writing or by e-mail that these arrangements meet with your approval. Thank you in advance.

Kind regards,  
Rachel

What is the minimal clinically important difference for helium-3 magnetic resonance imaging ventilation defects?  
Rachel L. Eddy, Sarah Svenningsen, David G. McCormack, Grace Parraga  
*European Respiratory Journal* 51 (6) 1800324; DOI: 10.1183/13993003.00324-2018 Published 28 June 2018  
Material: Figure 1

Acknowledgement Wording: Reproduced with permission of the © ERS 2019: *European Respiratory Journal* 51 (6) 1800324; DOI: 10.1183/13993003.00324-2018 Published 28 June 2018

European Respiratory Society hereby grants you permission to reproduce the material as requested in your thesis and full acknowledgement must be given.

Copyright remains with © ERS 2019. These publications are copyrighted material and must not be copied, reproduced, transferred, distributed, leased, licensed, placed in a storage retrieval system or publicly performed or used in any way except as specifically permitted in writing by the publishers (European Respiratory Society), as allowed under the terms and conditions of which it was purchased or as strictly permitted by applicable copyright law. Reproduction of this material is confined to the purpose and/or media for which permission is hereby given. Altering/Modifying Material: This is not permitted, however figures and illustrations maybe altered/adapted minimally to serve your work. Please be aware that the permission fee for the requested use of this material is waived in this instance but please be advised that your future requests for materials may attract a fee. This agreement is personal to you and may not be sublicense, assigned or transferred by you to any other person without our written permission. Any unauthorised distribution or use of this text may be a direct infringement of the publisher's rights and those responsible may be liable in law accordingly

#### "Green" open access and author archiving (where applicable)

Authors who do not wish to pay for their article to be published open access in the *ERJ* will still have their manuscripts made free to access via the *ERJ* online archive following the journal's 18-month embargo period. Authors also have licence to make their manuscripts available in an institutional (or similar) repository for public archiving, 12 months after final publication, provided the following requirements are met:

- 1) The final, peer-reviewed, author-submitted version that was accepted for publication is used (before copy-editing and publication).
- 2) A permanent link is provided to the version of the article published in the *ERJ*, through the [dx.doi.org](https://dx.doi.org) platform. For example, if your manuscript has the DOI 10.1183/13993003.06543-2018, then the link you provide must be <https://doi.org/10.1183/13993003.06543-2018>
- 3) The repository on which the manuscript is deposited is not used for systematic distribution or commercial sales purposes.
- 4) The following required archiving statement appears on the title page of the archived manuscript: "This is an author-submitted, peer-reviewed version of a manuscript that has been accepted for publication in the *European Respiratory Journal*, prior to copy-editing, formatting and typesetting. This version of the manuscript may not be duplicated or reproduced without prior permission from the copyright owner, the European Respiratory Society. The publisher is not responsible or liable for any errors or omissions in this version of the manuscript or in any version derived from it by any other parties. The final, copy-edited, published article, which is the version of record, is available without a subscription 18 months after the date of issue publication."

For manuscripts with Europe PMC funding, the journal acknowledges that the author retains the right to provide a copy of the final, peer-reviewed author-supplied manuscript (before copy-editing and publication) for public archiving in compliance with the requirements of the funder, i.e. 6 months after final publication for authors with funding from Europe PubMed Central Funders Group members.

Regards,

Kay

## Appendix C – Health Sciences Research Ethics Board Approval Notices



**Date:** 11 October 2019

**To:** Grace Parraga

**Project ID:** 7320

**Study Title:** Longitudinal  $^3\text{He}$  Magnetic Resonance Imaging of Healthy Lung (REB #17396)

**Application Type:** Continuing Ethics Review (CER) Form

**Review Type:** Delegated

**REB Meeting Date:** 15/Oct/2019

**Date Approval Issued:** 11/Oct/2019

**REB Approval Expiry Date:** 09/Nov/2020

---

Dear Grace Parraga,

The Western University Research Ethics Board has reviewed the application. This study, including all currently approved documents, has been re-approved until the expiry date noted above.

REB members involved in the research project do not participate in the review, discussion or decision.

Western University REB operates in compliance with, and is constituted in accordance with, the requirements of the TriCouncil Policy Statement: Ethical Conduct for Research Involving Humans (TCPS 2); the International Conference on Harmonisation Good Clinical Practice Consolidated Guideline (ICH GCP); Part C, Division 5 of the Food and Drug Regulations; Part 4 of the Natural Health Products Regulations; Part 3 of the Medical Devices Regulations and the provisions of the Ontario Personal Health Information Protection Act (PHIPA, 2004) and its applicable regulations. The REB is registered with the U.S. Department of Health & Human Services under the IRB registration number IRB 00000940.

Please do not hesitate to contact us if you have any questions.

Sincerely,

Daniel Wyzynski, Research Ethics Coordinator, on behalf of Dr. Joseph Gilbert, HSREB Chair

*Note: This correspondence includes an electronic signature (validation and approval via an online system that is compliant with all regulations).*



**Office of Research Ethics**

The University of Western Ontario

**Use of Human Subjects - Ethics Approval Notice**

**Principal Investigator:** Dr. G. Parraga **Review Level:** Expedited  
**Review Number:** 15928 **Revision Number:** 6  
**Review Date:** January 06, 2011 **Approved Local # of Participants:** 34  
**Protocol Title:** Hyperpolarized Helium-3 Magnetic Resonance Ventilation Heterogeneity and Airway Hyper-Responsiveness in Asthma  
**Department and Institution:** Imaging, Robarts Research Institute  
**Sponsor:** INTERNAL RESEARCH FUND-UWO  
**Ethics Approval Date:** January 07, 2011 **Expiry Date:** March 31, 2011  
**Documents Reviewed and Approved:** Addition of healthy volunteers (10), revised study methodology, revised inclusion criteria and revised letter of information & consent form dated Nov.25/10

**Documents Received for Information:**

This is to notify you that The University of Western Ontario Research Ethics Board for Health Sciences Research Involving Human Subjects (HSREB) which is organized and operates according to the Tri-Council Policy Statement: Ethical Conduct of Research Involving Humans and the Health Canada/ICH Good Clinical Practice Practices: Consolidated Guidelines; and the applicable laws and regulations of Ontario has reviewed and granted approval to the above referenced revision(s) or amendment(s) on the approval date noted above. The membership of this REB also complies with the membership requirements for REB's as defined in Division 5 of the Food and Drug Regulations.

The ethics approval for this study shall remain valid until the expiry date noted above assuming timely and acceptable responses to the HSREB's periodic requests for surveillance and monitoring information. If you require an updated approval notice prior to that time you must request it using the UWO Updated Approval Request Form.

During the course of the research, no deviations from, or changes to, the protocol or consent form may be initiated without prior written approval from the HSREB except when necessary to eliminate immediate hazards to the subject or when the change(s) involve only logistical or administrative aspects of the study (e.g. change of monitor, telephone number). Expedited review of minor change(s) in ongoing studies will be considered. Subjects must receive a copy of the signed information/consent documentation.

Investigators must promptly also report to the HSREB:

- a) changes increasing the risk to the participant(s) and/or affecting significantly the conduct of the study;
- b) all adverse and unexpected experiences or events that are both serious and unexpected;
- c) new information that may adversely affect the safety of the subjects or the conduct of the study.

If these changes/adverse events require a change to the information/consent documentation, and/or recruitment advertisement, the newly revised information/consent documentation, and/or advertisement, must be submitted to this office for approval.

Members of the HSREB who are named as investigators in research studies, or declare a conflict of interest, do not participate in discussion related to, nor vote on, such studies when they are presented to the HSREB.

Chair of HSREB: Dr. Joseph Gilbert  
FDA Ref. #: IRB 00000940

Ethics Officer to Contact for Further Information		
<input checked="" type="checkbox"/> Janice Sutherland	<input type="checkbox"/> Elizabeth Wambolt	<input type="checkbox"/> Grace Kelly

*This is an official document. Please retain the original in your files.*

cc: ORE File  
LHRI



**Date:** 15 January 2019

**To:** Dr. Grace Parraga

**Project ID:** 6014

**Study Title:** Longitudinal Study of Helium-3 Magnetic Resonance Imaging of COPD

**Application Type:** Continuing Ethics Review (CER) Form

**Review Type:** Delegated

**REB Meeting Date:** 29/Jan/2019

**Date Approval Issued:** 15/Jan/2019

**REB Approval Expiry Date:** 10/Feb/2020

---

Dear Dr. Grace Parraga,

The Western University Research Ethics Board has reviewed the application. This study, including all currently approved documents, has been re-approved until the expiry date noted above.

REB members involved in the research project do not participate in the review, discussion or decision.

Western University REB operates in compliance with, and is constituted in accordance with, the requirements of the TriCouncil Policy Statement: Ethical Conduct for Research Involving Humans (TCPS 2); the International Conference on Harmonisation Good Clinical Practice Consolidated Guideline (ICH GCP); Part C, Division 5 of the Food and Drug Regulations; Part 4 of the Natural Health Products Regulations; Part 3 of the Medical Devices Regulations and the provisions of the Ontario Personal Health Information Protection Act (PHIPA 2004) and its applicable regulations. The REB is registered with the U.S. Department of Health & Human Services under the IRB registration number IRB 00000940.

Please do not hesitate to contact us if you have any questions.

Sincerely,

Daniel Wyzynski, Research Ethics Coordinator, on behalf of Dr. Joseph Gilbert, HSREB Chair

*Note: This correspondence includes an electronic signature (validation and approval via an online system that is compliant with all regulations).*



**Date:** 29 January 2019

**To:** Grace Parraga

**Project ID:** 103516

**Study Title:** Structure and Function MRI of Asthma

**Application Type:** Continuing Ethics Review (CER) Form

**Review Type:** Delegated

**REB Meeting Date:** 12/Feb/2019

**Date Approval Issued:** 29/Jan/2019

**REB Approval Expiry Date:** 19/Feb/2020

---

Dear Grace Parraga,

The Western University Research Ethics Board has reviewed the application. This study, including all currently approved documents, has been re-approved until the expiry date noted above.

REB members involved in the research project do not participate in the review, discussion or decision.

Western University REB operates in compliance with, and is constituted in accordance with, the requirements of the TriCouncil Policy Statement: Ethical Conduct for Research Involving Humans (TCPS 2); the International Conference on Harmonisation Good Clinical Practice Consolidated Guideline (ICH GCP); Part C, Division 5 of the Food and Drug Regulations; Part 4 of the Natural Health Products Regulations; Part 3 of the Medical Devices Regulations and the provisions of the Ontario Personal Health Information Protection Act (PHIPA 2004) and its applicable regulations. The REB is registered with the U.S. Department of Health & Human Services under the IRB registration number IRB 00000940.

Please do not hesitate to contact us if you have any questions.

Sincerely,

Daniel Wyzynski, Research Ethics Coordinator, on behalf of Dr. Joseph Gilbert, HSREB Chair

*Note: This correspondence includes an electronic signature (validation and approval via an online system that is compliant with all regulations).*



# Western Research

**Date:** 17 August 2019

**To:** Grace Parraga

**Project ID:** 104200

**Study Title:** Hyperpolarized Magnetic Resonance Imaging in Asthma Pre- and Post-Bronchial Thermoplasty

**Application Type:** Continuing Ethics Review (CER) Form

**Review Type:** Delegated

**REB Meeting Date:** 03/Sep/2019

**Date Approval Issued:** 17/Aug/2019

**REB Approval Expiry Date:** 03/Sep/2020

---

Dear Grace Parraga,

The Western University Research Ethics Board has reviewed the application. This study, including all currently approved documents, has been re-approved until the expiry date noted above.

REB members involved in the research project do not participate in the review, discussion or decision.

Western University REB operates in compliance with, and is constituted in accordance with, the requirements of the TriCouncil Policy Statement: Ethical Conduct for Research Involving Humans (TCPS 2); the International Conference on Harmonisation Good Clinical Practice Consolidated Guideline (ICH GCP); Part C, Division 5 of the Food and Drug Regulations; Part 4 of the Natural Health Products Regulations; Part 3 of the Medical Devices Regulations and the provisions of the Ontario Personal Health Information Protection Act (PHIPA 2004) and its applicable regulations. The REB is registered with the U.S. Department of Health & Human Services under the IRB registration number IRB 00000940.

Please do not hesitate to contact us if you have any questions.

Sincerely,

Daniel Wyzynski, Research Ethics Coordinator, on behalf of Dr. Joseph Gilbert, HSREB Chair

*Note: This correspondence includes an electronic signature (validation and approval via an online system that is compliant with all regulations).*

## Appendix D – Curriculum Vitae

### EDUCATION

**2015-2020** Doctor of Philosophy in Medical Biophysics  
Department of Medical Biophysics  
**Western University, London, Canada**  
Supervisor: Dr. Grace Parraga  
*Thesis:* Pulmonary Structure and Function of Asthma Evaluated  
Using Pulmonary Imaging

**2011-2015** Bachelor of Engineering  
Electrical and Biomedical Engineering  
Department of Electrical and Computer Engineering  
**McMaster University, Hamilton, Canada**

### POSITIONS

**2017-2020** **Schulich School of Medicine and Dentistry**  
*Teaching Assistant*  
Western University, London Canada  
*Supervisor:* Dr. Nicole Campbell  
*Course:* Medical Science 4930F/G, Interdisciplinary Medical  
Sciences

**2016-2018** **Robarts Research Institute**  
*Research Assistant*  
Robarts Research Institute, Western University  
*Supervisor:* Dr. Grace Parraga  
*Project:* Calibration, quality control and data collection in pulmonary  
function lab for Acorda clinical trial

**2015** **Robarts Research Institute**  
*Summer Student*  
Western University, London, Canada  
*Supervisor:* Dr. Grace Parraga  
*Project:* Image-guided Thermo-ablation of Severe Asthma

## HONOURS AND AWARDS

2020

### **ISMIRM Educational Stipend Award**

*Awarded to support the attendance of students, postdoctoral and clinical trainees to present abstracts at the scientific meeting International (\$815 USD)*

2019

### **PSAC 610 GTA Academic Achievement Scholarship**

*Awarded on the basis of academic achievement and research excellence to graduate teaching assistant (GTA) members in good standing of PSAC Local 610 (Teaching Assistants and Postdocs at Western University) Institutional (\$500)*

### **Brian Keith Reid Scholarship Award**

*Awarded annually to a full-time graduate student in Medical Biophysics at the Schulich School of Medicine & Dentistry based on academic achievement and research merit Institutional (\$1,900)*

### **IWFPI 2019 Young Investigator Award Finalist**

*Three finalists selected from abstract submissions based on innovation, significance, approach and completeness International*

### **Nellie Farthing Fellowship in Medical Sciences**

*Recognizes excellence in research to a full-time doctoral student in medical sciences, candidate's record of research is of primary importance Institutional (\$3,000)*

### **First Place Oral Presentation Award**

*London Imaging Discovery Day 2019 Recognized for having the top oral presentation out of all participants at the annual meeting Regional*

### **Third Place Canadian Thoracic Society Poster Competition**

*Top 30 abstracts out of all Canada-based trainees that submitted to the American Thoracic Society Meeting 2019 selected to compete in poster competition National*

### **ISMIRM Summa Cum Laude Merit Award**

*Awarded to those whose abstract score was in the top 5% of those submitted for review International*

**Institute Community Support (ICS) Travel Award**

Canadian Institute for Health Research (CIHR) – Institute of Circulatory and Respiratory Health (ICRH)

*Competition for students, post-doctoral fellows, new investigators and knowledge users to present their own research at national and international meetings and/or conferences*

National (\$1,000)

**Respiratory Structure and Function Abstract Scholarship**

ATS 2019 International Conference Dallas TX

*Awarded to individuals based on quality of abstracts submitted as reviewed by the Assembly Program Committees*

International (\$550 USD)

**ISMRM Educational Stipend Award**

*Awarded to support the attendance of students, postdoctoral and clinical trainees to present abstracts at the scientific meeting*

International (\$535 USD)

**2018**

**Western Graduate Research Scholarship, Western University**

*Awarded to a full time graduate student for stipend support who has maintained an average of 80% or more*

Institutional (\$5,000)

**Honourable Mention Oral Presentation Award**

London Imaging Discovery Day 2018

*Recognized for having the third place oral presentation out of all participants at the annual meeting*

Regional

**Institute Community Support (ICS) Travel Award**

Canadian Institute for Health Research (CIHR) – Institute of Circulatory and Respiratory Health (ICRH)

*Competition for students, post-doctoral fellows, new investigators and knowledge users to present their own research at national and international meetings and/or conferences*

National (\$1,000)

**ISMRM Educational Stipend Award**

*Awarded to support the attendance of students, postdoctoral and clinical trainees to present abstracts at the scientific meeting*

International (\$525 USD)

**2017**

**Western Graduate Research Scholarship, Western University**

*Awarded to a full time graduate student for stipend support who has maintained an average of 80% or more*

Institutional (\$4,500)

**ISMRM Magna Cum Laude Merit Award**

*Awarded to those whose abstract score was in the top 15% of those submitted for review*

International

**Respiratory Structure and Function Abstract Scholarship (Declined)**

ATS 2017 International Conference Washington DC

*Awarded to individuals based on quality of abstracts submitted as reviewed by the Assembly Program Committees*

International (\$500 USD)

**Post-Graduate Scholarship – Doctoral (PGS-D)**

Natural Sciences and Engineering Research Council (NSERC)

*Awarded to high-caliber scholars who are engaged in doctoral programs*

National (\$63,000)

**IWPMI 2017 Best Scientific Presentation Award**

*One of six awards for the top abstracts submitted to the 8th International Workshop on Pulmonary Functional Imaging*

International

**ISMRM Educational Stipend Award (Declined)**

*Awarded to support the attendance of students, postdoctoral and clinical trainees to present abstracts at the scientific meeting*

International (\$545 USD)

**2016**

**Western Graduate Research Scholarship, Western University**

*Awarded to a full time graduate student for stipend support who has maintained an average of 80% or more*

Institutional (\$4,500)

**Respiratory Structure and Function Abstract Scholarship**

ATS 2016 International Conference San Francisco

*Awarded to individuals based on quality of abstracts submitted as reviewed by the Assembly Program Committees*

International (\$500 USD)

**Canada Graduate Scholarship – Masters (CGS-M)**

Natural Sciences and Engineering Research Council (NSERC)

*Awarded to high-caliber scholars who are engaged in master's programs, CGS is offered to the top-ranked applicants*

National (\$17,500)

- 2015**      **Western Graduate Research Scholarship, Western University**  
*Awarded to a full time graduate student for stipend support who has maintained an average of 80% or more*  
 Institutional (\$4,500)
- Dean's Honour List, McMaster University**  
*Awarded each year to outstanding students with a minimum average of 9.5 on at least 30 units*  
 Institutional
- 2014**      **Dean's Honour List, McMaster University**  
*Awarded each year to outstanding students with a minimum average of 9.5 on at least 30 units*  
 Institutional
- 2012**      **Dean's Honour List, McMaster University**  
*Awarded each year to outstanding students with a minimum average of 9.5 on at least 30 units*  
 Institutional
- 2011**      **Honour Award, McMaster University**  
*Awarded to entering undergraduate students for a final admission average of 90-94.99%*  
 Institutional (\$1,200)
- USW Post-Secondary Scholarship, United Steelworkers Local 2724**  
*Awarded to children of members of the USW who are completing high school and starting post-secondary studies, based on original essay on a selected topic*  
 Regional (\$1,000)

## **PUBLICATIONS AND PRESENTATIONS**

### **A Peer-Reviewed Journal Manuscripts**

#### **Submitted (1)**

1. S Svenningsen, **RL Eddy**, M Kjarsgaard, G Parraga, P Nair. Effect of Anti-T2 Biologics on MRI Ventilation in Prednisone-dependent Asthma. *Chest*. Submitted with revisions March 26, 2020. Manuscript ID CHEST-19-2866.R1

## Published and in press (21)

1. AL Barker, **RL Eddy**, JL MacNeil, M Kirby, DG McCormack, G Parraga. CT Pulmonary Vessels and MRI ventilation in Chronic Obstructive Pulmonary Disease: Relationship with Worsening FEV<sub>1</sub> in the TINCan Cohort Study. *Acad Radiol*. 2020. *In press*. Manuscript ID ARAD-S-20-00144.
2. JL MacNeil, DPI Capaldi, A Westcott, **RL Eddy**, AL Barker, DG McCormack, M Kirby, G Parraga. Pulmonary Imaging Phenotypes of Chronic Obstructive Pulmonary Disease using Multiparametric Response Maps. *Radiology*. 2020;295(1):227-236.
3. **RL Eddy**, S Svenningsen, M Kirby, D Knipping, DG McCormack, C Licskai, P Nair, G Parraga. Is Computed Tomography Airway Count Related to Asthma Severity and Airway Structure-function? *Am J Respir Crit Care Med*. 2020 [Epub ahead of print]  
*EDITORIAL HIGHLIGHT*
4. H Serajeddini\*, **RL Eddy**\*, C Licskai, DG McCormack, G Parraga. FEV<sub>1</sub> and MRI Ventilation Defect Reversibility in Asthma and COPD. *Eur Respir J*. 2020;55(3):1901947 \*contributed equally as first authors
5. **RL Eddy**, G Parraga. Pulmonary <sup>129</sup>Xe MRI: New Opportunities to Unravel Enigmas in Respiratory Medicine. *Eur Respir J*. 2020;55(2):1901987.
6. **RL Eddy**, AM Matheson, S Svenningsen, D Knipping, C Licskai, DG McCormack, G Parraga. Nonidentical Twins with Asthma: Spatially-matched CT Airway and MRI Ventilation Abnormalities. *Chest*. 2019;156(6):e111-6.
7. S Svenningsen, E Haider, **RL Eddy**, G Parraga, P Nair. Normalisation of MRI Ventilation Heterogeneity in Severe Asthma by Dupilumab. *Thorax*. 2019;74(11):1087-8.  
*FEATURED ON JOURNAL COVER*
8. **RL Eddy**, S Svenningsen, C Licskai, DG McCormack, G Parraga. Hyperpolarized Helium 3 MRI in Mild-to-Moderate Asthma: Prediction of Postbronchodilator Reversibility. *Radiology*. 2019;293(1):212-20.  
*EDITORIAL HIGHLIGHT, FEATURED ON JOURNAL COVER*
9. S Svenningsen, E Haider, C Boylan, M Mukherjee, **RL Eddy**, DPI Capaldi, G Parraga, P Nair. CT and Functional MRI to Evaluate Airway Mucus in Severe Asthma. *Chest*. 2019;155(6):1178-89.
10. **RL Eddy**, A Westcott, GN Maksym, G Parraga, RJ Dandurand. Oscillometry and Pulmonary Magnetic Resonance Imaging in Asthma and COPD. *Physiol Rep*. 2019;7(1):e13955.
11. **RL Eddy**, S Svenningsen, DG McCormack, G Parraga. What is the Minimal Clinically Important Difference for Helium-3 Magnetic Resonance Imaging Ventilation Defects? *Eur Respir J*. 2018;51(6).
12. HM Young, F Guo, **RL Eddy**, GN Maksym, G Parraga. Oscillometry and Pulmonary MRI of Ventilation Heterogeneity in Obstructive Lung Disease: Relationship to Quality of Life and Disease Control. *J Appl Physiol*. 2018;125(1):73-85.
13. S Svenningsen, **RL Eddy**, HF Lim, PG Cox, P Nair, G Parraga. Sputum Eosinophilia and Magnetic Resonance Imaging Ventilation Heterogeneity in Severe Asthma. *Am J Respir Crit Care Med*. 2018;197(7):876-84.  
*EDITORIAL HIGHLIGHT*
14. DPI Capaldi, **RL Eddy**, S Svenningsen, F Guo, JSH Baxter, AJ McLeod, P Nair, DG McCormack, G Parraga for the Canadian Respiratory Research Network. Free-breathing

- Pulmonary MR Imaging to Quantify Regional Ventilation. *Radiology*. 2018;287(2):693-704.
15. **RL Eddy**, S Svenningsen, A Kassay, DG McCormack, P Nair, G Parraga for the Canadian Respiratory Research Network. *This is what Asthma Looks Like: Review of New and Emerging Functional Imaging Methods and Results*. *Canadian Journal of Respiratory, Critical Care and Sleep Medicine*. 2018;2(1):27-40.
  16. HM Young, **RL Eddy**, G Parraga. MRI and CT Lung Biomarkers: Towards an In Vivo Understanding of Lung Biomechanics. *Clin Biomech*. 2019;66:107-122.
  17. DPI Capaldi, K Sheikh, **RL Eddy**, F Guo, S Svenningsen, P Nair, DG McCormack, G Parraga for the Canadian Respiratory Research Network. Free-breathing Pulmonary MRI: Response to Bronchodilator and Bronchoprovocation in Severe Asthma. *Acad Radiol*. 2017;24(10):1268-76.
  18. M Kirby, **RL Eddy**, D Pike, S Svenningsen, DD Sin, HO Coxson, DG McCormack, G Parraga for the Canadian Respiratory Research Network. MRI Ventilation Abnormalities Predict Quality-of-Life and Lung Function Changes in Mild-to-Moderate COPD: Longitudinal TINCan Study. *Thorax*. 2017;72(5):475-7.
  19. K Sheikh, F Guo, DPI Capaldi, A Ouriadov, **RL Eddy**, S Svenningsen, G Parraga for the Canadian Respiratory Research Network. Ultra-short Echo Time MRI Biomarkers of Asthma. *J Magn Reson Imaging*. 2016;45(4):1204-15.
  20. F Guo, S Svenningsen, **RL Eddy**, DPI Capaldi, K Sheikh, A Fenster, G Parraga. Anatomical Pulmonary Magnetic Resonance Imaging Segmentation for Regional Structure-Function Measurements of Asthma. *Med Phys*. 2016;43(6):2911-26.
  21. D Pike, M Kirby, **RL Eddy**, F Guo, DPI Capaldi, A Ouriadov, DG McCormack, G Parraga. Regional Heterogeneity of Chronic Obstructive Pulmonary Disease Phenotypes: Pulmonary <sup>3</sup>He Magnetic Resonance Imaging and Computed Tomography. *COPD*. 2016;13(5):601-9.

### **In Revision (1)**

1. S Svenningsen, MJ McIntosh, A Ouriadov, NB Konyer, **RL Eddy**, DG McCormack, MD Noseworthy, P Nair, G Parraga. Reproducibility of Hyperpolarized <sup>129</sup>Xe MRI in Severe Asthma to Evaluate Clinical Trial Feasibility. Manuscript ID ARAD-S-19-01476.R1.

### **B Book Chapters (2)**

1. AL Barker, **RL Eddy**, H Yaremko, M Kirby, G Parraga. Structure-Function Imaging of Asthma: Airways and Ventilation Biomarkers. In: *Pulmonary Functional Imaging – Basics and Clinical Applications*. Ohno Y, Hatabu H and Kauczor HU (Eds). Springer 2018. Submitted September 1, 2018.
2. DPI Capaldi, **RL Eddy**, G Parraga. Pulmonary MRI in Clinical Trials. In: *MRI of the Lung Second Edition*. p. 453-478. Kauczor HU and Wielpütz MO (Eds). ISBN: 978-3-319-42616-7. Medical Radiology. Springer, Cham 2016.

## C Peer-Reviewed Published Conference Proceedings (2)

1. AM Matheson, DPI Capaldi, F Guo, **RL Eddy**, DG McCormack, G Parraga. Fourier Decomposition Free-breathing  $^1\text{H}$  MRI Perfusion Maps in Asthma. Proc. SPIE 10949, Medical Imaging 2019: Image Processing, 1094912 (15 March 2019).
2. JL MacNeil, DPI Capaldi, **RL Eddy**, AR Westcott, AM Matheson, AL Barker, C Ong Ly, DG McCormack, G Parraga. Development and Evaluation of Pulmonary Imaging Multi-Parametric Response Maps for Deep Phenotyping of Chronic Obstructive Pulmonary Disease. Proc. SPIE 10953, Medical Imaging 2019: Biomedical Applications in Molecular, Structural, and Functional Imaging, 109530J (15 March 2019).

## ABSTRACTS AND PRESENTATIONS

### A Submitted Abstracts (9)

1. MJ McIntosh, **RL Eddy**, JL MacNeil, AM Matheson, G Parraga. Automated Quantification of Spatially Abnormal  $^{129}\text{Xe}$  MRI Ventilation and Perfusion: Implications for Lung Cancer, Asthma and COPD. Joint American Association of Physicists in Medicine – Canadian Organization of Medical Physicists Meeting Vancouver, Canada July 12-16, 2020.
2. FR Salerno, TJ Lindenmaier, AM Matheson, **RL Eddy**, MJ McIntosh, J Dorie, G Parraga, CW McIntyre. Noninvasive assessment of pulmonary hypertension using quantitative imaging in hemodialysis patients. European Renal Association – European Dialysis and Transplant Association 2020 Milan, Italy June 6-9, 2020.
3. **RL Eddy**, C Licskai, DG McCormack, G Parraga. Novel MRI-based Clusters of Asthma: Pulmonary Functional MRI and CT. International Society of Magnetic Resonance in Medicine Annual Scientific Meeting 2020 Sydney, Australia April 18-23, 2020. *Accepted oral presentation*
4. AM Matheson, **RL Eddy**, JL MacNeil, MJ McIntosh, G Parraga. Fully-automated  $^1\text{H}$  Thoracic Cavity Segmentation for Hyperpolarized Gas Imaging Using a Convolutional Neural Network. International Society of Magnetic Resonance in Medicine Annual Scientific Meeting 2020 Sydney, Australia April 18-23, 2020. *Accepted oral presentation*
5. MJ McIntosh, **RL Eddy**, D Knipping, T Lindenmaier, DG McCormack, C Licskai, C Yamashita, G Parraga. Supervised Shallow Learning of  $^{129}\text{Xe}$  MRI Texture Features to Predict Response to Anti-IL5 Biologic Therapy in Severe Asthma. International Society of Magnetic Resonance in Medicine Annual Scientific Meeting 2020 Sydney, Australia April 18-23, 2020. *Accepted oral presentation*
6. **RL Eddy**, MJ McIntosh, AM Matheson, D Knipping, C Licskai, DG McCormack, G Parraga.  $^{129}\text{Xe}$  MRI Ventilation Heterogeneity Phenotypes of Asthma. American Thoracic Society Annual Scientific Meeting 2020 Philadelphia, PA May 15-20, 2020. *Accepted oral presentation*
7. MJ McIntosh, **RL Eddy**, D Knipping, AL Barker, T Lindenmaier, C Yamashita, G Parraga. Response to Benralizumab in Severe Asthma:  $^{129}\text{Xe}$  MRI, Oscillometry and Clinical Measurements. American Thoracic Society Annual Scientific Meeting 2020 Philadelphia, PA May 15-20, 2020. *Accepted oral presentation*

8. AM Matheson, **RL Eddy**, AL Barker, DG McCormack, G Parraga. Perfusion Abnormalities in COPD: How do Emphysema and Airways Contribute? American Thoracic Society Annual Scientific Meeting 2020 Philadelphia, PA May 15-20, 2020. *Accepted poster discussion presentation*
9. H Serajeddini, **RL Eddy**, D Knipping, T Lindenmaier, KJ Bosma, I Dhaliwal, G Parraga. Longitudinal  $^{129}\text{Xe}$  MRI in a Survivor of Respiratory Failure Related to E-cigarette Use. American Thoracic Society Annual Scientific Meeting 2020 Philadelphia, PA May 15-20, 2020. *Accepted thematic poster presentation*

#### **B Invited Oral Presentations (7)**

1. Y Habis, **RL Eddy** (co-presenters). Airway Remodeling: A Clinical and Imaging Review. London, ON March 3, 2020.
2. **RL Eddy**. MRI Ventilation Heterogeneity and Oscillometry: Where Do We Go Next? Montreal Oscillometry Summer Seminar Montreal, QC July 25-26, 2019.
3. **RL Eddy**. Undergrad to Grad School to Post-PhD: Polarizing Perspectives. Summer Student Lunch Seminar Series, Robarts Research Institute, London, ON July 9, 2019.
4. **RL Eddy**. Pulmonary MRI of Airways Disease: Space-time Explorations. Centre for Heart Lung Innovation Seminar, University of British Columbia and St. Paul's Hospital Vancouver, BC June 28, 2019.
5. **RL Eddy**. Pulmonary MRI: Polarizing Perspectives. Department of Radiology Grand Rounds, University of British Columbia Vancouver, BC June 26, 2019.
6. **RL Eddy**, G Parraga. Oscillometry and Pulmonary MRI Measurements of Ventilation Heterogeneity in Obstructive Lung Disease: Relationship to Quality of Life and Disease Control. American Thoracic Society Respiratory Structure and Function Assembly Journal Club Webinar. February 26, 2019.
7. **RL Eddy**, RJ Dandurand, HM Young, GN Maksym, G Parraga. Relationship Between Pulmonary Functional MRI and Oscillometry. Montreal Oscillometry Summer Seminar Montreal, QC August 2, 2018.

#### **C Proffered Oral Presentations (18) \*presenter**

1. **RL Eddy**,\* C Licskai, G Parraga. Severe Asthma: Where do the Airways Go and Does it Matter? 9<sup>th</sup> International Workshop on Pulmonary Functional Imaging New Orleans, LA October 18-20, 2019. *Selected for Top 3 Young Investigator Finalist*
2. **RL Eddy**,\* A Westcott, GN Maksym, DG McCormack, G Parraga. Differences Between  $^3\text{He}$  and  $^{129}\text{Xe}$  Ventilation Heterogeneity Explained Using Oscillometry. International Society of Magnetic Resonance in Medicine Annual Scientific Meeting 2019 Montreal, Canada May 11-16, 2019.
3. **RL Eddy**,\* A Westcott, GN Maksym, DG McCormack, G Parraga. Can Oscillometry Explain Differences Between  $^3\text{He}$  and  $^{129}\text{Xe}$  Ventilation Heterogeneity? 17<sup>th</sup> Annual Imaging Network Ontario Symposium London, ON, Canada, March 28-29, 2019.
4. AL Barker,\* **RL Eddy**, AM Matheson, A Westcott, GR Washko, G Parraga. Are MRI Ventilation Defects and CT Vascular Pruning Related in Bronchiectasis and COPD Patients? 17<sup>th</sup> Annual Imaging Network Ontario Symposium London, ON, Canada, March 28-29, 2019.

5. AM Matheson,\* **RL Eddy**, DPI Capaldi, F Guo, DG McCormack, G Parraga. Multi-scalar Perfusion and Ventilation Defects in Asthma. 17<sup>th</sup> Annual Imaging Network Ontario Symposium London, ON, Canada, March 28-29, 2019.
6. HM Young, F Guo, **RL Eddy**,\* GN Maksym, G Parraga. Pulmonary MRI Measurements of Ventilation Heterogeneity in Obstructive Lung Disease: Relationships to Oscillometry, Quality of Life and Disease Control. International Society of Magnetic Resonance in Medicine Annual Scientific Meeting 2018 Paris, France June 16-21, 2018.
7. **RL Eddy**\*, S Svenningsen, DG McCormack, G Parraga. What is the Minimal Clinically Important Difference for MRI Ventilation Defects? London Imaging Discovery Day 2018 London ON, June 14, 2018.
8. **RL Eddy**\*, S Svenningsen, DG McCormack, G Parraga. What is the MCID for MRI Ventilation Heterogeneity? Canadian Respiratory Research Network 2018 Annual General Meeting Ottawa, ON January 18-19, 2018.
9. DPI Capaldi,\* JSH Baxter, AJ McLeod, **RL Eddy**, S Svenningsen, F Guo, DG McCormack, G Parraga. Measuring Specific Ventilation using Four-dimensional Magnetic Resonance Imaging: A Novel Physiological Biomarker of Asthma. 103<sup>rd</sup> Scientific Assembly and Annual Meeting of the Radiological Society of North America Chicago, IL November 26-December 1, 2017.
10. **RL Eddy**\*, K Sheikh, DPI Capaldi, S Svenningsen, DG McCormack, G Parraga. Ventilation Heterogeneity Reversibility: Asthma, COPD or ACOS? European Respiratory Society International Congress 2017 Milan, Italy September 9-13, 2017.
11. S Svenningsen,\* **RL Eddy**, HF Lim, P Nair, G Parraga. Inflammatory and Non-Inflammatory Contributions to Ventilation Heterogeneity in Severe, Poorly-controlled Asthmatics. American Thoracic Society Annual Scientific Meeting 2017 Washington DC May 19-24, 2017.
12. **RL Eddy**, DPI Capaldi, K Sheikh, S Svenningsen, DG McCormack, G Parraga. Pulmonary MRI Ventilation Defects in Asthma: Stochastic or Deterministic? International Society of Magnetic Resonance in Medicine Annual Scientific Meeting 2017 Honolulu, HI April 22-27, 2017.
13. **RL Eddy**\*, DPI Capaldi, K Sheikh, S Svenningsen, DG McCormack, G Parraga. Pulmonary MRI Ventilation Defects in Asthma: Stochastic or Deterministic? 8<sup>th</sup> International Workshop on Pulmonary Functional Imaging Seoul, South Korea March 24-26, 2017.
14. **RL Eddy**\*, DPI Capaldi, K Sheikh, S Svenningsen, DG McCormack, G Parraga. Pulmonary MRI Ventilation Defects in Asthma: Stochastic or Deterministic? 15<sup>th</sup> Annual Imaging Network Ontario Symposium London, ON, Canada, March 15-16, 2017.
15. **RL Eddy**\*, S Svenningsen, DG McCormack, G Parraga. MRI Ventilation Defects in Asthma: Space and Time Explorations of Non-randomness. Canadian Respiratory Research Network 2017 Annual General Meeting Ottawa, ON January 12-13, 2017.
16. **RL Eddy**, D Pike, K Sheikh, GA Paulin, M Kirby,\* DG McCormack, G Parraga. Testing the Fletcher-Peto Assumptions using Pulmonary Imaging Biomarker Longitudinal Measurements. American Thoracic Society Annual Scientific Meeting 2016 San Francisco, CA May 13-18, 2016.
17. K Sheikh,\* F Guo, S Svenningsen, A Ouriadov, DPI Capaldi, **RL Eddy**, DG McCormack, G Parraga. What does Magnetic Resonance Imaging Signal-Intensity

mean in Asthma? American Thoracic Society Annual Scientific Meeting 2016 San Francisco, CA May 13-18, 2016.

18. K Sheikh,\* F Guo, S Svenningsen, A Ouriadov, DPI Capaldi, **RL Eddy**, DG McCormack, G Parraga. What does Magnetic Resonance Imaging Signal-Intensity mean in Asthma? London Health Research Day 2016, London, Ontario, Canada. March 29, 2016.

#### **D Proffered Poster Presentations (31) \*presenter**

1. FR Salerno,\* **RL Eddy**, AM Matheson, G Parraga, CW McIntrye. Lung Ventilation Abnormalities in Chronic Hemodialysis Patients with Hyperpolarized  $^{129}\text{Xe}$  Gas Magnetic Resonance Imaging. American Society of Nephrology Kidney Week 2019 Washington DC November 5-10, 2019.
2. **RL Eddy**, A Westcott, M Kirby, DG McCormack, G Parraga. CT Pulmonary Vessel Volume in Ex-smokers with Normal FEV<sub>1</sub>. European Respiratory Society International Congress 2019 Madrid, Spain September 28-October 2, 2019. *Traditional poster*.
3. **RL Eddy**,\* GN Maksym, RJ Dandurand, G Parraga. Oscillometry Detects Different Airway Abnormalities that Manifest as MRI Ventilation Heterogeneity in Asthma and COPD. American Thoracic Society Annual Scientific Meeting 2019 Dallas, TX May 17-22, 2019. *Poster discussion*.
4. **RL Eddy**,\* DG McCormack, M Kirby, G Parraga. CT Airway Count as a Biomarker of Asthma Pathogenesis: Severe Asthma and ACOS in Never-smokers. American Thoracic Society Annual Scientific Meeting 2019 Dallas, TX May 17-22, 2019. *Poster discussion. \*Selected for Canadian Thoracic Society Annual Poster Competition*
5. AL Barker,\* **RL Eddy**, AM Matheson, AR Westcott, GR Washko, G Parraga. Bronchiectasis, Vascular Pruning and Ventilation Defects in COPD and Bronchiectatic Patients: Are They Related? American Thoracic Society Annual Scientific Meeting 2019 Dallas, TX May 17-22, 2019. *Poster discussion*.
6. AM Matheson,\* **RL Eddy**, DPI Capaldi, F Guo, DG McCormack, G Parraga. Perfusion Abnormalities and Ventilation Heterogeneity in Asthma. American Thoracic Society Annual Scientific Meeting 2019 Dallas, TX May 17-22, 2019. *Poster discussion*.
7. S Svenningsen,\* E Haider, C Boylan, M Mukherjee, **RL Eddy**, DPI Capaldi, G Parraga, P Nair. Airway Luminal Contributors to MRI Ventilation Heterogeneity in Severe Asthma. American Thoracic Society Annual Scientific Meeting 2019 Dallas, TX May 17-22, 2019. *Poster discussion*.
8. A Westcott,\* A Ouriadov, **RL Eddy**, DG McCormack, M Kirby, G Parraga. Compressed Sensing Hyperpolarized Gas Ventilation MRI: Towards a Maximal Clinically Acceptable Acceleration Factor. International Society of Magnetic Resonance in Medicine Annual Scientific Meeting 2019 Montreal, Canada May 11-16, 2019. *Digital poster*.
9. AL Barker,\* A Westcott, **RL Eddy**, DG McCormack, G Parraga, A Ouriadov. Feasibility of Single Breath-hold Isotropic Voxel  $^{129}\text{Xe}$  in Patients. International Society of Magnetic Resonance in Medicine Annual Scientific Meeting 2019 Montreal, Canada May 11-16, 2019. *Digital poster*.
10. S Svenningsen,\* A Ouriadov, NB Konyer, **RL Eddy**, A Westcott, DG McCormack, M Kjarsgaard, MD Noseworthy, P Nair, G Parraga. Two-site Reproducibility of Hyperpolarized  $^{129}\text{Xe}$  MRI Ventilation in Severe Asthma: Implications for Multicenter

- Clinical Studies. International Society of Magnetic Resonance in Medicine Annual Scientific Meeting 2019 Montreal, Canada May 11-16, 2019. *Digital poster*.
11. **RL Eddy**,\* HM Young, A Kassay, DPI Capaldi, S Svenningsen, DG McCormack, G Parraga. Contributions of Large Versus Small Airways to MRI Ventilation Heterogeneity in Asthmatics. International Society of Magnetic Resonance in Medicine Annual Scientific Meeting 2018 Paris, France June 16-21, 2018. *Traditional Poster*.
  12. S Svenningsen,\* N Zha, **RL Eddy**, DPI Capaldi, M Kjarsgaard, K Radford, P Nair, G Parraga. MRI Ventilation Texture Features Discriminate Severe Asthmatics with and without Eosinophilic Airway Inflammation. International Society of Magnetic Resonance in Medicine Annual Scientific Meeting 2018 Paris, France June 16-21, 2018. *Traditional Poster*.
  13. A Westcott,\* **RL Eddy**, DPI Capaldi, HM Young, DG McCormack, G Parraga. Novel Quantification of Ventilation Heterogeneity Patterns in Hyperpolarized <sup>3</sup>He MRI. International Society of Magnetic Resonance in Medicine Annual Scientific Meeting 2018 Paris, France June 16-21, 2018. *E-poster*.
  14. **RL Eddy**,\* S Svenningsen, DG McCormack, G Parraga. Determining the Minimal Clinically Important Difference: MRI Ventilation Defect Percent in Asthmatics. American Thoracic Society Annual Scientific Meeting 2018 San Diego, CA May 17-23, 2018. *Poster Discussion*.
  15. S Svenningsen,\* **RL Eddy**, DPI Capaldi, M Kjarsgaard, K Radford, G Parraga, P Nair. Effect of anti-Th2 Therapy on MRI Ventilation Heterogeneity in Prednisone-dependent Asthma. American Thoracic Society Annual Scientific Meeting 2018 San Diego, CA May 17-23, 2018. *Poster Discussion*.
  16. **RL Eddy**,\* S Svenningsen, DG McCormack, G Parraga. What is the Minimal Clinically Important Difference for MRI Ventilation Defects? London Health Research Day 2018, London, Ontario, Canada. May 10, 2018. *Traditional Poster*.
  17. **RL Eddy**,\* S Svenningsen, DG McCormack, G Parraga. Five-year MRI Study of Ventilation Heterogeneity in Asthma. European Respiratory Society International Congress 2017 Milan, Italy. September 9-13, 2017. *Thematic Poster*.
  18. HM Young, F Guo, **RL Eddy**,\* C Church, G Maksym, G Parraga. Forced Oscillation Technique and MRI Predictions of Airway Reactance in Moderate-Severe Asthma. European Respiratory Society International Congress 2017 Milan, Italy. September 9-13, 2017. *Poster Discussion*.
  19. DPI Capaldi, K Sheikh, **RL Eddy**,\* S Svenningsen, DG McCormack, G Parraga. Fourier-decomposition of Free-breathing Pulmonary Proton MRI in Asthma. European Respiratory Society International Congress 2017 Milan, Italy. September 9-13, 2017. *Thematic Poster*.
  20. **RL Eddy**, S Svenningsen, DG McCormack, G Parraga. Five-year MRI Study of Ventilation Heterogeneity in Asthmatics: Where Do the Defects Go? American Thoracic Society Annual Scientific Meeting 2017 Washington DC May 19-24, 2017. *Thematic Poster*.
  21. **RL Eddy**, K Sheikh, DPI Capaldi, S Svenningsen, C Licskai, DG McCormack, G Parraga. Ventilation Heterogeneity Reversibility: Asthma, COPD or ACOS? American Thoracic Society Annual Scientific Meeting 2017 Washington DC May 19-24, 2017. *Poster Discussion*.

22. **RL Eddy**, DPI Capaldi, K Sheikh, S Svenningsen, DG McCormack, G Parraga. Probability Mapping of Lung Functional Abnormalities in Asthma using MRI: Lung Atlas Explorations of Non-randomness. American Thoracic Society Annual Scientific Meeting 2017 Washington DC May 19-24, 2017. *Poster Discussion*.
23. A Bhalla,\* K Sheikh, HM Young, **RL Eddy**, DG McCormack, TM Luu, S Katz, G Parraga. Asthma Phenotypes in Adult Survivors of Premature Birth Using Functional Magnetic Resonance Imaging. American Thoracic Society Annual Scientific Meeting 2017 Washington DC May 19-24, 2017. *Poster Discussion*.
24. DPI Capaldi, K Sheikh, **RL Eddy**, S Svenningsen, M Kirby, DG McCormack, G Parraga. Asthma Ventilation Abnormalities Measured using Fourier-Decomposition Free-breathing Pulmonary <sup>1</sup>H MRI. International Society of Magnetic Resonance in Medicine Annual Scientific Meeting 201 Honolulu, HI April 22-27, 2017. *E-poster*.
25. **RL Eddy**,\* K Sheikh, DPI Capaldi, S Svenningsen, C Licskai, DG McCormack, G Parraga. Ventilation Heterogeneity Reversibility: Asthma, COPD or ACOS? London Health Research Day 2016, London, Ontario, Canada. March 28, 2017. *Thematic Poster*.
26. M Fennema, **RL Eddy**,\* DPI Capaldi, K Sheikh, S Svenningsen, C Licskai, DG McCormack, G Parraga. The Abnormal Airways that Dominate Asthma Attack: New clues using ventilation MRI during Exercise- and Methacholine-Challenge. American Thoracic Society Annual Scientific Meeting 2016 San Francisco, CA May 13-18, 2016. *Poster Discussion*.
27. F Guo, S Svenningsen, **RL Eddy**, M Fennema, DG McCormack, G Parraga. Towards Image-guided Asthma Therapy: A clinical pipeline to generate MRI Sub-segmental Ventilation Measurements. American Thoracic Society Annual Scientific Meeting 2016 San Francisco, CA May 13-18, 2016. *Poster Discussion*.
28. F Guo, K Sheikh, **RL Eddy**, DPI Capaldi,\* DG McCormack, A Fenster, G Parraga. A Segmentation Pipeline for Measuring Pulmonary Ventilation Suitable for Clinical Workflows and Decision-making. International Society of Magnetic Resonance in Medicine Annual Scientific Meeting 2016 Suntec City, Singapore May 7-13, 2016. *E-poster*.
29. M Fennema, S Svenningsen, **RL Eddy**, D Leary, G Maksym, G Parraga. Can the Forced Oscillation Technique and a Computational Model of Respiratory System Mechanics Explain Asthma Ventilation Defects? International Society of Magnetic Resonance in Medicine Annual Scientific Meeting 2016 Suntec City, Singapore May 7-13, 2016. *Thematic Poster*.
30. **RL Eddy**,\* M Kirby, D Pike, K Sheikh, GA Paulin, DG McCormack, G Parraga. Testing the Fletcher-Peto Assumptions using Pulmonary Imaging Biomarker Longitudinal Measurements. London Health Research Day 2016, London, Ontario, Canada. March 29, 2016. *Thematic Poster*.
31. **RL Eddy**,\* M Doughty, I Hegazzi. Breast Imaging Using Electrical Impedance Tomography. McMaster University Electrical and Computer Engineering (ECE) Expo 2015 Hamilton, Ontario, Canada. April 7, 2015 (Engineering Design Project poster).

## POST-GRADUATE EDUCATION DEVELOPMENT AND EXPERIENCES

- 04/2019                    **Poster Judge**  
Medical Biophysics Undergraduate Research Day, Western University
- 03/2019                    **Biotechnology Debate Judge**  
Western Advancement in Medicine Society (AIMS) Club  
*Role:* Judge 20-minute debate by presenting feedback to debate teams on validity and strength of arguments and determine a winning side.
- 09/2018-04/2019        **Career Profile Advisor**  
The Student Success Centre, Western University  
*Role:* Deliver career and employment support to Western University students as part of the Career Counselling team with extensive training on resume, cover letter, CV and LinkedIn Profile development
- 05/2018-                    **Oscillometry Standardization Project**  
Oscillometry Unit, Centre for Innovative Medicine, Montreal, Canada  
*Objective:* Standardization of oscillometry results across five commercially marketed devices and a wave tube  
*Role:* Attend meetings, and read and edit draft manuscript(s)
- 10/2017-12/2019        **Deep Learning Club Co-coordinator**  
*Co-coordinators:* Andrew Westcott, Wenyao Xia, Patricia Johnson  
*Goal:* Monthly seminar for introductory deep learning with specific applications in medical imaging and health information science, for multi-disciplinary trainees  
*Role:* meeting scheduling and organization, preparation of meeting content, presentations during meetings
- 06/2017/-04/2018        **Graduate Student Mentor/Supervisor**  
Undergraduate Student: Robert DiCesare, BSc Candidate Physiology and Pharmacology  
Project: “Resting State Brain Connectivity & Lung Function in Healthy Volunteers during Methacholine-induced Bronchoconstriction Mimicking Asthma Attack”
- 01/2017-03/2018        **Graduate Student Mentor/Supervisor**  
Undergraduate Student: Andrea Kassay, BSc Candidate Medical Biophysics  
Project: “Intraobserver Repeatability of CT Airway Measurements in Patients with Asthma”

04/2016-03/2017

**Volunteer Research Assistant**

*Study:* Canadian Alliance for Healthy Hearts and Minds, Robarts Research Institute

*Role:* Calling and scheduling study visit appointments for participants, performing participant study visits including physical measurements, cognitive assessments (Montreal Cognitive Assessment, Digital Symbol Substitution) and preparation for MRI and completing appropriate study forms and paperwork

**RESEARCH FUNDING APPLICATIONS**

**Lawson Health Research Institute Spring 2016 Internal Research Fund** (*Successful*)

MRI-guided Endobronchial Thermoplasty for Severe Uncontrolled Asthma

June 2016

**PROFESSIONAL SOCIETIES**

2017- European Respiratory Society (ERS)

*Student Member*

2016- Canadian Respiratory Research Network (CRRN)

*Trainee Member*

2015- International Society for Magnetic Resonance in Medicine (ISMRM)

*Student Member*

2015- American Thoracic Society (ATS)

*Trainee Member*

2015- Canadian Thoracic Society (CTS)

*PhD Student Member*

2015- Canadian Organization of Medical Physicists (COMP)

*Student Member*